Department of Earth Sciences

Institute of Geographic Sciences

Physical Geography

Abraha Adugna Ashenafi

Dissertation to obtain the doctoral degree

Modeling Hydrological Responses to Changes in Land Cover and Climate in Geba River Basin, Northern Ethiopia

Chairman of the Examination Board:

Univ.-Prof. Dr. Tilman Rost — Freie Universität Berlin

Date of the (final) oral examination: 2014-01-20

Supervisors:

Univ.-Prof. Dr. Brigitta Schütt — Freie Universität Berlin

Jun.-Prof. Dr. Wiebke Bebermeier — Freie Universität Berlin

Co-Advisor:

Dr.-Ing. Joachim Lengrich — Ethiopian Institute of Technology-Mekelle

This page intentionally left blank.

Abstract

This study addresses the past and potential future land cover and climate changes and their impacts on the hydrological response of Geba River Basin, Northern Ethiopia. The study analyses the historical climatic (1961–2003) and land cover changes (1972–2003) that took place and the effect these had on the hydrology of the basin. It makes use of land cover and climate change scenarios for the future to determine the potential effects these changes will have on the basin.

Geba River Basin was selected as a case study due to its socio-economical importance in the region. However, the socio-economic development and food security is limited by the high variable rainfall, serious water shortage and poor watershed management. The erratic rainfall, both in time and space, together with high land degradation makes the regional food unsecured only using rain-fed agriculture. In order to supplement rain-fed agriculture with other technological options, detailed understanding of the hydrological response of the basin and the impact to changes in land cover and climate on hydrological responses is crucial. Hence, spatially and temporally detailed assessment of the hydrologic processes is vital for watershed management to cope with the pressing water problems due to burgeoning population growth, a growing demand for water, irrigation for food production and possible climate change.

The analysis of the long-term hydrological and meteorological data reveals that the climate in the Geba River Basin is changing slower than the global average. Though no definite trends can be found in the annual precipitation records using Mann-Kendell methods, clear decreasing trends can be seen in the annual number of rainy days during the study period of 1961–2003. Climate change scenarios were obtained from general circulation models (GCMs) for the years 2030, 2050 and 2080. The Intergovernmental Panel on Climate Change (IPCC) Special Report on Emission Scenarios (SRES) scenarios A2 and B2 for rainfall and temperature from GCMs (HADCM3 and CGCM3) model are used. From the classified Landsat satellite images past changes are analyzed. Using these change detection analysis and Ethiopian Climate-Resilient Green Economy (CRGE) strategies on agricultural development, three future lands cover scenarios are developed for the year 2030.

An intensive field campaign has been undertaken in 2010/11 and 2011/12 for a total of six months to collect relevant data for the model. Based on the collected primary and secondary data, the Soil and Water Assessment Tool (SWAT2009) model was used to investigate the impact of land cover and climatic change on stream flow. The model is set up using readily available spatial and temporal data, and calibrated against measured monthly and daily discharge. It is done by superimposing the climate, soil and land cover data and evaluated in different time periods and scenarios to investigate the impact it had in hydrological response.

To familiarize with the watershed, six exemplary test sites in the order of 2–20 km^2 area were selected and detail soil mapping, geomorophological mapping and soil logging were performed. Moreover, more than 112 soil samples and 120 ground truth points were collected for soil texture classification and land cover classification. Soil texture and hydraulic conductivity were analyzed in the geotechnical laboratory of Mekelle University. Stream flow data at the outlet of the Geba watershed near Mekelle is utilized to analyze stream flow variability due to changes in land use and land cover and climate.

The model performances are evaluated through a modeling protocol i. e. sensitivity, calibration, validation and uncertainty analysis. The model performance is with acceptable range of Nash-Sutcliffe coefficient and coefficient of determination. It is well bracketing 90% of the observed river discharge and introducing an R^2 of 0.6 and Nash-Sutcliffe (NS) of 0.5 for calibration and R^2 of 0.77 and NS of 0.86 for validation. Surface runoff, interflow, base flow, ground water recharge and seasonal and annual evapotransipration are the main outputs of the model. Accordingly, about 61% of the precipitation in the basin is lost through evapotransipration, 18% becomes surface runoff, and 8% is recharging the deep aquifer.

The scenario analysis results show the implication of reduced water availability and impacts on agricultural production. Thus, to mitigate possible shortage of stream flow which has been a major problem for the Mekelle City water supply and irrigation in the watershed, it is needed to implement Ethiopian Green Economy Climate-Resilience strategies to reverse trends in deforestation and land degradation. In addition, water harvesting techniques during excess flow could alleviate water shortage that may be experienced with a changing climate. Eventually, the scenario analyses results guides how to allocate available water resources among competing users to avoid a substantial negative impact on the socioeconomic condition of the area.

Acknowledgements

First and above all, I praise the almighty God, for providing me this opportunity and granting me the capability to proceed successfully. Next, the funding for this study, the Engineering Capacity Building Program of Ethiopia (ECBP) and Mekelle University are deeply acknowledged.

I thank my supervisor Prof. Dr. B. Schütt for her great support, invaluable and constructive advice, and guidance to make this PhD study come to fruition. I very much appreciate her encouragement, follow up, and understanding for my study. Dear Prof. Schuett, what I learned working with you would unquestionably continue to influence my research career and thinking in years to come.

I also thank Jun.-Prof. Dr. Wiebke Bebermeier for her regular advice in the working group discussion and reviewing my thesis.

I wish to express my sincere thanks to Dr. Jan Krause for the encouragements and many useful contributions in my study both in the field work, office work and day to day life in Berlin.

I also thank all staff and PhD students at physical geography (Freie Universität Berlin) for their regular advice and provided an excellent working environment. Special thanks to Fabian Becker for editing my thesis day and night and improve the quality of the thesis.

I would like to forward my heartfelt thanks to my counterpart advisor Dr.-Ing. Joachim Lengrich and all my colleagues Mr. Daniel Asefa, Mr. G/tensay Teklu, Mr. Eskinder Giday, Mr. G/mariam G/selassie, Dr. Abdulwassie Hussien, Dr. Messay Daniel, Mr.Yisehak G/egzabher, Mr. Befekadu Getachew, Dr. Asmelash Abay, Dr. Hadush Goitom and others not mentioned, for their assistance, guidance and realization of this work. The brevity of this acknowledgement does not in any way downplay the support I have received from anyone mentioned, or not mentioned, herein.

I thank Ethiopian Institute of Technology - Mekelle and the Department of Civil Engineering for allowing me to use the resources and facilities during my field work.

I would also like to thank the DAAD and Mrs. Ada Osinski for facilitating all the necessary administrative matters and takes care of matters pertaining to visa and monthly stipend.

Mr. Negusie W/Georgis and Mr. Alula Araya thanks to your willings to take care of matters pertaining to Mekelle University. Special thanks to Mr. Bizuneh Asfaw for the great time we had together in Berlin and sharing a common office at Freie Universität Berlin.

I thank my entire family for always being there for me knowing that they always held me in their thoughts and prayers gave me strength to go on. Every family member is so dear to me. Special thanks to my brother Eshetu Adugna for his help and patience, for every period I was away.

Most importantly, I would like to forward the leading and loving thanks to my helpful wife Mrs. *Helen Debebe Mekonon* for her never ending concern, support and encouragement. None of this would have been possible without her strong believe. Her patience during my long absence from home and take caring

our childrens was quite incredible. *Heli*, without your love and patience this achievement would have not been possible. The success belongs to both of us. Special thanks go to my lovely kids, *Yisehak, Solyana* and *Eureka*. They are always the source of my strength, happiness and permanent inspirations. Love you.

Abraha Adugna Ashenafi

Oct, 2013. Berlin, Germany.

Table of Contents:

List of figures

List of tables

1 Introduction

Land cover and climate change associated with increased emissions of greenhouse gases (GHGs) due to natural and anthropogenic effects are of great concern. Its impacts on hydrological systems threaten the availability, supply and sustainability of water resources. One of the main aims of this study is to quantify and identify the scale and impact of land cover and climate change on the watershed hydrological responses. It is important to understand the hydrology of the watershed particularly the physical processes occurring and the controlling factors within the watersheds. Studying the hydrological processes reacting to changes in land cover, climate variability and potential future climatic changes, give valuable insights how the river flow will respond to these changes. River flow is known to be an integrated indicator of the entire watershed processes. Besides, the projection of watershed hydrology based on different climate change scenarios and land cover dynamics are used to prioritize options for water resources planning and management for future watershed management.

The study was conducted for the Geba basin, Northern Ethiopia, which is highly prone to changes imposing impact on hydrological processes. Excessive land degradation due to increasing population density within the watershed have created environmental changes, economical and social effects, all resulting in degradation of raw water in the basin. Hence, understanding the impact of climatic and land cover change enhances the water users and mangers to allocate and use the available water resources in supporting the dominant agriculture based economic and social developments. It is also used to implement techniques that control water yields, including rainfall, temperature and stream flows and, finally, to optimize the resources.

The semi-distributed Soil Water Assessment Tool (SWAT) is a hydrologic simulation model coupled with ArcGIS9.3 (ArcSWAT2009.97 release version 488) and is applied in the study. Using this tool hydrological response is critically evaluated, calibrated and validated. It provides a watershed scale model that enables to conduct impact studies. This calibrated and validated model is used for watershed mangers and decision makers to plan, allocate and optimize the scarce water resources in a watershed.

1.1 Background

Ethiopia is a country highly affected by desertification and droughts (UNCCD, 1999). The situation is aggravated by a number of other problems such as over-cropping of marginally productive land, poor water use and water management, and deforestation. These human and natural factors cause devastating effects on the socio-economic activities, ecological systems and general development of the region (Bai et al., 2008, cited in Abraha, 2009).

The environmental instabilities due to natural and anthropogenic effects have potential treats on the water resource management and development as weather and land cover influences the water balance (Githui, 2009). Based on current water use efficiencies, global weather phenomena, and poor watershed management techniques, it can easily be predicted that water demand will rise in the near future unless water management and development techniques are implemented.

The rapid population growth has caused an increasing pressure on land and water resources in almost all regions of the world. This increased demand and pressure makes water resources becoming a scarce natural resource (Yazew, 2005). Furthermore, variability in stream flow produced by complex interactions of land use, land management, and climate, combined with competing and increased demand, make management of water resources at watershed scales extremely challenging (Mengistu, 2009; Setegne, 2010). This all forced that managing water resources is a must to fully understand its importance for the social and economic development in an integrated way.

Globally, an unbalanced water potential occurs. In some parts of the world, there will be more available water but in other parts less. It results a conflict in water use and demand (Global Water Partners, 2012). Improved water resources management tools and a thorough understanding of the interaction of water with land and climate are required to solve the increased water resources problem. The tools have to involve, amongst others, an integrated description of the land phase of the hydrological cycle, an integrated description of water quantity, quality and ecology, and an integration of hydrological, ecological and economical information designed for decision makers at different levels (Abbot and Refsgaard, 1996).

The potential effects of land cover changes and global climate changes on water resource have been of great concern in the past few decades (Githui, 2009). However, techniques for the analysis of the impact of land cover change and climate change on hydrological responses are still very much at an early stage. The prediction of the effect of future changes has hardly even started (Beven, 2001). At present, watershed management models are fundamental to water resources assessment, development, and management (Singh, 1995). They are, for example, used to analyze the quantity and quality of stream flow, reservoir system operations, groundwater development and protection, surface water and groundwater conjunctive use, water distribution systems, water use, and a range of water resources management activities (Singh and Woolhiser, 2002).

The relationship between land and water is of global interest. In many developing countries, changes in land use are rapidly taking place and the largest change in terms of land area, and perhaps also in terms of water resource impact, is arising from deforestation activities (Githui, 2009). The dynamic nature of land use emanating from increasing population and infrastructural development is of paramount stage in northern Ethiopia and needs primary concern. Expansion and intensification of agriculture, growth of urban areas, and extraction of timber and other natural resources will likely accelerate over the coming decades to satisfy demands of increasing population (Mengistu, 2009; Githui, 2009). Since the 1970s, there has been a growing awareness that natural resources are limited and that future development must come to terms with this fact (WMO, 2009).

The Ethiopian government's water resources policy Minstry of Water Resource (MoWR, 2008) is focused on enhancing and promoting all national efforts towards the efficient, equitable and optimum utilization of the available water resources of the country for significant socioeconomic development on a sustainable basis. The policy emphasises on allocation and apportionment of water based on comprehensive and integrated plans and optimum allocation principles that incorporate efficiency of use, equity of access, and sustainability of the resource (MoWR, 2008).

1.2 Objectives

Following the country's water resource policy and water stress in Geba river basin (northern Ethiopia) due to high population growth and environmental instabilities, there is still need to undertake comprehensive study. The study needs to examine the mechanisms associated with physical and dynamical processes influencing the hydrology of the Geba River basin, especially under a changing land cover and climate. Consequently, the central theme of this research aims

to quantify and identify the degreeof impact of land use, land cover and climate change on the hydrological processesin the northern Ethiopia Geba Basin. Based on this remedial measures will be suggested.

The specific objectives are:

- Understanding of the anthropogenic effect on hydrology, water balance and stream flow variability in the Geba basin and determination of the past changes in the environment.
- Modeling the hydrological processes/dynamics to assess the impacts of environmental change (land cover and climate).
- Assessment of the past impacts of environmental change on the water balance components: climate (between 1961 and 2003), and land cover (between 1972 to 1986 and 1986 to 2003). Integrating this information into the hydrological model will give valuable information on the sensitivity of the Geba basin to changes in land cover and climate.
- The projection of the watershed hydrology based on different climate change scenarios and land cover dynamics: This includes generating land cover change scenarios for the years 2011–2040, 2041–2070 and 2071–2100.

2 State of the Art

2.1 Water resources management

Water resource management is the activity of planning, developing, and managing the optimum use of water (WSSD, 2002). In an ideal world, water resource management is regarded to all the competing demands for water and seeks to allocate water on an equitable basis to satisfy all uses and demands. This is rarely possible in practice. Water resource management controls water resources systems that are combinations of constructed water control facilities and natural or environmental elements that work together to achieve water management (Grigg, 2005).

A constructed water resources system, consisting of structural facilities, provides control of water flow and quality. Examples include conveyance systems, diversion structures, dams and storage facilities, etc. Whereas, natural water resource systems comprise sets of environmental or hydrologic elements in nature that include the atmosphere, watersheds, stream channels, wetlands, floodplains, aquifers and groundwater systems (Grigg, 2005). Water resource management is, therefore, a controlling system of this phenomenon and understanding the processes within the system.

2.1.1 Water resource management in Ethiopia

Ethiopia is a country with a broad range of geomorphic provinces; a high and rugged mountainous core cut by deep gorges and incised river valleys, fault bound plateaus and basins, a prominent rift valley that hosts a number of lakes (Ferriz and Gebeyehu, 2002; Yosuf, 2007). The total surface water is estimated about 123 billion meter cube and ground water resource about 2.6 billion meter cube (MoWR, 2008; Table 2-1). According to FAO (2005; cited in Abdurahman, 2010) survey base year 2002, Ethiopia withdraws 5.5 billion m^3/year, which is about 5% of the total surface flow, while the difference is lost as runoff to the neighboring countries. From the 5% withdrawal, 6% are used by the domestic sector, 0.34% by the industry and 93.6% are allocated for agriculture, especially to irrigate (Awulachew et al., 2005).

Ethiopia receives a significant amount of rainfall in the highlands. At a broader scale, the abundant rainfall feeds the groundwater system and streams that go from small seasonal rivulets to the mighty Blue Nile. However, most of this water evaporates, runs away as stream flow, or is stored in aquifers which are difficult to use by simple technologies (NEDECO, 1997a; Ferriz and Gebeyehu, 2002).

The country's water resource management is mainly focused on the surface water potential for irrigation and hydropower developments with little attention to the groundwater potential. Most of the accessible groundwater resources are used for domestic and industrial water supply. Nowadays, to utilize ground water potential for irrigation, studies are undertaken in different parts of the country like Ada Bucho in the Oromiya region and Alaydege in the Afar region, Kobo-Girana in the Amhara region and Raya-Azobo in the Tigray Region (http://www.mowr.gov.et).

In Ethiopia, accessible groundwater is still limited. The Precambrian metamorphic complexes are notoriously problematic as aquifers. Fractured rock aquifers locally exist, but in their shallow reaches provide only modest amounts of ground water, often barely sufficient to satisfy the drinking needs of small settlements (Yosuf, 2007). Deeper aquifers might have higher yields, but exploration and deep drilling will be expensive and time consuming (Ferriz and Gebeyehu, 2002).

Table 2-1: Surface water resource potential of Ethiopia (modified after MoWR, 2001).

No.	River basin	Area (km^2)	Volume ($10^9 * m^3 * year^{-1}$)	% of the volume of water
1	Abbay (Blue Nile)	210,846	54.84	44.1
2	Awash	112,696	4.60	3.7
3	Aysha	2,223	0	0
4	Baro-Akobo	75,912	23.24	18.9
5	Denakil	62,882	0.86	0.7
6	Genale-Dawa	171,042	5.88	4.8
7	Mereb	5,900	0.65	0.6
8	Rift-Valley	52,739	5.63	4.6
9	Ogaden	72,121	0	0
10	Omo-Gile	79,000	16.60	13.5
11	Tekeze (Atbara)	90,001	8.20	6.7
12	Wabi-shebele	202,697	3.16	2.6
		Total	123.66	100

Some of the strategies to develop water resource in Ethiopia are rainfall harvesting by constructing small reservoirs, use of surface water by diverting rivers and tapping the ground water potential (MoWR, 2001).The country pursues the development of medium and large-scale irrigation schemes while the development of small-scale irrigation schemes is continued under regional water, mines and energy bureaus (MoWR, 2008).

Ethiopia covers a total area of about 1.13 million km^2, with estimated arable land resources of 55 million hectares, or approximately 50% of its land mass (MoWR, 2008). The importance of introducing irrigated agriculture in to the economy is based on the fact that rain-fed agriculture is not capable to feed the increasing population (Abdurahman, 2009).

2.1.2 Regional water management

Tekeze River is perennial with a minimum flow of 2 m^3/s (NEDECO, 1996). The Geba watershed, which this study focuses on, contributes 17% to the runoff of Tekeze and is one of the major focus areas vital for sustainable economic and social development of the region. In the head water area of the Tekeze basin only the major sources are perennial. The minimum dry season discharge of those streams ranges between 0.5 to 70 l/s (Leul, 1994). The mean annual rainfall of Tekeze basin is spatially and temporally highly variable.In the northeastern part, directly adjoining the rift valley, mean average rainfall averages 300–700 mm, wheras in the southwestern part more than 1200 mm average rainfall is observed. The yearly sum of the rainfall is allover sufficient for crop production. However, the high

variability of rainfall in time and space (20% to 40%) impacts the environmental instability in the area and consequently affects the socio economic of the peoples (Leul, 1994).

At present a long term policy and strategy for the development and management of the region's water resources is developed. The Geba river basin is one of the development corridors to supply water for Mekelle city and to irrigate agricultural land within the basin. A commonly used strategy to irrigate the land is by building a low embankment dam, a diversion weir to raise the water level by division channels to feed the land. In addition to this, the regional government is working on small scale techniques constructing small hand dug ponds by the local farmers and medium scale irrigation projects constructed by the regional government to reserve water for supplementary irrigation during short period erratic of rainfalls and to irrigate more lands in dry periods. The local farmers are advised to have a hand dug ponds within their farms to store water and irrigate or supply water for domestic purposes.

The regional ground water management experiences focus mainly on extracting water through wells for domestic water supply purposes (Ferriz and Gebeyehu, 2002; Gebreyohannes, 2009). Where the water table is not very deep (< 10 m), large-diameter hand-dug wells are used. Very recently, the ground water sources are used on irrigation farms owned by small scale farmers. The water resource management practice in the country shows that there is a need of introducing integrated watershed management approaches to sustain the development.

2.2 Hydrological processes in a watershed

Investigations to understand the hydrological process are all about seeking answers to basic questions such as (McDonnell, 2003):

i. Where does water go when it rains?
ii. What flow path does it take to the stream?
iii. How long does it reside in the catchment?

These questions were articulated by John Hewlett within the context of his variable source area concept almost forty years ago (McDonnell, 2003). Attempts have been made to answer these and related questions by theoretical analysis and actual field measurement data. Still these questions are fundamental for hydrological process studies. Knowledge of the rainfall- runoff mechanisms and its factors that have directly or indirect effects is crucial to understand the hydrological processes.

The underlying fundamentals of the hydrological processes have been investigated for many decades. However, research is still ongoing and increasingly focuses on hydrological models used to simulate environmental changes in watershed responses, investigating impact of internal and external factors on landscape and hydrological processes. In recent years, an increasing number of studies have referred to the concept of land cover and climate change impacts to explain watershed hydrological responses. This process requires improved water resources management tools i.e. watershed modeling techniques based on sound scientific principles (Abbot and Refsgaard, 1996).

Watershed modeling techniques are useful tools to investigate interactions among the various components of a watershed as they are basic units of the landscape (Silberstein, 2006; Refsgaard, 2007). It is a geographical unit in which the hydrological cycle and its components should be analyzed (Singh, 1995). In watershed studiesthe topographic boundary of a watershed usually coincides with the hydrologic boundary causing that any precipitation falling on the watershed is routed to a stream from where it is transported out of the watershed. The stream flow at the outlet of a watershed is an integrated result of all meteorological and hydrologic processes in the watershed.

In any landscape a number of discrete processes occur to generate runoff from a watershed as an output which is a function of dominant environmental factors (Freese et al., 2010). Studies over the preceding decades have focused on how these dominant environmental factors are related to each other and how the hydrological/landscape connectivity of different landscape within the catchment generate runoff.

Hill slopes, hill foots (riparian) and streams are connected to generate runoff. How they are connected to generate runoff is the main issue. Hill slopes can be used to characterize different environmental sequences such as geology, landform, soils, land use and topography, to determine dominant response patterns resulting from different hill slope catenas (McGuire et al., 2005; Van Tol et al., 2010). The hill slope acts as an organizing principle which complements the hydrological cycle and conservation of mass.

2.3 Runoff generation processes

Surface runoff, is generated mainly in three ways:

- Infiltration overland flow, known as Horton principles (infiltration excess theory)
- Partial area infiltration excess
- Saturation excess which is a variable source area theory (non-Hortonian theory)

Research on the Blue Nile watershed shows that the temporal runoff dynamics are poorly captured by the infiltration excess theory (Liu et al., 2008; White, 2009; Awulachew et al., 2010). Runoff response patterns were investigated by plotting the biweekly sums of discharge as a function of effective rainfall comparatively during the rainy season and dry season. It is pointed out that, with progressing wet season the runoff coefficient increases (Liu et al., 2008). As rainfall continues to accumulate during a rainy season, each watershed eventually reaches a threshold point where runoff response can be predicted by a linear relationship with effective precipitation. This indicates that the proportion of the rainfall that becomes runoff is constant during the remaining rainy season, documenting that the saturation excess dominates runoff generation in the basin (Liu et al., 2008; Awulachew et al., 2008).

Similarly, Bryant et al. (2006) address factors that affect hydrologic modeling in different spatial scales through a combined knowledge of the system structure. It is documented that the volume of rain required to generate runoff varies as a function of storm size, rainfall intensity and rainfall duration (Bryant et al., 2006). This indicates that saturation excess dominates runoff generation processes.

On the other hand Tulu (2010), Smith and Goodrich (2005) and Bull and Kirkby (2002) articulate that in semi-arid regions runoff generation is dominated by Hortonian overland flow. Depending on the watershed properties and the high variability of runoff generation mechanisms with space, the runoff generation is dominated by infiltration excess mechanisms. Tulu (2010) conducted research in the Illala basin, tributary to the Geba basin, and indicates that the dominant runoff mechanism of runoff generation is infiltration excess.

Smith and Goodrich (2005) point out that the infiltration and saturation excess generating mechanisms are not mutually exclusive on a watershed, nor even mutually exclusive at a point on a watershed. The rainfall rate may exceed the infiltration rate for some storms, and for others the rain may come slowly until the surface soil layer is saturated (Bauer, 1974; Linsely et al., 1982; Dingman, 2002; Walter et al., 2003). Climate and landscape character will determine which mechanism is dominant at a given location and time (Smith and Goodrich, 2005).

To evaluate the runoff generation mechanism and to understand the hydrological processes, it is required to study the interactions of climate with hydrology. Hydro-climatic studies focus on the interactions between precipitation, evapotranspiration, soil moisture storage, ground water recharge, and stream flow (Tulu, 2010).

Different studies using rainfall-runoff simulations have been conducted to describe the factors, influencing the rate of overland flow generation (Renard and Keppel, 1967; Finlayson and McMahon 1988; Pilgram et al., 1988; Nyssen et al., 2005; Abraha, 2009; Tulu, 2010) and impacts of climate change on these processes (Mengistu, 2009; Setgne, 2009). Still it is needed to study the response of the hydrologic cycle to climate change on different timescales and their linkage to large-scale features of the general atmospheric circulation.

In arid and semi-arid regions, water resources are limited, and under severe and increasing pressure due to expanding populations, increasing per capita water use and irrigation (Wheater et al., 2008). Acute water scarcity due to less rainfall, seasonal inter-annual irregularities and high evapotranspiration leads to poor productivity of agricultural land. Changes in regional hydro-climatology highly affect these regions due to their high rainfall variability (Wheater et al., 2008).

2.4 Land cover and climate change

2.4.1 Land use and land cover change

For different parts of Ethiopia, land cover changes were studied from small scale to large scale, e.g. Abate, 1994 (west Ethiopia); Zeleke and Hurni, 2001 (north-western Ethiopia); Hadgu, 2008; Bewket and Sterk, 2005; Bewket, 2003; Belay, 2002 (north Ethiopia); Kassa, 2003 (north-eastern Ethiopia); Mekuria, 2005 (south-western Ethiopia) and Mengistu, 2009 (southern Ethiopia). All these studies show that agricultural land has expanded at the expense of natural vegetation, including forests, grazing land and shrub lands. In many parts of the highlands of Ethiopia, agriculture has gradually expanded from gently sloping land into the steeper slopes of the neighboring mountains (Mengistu, 2009). On the other hand Bewket and Sterk (2005) point to an increase of woodland area in recent years due to afforestation efforts in the Blue Nile basin.

Impacts of land use and cover changes on surface hydrology, surface energy balance and surface roughness are not straightforward but rather complex to warrant any generalization as it is dependent on the scale of the watershed, seasons, climate, and soil conditions (Lambin et al., 2003). The knowledge about the impact of land use and land cover changes on weather and climate is still limited, especially on the scales that are most relevant for local actors, such as farmers. Subsequently, many insights into consequences of land use and land cover change on hydrology and surface energy balances have been elucidated at small spatial, observable scales (Kiersch, 2001; DeFries and Eshleman, 2004; Lambin et al., 2006).

The impact of population growth on the environment is not one directional (Bewket, 2003). Basically, the complex relationship between human development and the environment is what causes land degradation, in which the use and management of the natural resources is a central issue. In view of the above mentioned research problems, this research seeks to investigate the problem of scale and temporal variability of land cover changes in the Geba river basin.

2.4.2 Future climate change

Climate has been changing ever since. Changes refer to the variability of the long term trends in the state of the climate or average changes in temperature and rainfall that persist for extended period (Intergovernmental Panel for Climate Change, IPCC, 2007). However, the United Nations Framework Convention on Climate Change (UNFCCC, 2006) defines climate change as “a change of climate which is attributed directly or indirectly to human activity that alters the composition of the global atmosphere and which is in addition to natural climate variability observed over comparable time periods“. The factors that determine the climate at a location are rainfall, sunshine, wind, humidity and temperature. Climate change may result from extra-terrestrial influences such as changes in the Earth's orbit, Earth’s tilt, or might result from human impact such as burning fossil fuels, greenhouse effect, deforestation, urbanization, desertification, volcanic eruption, flood, forest fire, storms, etc. In consequence, the observed changes in climate could be both natural and human induced. The natural one could be due to the flow of energy into and out of the earth-atmosphere system that affects the energy budgeted within the earth-ocean atmosphere system (Boukhris, 2008).

Recent analysis from the inter-governmental panel for climate change indicates that the earth as a whole has warmed by about 0.6°C ± 0.2°C over the past century with locally and seasonally varying amounts (IPCC, 2007). The non-uniformity warming system alters the temperature gradients and changes the regional pattern of winds and precipitation distribution. The changes in pattern and intensity of precipitation, melting of ice, increasing atmospheric water vapor and others has a significant natural variability on inter annual to decadal that masking the long term trend (Bates et al., 2008).

Among the different assessments that are carried out by the IPCC, the one published in 2008 states the projected global surface warming by 2100 using the Special Report for Emission Scenarios (SRES) scenarios as input. Estimated global temperature to increases for 2090–2099 (relative to 1980–1999) ranges from 1.8°C (best estimate, likely range 1.1°C to 2.9°C) for scenario B1, to 4.0°C (best estimate, likely range 2.4°C to 6.4°C) for scenario A1FI.

There is also an increased concern on climate change that alters the hydrologic cycles and changes in water availability and the hydrological responses of the watershed. Increased evaporation, combined with changes in precipitation characteristics, has the potential to affect runoff, frequency and intensity of floods and droughts, soil moisture, and water supply. Moreover, runoff production is influenced by several factors such as the condition of the soil surface and its vegetative cover (Laurence, 1998; Zhang et al., 2001; Brown et al., 2005), the soil texture and the antecedent soil moisture content, land use practice and spatial patterns of interactions (Richey et al., 1989; Schulze, 2000; Huang and Zhang, 2004; Setegn, 2010).

Since hydrologic conditions vary regionally and locally, the influence of climate change on local hydrological processes will likely differ between localities, even under the same climate scenarios. Important regional water resource vulnerabilities to changes in both temperature and precipitation patterns are documented (Lahmer et al., 2001). It is primarily at the regional and local scales that policy and technical measures could be taken to avoid or reduce the negative effects of climate change on the natural environment and the society.

2.3.2.1 Climate Models

Warming of climate system and change in its state variables are highly related to the atmosphere-land-ocean system. The climate modeling science integrates these complex systems with the Global Circulation Models (GCMs) to simulate future climate changes and forecast it for to decades and centuries. Climate change scenarios developed from General Circulation Models (GCMs) are the initial source of information for estimating plausible future climate changes. Most GCMs have a horizontal resolution of between 250 and 600 km, and 10 to 20 vertical layers (Bates et al., 2008). The spatial resolution of GCMs is too coarse to resolve regional scale effects. Therefore downscaling is required.

Downscaling of future climate from coarse resolution GCMs to regional scale to assess future impacts on environment, society and economy requires a baseline data corresponding to present day observed climate data. The world meteorological organization (WMO, 2009) recommends a 30 year normal period as a baseline just to cope weather varablity and superseded by a new 30 year period 1971/2000 as a new normal period for downscaling (Bates et al., 2008). Correspondingly, a 30 year normal period is required to compare the downscaled climate data with the observed ones (WMO, 1990). This will help to build confidence in future downscaling. Above, the data are used for calibration and testing GCMs.

2.5 Hydrologic modeling

The detailed processes that link the rainfall over the catchment with the stream flow may be studied by applying physical laws. However, the complexity of the boundary conditions (i.e. the physical description of the catchment and the initial conditions and distribution of the variables) makes a solution based on the direct application of the laws of physics impracticable (Fekadu, 1999). Moreover, direct application of these laws requires subdividing the catchment into homogenous and isotropic regions. The subdivision depends on catchment characteristics (soil type, land use, slope, vegetation

cover, etc.) which may also vary in space and time. For these reasons, instead of exact representation of the processes effort is directed to the construction of a hydrological model (Fekadu, 1999).

Hydrological modeling involves the application of mathematical expressions that define quantitative relationships between inputs (e.g. flow-forming factors) and outputs (e.g. flow characteristics). It is related to the spatial processes of the hydrologic cycle and is often used to estimate basin water resources as well as for impact assessment (Githui, 2009).

Many hydrologic models have been developed in the past and more will be developed. Nowadays, different models are used to determine the performance of watersheds under inevitable land use changes, climate change, and effects of increased climate variability on hydrological process with minor modification and direct application (Bormann and Diekkrüger, 2003; Giertz and Diekkrüger, 2003; Legesse et al., 2003; Githui, 2009; Mengistu, 2009). This is done by establishing baseline data of climate, land cover and stream flow, and then used to compare the effect on stream flow due to changes in precipitation, temperature, land cover and other climate variables.

2.5.1 Hydrological model classification

Hydrological models can reduce highly complex processes in the watershed to simple outputs. Since these hydrological models are developed for mulit-purposes, they require a large quantity of data. This fact forces to classify the hydrology models based on the data requirement and the purpose of the model. Singh (1995) classified hydrologic models based on the process description, the time and space scale, needed technique to get solution and model use.

In general, models are classified as (Refsgaard, 1996):

- Physically based models
- Black-box or Data driven models
- System models or cybernetics

Based on the hydrological process description, hydrological models can be either lumped (conceptual) or spatially distributed. In a conceptual model the internal descriptions of the various sub processes are modeled attempting to represent. It is partitioned into components that are routed through the sub processes either to the catchments outlet as stream flow or to the surface and deep storages or to the atmosphere as evapotranspiration (Price, 2001). Conceptual approaches were recognized to be able to improve the description of the hydrological response of a basin (Refsgaard, 1996). The lumped models are especially well suited for the simulation of the rainfall-runoff process when hydrological time series exist that are sufficiently long for a model calibration (Refsgaard, 1996).

Contrary to lumped models, a distributed physical-based model does not consider the water flows in an area to take place between a few storage units**.** Instead, the flows of water and energy are directly calculated from the governing continuum equation and partial differential equations. Today, several general-purpose catchment models of this type exist, including the soil and water assessment tool (SWAT) which combines the lumped and distributed model called semi-distributed model (Arnold and Allan, 1996).

Data driven models require extract information from data and define the relation-ship between system state variables (input, internal, and output variables) with out understanding the physical situations (Jembere, 2004).

Hydrological models are also classified as event based or continuous models. The hydrological cycle in nature is a sequence of dry and wet periods. In semi-arid areas the rainfall is dominated by convective rainfall and results in flash floods (Tulu, 2010). To forecast runoff or model the flood, event based models are appropriate since they are simulating individual peaks. On the other hand to study impacts and to quantify average water balance in the watershed, an extended simulation is needed to get long period average output of the drainage basin. Usually for long average runoff conditions modeling the continuous model is an appropriate option. One such model is the soil and water assessment tool (SWAT) which allows studying the impact of land management and climate on the hydrological responses in an extended period (Arnold and Allen, 1996).

2.5.2 The Soil and Water Assessment Tool (SWAT)

The Soil and Water Assessment Tool (SWAT) was developed at United States Department of Agriculture – Agricultural Research Service in a modeling experience that span roughly 30 years (Arnold et al., 1998). The model is a semi-distributed, physically based simulation model and can predict the impact of land use change on hydrological regimes in watersheds with varying topography, climate and soils, land use and management over long periods and serves primarily as a strategic planning tool. The model development was an outgrowth of SWRRB (Simulators for water resources in rural basin) model with coupling with United State Agricultural Development research services ARS (Agricultural Research service) (Arnold and Williams, 1987).

A SWAT2009 interface compatible with ArcGIS version 9.3 (ArcSWAT 93. ver 488) has recently been developed. It uses a geo-database approach and a programming structure consistent with a component object model protocol. In SWAT2009 modeling subdivision into sub-basins is made by considering the impact of spatial variation of topography, land use, soil and other watershed characteristics on hydrology (Olivera et al. 2006). There are two-level scales of subdivisions: (1) a sub division based on the drainage area of the tributaries, and (2) based on the threshold level of land use and land cover. Soil and slope are assigned by the user on each sub-watershed, further divided into a number of Hydrologic Response Units (HRUs) (Wu and Xu, 2005). The model uses continuous daily time steps and focuses on land and water interaction in predicting runoff simulation over for long time span.

The SWAT2009 model was built with an attempt to simulate the stream flow processes and the effects of land management on water quality and quantity. The model uses readily available inputs as it is coupled with an ArcGIS environment. This enables the users to study long-term impacts of land cover and climate, land management and nutrient supply on the water resource potential.The major components simulated by SWAT are: hydrology, weather, sedimentation, soil temperature, crop growth, nutrients, pesticides, and agricultural management (Neitsch et al., 2005). Evapotransipration, surface runoff, infiltration, percolation, shallow aquifer and deep aquifer flow, and channel routing are simulated by the hydrologic componenet of the SWAT model (Arnold and Allan, 1996). The hydrological component divides the simulation into four processes: surface flow, subsurface flow, and

interflow, shallow aquifer and deep aquifer, and open channels. Total stream flow is determined by summing the surfaceflow into lateral flow and base flow which are returned to the stream from the shallow aquifer.The deep recharge to the aquifer is considered as a loss from the hydrologic components (Arnold and Allan, 1996).

2.4.3 Application of selected model in watershed study

SWAT hydrological model has been used to predict stream flow; output data performed well to measured data for a variety of watersheds (Saleh et al., 2000; Santhi et al., 2001; Van Liew and Garbrecht, 2003; Govender and Everson, 2005). Intention of the application was to predict various impacts of land management on water quantity (Srinivasan and Arnold 1994; Muttiah and Wurbs, 2002), and to evaluate the impacts of conservation practices on the environment at both, large and small scale basins (Mausbach and Dedrick, 2004), to estimate base flow and groundwater flow (Arnold et al., 2000; Kalin and Hantush, 2006), to predict potential climate change impacts on water resource (Rosenberg et al., 2003; Gosain et al., 2006) and to evaluate effects of land use changes on the annual water balance and temporal runoff dynamics (Fohrer et al., 2005)

Table 2-2: SWAT model applications in Nilotic countries and Ethiopia.

Purpose	Country	Basin	References
Land and water management	Tanzania	Simiyu	Mulungu and Munishi, 2007
Sediment yield	Tanzania	Simiyu and Ndagalu	Ndomba and Birhanu, 2005
Water resource assessment	Tanzania	Weruweru	Birhanu et al., 2006
Land use and climate	Kenya	Nyando and Sondu	Jayakrishan et al., 2005; Sang, 2005
Environmental change in Hydrology	Kenya	Nozoia, Lake Victoria	Githui (2009)
River flow simulation	Ethiopia	Blue Nile	White, 2009; Stegne, 2008
Impact assessment	Ethiopia	Blue Nile	Birhanu et al., 2006; Tekleab, 2011; Stegne et al., 2009a; Setegn, 2010
Watershed responses, land use and land cover and climate	Ethiopia	Lake Abaya-Chamo, Hare	Mengistu and Förch, 2007
Climate Change and water	Ethiopia	Lake Ziway	Zeray et al., 2007
Hydrology and Soil Erosion	Ethiopia	Upper Awash	Chekol, 2006

Most recently, the SWAT hydrological model has been applied to large and small river basins in the Nile basin countries (Table 2-2). Application of the SWAT model on Ethiopian watersheds of small and medium level shows good performance on a monthly data base for most of the studies (Table 2-2). The new water balance SWAT (SWAT-WB) and the original curve number (CN) based SWAT (SWAT-CN), were tested for headwaters of the Ethiopian Blue Nile basin. The objective of the model testing was to check the SWAT model performanceunder dry-subhumid tropical climate (White, 2009).

3 Methodology

3.1 Approach and Methods

3.1.1 Conceptual Frame Work

The conceptual framework showing the components and relationships that have been used as a framework for the analysis in this research is indicated in Figure 3-1.

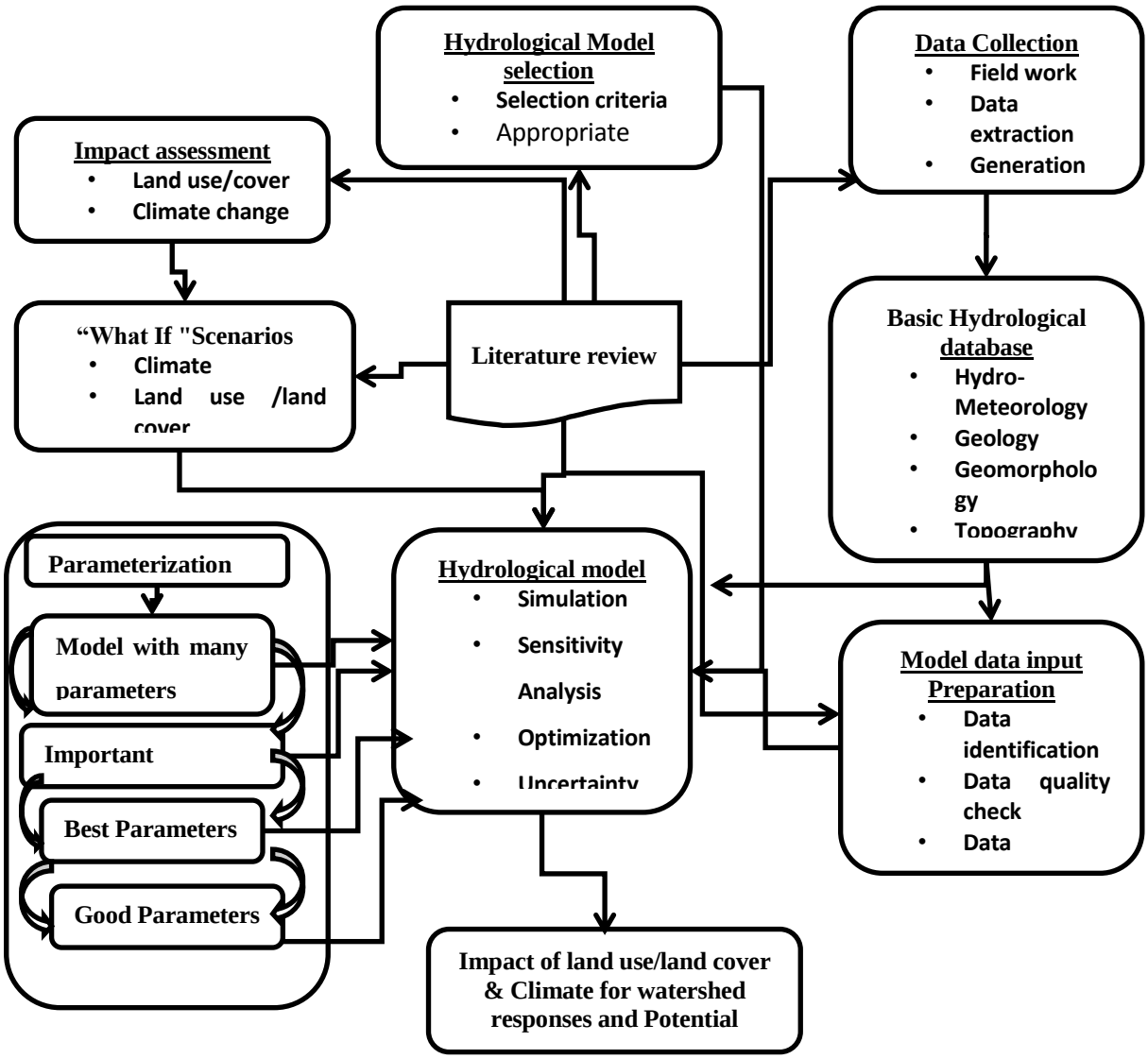

Figure 3-1: General approach for modeling in the Geba basin.

3.1.2 Methods

The workflow in Figure 3-2 is applied in the modeling processes. Subtitles of the chapter brief the mapping, sampling and processing of the input data and archiving results.

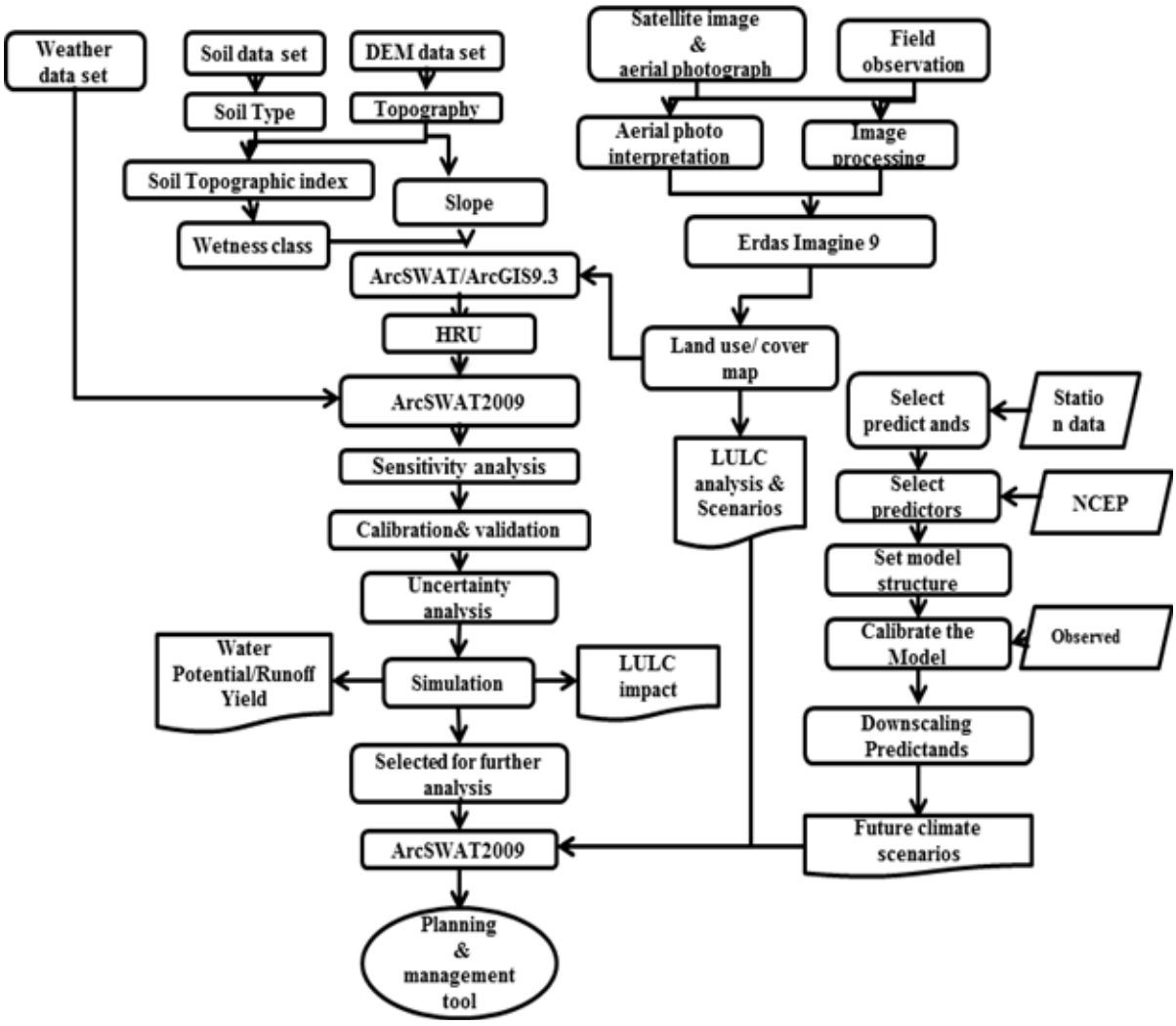

Figure 3-2: General conceptual methodology used for modelling in the Geba basin.

3.2 Mapping and sampling

Field campaigns mainly on sampling and mapping were conducted between April and September 2011 and from March to April 2012. Field work included geomorophological and land cover mapping of selected test sites. Besides, the field work includes GPS-based observations of soils profile, geological sections, geomorophological processes and units. Additionally, soil samples were taken for further laboratory analysis.

3.2.1 Sampling

During the field surveys a total of 112 disturbed and undisturbed soil samples were collected from the top soil layer. The disturbed samples were taken by digging the topsoil after removing the roots of different vegetation on the first 5 cm soils layers. The undisturbed soil samples were taken on different soil types classified by FAO (1998) using a standard 10 cm long by 8.3 cm diameter cylindrical metal core. Then sampling core was inserted into a ring holder, and inverted onto the soil. Until the top of the soil core was about 0.5 cm below the soil surface, the handle of the holder was tapped gently with a mallet. After inserting the handle to the specified depth from surface, the soil around the holder was dug, the soil sample core brought out and excess soil cut off with a soil knife (ASTM, 1998).

3.2.2 Mapping and selection of test sites

The FAO soil map data at a scale 1:1,000,000 (FAO, 1998) and the Ethiopian soil classification map at a scale of 1:1,000,000 provide small scale information on the spatial distribution of soil types. A soil texture map was derived from the soil samples collected during the field surveys after texture analysis (cf. 3.3.1). The map provides the soil textural physical properties needed for modeling, as well as for verifying FAO soil map data.

Large scale geomorophological mapping was conducted for test sites on the basis of visually analized ETM images, terrain data and a geological map (Gebreyohannes et al., 2010). Differentiation of the study site into geomorphologic units considers a combination of geological characters and character of overall relief (Schütt and Thiemann, 2001). The characteristic of the individual formations strongly affect the types of landforms and soils developed on them (Hunting Technical Service, 1976).

- Criteria for identification of these test sites were:
- Size: small watershed (2–10 km^2)
- Representative landscape characteristics of the study site and region
- Different landscape and land use within the test site
- Accessibility

During mapping the landform designation (Table 3-1; after Schütt and Thiemann, 2001) and slope description (Table 3-2; after Schütt and Thiemann, 2001) were used. Slope is the most important criteria in view of its effects on geomorphological-pedeological mapping and the landform refers to the shape of the land surface in the area in which the soil observation is made (Hunting Technical Service, 1976).

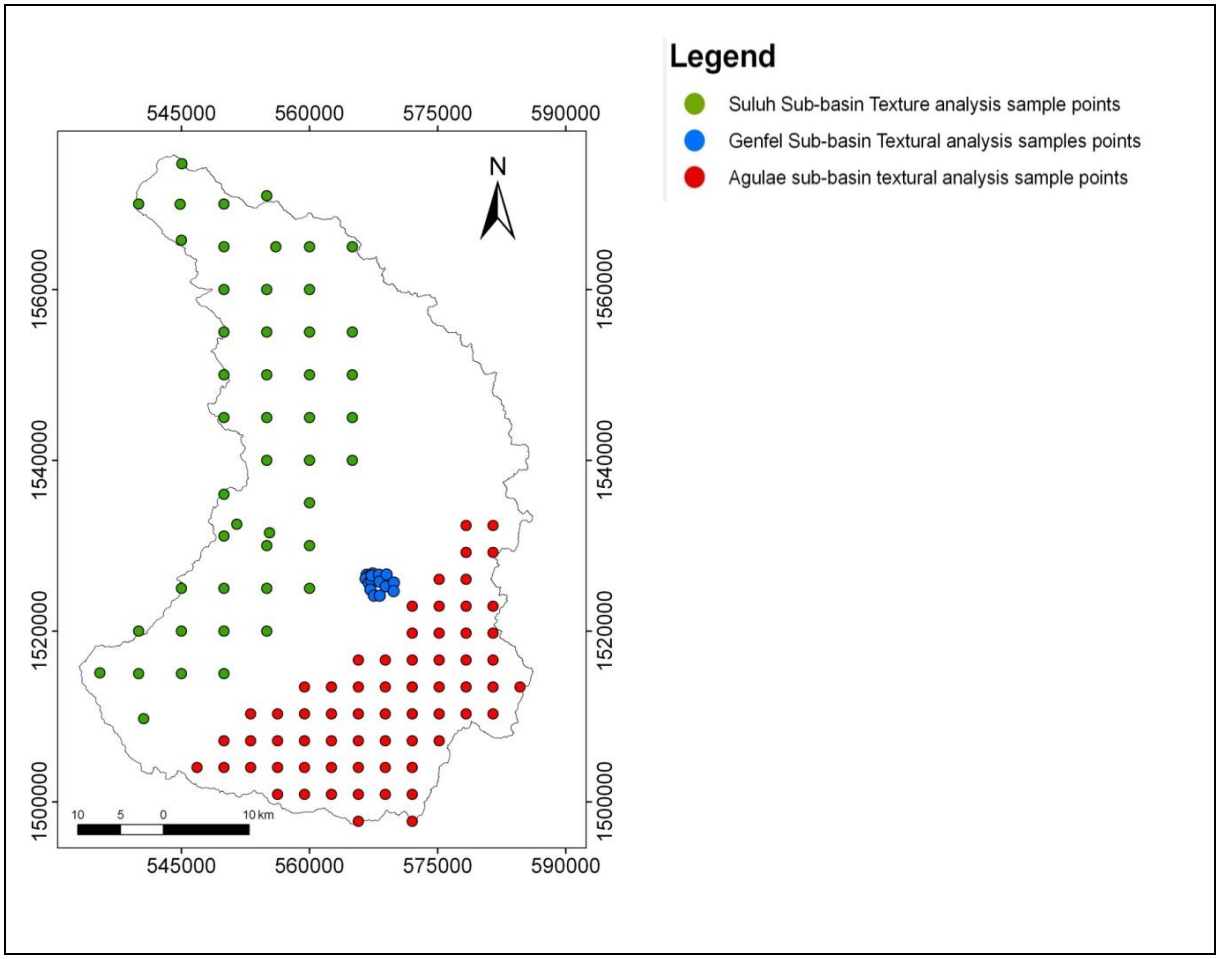

Figure 3-3: Soil sample collected in the Geba basin (Data base: Jarvis et al., 2008 for boundary delination).

Table 3-1: Landform designation (modified after Schütt and Thiemann, 2001).

Description	Mountain	Plateau	Plain	Hill	Escarpment	Valley
Symbol	MO	PT	PL	HI	ES	VA

Table 3-2: Slope description (modified after Schütt and Thiemann, 2001).

Symbol	Slope (%)	Slope (°)	Description	Remarks
F	0–0.9	0–0.5	Flat	
A	0.9–3.5	0.5–2	Almost flat	
G	3.5–8.8	2–5	Gently undulating	
U	8.8–17.6	5–10	Undulating	
R	17.6–26.8	10–15	Rolling	
H	26.8–57.7	15-30	Hilly	
S	>57.7	>30	Steeply dissected	Moderate range of elevation
M	>57.7	>30	Mountainous	Greater range of elevation

The land use and land cover mapping and subsequent change detection analysis were done by classifying Landsat images from 1972, 1986 and 2000. Data were and processed using Erdas Imagine 9.2 and ArcGIS9.3 software. In addition, the Ethiopian Ministry of Agriculture, Woody Mass Project from 2003 provides a land cover map in the scale 1:50,000. This map is used for verification of satellite image based land cover classfication. Based on this map, also field verification for different land cover and land use classes was done. Several field visit and visualization of the specific land cover were made to collect ground truth points for classification and to visualize human impact on land cover changes. More than 120 ground truth points were taken during the two field campaigns.

3.3 Laboratory works

The analysis of the physical soil characteristics is performed based on the procedure of the Geotechnical Laboratory Manual prepared at Mekelle University Department of Civil Engineering. The manual is adapted to the ASTM (originally known as the American Society for Testing and Materials) and the AASHTO (American Association of State Highway and Transportation Officials) standard. The following are the tests modified for the geotechnical laboratory of Mekelle University:

- ASTM D422 / AASHTO T88/ FM1-T88: Particle Size Analysis of Soil
- ASTM D422 / AASHTO T88: Hydrometer Analysis of Soil
- ASTM D1140 / AASHTO T11/ FM1-T88: -200 Sieve Analysis of Soil
- ASTM advanced test FM5-513: Falling Head Permeability test

3.3.1 Grain size analysis

Grain size analysis of the soils is performed based on the Geotechnical Laboratory Manual (2000) with the objective of grouping particles into separate ranges of sizes to determine the relative proportion by weight of each size range. The method employs sieving and sedimentation of a soil/water/dispersant suspension to separate the particles. The Hydrometer analysis was used to obtain information on the distribution of soil particle sizes < 0.075 mm. The data are presented on a semi-log plot of percent finer vs. particle diameters and are combined with the data from a sieve analysis. The principal value of the hydrometer analysis shows the clay fraction. This test is applied when more than 20% of the sample pass through the No. 200 sieve (∅ <0.075mm) and 90% or more passes the No. 4 sieve (∅ <4.75 mm). Using Stokes's law, relations were created between the falling velocity with particle diameter and specficg gravity (Annex-5).

3.3.2 Hydraulic conductivity analysis

Hydraulic conductivity measurements (ks) were made in the laboratory using both, the constant and falling head permeameter methods. The soil sample collected from the field was soaked in water until the soil pores were completely filled with water. The fully saturated soil sample was fitted with a 20 cm height cylinder that acts as a water head to create flow within the sample. The bottom part of the

cylinder was filled with gravels of Ø < 2 cm acting as discharge of water from sample core. In addition, to grant that only water will flow within the core, on the top of the core a fast filtration paper is placed. Then water is gently added into the core maintaining the cylinder height, that acts as the level of water over the saturated core.The decrease in height of water within time is the velocity of the water; together with the crossectional area of the cylinder and the height of the cylinder, hydraulic conductivity is calculated (ASTM, 1998).

3.3.3 Chemical soil analysis

Soil pH and cation exchange capacity (CEC) were determined following the standard procedures as provided by FAO (1970). After preparation of water extracts of the soil samples, the ethylene diamine tetra acetate (EDTA) method was applied to determine calcium (Ca_2^+) and magnesium (Mg_2^+) contents. Sodium (Na^+) and potassium (K^+) were detected by flame protometer at 589 nm and 766 nm wavelengths. After calculating the miliequivalent per 100 g (meq/100 g) for each cation, they were summed up to receive cation exchange capacity (CEC).

In tropical soils, the cation exchange capacity (CEC) of a soil is determined by the clay percentage and the amount of organic carbon (OC) so that:

$$\mathrm{CEC_{soil}} = \mathrm{CEC_{Clay}} + \mathrm{CEC_{OC}} \qquad \text{Equation 3-1}$$

Where CEC_{soi} is the CEC of a soil in cmolc/kg or meq/100g, CEC_{clay} is the portion of CEC soil added by clay and CEC_{OC} is the portion of CEC soil added by OC.

Soil pH measures have been identified as the principal indicator of the chemical characteristic of a particular soil (Sander, 2012). Soil pH was determined from prepared soil suspension with a ratio of one part air dried soil to five part aqua dest using a direct reading pH meter.

3.4 Computer laboratory work

3.4.1 Relief analysis and watershed characterization and delineation

Relief analysis was carried out utilizing the ArcGIS9.3 Spatial analysis tool. The Shuttle Radar Topography Mission (SRTM) data were used as a raw data for the digital elevation model, being processed with the ArcGIS9.3 as follows: Raw data were projected into the UTM coordinate system zone 37 N. Sinks of the Grid-DEM were filled using ArcGIS9.3 spatial analysis tool. The resulting DEM with the cell size of 90 m x 90 m is the basis for the further analysis of flow direction, flow accumulation, slope and aspect, topographic wetness index, relief, hillshade as well as plan curvature, profile curvature and complex curvature.

Topographical maps 1:50,000 from Ethiopian mapping agency were geo-referenced in Erdas Imagine 9.2 and saved as GeoTIFF. These GeoTIFF files were taken as the basis for all digitized information as well as for the geo-referencing (image to image) of individual images, thematic maps or ground data. Additionally they served for the verification of the digital elevation model. For the test sites, elevation

data were generated from the topographical maps digitizing contour lines and transforming them into a raster format with a resolution of 30 m x 30 m cell size. The DEM was used to delineate the topographic characterization of the watersheds and to determine the hydrological parameters of the watershed such as slope, flow accumulation and direction, and stream network.

3.4.2 Data acquisition and preparation

Spatial data were provided by different sources, including analogous maps, digital maps, air photographs and satellite images. Data acquisition and processing included the following steps (modified after Mengistu, 2009):

1. Collecting of land use land cover maps from the Ministry of Agriculture (WBISPP, 2004), collecting panchromatic aerial photos from 1986 and 1994 (scale of 1:50,000) and topographic maps with a scale of 1:50,000 from the Ethiopian Mapping Agency (EMA).
2. Downloading Landsat images from the Global Land Cover Facility (GLCF) website (www.landcover.org) for the years 1972, 1986 and 2000 (Table 3-3). These Landsat images were georeferenced and radiometrically corrected.
3. Identification of ground control points before analysis and interpretation of the aerial photo and satellite images. At each ground control points location, GPS measurements were taken.
4. Geo-referencing of the aerial photos and satellite images using the topographic maps 1:50,000. On this basis the image were remapped and projected to UTM coordinates system.
5. Using aerial photo interpretation and supervised image classification techniques, land use and land cover maps of 1972, 1986 and 2000 were produced and organized for further processing (cf. 3.5.1.3). The satellite images based land use maps were compared with the 2003 land cover map of Ethiopia from the Woody Bio Mass project (WBISPP, 2004).

Table 3-3 Satellite images used for land use and land cover classification (Data were downloaded from www.landcover.org).

Sensor	Band	Date	Pixel Resolution (m)	Path/Row
Multi-Spectral Scanner	1–3 and 4	Feburary 1972	60	181/51
TM multi-spectral	1–5 and 7	January 1986	30	168/50 and 168/51
TM thermal	6		120	169/50 and 169/51
ETM^+ multi-spectral	1–5 and 7	January 2000	30	168/50 and 168/51
ETM^+ thermal	6.1 and 6.2		60	169/50 and 169/51
ETM^+ thermal	8		15	168/50 and 168/51 169/50 and 169/51

3.5 Data pre-processing

3.5.1 Pre-processing of mapping data

3.5.1.1 Geomorphological mapping

A geomorphological base map was prepared for each test site describing the site by landscape units. Transect were designed on the map running from divide to divide. Along the transects sample location were identified referring to the slopes. These maps were georeferenced and processed in ArcGIS9.3 for further analysis.

The landscape units were determined mainly by the differences in geomorphology. These units were subsequently sub divided in to landform units, mainly on the basis of geology and landform characteristics. At the lowest level of classification the landform units were divided into relief units according to topography, steepness of slope and inferred soil characteristics (Hunting Technical Service, 1976). Topographical cross sections were made across the drainage basin applying the ArcGIS9.3 surface analysis tool.

3.5.1.2 Image pre-processing

For land use and land cover classification Landsat image available for 1972, 1986 and 2000 (Table 3-3) included several images for each year to cover the Geba basin. To reduce data amounts for computer processing time images were joined for each band and cropped to smaller size fitting the minimum and maximum Easting and Northing dimensions of the Geba basin. The Land use and land cover classification was based on identifying and delineating training sites using geocoded ground observation points and visual interpreting Google Earth images.

3.5.1.3 Image classification

Image classification was first done by an unsupervised classification using ERDAS Imagine 9.2 by defining signature files and fixing the number of classes. Resulting output layer provides the delineation of land cover classes recoding to the raster of the satellite images. Main classes were grouped to merge classes with a similar value like the center class (following Leica Geosystems Geospatial Imaging manual, 2009). In total six land cover classes were identified, verified by field servey.

After field verification of the unsupervised land cover classification, pixels in a data set were clustered into classes corresponding to the areas of interest (AOIs), training classes which were selected as representative areas. Using parallelepiped supervised classification techniques different classes were identified (following Leica Geosystems Geospatial Imaging manual, 2009).

3.5.1.4 Evaluation of the land cover classification results

Accuracy assessment is used to evaluate the land cover classification results. It is usually done by comparing the classification product with some reference collected on field. Sources of reference data is the ground truth collected from the field, aerial photo interpretation campaign, land use map from woody mass project and hunting maps. The process was repeated until to get a realistic image classification is achieved. Finally it was determined by use of the Confusion Matrix. This matrix shows the accuracy of a classification result by comparing a classified result with ground truth information (Richards, 1995).

3.5.1.5 Post Classification and change detection and quantification

The post-classification comparison method, which is commonly applied for land cover change detection studies, was found to be the most suitable method to detect land use and land cover changes (Larsson, 2002; Liu and Zhou, 2004). To apply this technique independently land cover classified images were compared.

3.5.2 Pre-processing meteorological data

Meteorological data were collected from the Ethiopian Meteorological Services agency (Table 3-4). Meteorological stations considered are located within and adjacent to the Geba watershed. Hard copies of these daily meteorological data were edited in digital form. Most of the raw data are not complete; missing data were completed applying SWAT weather generator using the monthly weather generator parameters.

Table 3-4: Meteorological stations in Geba watershed (Data base: Ethiopian National Meteorological Service Agency).

Station	Location		Altitude (m a.s.l)	Annual mean	Period with missing values
	Easting	Northing			
Adigrat	548379	1578542	2506	590	1970-todate
Agula	569390	1514714	2016	441	1975-todate
Atsebi	580252	1534423	2729	633	1996-todate
Edagahamus	560828	1568223	2720	633	1973-todate
Hagereselam	518972	1508550	2608	732	1973-todate
Hawzen	546779	1544804	2255	535	1971-todate
Mekelle-airport	557678	1489249	2267	596	1962-todate
Mekelle-Illala	550694	1495184	2005	605	1962-todate
Senkata	562000	1554000	2467	816	1973-todate
Wukro	564675	1524313	1995	616	1963-todate

Data quality check was primarily made by time series plotting to identify outliers. Double mass analysis is made to check consistency of the weather station data. After checking the consistency and outliers, data were prepared for the weather statistics applying the weather statistics software WGNMAKER to fill missed data (http://swat.tamu.edu/software/links-to-related-software). The resulting data set is required to generate representative daily climate data on sub basins level. Detail formula and description is appended in Annex-1.

3.5.3 Pre-processing hydrological data

Hydrological data were collected from the Ministry of Water Resource (MoWR) (Table 3-5). For the gauging station data provided by high stage data are handeled with care as the existing rating curves might be developed without including high-flows. Consequently, due to the flashy nature of the runoff an additional uncertainty is introduced to cover the possibility of missing high-flows.

Table 3-5: Hydrological stations in the Geba basin (Data base: Minstry of Water Resource).

	Location		Operated by			Measurement	
Station Name	Easting	Northing	Staff gage	Autom. water level recorder	Bank operated cable way	Period	Resolution
Geba Nr.Mekelle 121004H2	540961	1508987	yes	yes	no	1967–1979 1995–2003	Daily, with missed data Daily, good quality
Suluh 121007	552902	1549135	yes	yes	yes	1973–2003	Daily, with missed data
Genfel 121010	563045	1521168	yes	yes	yes	1982–2003	Daily, with missed data
Agula 121013	562718	1513261	yes	no	yes	1993–2003	Daily, with missed data

The key station used for modeling purpose was Geba Nr. Mekelle station (121004 H2) which was installed in 1967. In 1991 the gauging station was slightly shifted downstream.The present day gauging station is located at the bridge along the road from Mekelle to Hagere-seleam. Water level data are available from June 1967 to 1979 and from 1991 to 2003.

Flow measurements at the Geba site from 1991–1993 were accounted by Tekeze master plan project. The results were compared with the data provided by the Ministry of Water Resource (MWR). From this comparison it can be concluded that the rating equation used by MWR could lead to an overestimation of peak discharges (DEVECON, 1998). The rating equation according to the Tekeze master plan study (DEVECON, 1998) is:

$$Q = 35.5\ (H + 0.096)^{2.393} \qquad \text{Equation 3-2}$$

Where Q is river discharge in m^3/s and H is the stage in meter.

For high flows above a stage of 1.0 m, the exponent 2.393 should be changed to approximately 1.7. This problem is addressed by Hunting (1976) constructing an approximate rating curve based on the Manning equation for the known river cross section.

Table 3-6: Result of annual runoff calculation applying different rating curves (Data source: DEVECON, 1998, Hunting Technical service and Ministry of Water Resource, 2001).

		Annual runoff (Mm^3)		
Year	Rainfall (mm)	MoWR	DEVECON, 1998	Hunting technical service, 1976
1968	471	80	246	229
1969	694	86	296	249
1970	609	84	287	264
1971	438	45	108	117
1972	625	61	179	201

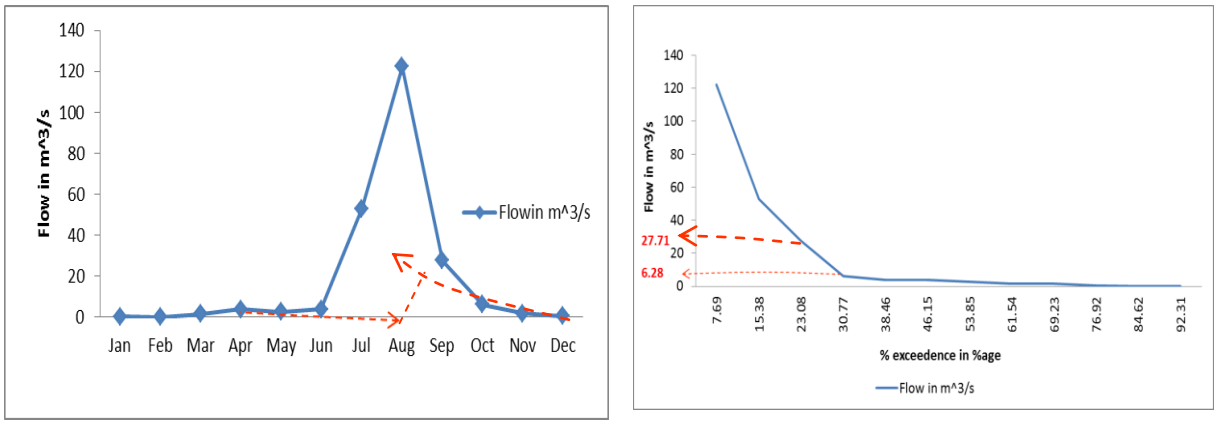

Figure 3-4: Base flow separation from stream flows and field measurement using current meter: a) low flow in Geba river, b) low flow gauge is above the flow and does not measure the flow, c) low flow measurement using current meter, d) meteorological data downloaded from the weather station, e) base flow separation using flow separation method, f) flow duration curve for Geba river (Data base: flow data from Ethiopian Minstry of Water Resource).

The base flow analysis is done by preparing a flow duration curve and applying the base flow separation techniques based on the Ministry of Water Resource data base and field measurements after rain periods and during dry periods at Geba Nr Mekelle outlet. A comparison was done with the

Soil and water assessment tool base flow separation program developed by Arnold and Allen (1999). The mean monthly stream flow is considered for the analysis. It was observed as it shown in the Figure 3-4, below; the base flow is not properly measured by the gauges.

3.6 Climate downscaling

In hydrological proceses modelling, climate change and weather varaibliy has different impacts on the watershed. To identify the climate change in the watershed, differentiating short-term weather varablity from climate change is crucial. Long-term trends of climate varability with its cycle require extended data series. To identify long-term trends in the data available the following tests are conducted:

- Homogeneity test of the trends conducted to test for abrupt change points,
- The long-term (monotonic) and seasonal trends test,
- Trend and seasonality were computed for the basin using thirty-eight year time series of the data by Mann-Kendall test method (Hirsch et al., 1982).

In this way local trends and cycles of local trend frequencies are identified. Based on these results future climate scenarios are generated.

3.6.1 Downscaling methods and tools

Studies on the impact of global warming on the hydrological cycle and water resources in the future usually rely on climate change scenarios projected by General Circulation Models (GCMs). However, the coarse scaled GCM projections cannot be applied directly in to hydrologic studies at a regional or basin scale. To derive local or station-based climate change scenarios from GCM outputsdata have to be downscaled (Wilby and Christian, 2007). In consequence, two techniques of downscaling are available: statistical downscaling and dynamical downscaling. For this study statistical downscaling was applied.

The statistical downscaling technique bases to establish a relationship between large state climate (e.g. precipitation, temperature, water vapour, etc) and local area features (e.g. topography, land-sea distribution) in local or regional stations data. This needs equations to convert coarse scale global data output to local or regional scale. The equations used for explaining one as a function of other and then used on the GCM data to obtain the local variables. Large climate variables are called Predictors and local variables are predictands (Wilby and Christian, 2007). Thus statistical downscaling models uses the predictors obtained from National Center for Enviropmental Prediction (NCEP) and predictands from lcal area to formulate locally used functions.

The large scale output of a GCM simulation is fed into this statistical model to estimate the corresponding local and regional climate characteristics. Through the analysis of the simulation results of the climate models climate scenarios were generated from the GCM data HadCAM3 and CGCM3 acting as drivers of the hydrological system. Based on these, impact of rainfall and evapotranspiration

to changes on floods and rivers dry water flows (low flows) were investigated using the rainfall-runoff models.

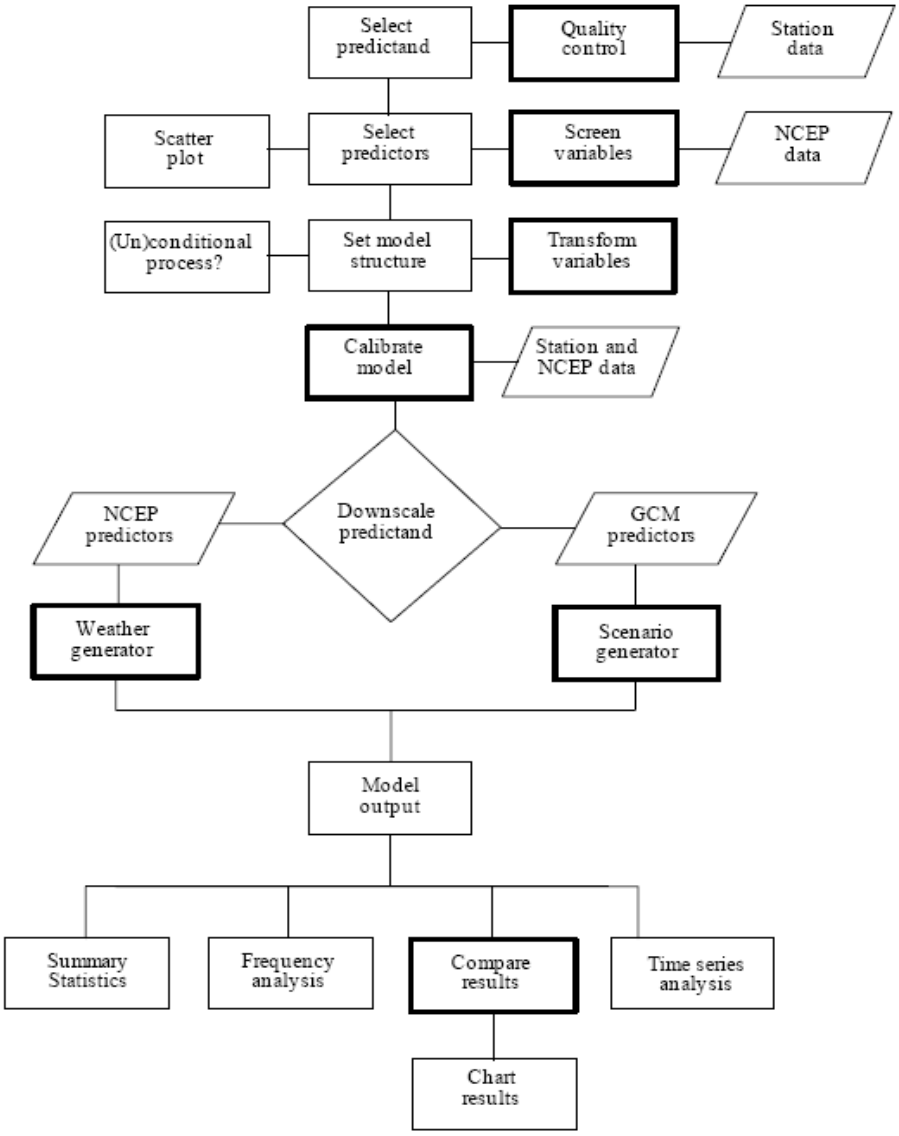

Figure 3-5: Climate scenario generation (modified after Wilby and Christian, 2007).

3.7 Basics formulas of the hydrological model

3.7.1 Hydrological processes model

The hydrological processes simulated by SWAT2009 include precipitation, evapotranspiration, surface run-off, lateral subsurface flow, groundwater flow and river flow. The simulation of the hydrology of a watershed is done in two separate divisions (Neitsch et al., 2005). The land phase process of the hydrological cycle and the routing phase of the hydrological cycle.

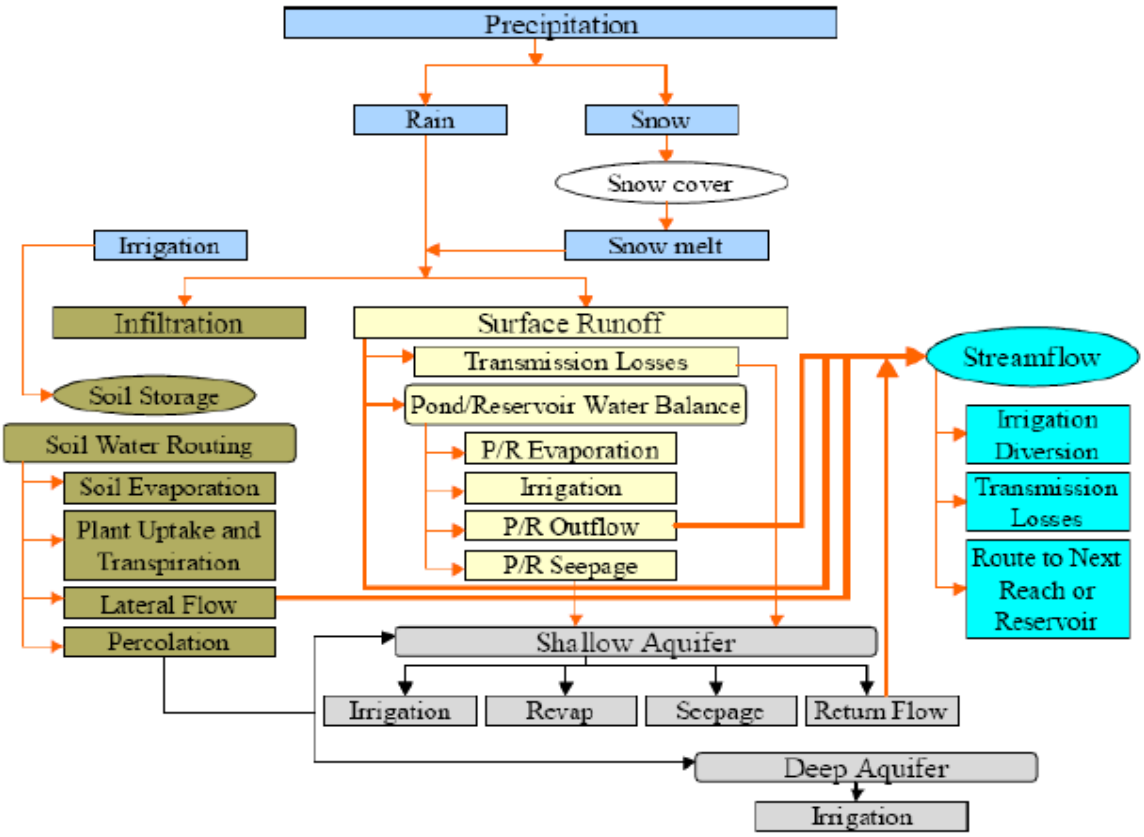

Figure 3-6: Pathways for water movement within SWAT2005 (after Neitsch et al., 2005).

3.7.2 Land phase processes

In the land phase process of the hydrological cycle, SWAT simulates the hydrological cycle based on the water balance of the soil profile (Equation 3.2).

$$SW_t = SW_o + \sum_{i=0}^{t} [R_{day} - Q_{surf} - E_a - W_{seep} - Q_{wg}] \qquad \text{Equation 3-3}$$

Where SW_t is the final soil water content (mm H_2O); SW_o is the initial soil water content on day I (mm H_2O); t is the time in days; R_{day} is the amount of precipitation on day i (mm H_2O); Q_{surf} is the amount of runoff on day i (mm H_2O); Ea is the amount of Evapotranspiration on day i (mm H_2O); Wseep is the amount of water entering the vadose zone from the soil profile on day i (mm H_2O) and Qgw is the amount of return flow on day i (mm H_2O).

3.7.3 Surface runoff generation

Runoff is generated when on a sloping surface the precipitation reaching the ground is higher than the infiltration rate. This kind of flow is based on the Hortonian principles. Sometimes precipitation is reaches the ground surfaces after saturation, the resultin runoff is called saturation overland flow. The surface runoff generation in SWAT2009 is mainly based on the soil conservation service curve number method (SCS) (USDA, Soil Conservation Service, 1972) which estimates the amount of runoff based on land use, soil type and antecedent moisture condition (Arnold et al., 1998):

$$Q_{surf} = \frac{(R_{day} - I_a)^2}{(R_{day} - I_a + S)}, \; Q_{surf} \text{ in } m^3/s \qquad \text{Equation 3-4}$$

Where Q_{surf} is the accumulated rainfall excess (mm H_2O); R_{day} is the rainfall depth for the day (mm H_2O); I_a is the initial abstraction which includes surface storage, infiltration and infiltration prior to runoff (mm H_2O) and S is the retention parameter (mm H_2O).

The soil retention parameter which is derived from the curve number varies spataially and temporarly.The varaiblity depend on varations in soil watercontents, soil, land use, land mangement and slope with time and space with in the watershed.

The retention parameter is defined as

$$S = 25.4 \, (\frac{1000}{CN} - 10) \qquad \text{Equation 3-5}$$

Where CN is the curve number, a basic parameter that includes the areas, hydrologic soil group, land use and hydrologic conditions (Williams, 1995).

The initial abstractions, I_a, is commonly approximated as 0.2S and the above equation becomes (USDA, Soil Conservation Service, 1972):

$$Q_{surf} = \frac{(R_{day} - 0.2S)^2}{(R_{day} + 0.8S)}, \; Q_{surf} \text{ in } m^3/s \qquad \text{Equation 3-6}$$

3.7.1 Computation of evapotranspiration

Three methods for estimating potential evapotransipration (PET) are provided by the Soil and Water Assessment Tool (SWAT). In this study the Penman-Monteith method (Monteith, 1965) is used.

$$ET = \frac{\Delta(R_n - G) + \rho_a C_p (e_s - e_a)/r_a}{\left(\Delta + \gamma\left(1 + \frac{r_s}{r_a}\right)\right)\lambda\rho_w} \qquad \text{Equation 3-7}$$

Where Δ is the slope of the saturation vapor pressure vs. temperature curve; R_n is the net radiation flux at the surface; G is the sensible heat exchange from the surface to the soil (positive if the soil is warming); ρ_a is air density; C_p is specific heat of dry air; e_s is the saturation vapor pressure of the air at some height above the surface; e_a is the actual vapor pressure of

the air; r_a is aerodynamic resistance to turbulent heat and/or vapor transfer from the surface to some height z above the surface; γ is the psychometric constant (defined later); r_s is a bulk surface resistance that describes the resistance to flow of water vapor from inside the leaf, vegetation canopy, or soil to outside the surface; λ is the latent heat of vaporization, defined as the energy required to convert a mass of liquid water into vapor (having typical units of joules per kilogram) and ρ_w is density of liquid water.

3.7.4 Water movement in soils

The Soil and Water Assessment Tool assumes the shallow and the deep aquifers to address ground water. Ground water movement in the shallow aquifer is modeled by classifying in to three processes: upward migration by capillary rise to unstautrated zone, losses to deep aquifer and return flow to the stream (Neitsch et al., 2005). SWAT2009 allows simulating water perculation from one layer if the water content exceeds the field capacity of the layer considered. Using the storage routing method, the water that moves to the the underlying layer is calculated. Water that percolates to the next layer is computed as (Neitsch et al., 2005):

$$W_{p,ly} = SW_{ly,excess}\left[1 - \exp\left(\frac{-\Delta t}{TT_p}\right)\right] \qquad \text{Equation 3-8}$$

Where the travel time for percolation is unique for each layer and is calculated as:

$$TT_p = \frac{Sat_{ly} - FC_{ly}}{K_s} \qquad \text{Equation 3-9}$$

Where Wp,ly is the amount of water percolating to the underlying soil layer on a given day (mm), SWly,excess is the drainable volume of water in the soil layer on a given day (mm), Δt is the length of the time step (hrs), TTp is the travel time for percolation (hrs), Sat_{ly} is the amount of water in the soil layer when completely saturated (mm), FC_{ly} is the water content of the soil layer at field capacity (mm) and K_s is the saturated hydraulic conductivity for the layer (mm hrs^{-1}).

3.7.5 Lateral subsurface flow

The Soil and Water Assessment Tool incorporates a kinematic storage model (Sloan and Moore, 1984 cited in SWAT2009 manual) to compute subsurface flow as a function of the drainable volume of water, saturated hydraulic conductivity, soil slope, hill slope length, and drainable porosity. The equation to compute lateral flow is given as (Arnold et al., 1998):

$$q_l = 0.024\left[\frac{2.SW.K_s.sl}{\emptyset_d.L_h}\right]$$ Equation 3-10

Where q_l is lateral flow (mm*d^{-1}); SW is drainable volume of soil water (mm), sl is slope (m/m^{-1}); $\emptyset_d$is drainable porosity (mm*mm^{-1}); Ks is saturated hydraulic conductivity (mm/ hrs) and Lh is the hill slope length (m).

3.7.6 Base flow estimation

The SWAT2009 model estimates the base flow by separating the groundwater in two aquifers: confined deep aquifer and unconfined shallow aquifer.The unconfined aquifer which is not fully saturated has a contribution to streamflow during dry periods as baseflow due to the water pressure differences in the aquifer.Wheras the deep aquifer is treated as a loss in the hydrologic system and contributes flow to the stream outside the basin (Arnold and Allen, 1993).

The contribution of groundwater to stream flow is simulated by creating a shallow aquifer storage which is recharged by percolation from the unsaturated zone, and discharges to the reach of the watershed. The water balance for the shallow aquifer is (Arnold et al., 1998):

$$\mathrm{Aq_{sh,i}} = \mathrm{Aq_{sh,i-1}} + \mathrm{W_{rec}} - \mathrm{Q_g} - \mathrm{W_{rev}} - \mathrm{W_d} - \mathrm{WU_{sa}}$$ Equation 3-11

And groundwater flow into the main channel on day *i* is calculated using (Arnold et al., 1998):

$$\mathrm{Q_{g,i}} = \mathrm{Q_{g,i}} * \mathrm{e}^{-\alpha\Delta t} + \mathrm{W_{rec}}\left(1 - \mathrm{e}^{-\alpha\Delta t}\right)$$ Equation 3-12

Where Aqsh,i and Aqsh,i-1 is the shallow aquifer storage (mm) on day *i* and *i*-1 respectively; Wrec is the recharge entering the aquifer on day *i* (mm); Qg is the groundwater flow or base flow, into the main channel on day *i* (mm); Wrev is the amount of water moving into the soil zone in response to water deficiencies on day *i* (mm); Wd is the amount of water percolating from the shallow aquifer into the deep aquifer on day *i* (mm); WUsa is the water use from the shallow aquifer (mm); α is the recession constant which describes the lag flow from the aquifer and Δt is the time step and α can be best estimated by analyzing measured stream flow during periods of no recharge in the watershed.

3.7.7 Routing phase

The second phase of the SWAT hydrologic simulation, the routing phase, consists of the movement of water, sediment and other constituents (e.g. nutrients, pesticides) in the stream network. Two options are available to route the flow in the channel networks: the variable storage and Muskingum methods.

For this study, the variable storage method was adopted. The method was developed by (Williams, 1969).

Storage routing is based on the continuity equation (Williams, 1969):

$$\nabla V_{stored} = V_{in} - V_{out} \qquad \text{Equation 3-13}$$

Where *Vin* is the volume of inflow during the time step (m^3 water); *Vout* is the volume of outflow during the time step (m^3 water); and $\nabla Vstored$ is the change in volume of storage during the time step (m^3 water).

3.7.8 Model evaluation

The general procedure of the sensitivity analysis, optimization (calibration and validation) and uncertainty analysis is provided in Figure 3-6.

The sensitivity analysis is done by using a combined method of Latin Hypercube (LH) sampling and One-Factor-At-a-Time (OAT), integrated toArcSWAT2009 and Soil and water assessment tool calibration uncertainty prediction tool (SWAT-CUP). It was performed for twenty seven parameters that may have the potential to influence Geba river flow. The ranges of parameter variations are based on a listing provided in the SWAT2009 manual (Neitsch et al., 2005) and are sampled by considering a uniform distribution. For each parameter, changes were made a number of times within its allowable range to test its sensitivity; during this process the other parameters were kept unchanged.

Model calibration involves adjustment of parameter values of the models to reproduce the observed response of the Geba watershed within the range of accuracy specified in the performance criteria. Consequently, tests were conducted to validate the calibrated model that is capable of making sufficiently accurate predictions. The approach to calibrate and validated the SWAT2009 model was based on manual calibration helper and auto calibration procedures. The Sequential Uncertainty Fitting, ver. 2 (SUFI-2) is incorporated in an independent program called Soil and Water Assesement Tool-Calibration and Uncertainty Program (SWAT-CUP) and is used for automatic calibration (Abbaspour, 2007).

3.7.8.1 Performance evaluation

After selecting suitable parameters, the performance of the models is checked using coefficient determination (R^2) and the Nash-Sutcliffe model efficiency (E_{NS},) (Nash and Sutcliffe, 1970; Santhi et al., 2001; Moriasi et al., 2007). The appropriateness of the models is evaluated based on three criteria after Van Griensven et al. (2012):

1. Analysis of the performance indicators (fit-to-observations, Equation 3-8 to Equation 3-13),
2. Evaluation the realistic representation of the hydrological processes by means of parameter and mass balance evaluation (fit-to-reality)
3. Assessment, how far the models are able to tackle the problem (fit-to-purpose).

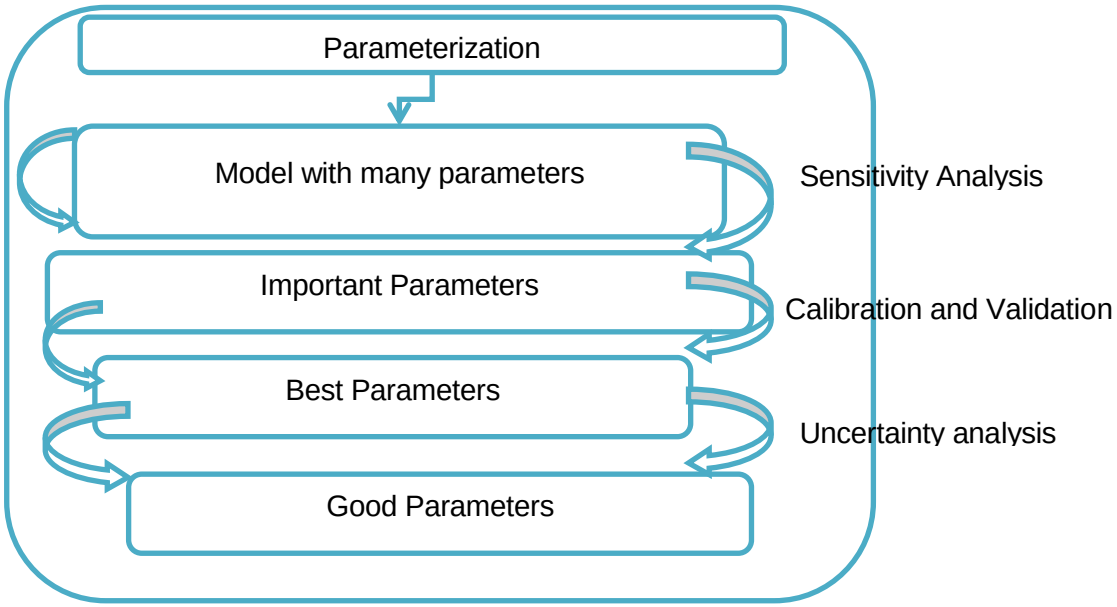

Figure 3-7: Procedures of sensitivity analysis, optimization (calibration and validation) and uncertainty analysis (after Van Griensven et al., 2006).

$$R^2 = \left\{ \frac{\sum_{i=0}^{n}(q_{obs} - \bar{q}_{obs})(q_{sim} - \bar{q}_{si\,m})}{\left[\sum_{i=0}^{n}(q_{obs} - \bar{q}_{obs})^2\right]^{0.5}\left[\sum_{i=0}^{n}(q_{sim} - \bar{q}_{sim})^2\right]^{0.5}} \right\}$$ Equation 3-14

$$E_{Ns} = 1 - \frac{\sum_{i=0}^{n}(q_{sim} - q_{obs})^2}{\sum_{i=0}^{n}(q_{obs} - \overline{q_{obs}})}$$ Equation 3-15

$$MBE = \frac{\bar{q}_{sim} - \bar{q}_{obs}}{\bar{q}_{obs}}$$ Equation 3-12

$$PBIAS = \left(\frac{\sum_{t=0}^{T}(q_{sim} - q_{obs})}{\sum_{t=1}^{T} q_{obs}}\right) x100$$ Equation 3-13

Where: q_{obs} is the observed discharge; q_{sim} is the simulated discharge; ,$\overline{q}_{obs,}$ is the average observed discharge; $\bar{q}_{si\,m}$ is the average simulated discharge.

4 Study area

The Geba watershed drains the north-eastern part of the Tekeze River Basin and is located in northern Ethiopia, Tigray Regional State. The watershed has a size of 5,260 km^2 (Abraha, 2009). This research focuses on the upper part of the watershed which covers about 2,440 km^2.

4.1 Regional settings and landscape units

The study area is bounded between latitudes 13^{0}16' and 14^{0}16' North and longitudes 38^{0}38' and 39^{0}49' East (Figure 4-1).

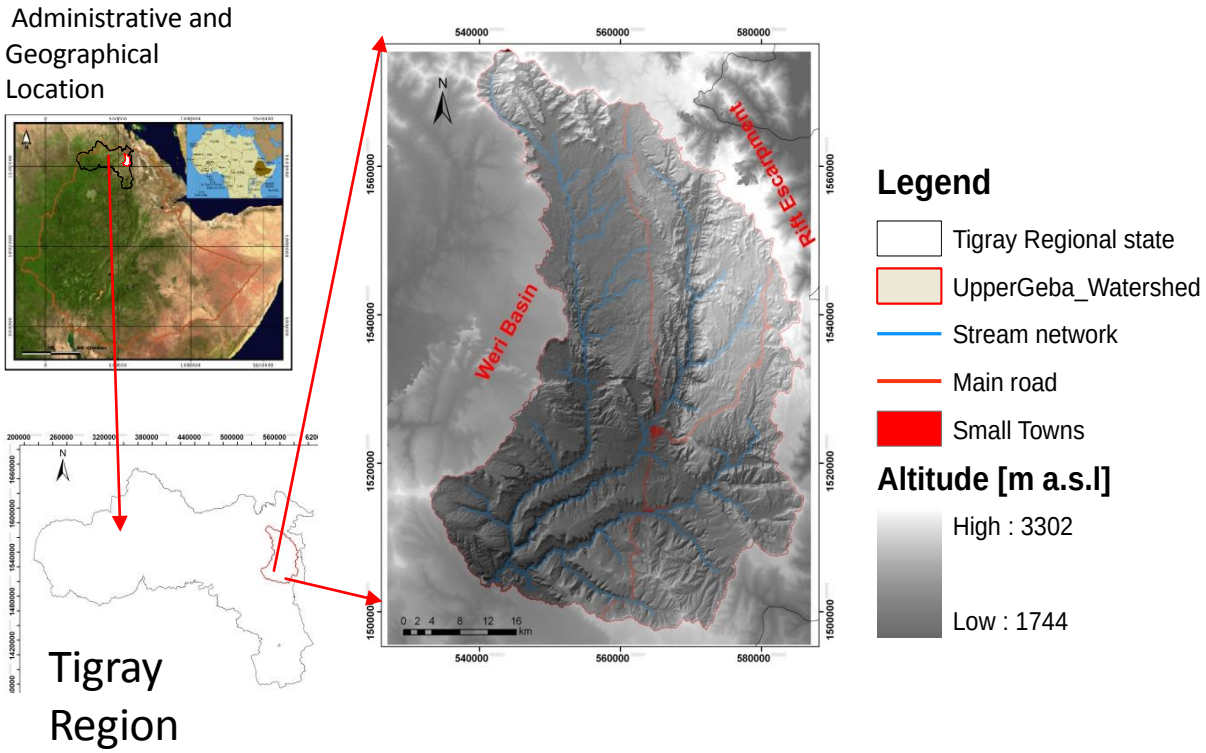

Figure 4-1: Location map of the Geba basin. (Data base: Jarvis et al., 2008 and topographic map 1:50,000 from Ethiopian Mapping Authority, and www.fews.net for the map of Ethiopia)

The headwater area lies between altitudes of 2600 and 3300 m a.s.l. and is bordered by higher mountains areas of Mugulat to the north and Atsebi Horst to the north east. The central plateau, which lies between 2000 to 2400 m a.s.l., becomes increasingly dissected by rivers flowing south west. The fault-controlled Mekelle, Wukro and Senkata areas, and the Atsbi horst, build the major plains of the Geba basin and lie between 1800 to 2400 m a.s.l.

4.2 Climate

4.2.1 Rainfall

The watershed receives two rainy seasons: the main rainy season (June to September) and the small rainy season (Feburary to May). The annual rainfall totals between 500 to 800 mm. Annual rainfalls shows very pronounced annual and seasonal fluctuations. Moreover the local rainfall pattern highly depends on the topography.

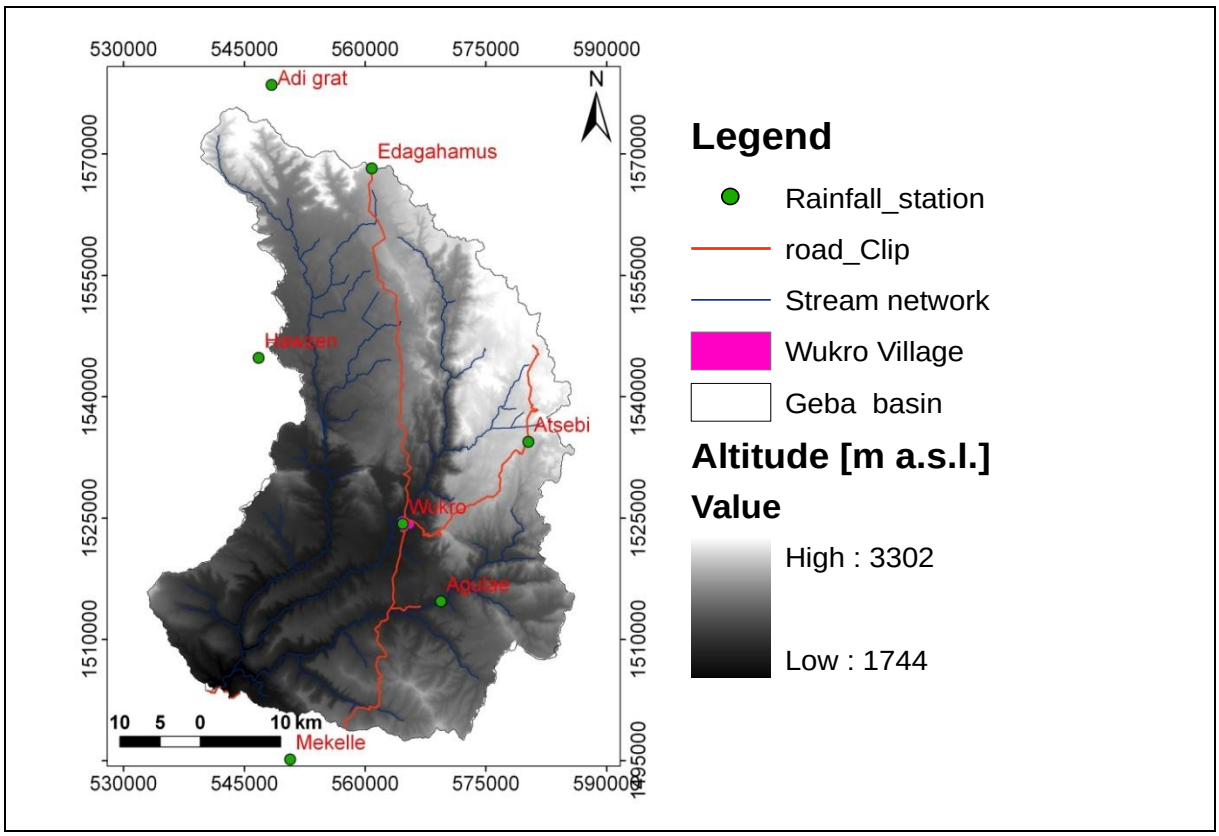

Figure 4-2: Meteorological station distribution within and around the Geba basin (Data base: Jarvis et al., 2008; Topographic map 1:50,000 from Ethiopian Mapping Authority; rainfall data from Ethiopian National Meteorological Service Agency).

In the study area around 70% of the annual rainfall occurs between July and August (Figure 4-3). At all rain gauge stations in the study area (Figure 4-2) annual precipitation underlies a distinct seasonality. The rainfall distribution is bimodal at all stations, with a minor peak usually in March–April and July–August (for details see chapters 6 and 7).

Table 4-1: Meteorological stations in the Geba basin (Data base: Ethiopian Nation Meteorological Authority).

Station	Location UTM coordinate system		Altitude (m a.s.l)	Annual mean rainfall (mm)	Period with missed value
	Easting	Northing			
Adigrat	548379	1578542	2506	590	1970–todate
Agula	569390	1514714	2016	441	1975–todate
Atsebi	580252	1534423	2729	633	1996–todate
Edagahamus	560828	1568223	2720	633	1973–todate
Hagereselam	518972	1508550	2608	732	1973–todate
Hawzen	546779	1544804	2255	535	1971–todate
Mekelle-airport	557678	1489249	2267	596	1962–todate
Mekelle-Illala	550694	1495184	2005	605	1962–todate
Senkata	562000	1554000	2467	816	1973–todate
Wukro	564675	1524313	1995	616	1963–todate

4.2.2 Temperature

The National Meteorological Service Agency of Ethiopia (Gonfa, 1996) divides the country based on temperature into four zones; Kolla I (mean annual temperature > 20°C), Kolla II (mean annual temperature > 25°C), Woina Dega (mean annual temperature > 15°C) and Dega (mean annual temperature < 15°C). The study area is located in the Kolla II zone; here hot season mean temperatures range from between 25°C in the area close to Mekelle to about 22°C on the high plateaus. The temperature of the coldest month average less than 6°C on the high plateau and reaches 11°C near the Mekelle area (Figure 4-4). The highest mean monthly temperatures are reached just prior to the onset of the rainy season in April and May. The approximate lapse rate (decrease of temperature with altitude) averages 0.6°C /100 m (Gonfa, 1996).

4.1.1 Relative humidity

The mean monthly relative humidity is only available for five years of the two stations Mekelle (Quiha) and Mekelle (Illala). The data of 1996–2000 reveal that the average humidity is highest in August (72%), and least in May (43%) (Table 4-2). The humidity is highest in the early morning (06:00) and lowest in the afternoon (15:00). In July and August the relative humidity in the early morning might reach up to 90%.

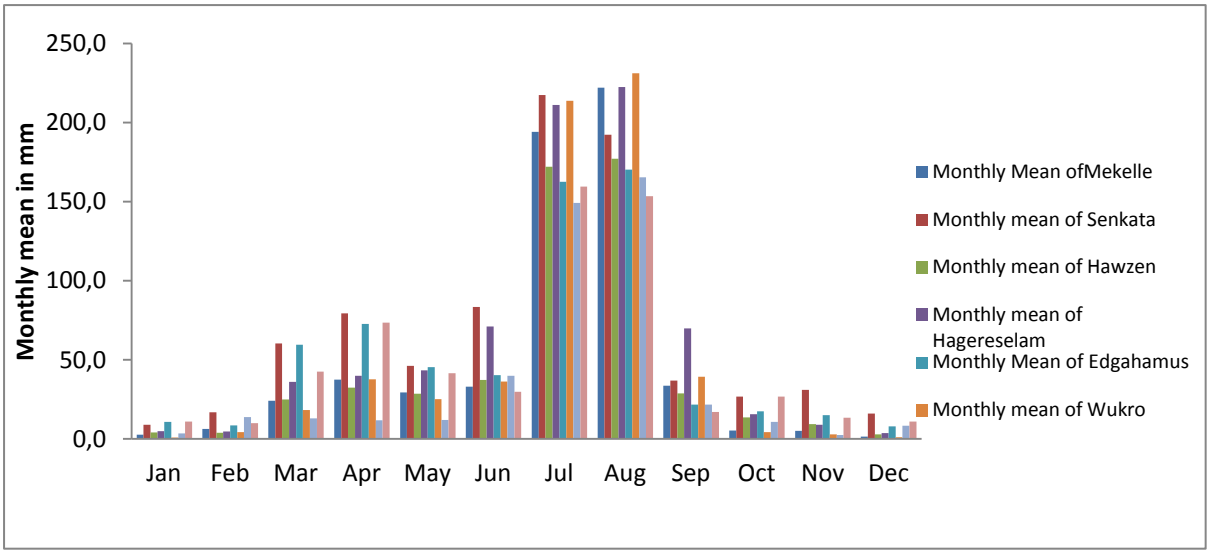

Figure 4-3: Mean monthly rainfall of all station in the Geba basin (Data base: Ethiopian Nation Meteorological Service Agency 1962–2010).

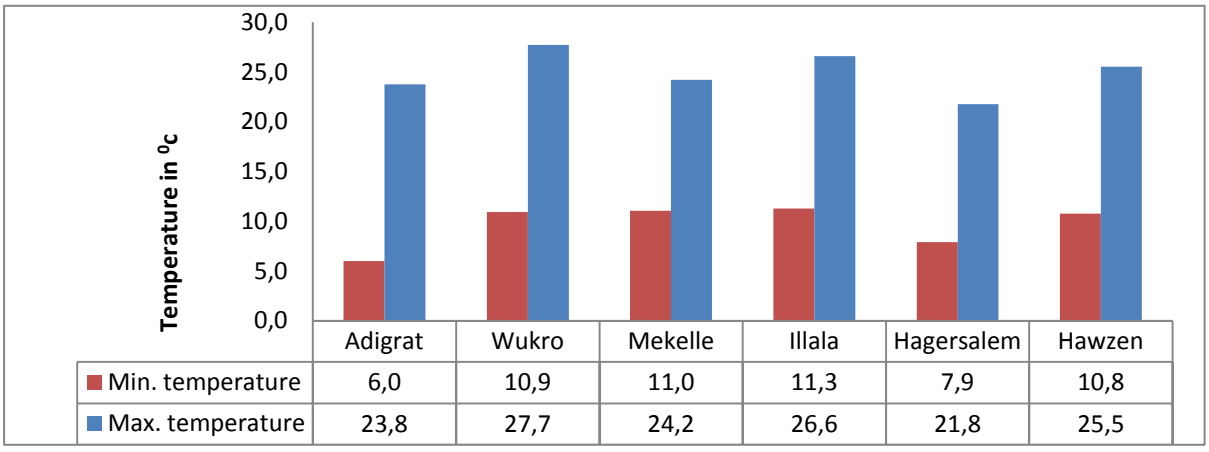

	Adigrat	Wukro	Mekelle	Illala	Hagersalem	Hawzen
Min. temperature	6,0	10,9	11,0	11,3	7,9	10,8
Max. temperature	23,8	27,7	24,2	26,6	21,8	25,5

Figure 4-4: Mean monthly temperature at the weather station of the Geba basin and its vicinity (1962–2010) (Data base: Ethiopian Nation Meteorological Service Agency)

4.1.2 Wind

Wind directions during dry season in most parts of Ethiopia is generally from the east direction (easterly or southeasterly), changing to westerly or north-westerly during the rainy season. Winds are not very strong and velocity generally averages 2.1 to 3.1 m/s with slight increase during the transition period between the dry and wet spell (WAPCOS, 2003).

Table 4-2: Mean Monthly Climate data from 1996–2000 from Mekelle and Illala stations (Data base: Ehiopian Nation Meteorological Service Agency 1962–2010)

Climate parameter	Month											
	Jan	Feb	Mar	Apr	May	Jun	Jul	Aug	Sep	Oct	Nov	Dec
Relative Humidity in%	53	48	50	48	43	46	66	72	51	50	49	49
Wind speed in m/s	3.0	3.5	3.5	3.5	2.6	1.5	1.2	1.0	1.4	2.6	3.2	3.1
Sunshine in hour	9.5	9.7	9.2	9.4	9.6	7.5	5.5	5.4	7.9	9.4	9.8	9.9
Evaporation in mm	6.9	9.2	9.3	10.4	10.1	7.3	4.1	3.8	6.1	7.7	7.8	7.4

4.1.3 Evaporation

Evaporation data are only available for Mekelle (Illala) station for five years (1996–2000). These station data are used for preliminary analysis. The evaporation is maximum in April (10.4 mm per day) and May (10.1 mm per day), when daily temperatures are high and winds are comparatively stronger than during other months. The evaporation is minimum in July (4.1 mm per day) and August (3.8 mm per day) when the atmosphere is more humid, day temperatures are low and wind speeds are less compared to other months (Table 4-2).

4.1.4 Sunshine

The sunshine data are available from 1996–2000 for Mekelle (Quiha) and Mekelle (Illala) weather stations. The sunshine hours average around 5.5 hours/day in July and August and around 10 hours a day in December. Obviously the decrease in sunshine hours in July and August is due to persistent cloudiness during rain.

4.2 Geology

The geology of the study area is dominated by the Mekelle outlier, a basement complex plateau having an upper sedimentary rock layer with some doleritic intrusions and a basalt capping. Fluvial deposits occur along narrow incised river valleys (Gebreyohannes et al., 2010). The following geological units (Figure 4-5) mainly underlie the study area:

- Agula formation southwest of Mekele Fault and the cliff forming lower Hintalo limestone units;
- Enticho sandstone and Edaga Arbi tillites are exposed locally;
- Quaternary gravels, sand, silt and clay along the river beds, banks and terraces;
- Adigrat Sandstone along the lower river valleys and northeast of the Mekelle Fault;
- The Precambrian basement rocks around Genfel river and
- Tertiary basalts around Mugulat

4.2.1 Agula formation along Geba river valley

In the southeast of the Geba river valley, between the Bridge of Geba River to Abi Adi and the confluence with Agula River, the exposed rocks are composed of black, fractured, and steep cliff forming limestone units, alternating with marls and shales. The limestone units are highly jointed (Figure 4-6, Photo-1).

4.2.2 Recent river deposits

The composition of recent river sediments in the Geba river banks varies from gravel to various grain sizes of sand, silt, and mud. The gravel is of different degree of roundness and might reach sizes of blocks (Figure 4-6, Photo-2).

4.2.3 Adigrat sandstone

The downstream parts of Geba River and Agula River north and northeast of the Mekelle Fault are underlain by Adigrat Sandstone and dolerite. The Adigrat sandstone is friable and porous, and forms a gently sloping relief compared to the overlying carbonate rocks. The rocks are regionally dipping to the northeast.

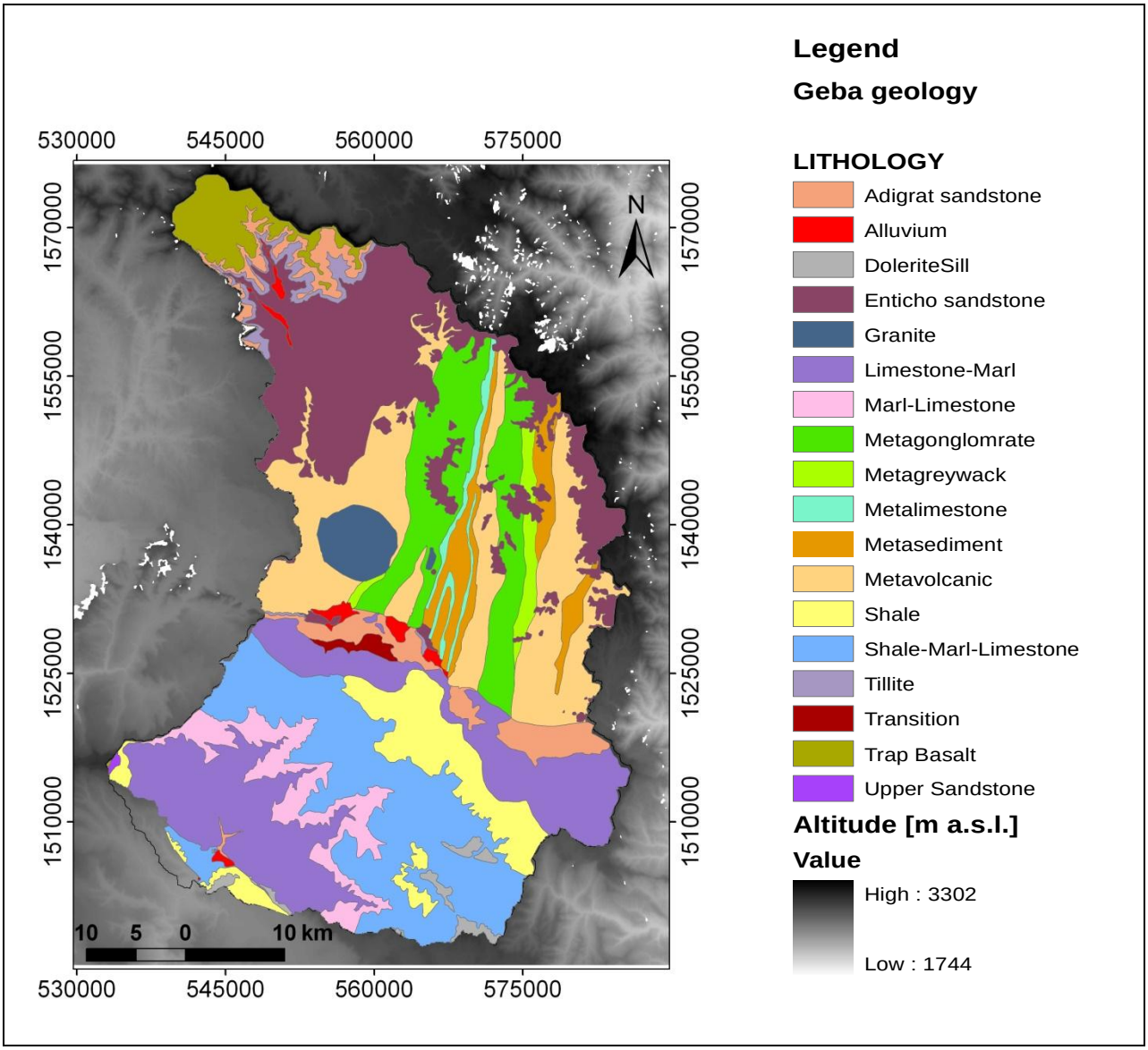

Figure 4-5: Geological Map of the Geba basin (Data base: Gebreyohanes et al., 2010; Jarvis et al., 2008; Topographic map from Ethiopian Mapping Agency)

Photo 1. Joints terminating against soft rocks in the lower Agula River valley. The thin beds are also dipping towards Mekelle Fault. The lower joint has extended to the overlying soft rock.

Photo 2. Composition of recent river sediments in the Geba River banks.

Figure 4-6: Photographs on Agula shale and Mekelle Outlier

4.3 Relief and Hydrogeography

4.3.1 Relief and topograhic variables

The morphometric variables derived from 1:50,000 map and generated from the DEM are tabulated in Table 4-3.

Table 4-3: Topographic data derived from map and Digital Elevation Model (Data base: Jarvis et al., 2008).

Controlling Variable	Tributary of Geba			Upper Geba
	Suluh	Agulae	Genfel	
Catchment area in km² (A)	968.4	692	729.3	2441.3
Perimeter in km	236.2	171.4	206.16	309.82
Minimum elevation in m	1777	1764	1777	1747
Maximum elevation in m	3302	2864	3002	3302
Height Difference (HD) in m	1525	1100	1225	1555
Longest flow path length in km	97.54	79.46	92.48	120.4
Total drainage length(TDL) in km	2207.6	1496.9	1581.8	5378.2
Horizontal distance (HL) in km	66.6	49.73	58.86	77
Drainage density (TDL/A) in km/km²	2.28	2.16	2.17	2.2
Relief length ratio (HD/HL)	0.023	0.022	0.013	0.02
Slope along drainage line in%	4.1	5.2	5.3	5

4.3.2 Physiography, landform and relief for the upper Geba basin

Generally, the landscape can be classified in to six units (Figure 4-8). There is a considerable variation in altitudes over the basin with a maximum altitude of 3302 m a.s.l., a minimum altitude of 1700 m a.s.l and an average altitude of 2000 m a.s.l.

The topography of the basin is highly controlled by erosion features and geological structures. Sharp cliffs and steep slopes occurs along the major rivers (Figure 4-7)

Figure 4-7: Geba at confluence of Suluh and Genfel, sharp cliff and steep slope.

A series of faults in the Mesozoic sediments and folds in the basement terrains create remarkable topographic breaks in the basin (Hunting technical service, 1976). The entire basin landscape is characterized by a strong incised network of gullies. The presence of major faults and some minor faults are responsible for steep cliff that is common in the area (Hunting technical service, 1976).

The northern and northeastern part of the basin are mountainous, with the eastern part comprising several upland plateau flanked by mountainous (Hunting technical service, 1976; Gebreyohannes et al., 2010).

4.3.3 Drainage

The Geba River is a major tributary of the Tekeze River. Suluh, Genefel and Agulae River build the head water streams of the Geba River. The drainage system of the Geba basin can be described as dendritic with some significant influence of major structures like folds and faults (Hunting technical service, 1976; Gebreyohannes et al., 2010). Overall, the drainage pattern in the northern and eastern parts of the basin is highly influenced by the foliation direction of the Precambrian rocks while the central part is influenced by the Neo-tectonic faults of the Mekelle outlier (Gebreyohannes et al., 2010).

4.3.4 Geomorophological processes

The upper Geba river basin is in a continuous process of change that is mainly marked by stepped morphology and strong relief variations (Figure 4-10). Present day relief changes are mainly attributed to exogenic forces (Hunting technical service, 1976; WWDSE, 2008. The main geomorphological processes shaping hilly slopes in the Geba watershed are:

- Mass movement due to forces of gravity;
- Sheet and rill erosion related to rain splash;
- Gully and channel erosion associated with fluvial processes.

The effect of gravity is spatially linked mostly to the steep cliffs bordering the plateau and rugged terrain in the lowlands (Figure 4-11). It commonly involves detachment of blocks of rocks along litho-structural discontinuities initiated by positive porewater pressure during wet seasons. The detached earth material slides and falls downslope with much of it being temporarily deposited along mid and down slopes (Figure 4-11) (Hunting technical service, 1976). Sheet and rill erosions are widely common wherever the natural vegetation cover has been depleted. The development of rills is frequently associated with geologic structures that weaken strength of rock materials, which they intersect. This phenomenon has been noted on scarps/plateau cliffs incapable of supporting vegetation growth, and also gently sloping plains in the periphery of stream courses (Hunting technical service, 1976; WWDSE, 2008). Gully and channel erosion dominate the fluvial processes and commonly occur along valley sides. The processes are basically initiated by high runoffs generated from the upland plateaus, overflowing river banks and channel ways (WWDSE, 2008).

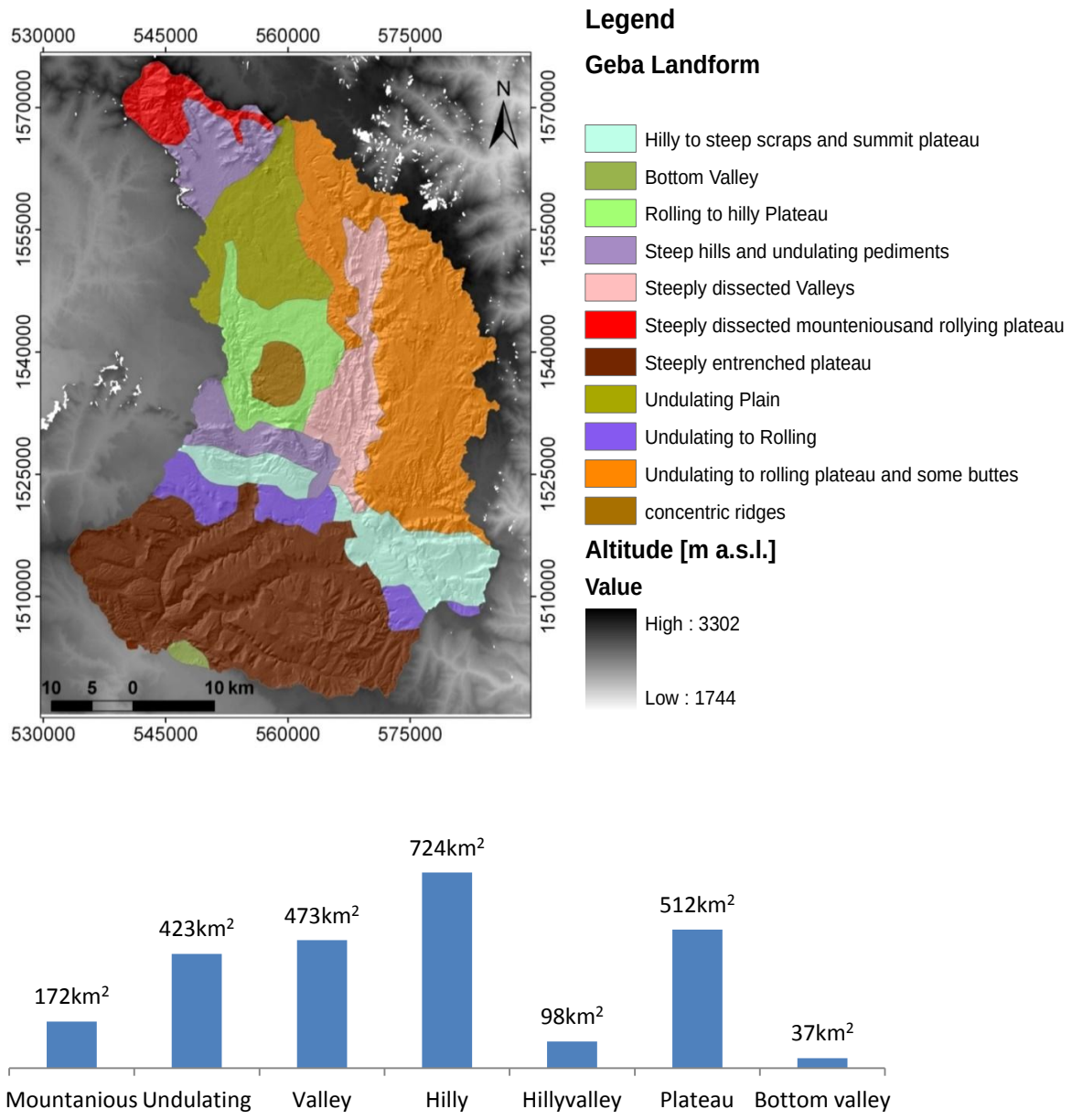

Figure 4-8: Geomorphological unit of the Geba drainage basin (above); the histogram (belowe) shows the areal distribution of the geomorphological units (Data base: Jarvis et al., 2008; Huntingten technical service, 1976 and 1:50,000 Topographic Map from Ethiopian mapping agency).

4.3.5 Slope gradients and assessment of geomorphical processes

The slope gradients range from 0–74°. Very steep slope gradients of 30° to 74° are recorded in the north and north east highland plateaus (Mugulat and Atsebi mountainous area, escarpment cliffs). The escarpment cliffs are mainly affected by mass (Figure 4-3, Photo-1, below).

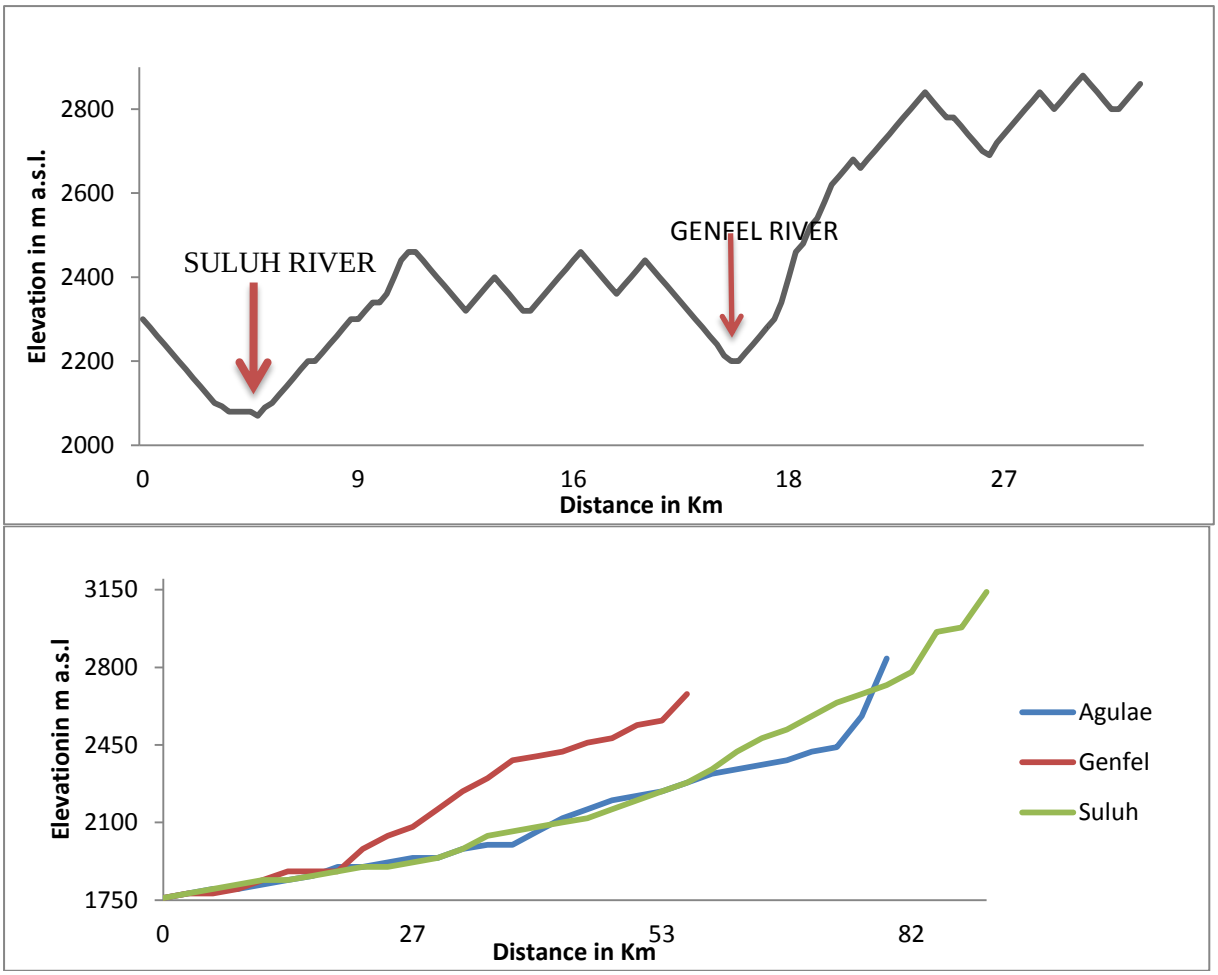

Figure 4-9: Cross profile (a) and longitudinal profile (b) of the Geba watershed. For the location of the cross profile see Figure 4-8a. The longitudinal profile follows the channel beds of the three major headwater streams (Data base: Jarvis et al., 2008; Topographic map 1:50,000 from Ethiopian Mapping Agency).

Slope gradients of 25–30 intermittently follow the cliffs for small distances and ends shortly down slope. This area corresponds to the debris slope. The debris slope gradually merges into moderately sloping ground (7°–15°) that is highly affected by gully erosion. Slopes 0°–4° characteristically occurs at the plateaus flat, at mid slopes and along valley side plains. Erosion activity in these areas is relatively low.

Photo-1: Small lobes of colluvial deposits along foot of dolerite scarp in red line, eastern part plateau margin, Mekelle.

Photo-2 :Mass movement and rill development along steep and long cliffs, in the northern plateau margin

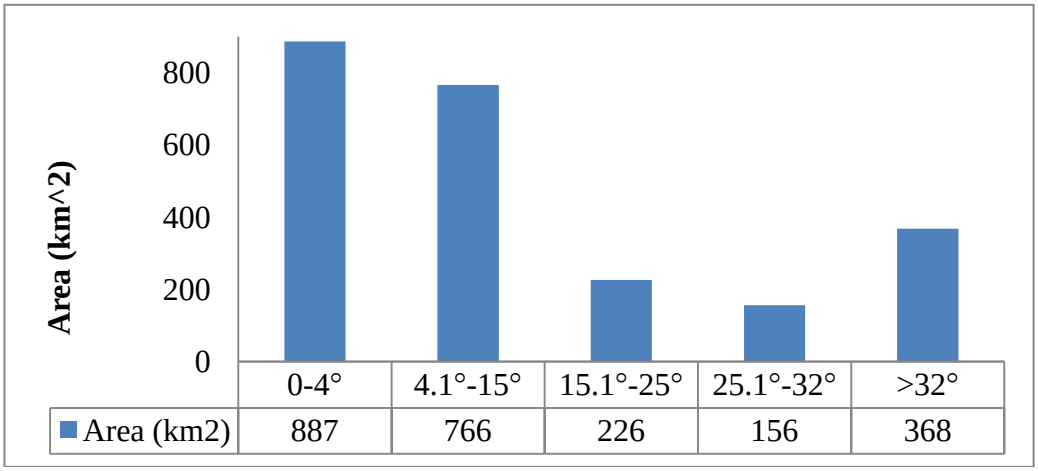

Figure 4-10: Field view of Geba basin (photos) and slope distribution in the area.

Table 4-4 Slope gradient, associated geomorphic processes in the study area

Slope (°)	Slope Description (modified after Schütt and Thiemann, 2001)	Geomorphic process dominating
0–4	Flat to gently undulating	Splash rain
7–15	Undulating to rolling	Valley side fluvial and splash rain
25–30	Hilly	Deposition and transportation (debris flow)
>30	Steeply dissected to mountainous	Mass Movement

Table 4-5: Physiographic units across the Geba river

Landform unit	Geology or Soil Parent Material	Relief unit and slope ranges	Altitude m a.s.l.	Soil
Plateau	Agula shale and marl with some limestone, dolorite and sandstone locally	Flat to gentle undulating valley floors and Cliff forming Limestone	1900–2100	Shallow to deep very dark grey calcareous clay soils; Chromic vertisol and Vertic Cambisol
	Agula marl and shale with some limestone, dolorite and sandstone locally on the right side of Suluh river	Flat to undulating plains with low hills and ridges (2–7%)	1900–2200	Shallow to moderately deep brown to dark grayish brown calcareous clay soils; often stonney Chromic vertisol and Vertic Cambisol
Hilly	Limestone and marl	Rolling to hilly terrain of low hills and wide valleys, locally steep slopes.	2200–2400	Shallow to very shallow medium textured stony Eutric cambisol with frequent rocks outcrops on slopes
Mountaineous	Limestone and marl	Hill and dissected slopes >100%	2300–2400	Lithic leptosols Shallow to very shallow medium textured

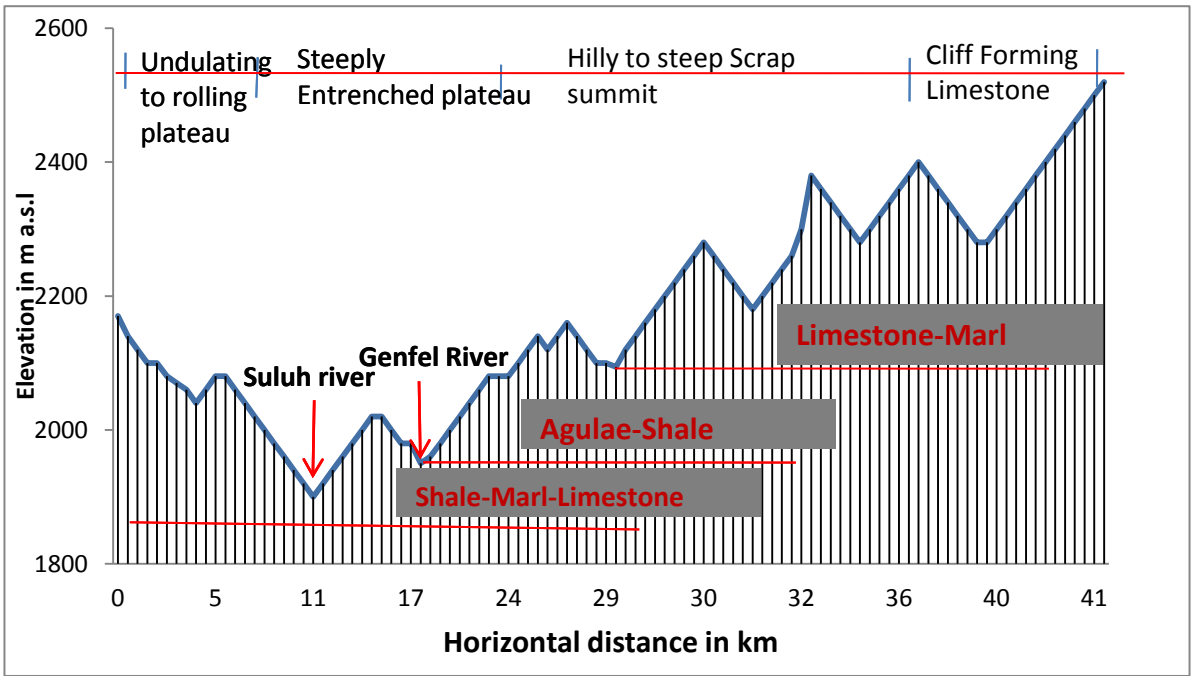

Figure 4-11: Cross-sectional profile on the Geba Plateau across the River.

4.3.6 Hydrogography

Most of the plateau area shows undulating to rolling relief, interspersed by very steep hills. Deep incised valleys dissect the terrain to the northwest of Mekelle. The extreme ranges in elevation and steep slopes result in rapid erosion and shallow soils. Only on the more stable relief of the flatter upland plateaus and the graben valleys bottom soils with moderate depths developed (Hunting technical service, 1976). Locally slopes are terraced as soil conservation measure.

4.4 Soils

At a local level relief has strong influence on soil development. In the idealized sequence deeply weathered soils occur on the upper plateau, rocky or even shallow soils occur on vertical scarps, unconsolidated coarse stony soils occurs on steep debris slopes finer textured soils varying in texture occur on the undulating pediments and deep alluvial soils occur on the alluvial terraces and lower parts of alluvial deposits.

Leptosols are a widespread soil type in the Geba basin (Abraha, 2009; Gebreyohannes, 2009; Sander, 2012). Leptosols are very shallow soils where the unweathered rock is reached within 10 cm below the surface. They occur on all rock types and, thus, include all textures (Hunting Technical Service, 1976; Sander, 2012). Leptosols are most common on steep land however, thier distribution increases as soil erosion results in the depletion of soil depth. These soils are not suitable for crop production, but farmers use it for cultivation due to shortage of arable land.

Table 4-6: The soil types and their main characteristics in the Geba basin.

Code	Soil Unit		Slope (°)	Texture Class	Geomorphic unit
	Major unit	Sub unit			
LPe.ca	Eutric Leptsols	Calcaric soils	16–30	Clayloam	Hilly/valley bottom
LPe.cm	Eutric Leptsols	Cambic soils	8–16	Loam	Hilly/valley
LPe.cm	Eutric Leptsols	Cambic soils	8–30	Clay	Hilly/valley
CMx.or	Chromic Cambic sols	Orthic soils	2–8	Clayloam	Plateau
CMv.or	VerticCambic sols	Orthic soils	2–8	Sandyclay	Plateau
LPq	Lithic leptosols		>30	Silty clayloam	Mountainous
			16–30	Clayloam	Hilly/valley
			>30	Clayloam	Mountainous
			16–30	Sandy clayloam	Hilly/valley
			>30	Clayloam	Mountainous
LXh.ch	Haplic Lixsols	Chromic Vertisols	8-16	Clayloam	Plateau/Hilly

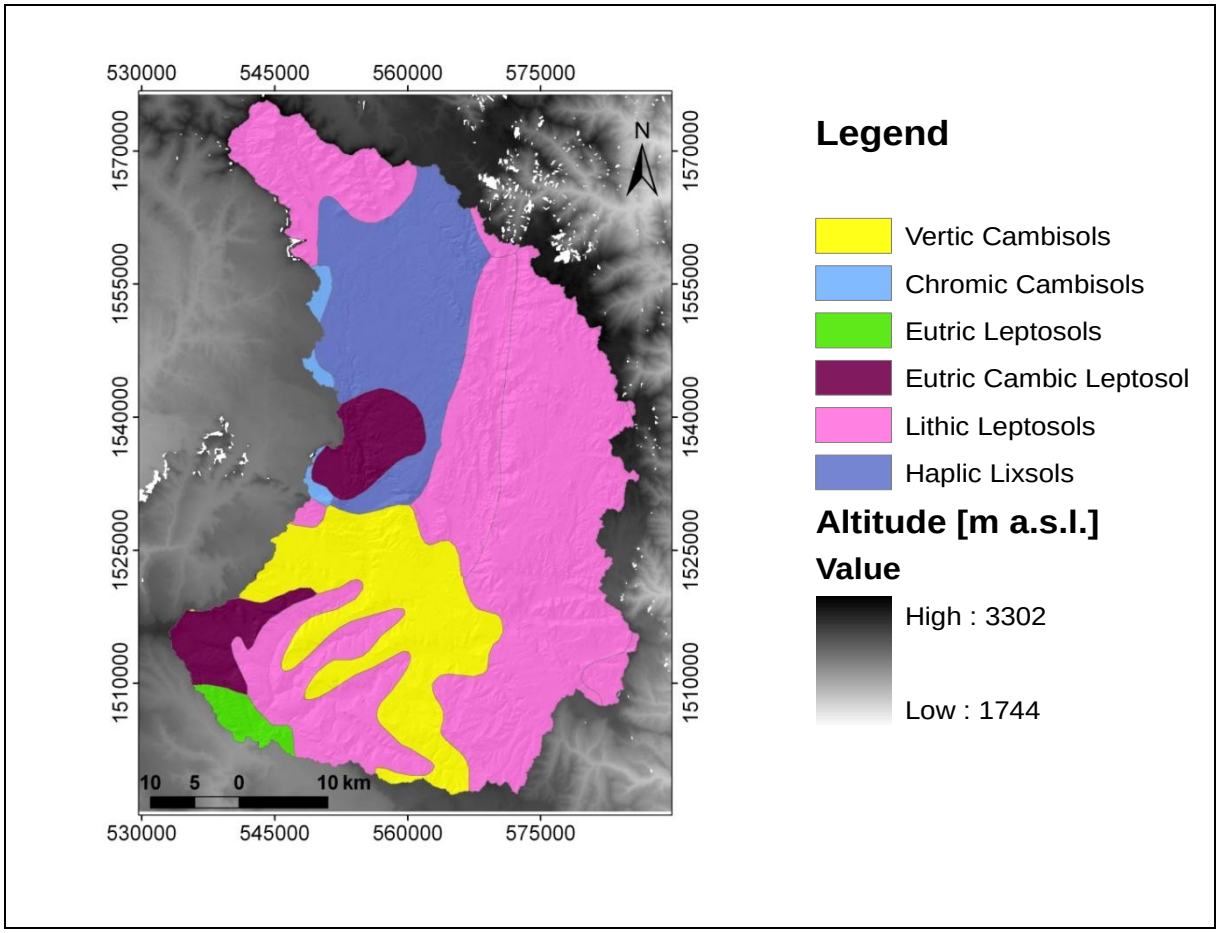

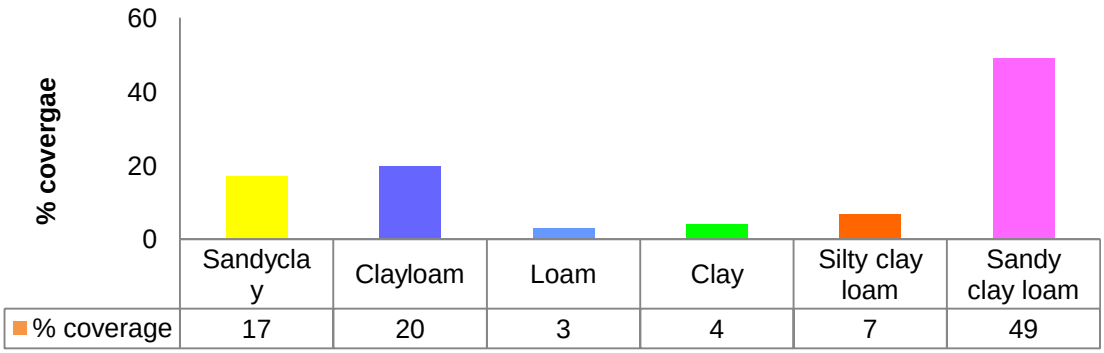

Figure 4-12: Soil map and soil texture type of Geba (modified after FAO,1998) (Data base: Jarvis et al., 2008, FAO Soil Map (1998), 1:50000 topographic map from Ethiopian Mapping Agency)

The FAO soil map (1998) has been supplemented by field work. The objective of soil sampling is to verify the textural classification of the large scale FAO soil map (1998) and to develop input parameters for the hydrological modeling.

4.5 Vegetation and land use

The natural woodland vegetation of most of the region has been largely destroyed or severely modified by human activities. The original Acacia woodland of the plateau survived only locally in areas of mountain ranges, the main escarpment and locally around the churches. Elsewhere, the present vegetation comprises a sparse cover of low Acacia bush and scrub interspersed between cultivated lands.

Overgrazing builds a main reason for the reduction of the natural vegetation in the Geba basin. The progressive increase in the demand for fuel wood and for extra cultivation land has caused devastating effects in acceleration of erosion and, consequently depletion of soil depth and soil moisture (Abraha, 2009; Hadgu, 2008). Land degradation such as deforestation, poor agricultural practices, and inappropriate land use systems, disrupt the socio-economic activities, ecological systems and general development of the region. The watershed is mainly used for agricultural purposes. Cultivated fields cover more than 60% of the watershed.

5 Test sites

Seven test sites inside Geba basin have been selected for detailed geomorphological, pedological and land use mapping. The test sites are located in the four major geomorophological units of the Geba basin (Figure 5-1, Table 5-1).

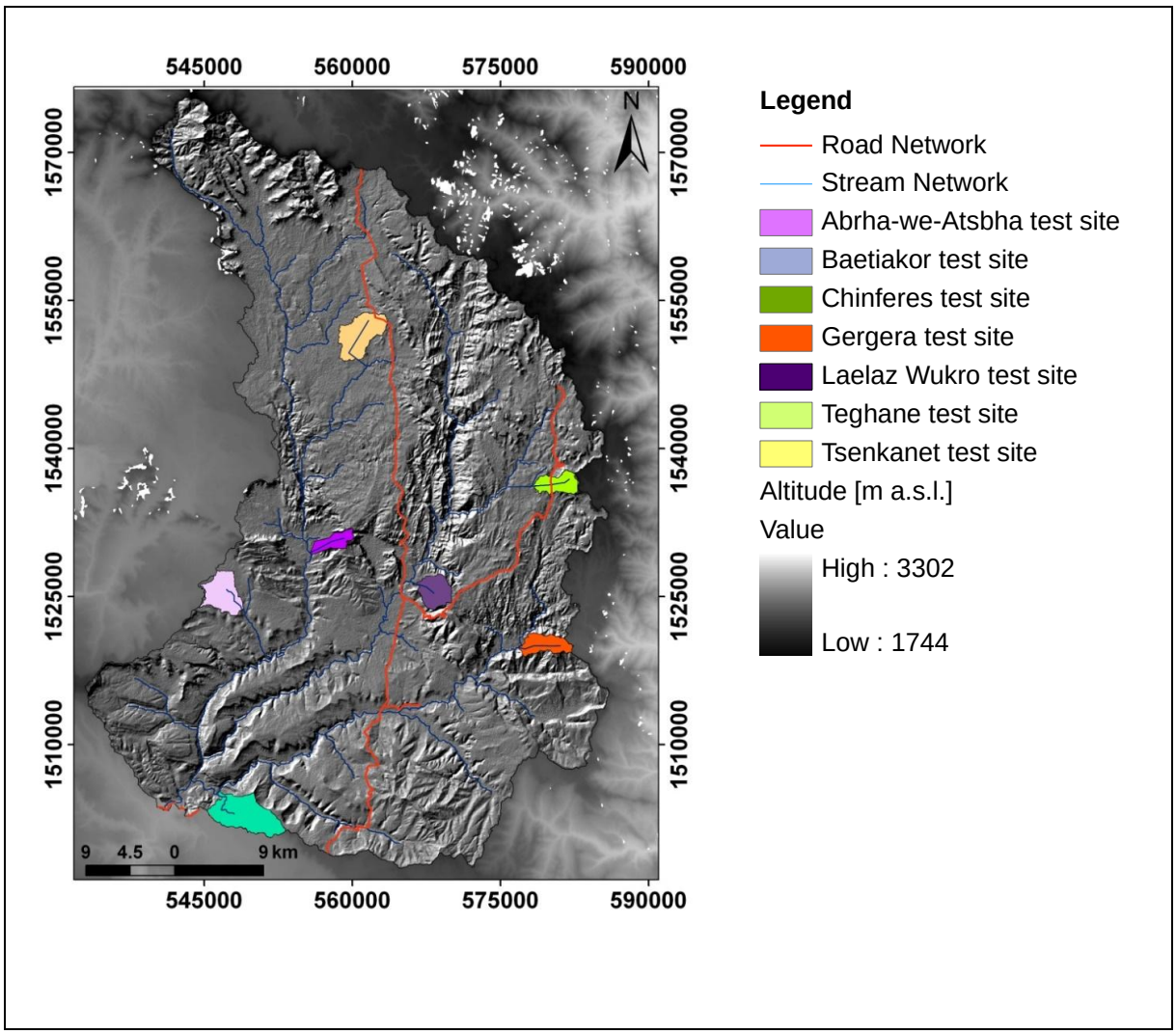

Figure 5-1: Test sites within the Geba basin (Data base: Jarvis et al., 2008).

Studying the geomorphological processes in selected test site is done to understand the hydrological responses of the basin. Runoff generation in the basin is highly influenced by relief parameters. However, these parameters are not directly fed into the model and consequently need indirect evaluation to verify the modeling processes. The slope length, concavity and convexity have a great impact on the time of runoff concentration and runoff generation. Infiltration rate is highly dependent to the deposition material and soil depth. Quaternary deposits like alluvial infills or debris flows significantly influence the hydraulic conductivity of the soils. Therefore, detailed morphological and pedological investigation of the test sites is used for an internal model calibration and an evaluation of the hydrological response units.

Table 5-1: Distribution of test sites in the watershed geomorphological and geological units

Test site Name	Chenferese	Gergera and Teghane	Tsenkenet	Abraha-we-Atsbeha	Laelay Wukro
Physiographic Unit	Mekelle/Geba Plateau	Atsbi Horst /Transition	Entcheo Plateau	Highland	Genfel Valley
Landform Unit	Steeply entrenched plateau and undulating to rolling plateau	High steep Ridges and undulating to rolling	Undulating Plain	undulating pediments hilly	Dissected Valley
Geology Unit	Mekelle outlier (Agula shall, Limestone-marl)	Adigrat sand-stone, Entcho sandstone and basement rock	Entcho sandstone	Adigrat sandstone	Basement rock

The climate of the test sites are interpolated from the nearest station or from the areal mean values of the watershed. This is due to non availability of meteorological station on the test sites except Laelay Wukro test site, which has fixed automatic weather stations.

5.1 Chenferese test site

The Chenferese test site is located in the Agulae sub-watershed in the south-west of the Geba basin. Geographically, it is located between 13°34'–13°35' N and 39°25'–39°29' E and has a surface area of about 19.8 km².

In the Chenferese test site lithology is closely coupled with morphology. The Chenferese test site is divided into three major geomorphological units: Mekelle Plateau, Mekelle fault belt escarpment and Agula River valley (Gebreyohannes et al., 2010). The Mekelle Plateau covers the largest part of the test site. Most parts of the Mekelle Plateau are highlands with altitudes around 2000 m a.s.l. The highlands extend from the central to the northern and eastern part of the test site. Land forms range from leveled plains to very steep scarps and rolling to hilly slopes. The Mekelle fault crosses the area in the north, characterized by an increased drainage pattern and an entrenched steeply dissected plateau (Figure 5-2 and Figure 5-4).

The meteorological stations near to the Chenferese test site are Mekelle and Quiha weather stations. Rainfall and temperature data recorded for over thirty eight years (1969–2010) show that the annual rainfall averages 605 mm at Quiha weather station and 590 mm at Mekelle weather station. The rainy season extends from June to September with major rainfall occurring in July and August. Temperature analysis shows that the lowest monthly temperature occurs from September to November with the monthly temperature averaging 9.6°C and maximum temperatures occurring in May with values peaking up to 27°C (see Table 4-6).

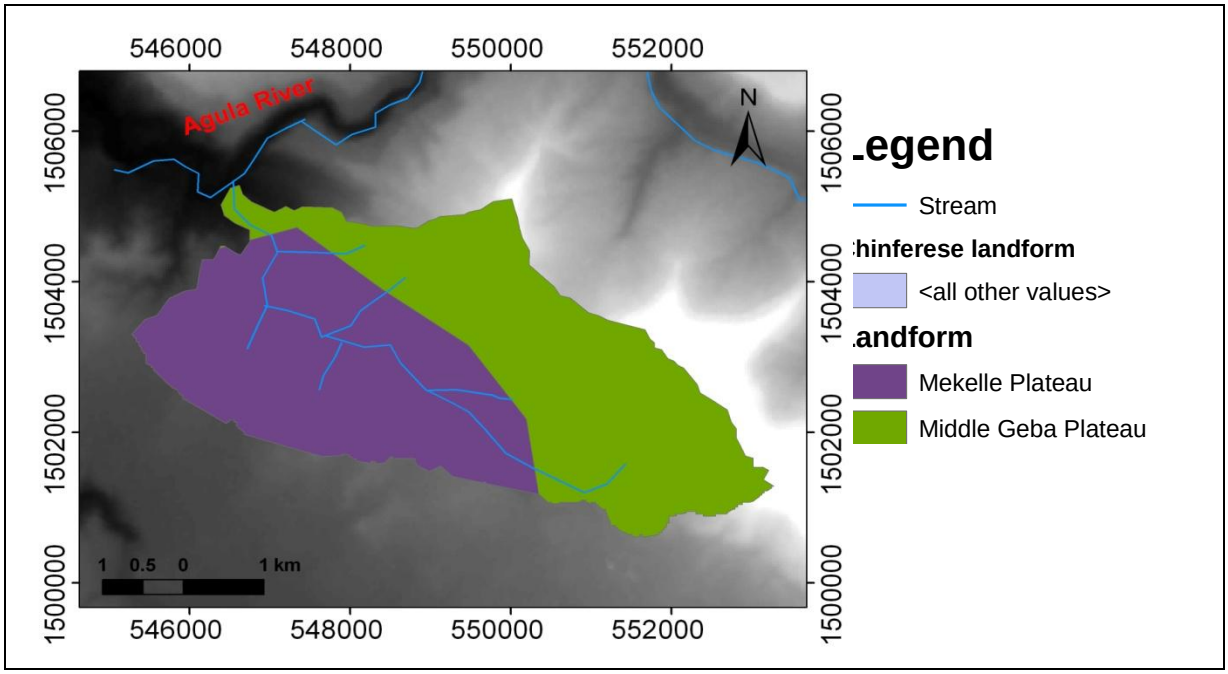

Figure 5-2: Landforms of the Chenferese test site. For location in the Geba basin see Figure 5-1 (Data base: Jarvis et al., 2008)

Chenferese test site is located in the Mekelle Outlier where Mesozoic sedimentary rocks have been preserved from erosion. The test site's bedrock is composed of Jurassic sedimentary rocks, Tertiary dolerites and Quaternary alluvial and colluvial deposits (Bosellini et al., 1997; Russo et al., 1996). Patches of dolerite are exposed along the fault and Adigrat sandstone is exposed along the valley (Gebreyohanness et al., 2010). Travertine is found around the Chenferese church. Marl interbedded with black and white limestones is located in the north of the Chenferese test site and is formed by marly limestone, rich in gastropods bivalves in the lower part, overlain by dark limestone (Figure 5-5, Photo 2).

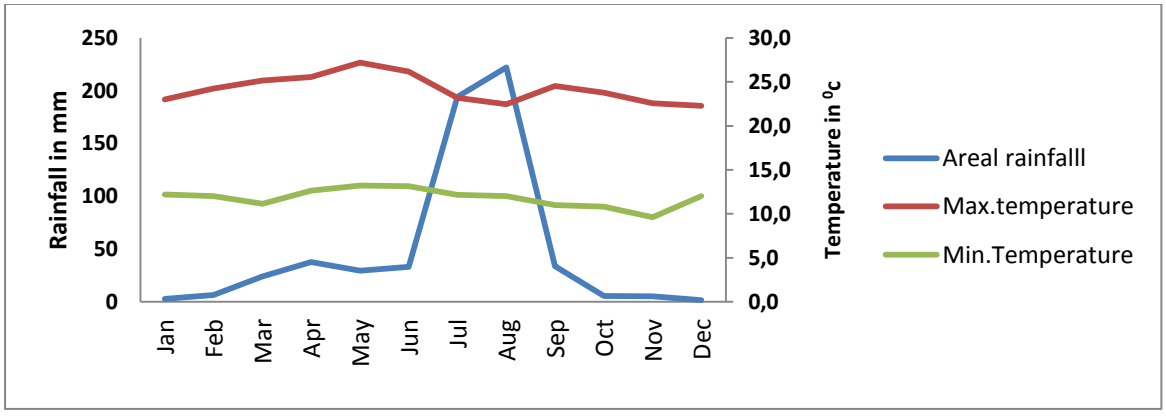

Figure 5-3: Monthly mean meteorological data for Chenferese Test site (Data base: National meteorological agency)

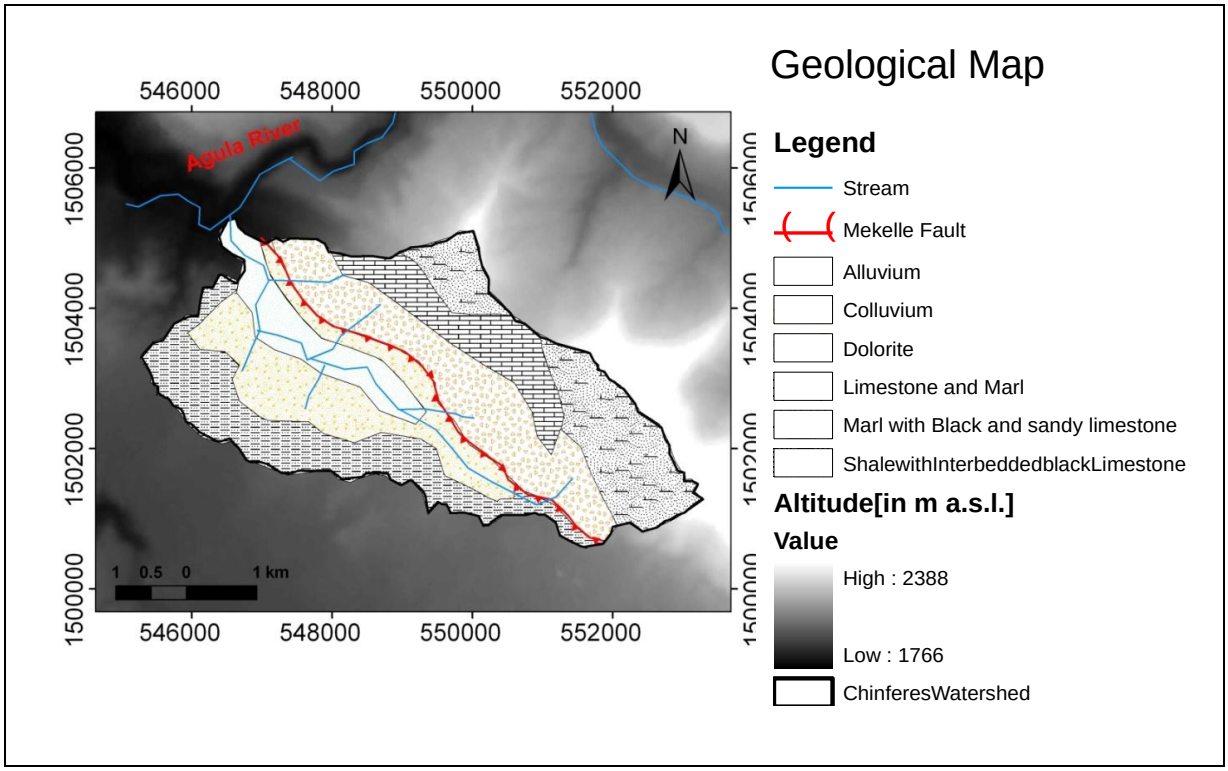

Figure 5-4: Geological map of chenferese test site (Data base: Gebreyohanes et al., 2010; Jarvis et al., 2008)

Fine to coarse grained dolorite occur along on the Mekelle fault (Figure 5-5, Photo 3). This dolorite occurs as sills or dykes discontinuously through the test site (Gebreyohaness et al., 2010). Agula Shale is composed by marl, black limestone, with fossiliferous limestone intercalations (Figure 5-5, Photo 4). The limestone is regionally used for construction. Slopes where Agula shale outcrops are moderately steep (30–50%). They are mostly covered by colluvial deposits.

The dominat soil types in the Chenferese test site are Leptosols, Cambisols, Calcisols and Vertisols (FAO, 1998). Bedrock, topographic features, landforms and human impact are main driving forces that define the variability of soil type in the test site. Soils in the steeply entrenched plateau (Figure 5-1), which builds the largest part of the test site, are shallow soils. The transition to the middle slopes is marked by a scarp face on which Leptosol and bare bed rock occur.

Photo 1 **Photo 2**

Photo 3 **Photo 4**

Figure 5-5: Geological units: black limestone (Photo 1); dark limestone (Photo 2); dolorite intrusion (Photo 3) and shale lime intercalation (Photo 4).

On the highly calcareous and fine-textured marls and shales of the middle slopes Eutric Cambisols documents good draining conditions. In contrast, the Vertic Cambisols occurring in depressions occur due to impeded drainage which favors the formation of montmorillonitic clays. Down slope increasing soil moisture favors the formation of deep Vertisols in lower slope positions and in the alluvial plains.

Landforms like colluvial deposit, alluvial deposit, debris flow or rock mass flow, alluvial fan and mass movement directly correlate with runoff generation and hydrological outputs. This is evaluated along transects across the test site running from divide to divide (adapted procedures from Schütt and Thiemann, 2001).

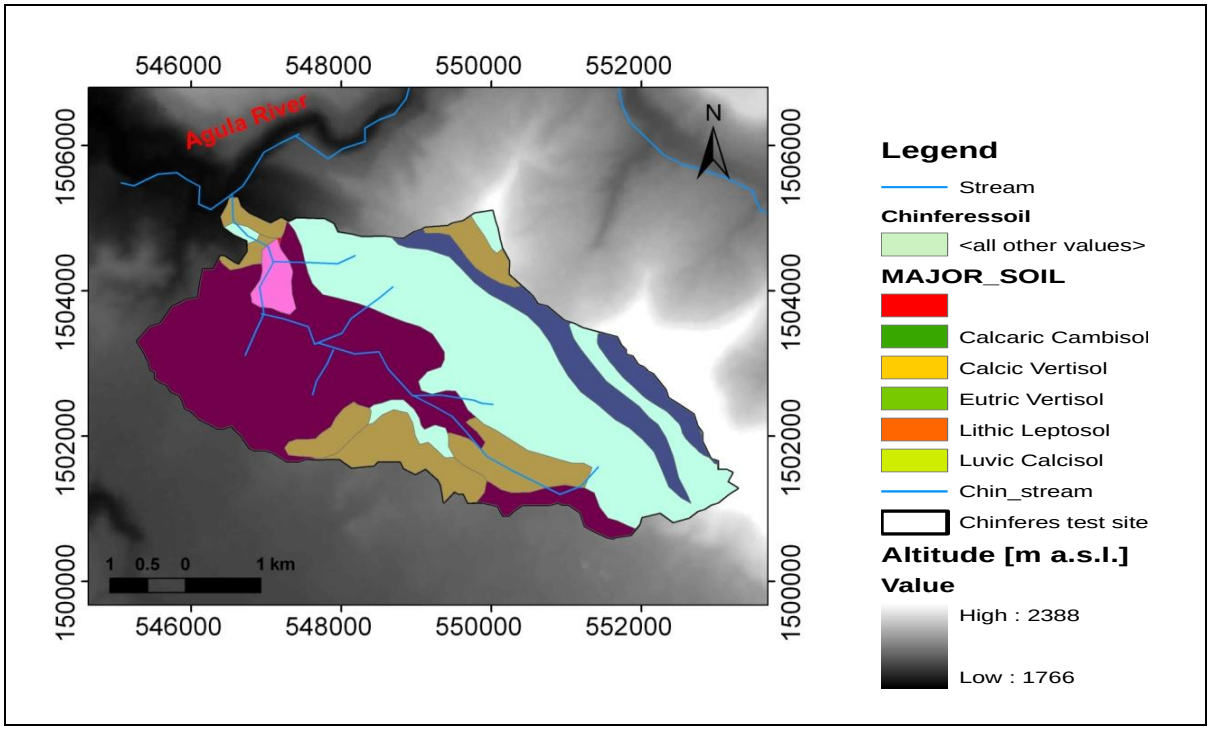

Figure 5-6: Soil map of the Chenferese test site (Data base: Jarvis et al., 2008).

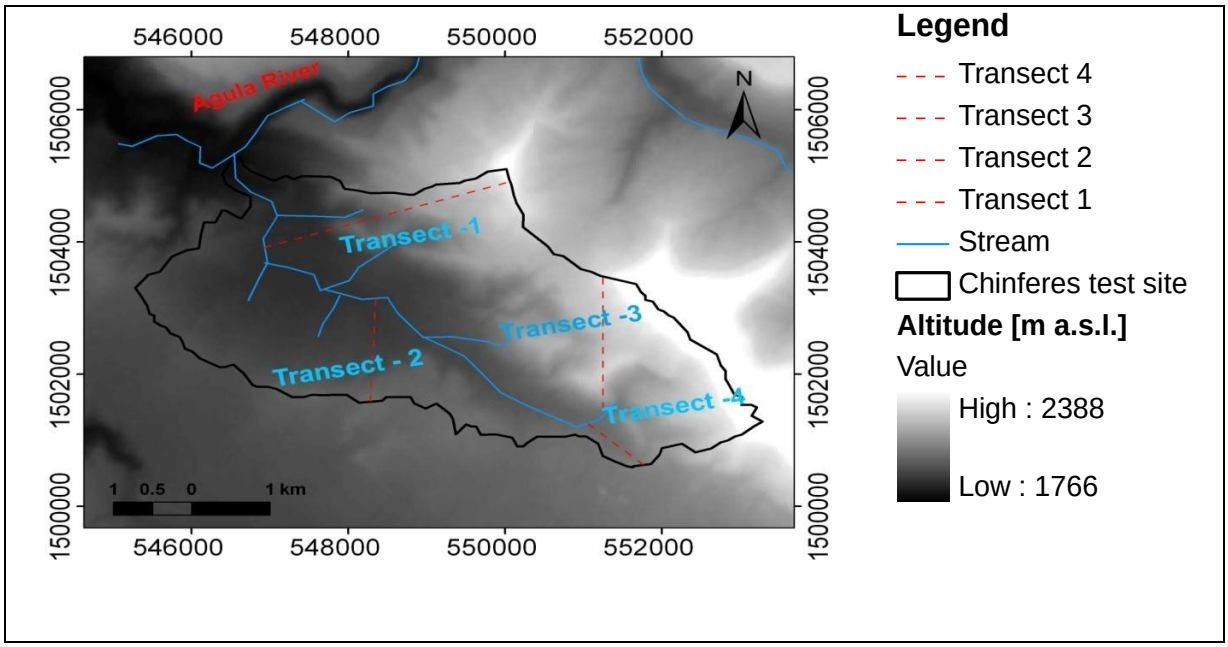

Figure 5-7: Location of geomorphological pedological transects in the Chenferese test site. (Data base: Jarvis et al., 2008)

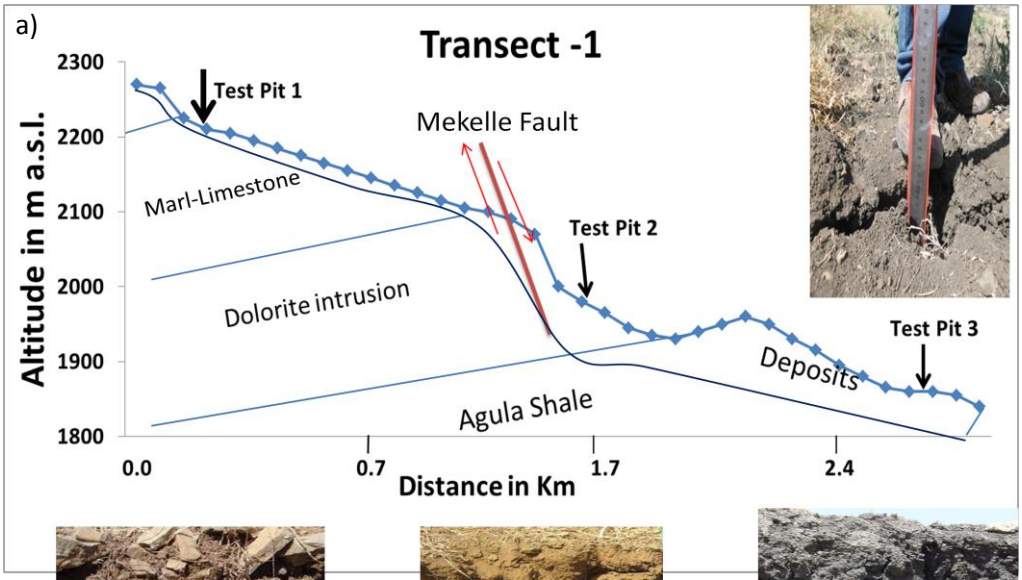

Calcaric cambisol

Calcaric Vertisol

Vertisol

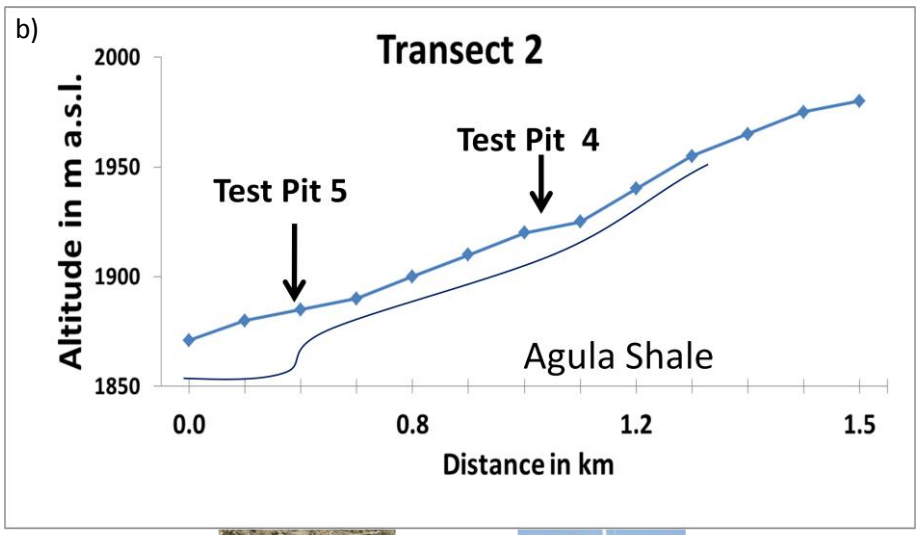

Vertisol

Chromic Vertisol

Figure 5-8: Transect 1 (a) and Transect 2 (b) of the Chenferese test site showing topographic level, bedrock and soils.

The flatness of the plateau in the southern part is affected by a northward flowing stream tributary to the Agula River. The central flat part shows depositions (Figure 5-8). In the northern part the steeped mountainous area corresponds to a cliff where the fault crosses the limestone. A small area in the western part is strongly affected by river erosion, forming a rugged topography. The Quaternary sediments are composed of alluvial and colluvial deposits, occupying the lower topographic terrains, structurally following the valleys.

The relief map prepared from the digital elevation model shows small variation between the northern and northeastern part of the Chenferese test site.

Alluvial deposit occurs in the wider parts of the flood plain, sometimes forming terraces. The alluvial deposits are predominantly composed of gravel, sand, silt and clay, moderately compacted and poorly sorted, characters which facilitate infiltration than runoff.The middle and the lower course of the river run through Agulae shales; colluvial deposits in this area have a good runoff potential. In contrast, colluvial deposits developed in dolerites, mostly occurring along the rivers upper course consist of loose to moderate compacted residual sediments, ranging in texture from clay to sand with rock fragments having different composition, size and shape. Similarly, the debris flow occurring in the foot zone of the limestone cliff due to the fault cuts the limestone as well as the alluvial fans have high infiltration capacity and most of the time reduce the surface runoff.

The type of land use varies with the topography or landform. Most of the hill tops are occupied by the churches and villages while the almost flat level areas are used for agriculture and as grazing land. Most of the land above the fault (northern part) is bare, locally covered with some bushes.

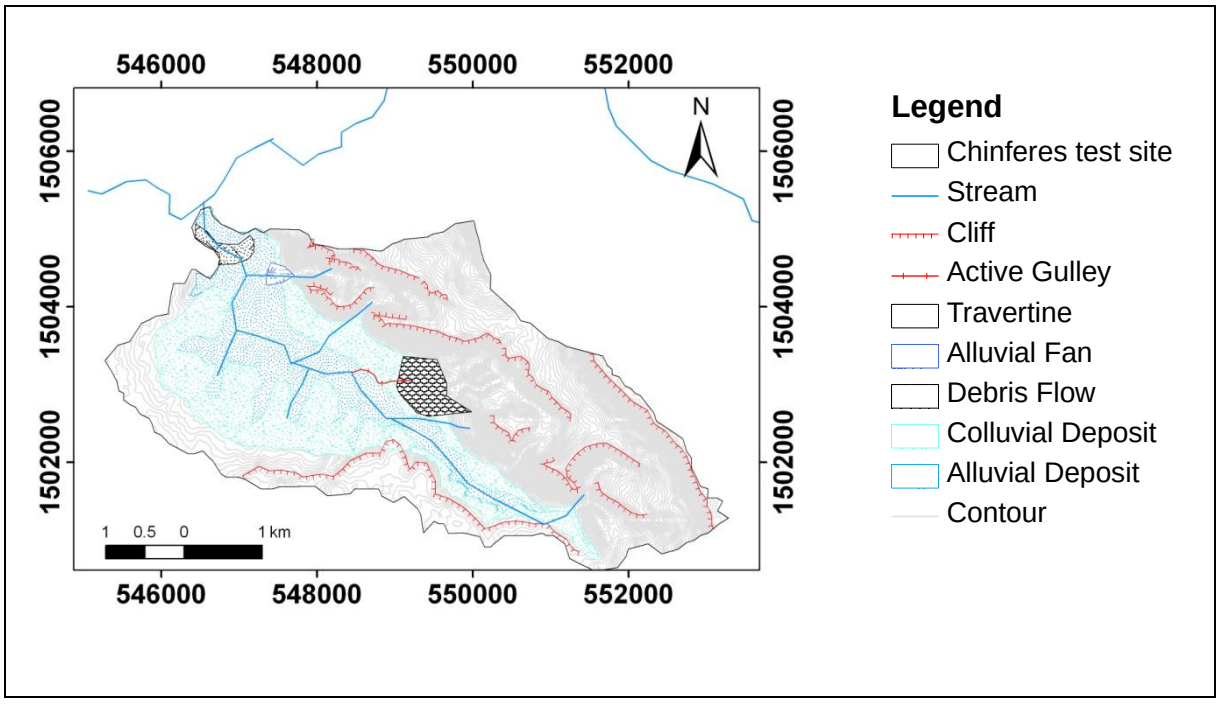

Figure 5-9: Geomorophological map of the Cheneferese test site (Data base: Jarvis et al., 2008).

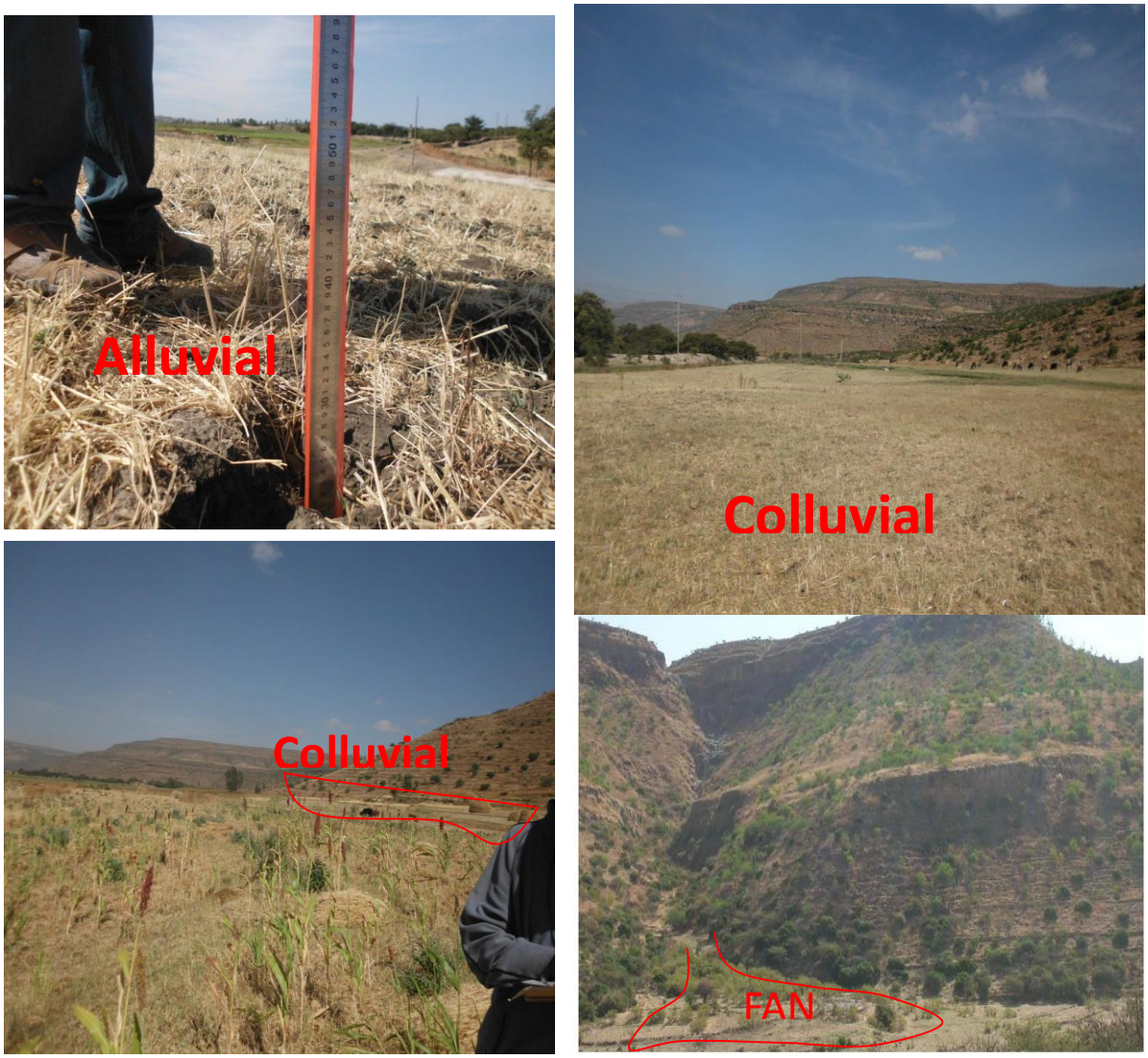

Figure 5-10: Geomorophological units in Chenferese test site: alluvial deposits (Photos 1 and 3, LT and LB); colluvial deposit (Photos 2 and 3, RT and LB); alluvial fan (Photo 4, RB).

5.2 Geregera test site

The Geregera test site is located in the Agula sub-basin in the eastern part of the study area. Geographically, it is located between 39º30'–39º45' E and 13º30'–13º45' N and has an aerial extent of about 8.02 km². The Geregera test site is located in the Atsbi Horst plateau which is undulating to rolling. The three major geomorphological units observed are mountains, hillslope and flood plains. The flood plain stretches from south-east to north-west and is bounded by highlands. The flood plains have deep alluvial deposits. The maximum peak reaches 2560 m a.s.l. in the Asagulo Ridge, which is found in the southern part of the study area and is dominated by Adigrat sandstone. The lowest point of the area is where its receiving stream discharge into the Agula River in the east.

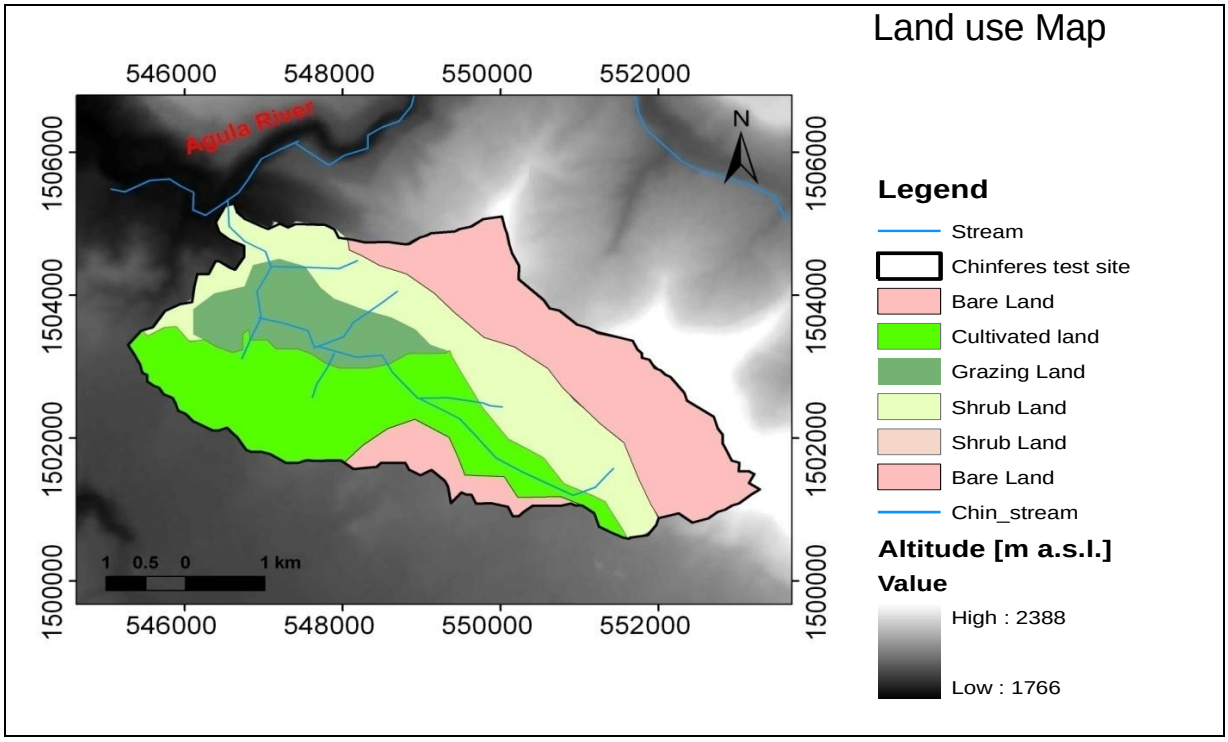

Figure 5-11: Land use of the Cheneferese test site (Data base: Jarvis et al., 2008).

The rainfall data of the Gergera test site are extrapolated from Wukro metrological station which is 14 km off the site. The mean annual rainfall totals 615 mm (1969–2010). Similarly, temperature data were taken from the Wukro meteorological station and extrapolated to the study area using 0.6°C increment for 100 m depression. The mean annual temperature of the area is 17.4°C (1991–2010).

Bedrock of the Gregera test site range from Precambrian to Quaternary age. 26.5% of the total basin area is covered by the basement rocks and their associated intrusives. Paleozoic sediments occur in 2.5% of the area, Mesozoic sediment occurs 31% of the area and Quaternary sediments cover 40% of the Geregera test site. Alluvial deposits occur at the valley bottom, overlying a Precambrian basement. The average thickness of the alluvial deposits is about 7 m (Gebreyohannes et al., 2010) (Figure 5-12).

The soil map of the Geregera test site is prepared based on the FAO soil map (1998). The soils found in the Geregra test site can be grouped into four different soil texture classes: sandy loam, clayey sand and sandy clay loam and clay. In the alluvial zone and in the Entecho sandstone Haplic Archsols are developed due to the sandy character of the parent material. Haplic Calcisols are developed in the lower course of the alluvial zone. Eutric Leptosols are developed in the colluvial deposits, Lithic Leptosols occur at the steeper slopes (Figure 5-13).

The northern part of Ethiopia is known for its mountainous and rough topography. The Atsbi-Wemberta area also shows such pronounced contrasts in the topography. Generally, the Geregera test site is plateau like with an average elevation of 2350 m a.s.l.

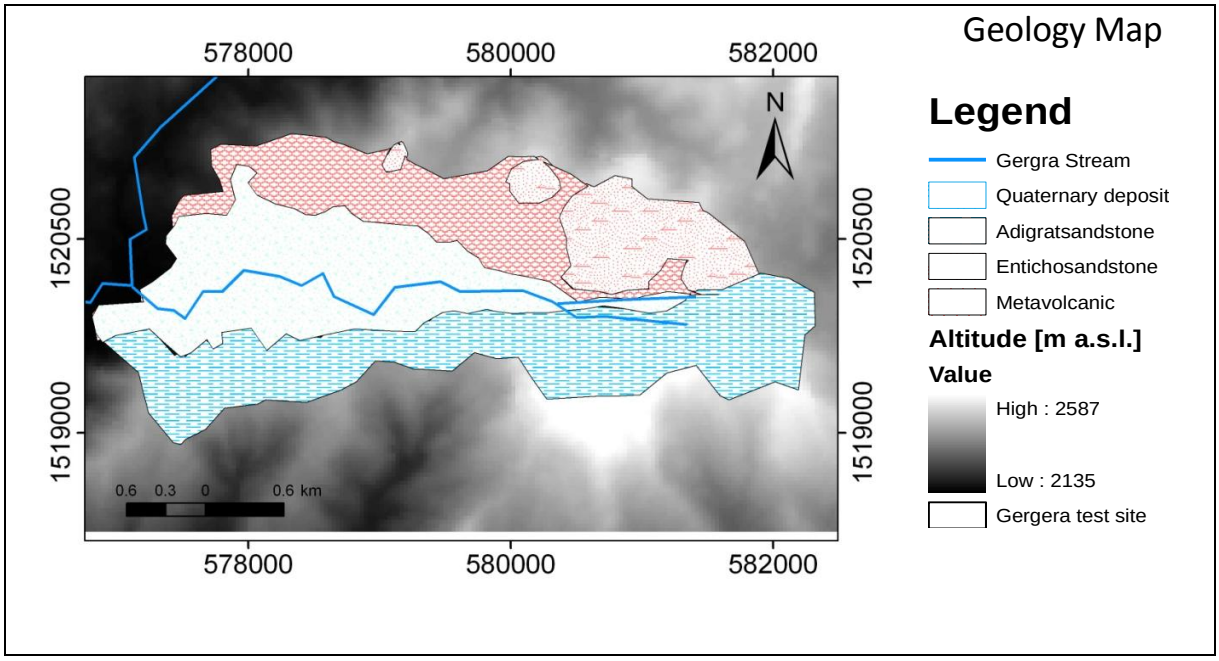

Figure 5-12: Geological map of Gergera test site (Data base: Jarvis et al., 2008; Gebreyohannes et al., 2010).

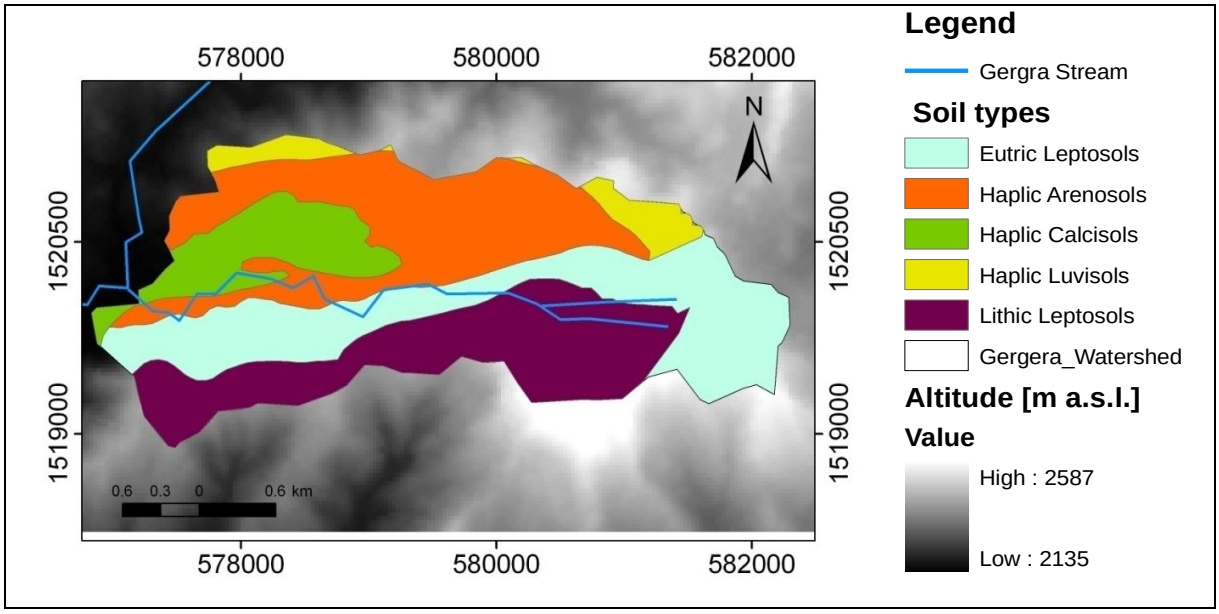

Figure 5-13: Soil map of Geregera test site (Data base: Jarvis et al., 2008).

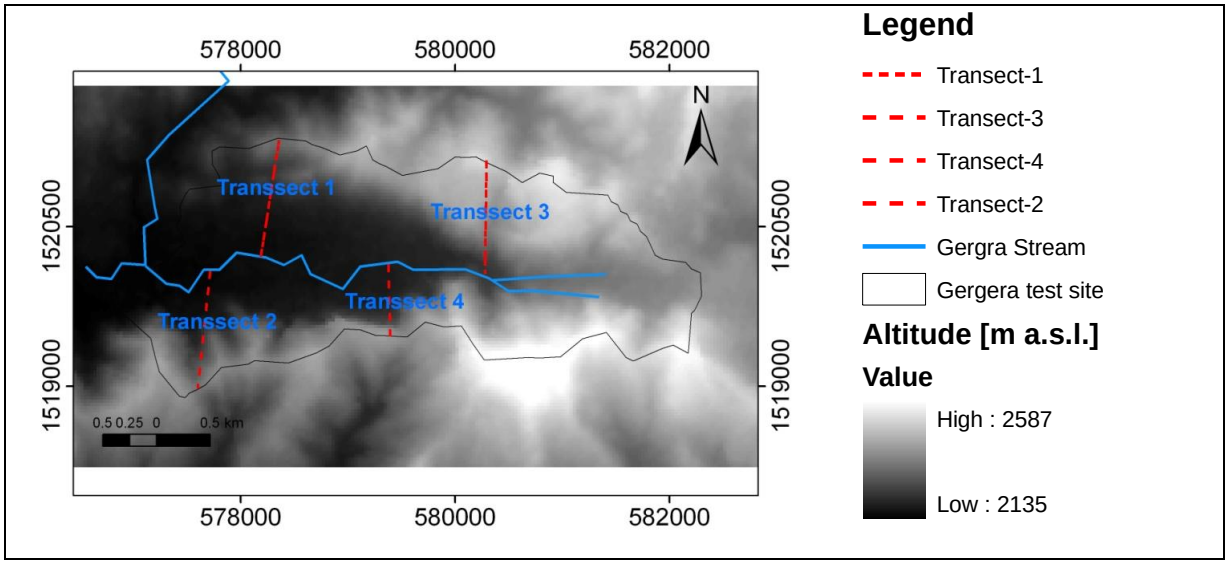

Figure 5-14: Location of geomorphological pedological transects in Gergera test site (Data base: Jarvis et al., 2008).

a)

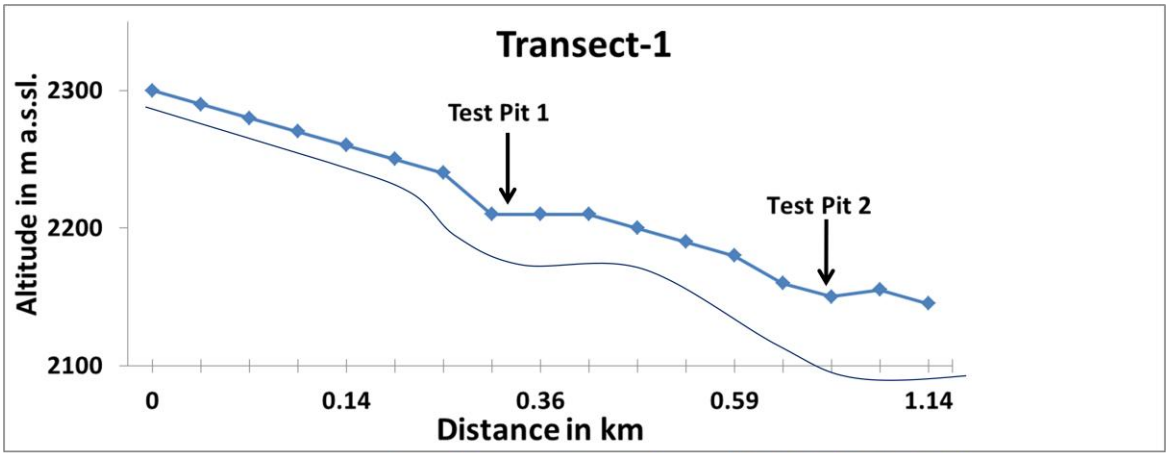

Loamy sand

Sandy loamy

b)

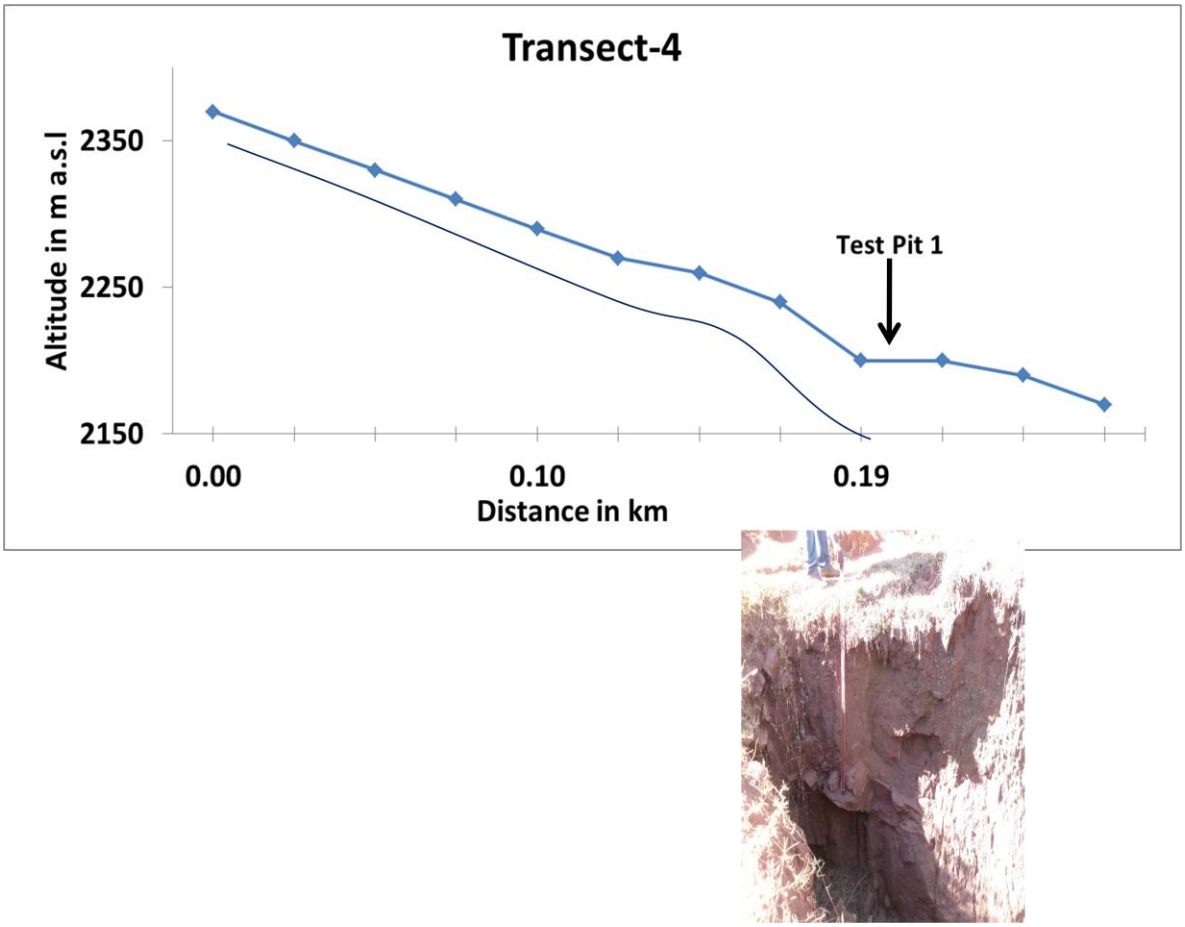

Figure 5-15: Transects 1 (a) and Transect 4 (b) of the Geregera test site showing topographic level, bedrock and soil.

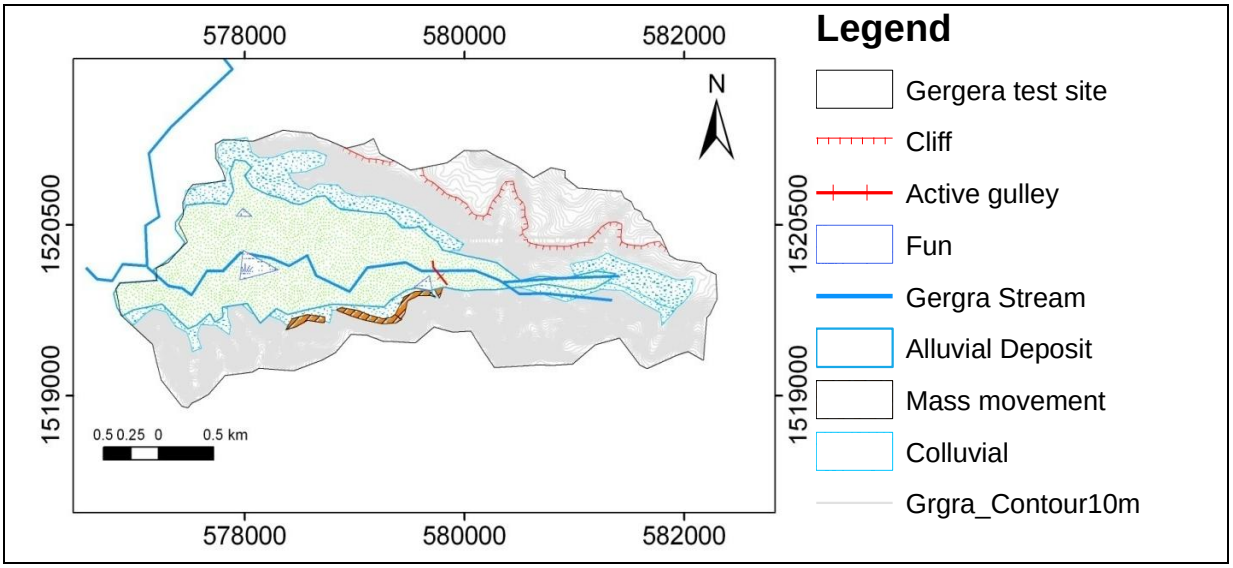

Figure 5-16: Geomorophological map of Geregera test site (Data base: Jarvis et al., 2008).

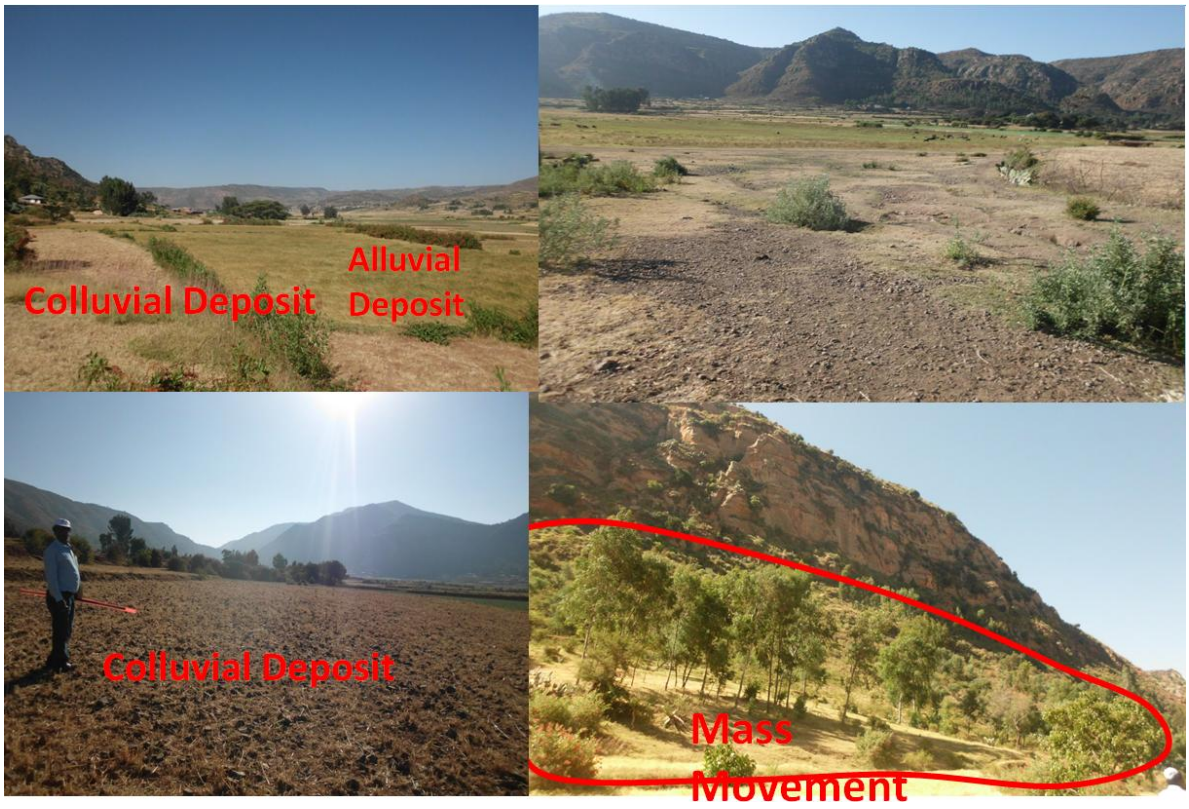

Figure 5-17: Geomorophological units; colluvial-alluvial (Photo 1, LT); overview of alluvial area (Photo 2, RT); colluvial deposit (Photo 3, LB); mass movement (Photo 4, RB).

Along the transects (Figure 5-15) it gets obvious that the thickness of the soil varies with slope and the resistance of geological formations for erosion. The alluvial deposit in the test site consists of sand, gravel, sandy gravel and clay. Even if these units are distributed variably in the area, sand dominates.

The alluvial deposits hold water during the rainy periods due to their high permeability and high soil depth and supplying water for agriculture and domestic uses. The sand unit, which corresponds to the weathered part of the Entecho sandstone occurs in the south and southeast and west of the test site. Colluvial deposits are coarse grained and partly well sorted. In the northern part due to the steep slopes, the material is displaced by mass movements and deposited as debris at the foot slope. Most of the settlements are located in the colluvial deposits.

The land cover of the Geregera test site is differentiated into seven different types. The dominant partof the hilly and mountainous is bare land, only locally covered by a thin soil layer. The flat land between the highlands is used for cultivation and grazing land. In the eastern part of the basin close to the divide, a swampy area occurs due to emerging springs at the contact of the Adigrat sandstone and Metavolcanic rocks. Only a small area around the Church, found on the alluvial fan of the confluence of two of the test sitse major source stream, is covered by forest.

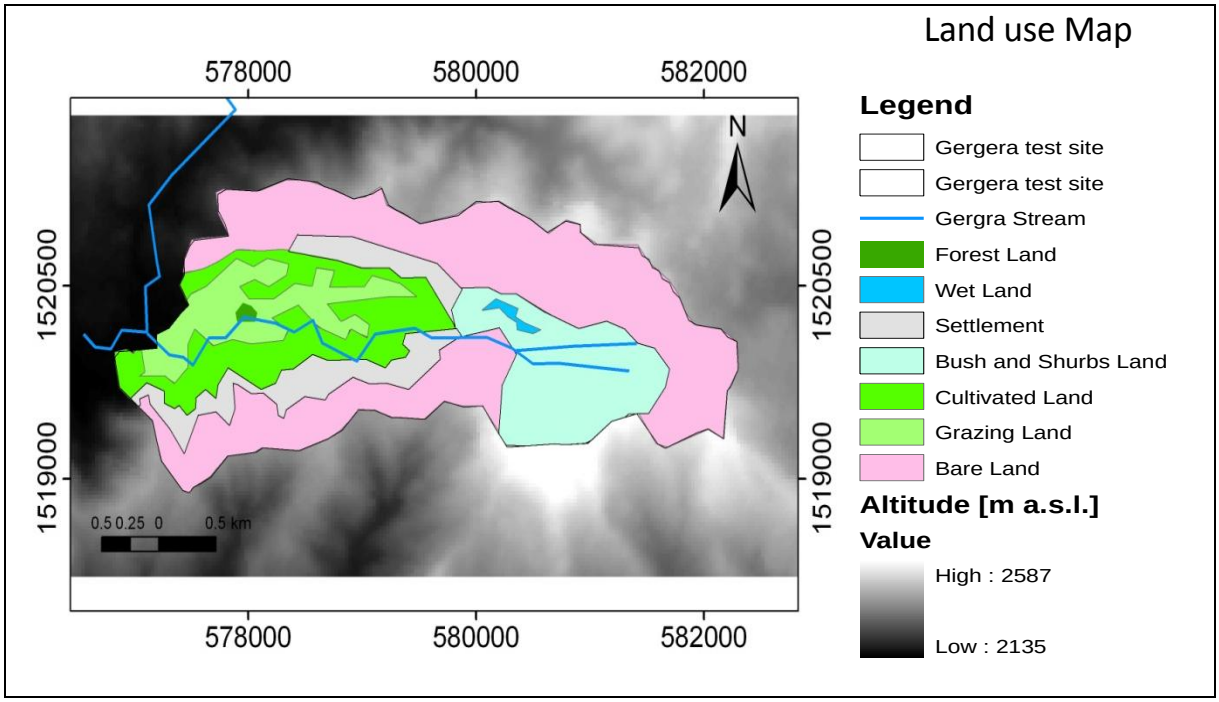

Figure 5-18: Land use map of Geregera test site (Data base: Jarvis et al., 2008).

5.3 Laelay Wukro test sites

The Laelay Wukro test site is located in the Genfel sub-basin. Geographically it is located between 39°36′–39°38′ E and 13°46′–13°47′ N and has an areal extent of about 12.48 km². The relief of the Laelay Wukro test site is dominated by steeply dissected valleys and an undulating to rolling plateau with some buttes. The undulating to rolling plateau as well as the head water area of the drainage system is developed Precambrian metavolcanics and met-sediments (Bosellini et al., 1997; Gebreyohanness et al., 2010) (Figure 5-19).

The Laelay Wukro test site had its own automatic weather station (2003–2008); the Wukro meteorological station is the nearby station. Rainfall data shows that the mean annual rainfall (1969–2010) is 615 mm. The mean annual temperature (1991–2010) is 19.4°C.

The bedrock of the Laelay Wukro test site is dominated by Precambrian metavolcanics, metasedmients and small patches of metalimestone. The metavolcanic unit covering more than half of the watershed area. They highly dissected valley in the northern part and forms an undulating plateau in the southeastern parts (Gebreyohaness et al., 2010). At the valley bottoms locally Quaternary alluvial deposit occur.

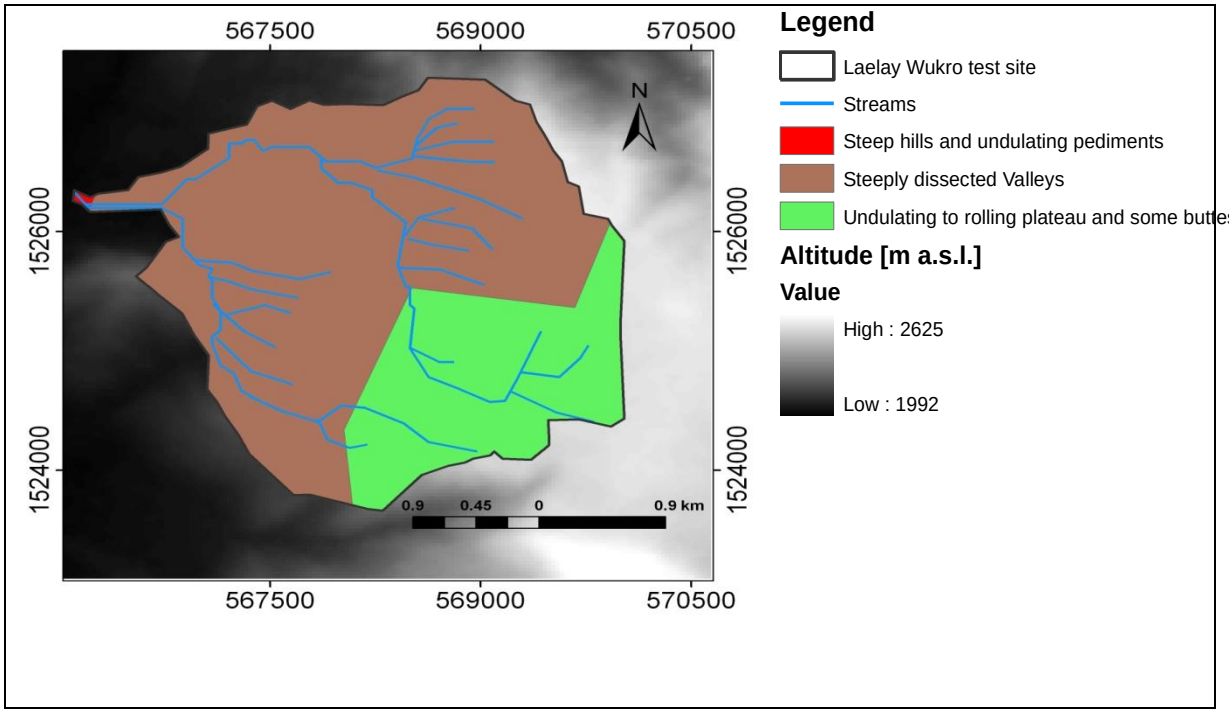

Figure 5-19: Landform units of the Laelay wukro test site (Data base: Jarvis et al., 2008).

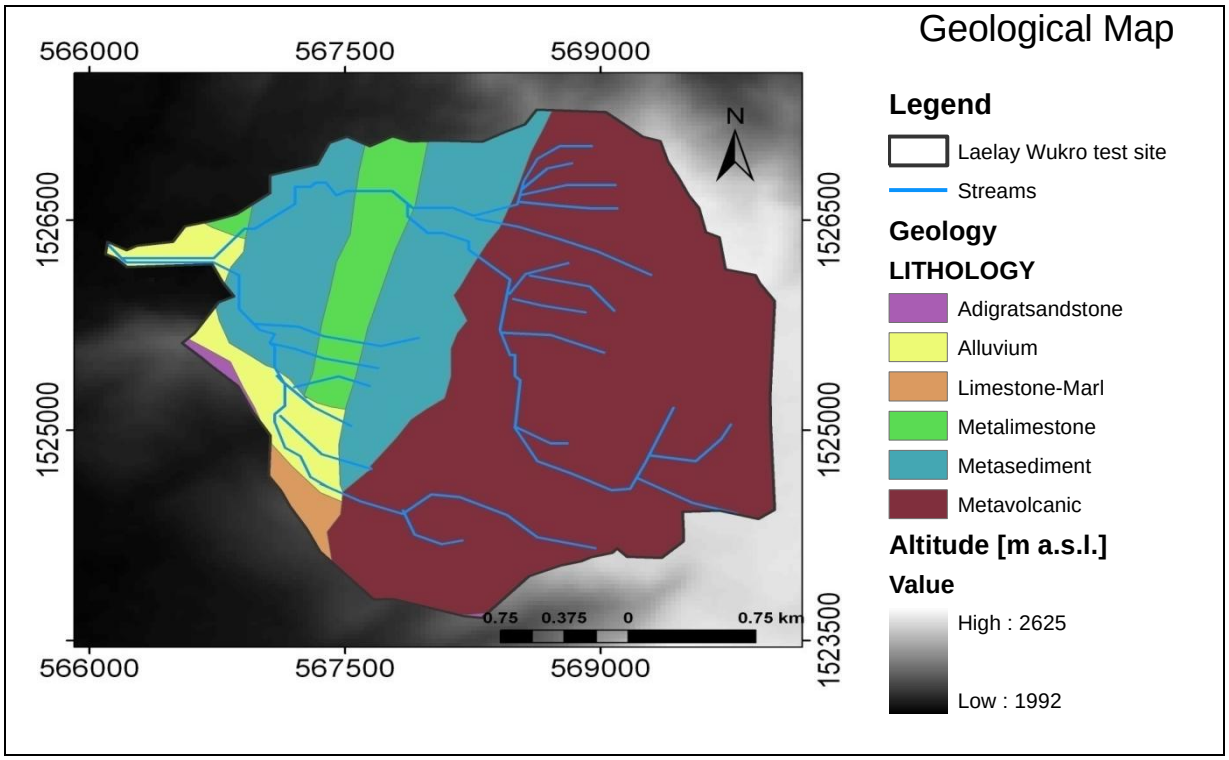

Figure 5-20: Geological map of Laelay Wukro test site (Data base: Jarvis et al., 2008).

The soil map of the test site is prepared based on the FAO soil map (1998). The dominant soil in the watershed is Lithic Leptosol which is shallow in depth. Texturally, the Lithic Leptosol is classified as silty clay loam and silt loam.

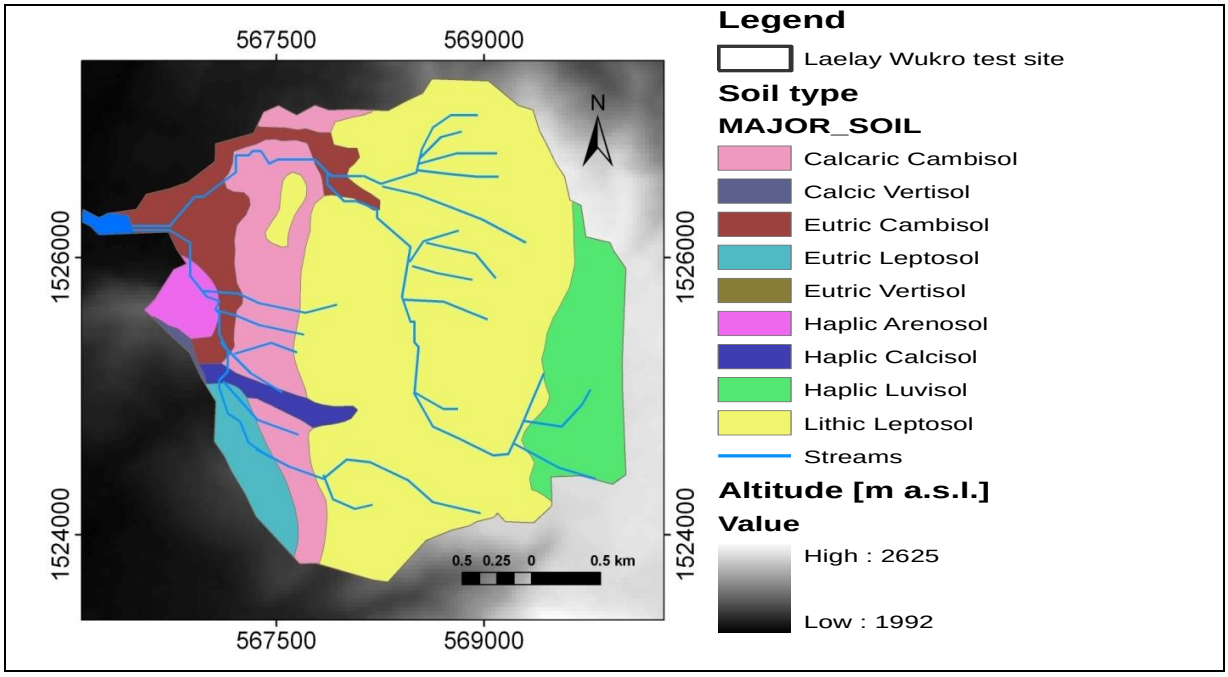

Figure 5-21: Soil map of the Laelay Wukro test site (Data base: Jarvis et al., 2008).

The Laelay Wukro test site is located in the highly dissected Genfel graben valley. The watershed is divided into mountainous with plateau peaks, hill sides with steep slopes, undulating areas with resulting steeper, highly eroded west facing slopes and gentle slope along the flood plain. The whole area is dominated by intensive agriculture.

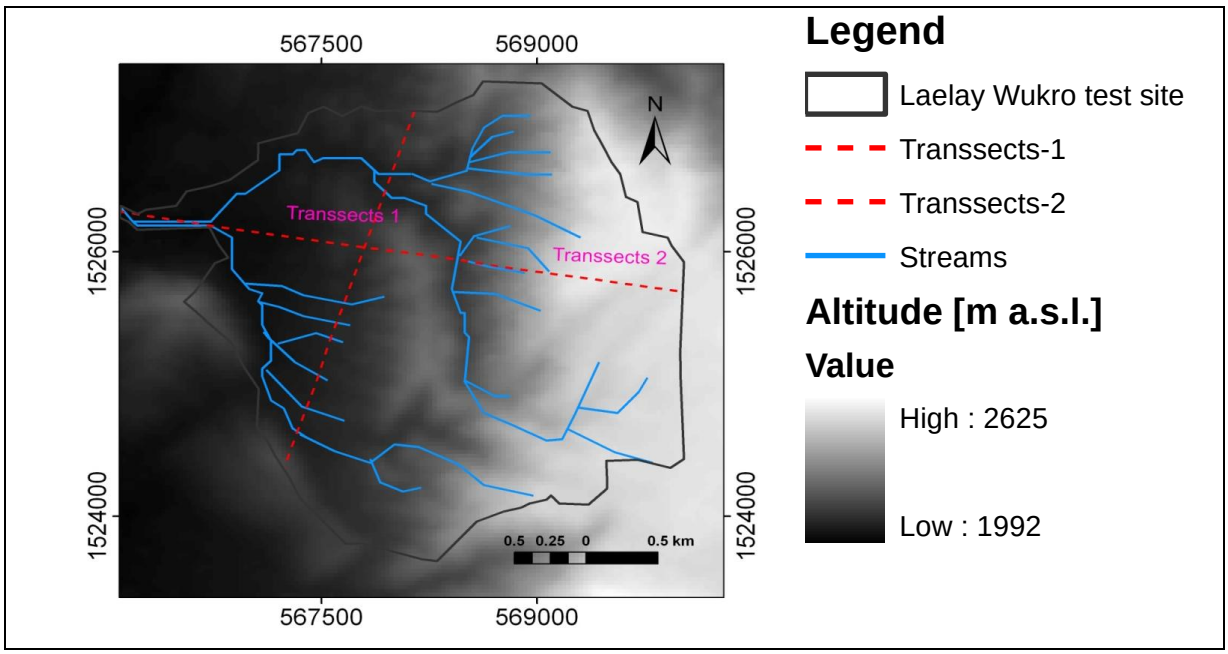

Figure 5-22: Location of geomorphological pedological transects in Laelay Wukro test site (Data base: Jarvis et al., 2008).

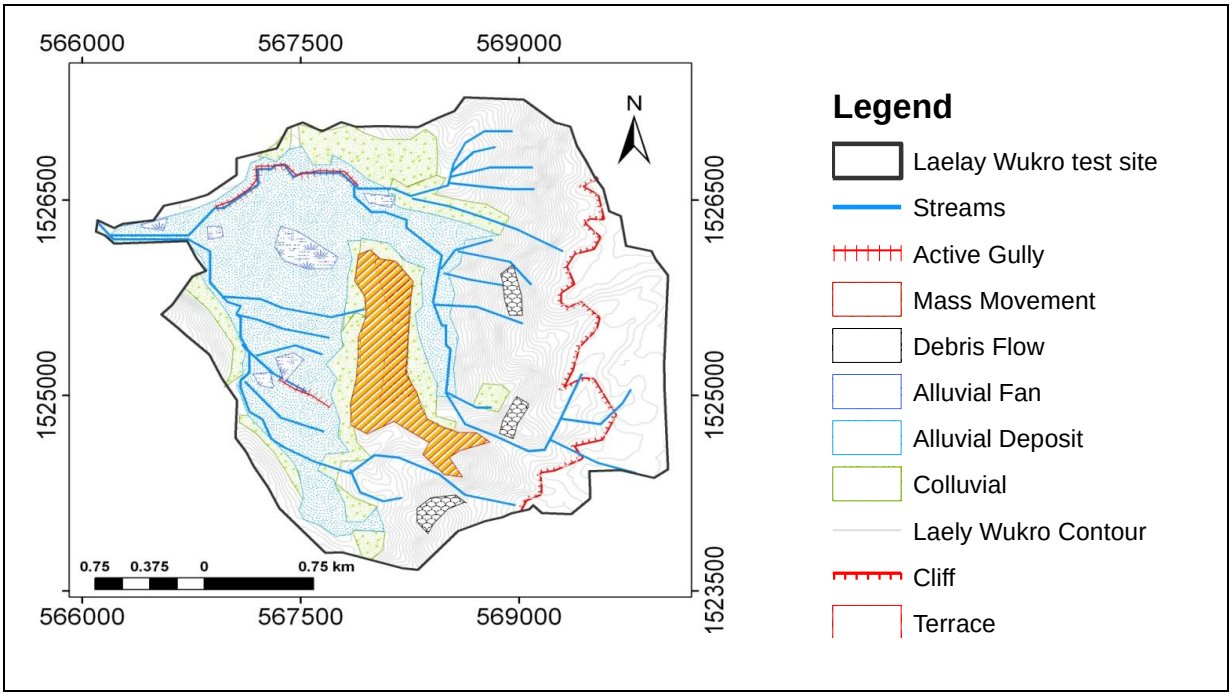

Figure 5-23: Geomorophological map of Laelay Wukro test site (Data base: Jarvis et al., 2008).

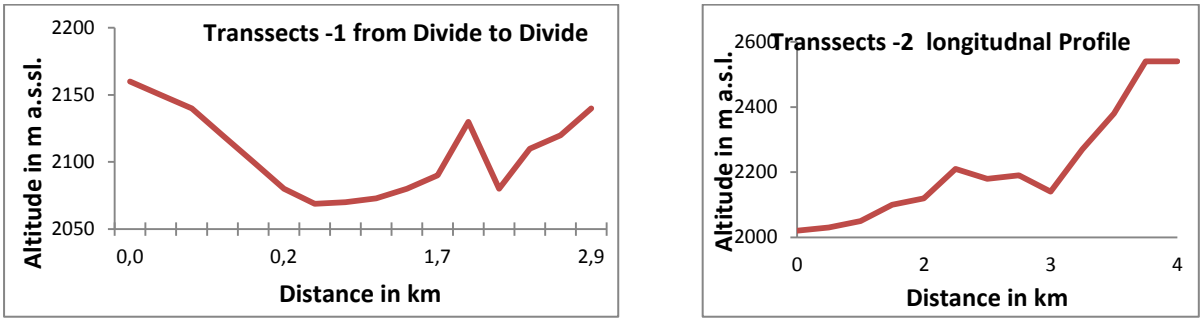

Figure 5-24: Detail profile along the Transects (cf. Figure 5-23).

Table 5-2: Profile along the transects: Details of landform and geology.

Transect 1				Transect 2			
Elevation	Lithology	Soil Type	Landform	Elevation	Lithology	Soil Type	Landform
2160-2100	Limestone-marl	Eutric Leptosol	Hillyslope	2020-2040	Alluvium	Eutric vertisol	Alluvial Deposit
2100-2080	Limestone-marl	Eutric Leptosol	Colluvial deposit	2050	Meta-sediment	Calcaric cambisol	Fan
2080-2069	Alluvial	Cacaric Cambisol	Alluvial deposit	2070-2200	Meta-sediment	Lithic Leptosol	Colluvial
2060	Meta-sediment	Eutric Cambisol	Alluvial Fan	2210	Meta-sediment	Lithic Leptosol	Terrace
2110-2120	Meta-sediment	Eutric Cambisol	Colluvial deposit	2180	Meta-volcanic	Lithic Leptosol	Colluvial
2140	Meta-sediment	Cacaric Cambisol	Hilly slope	2150-2500	Meta-volcanic	Lithic Leptosol	Hilly slope

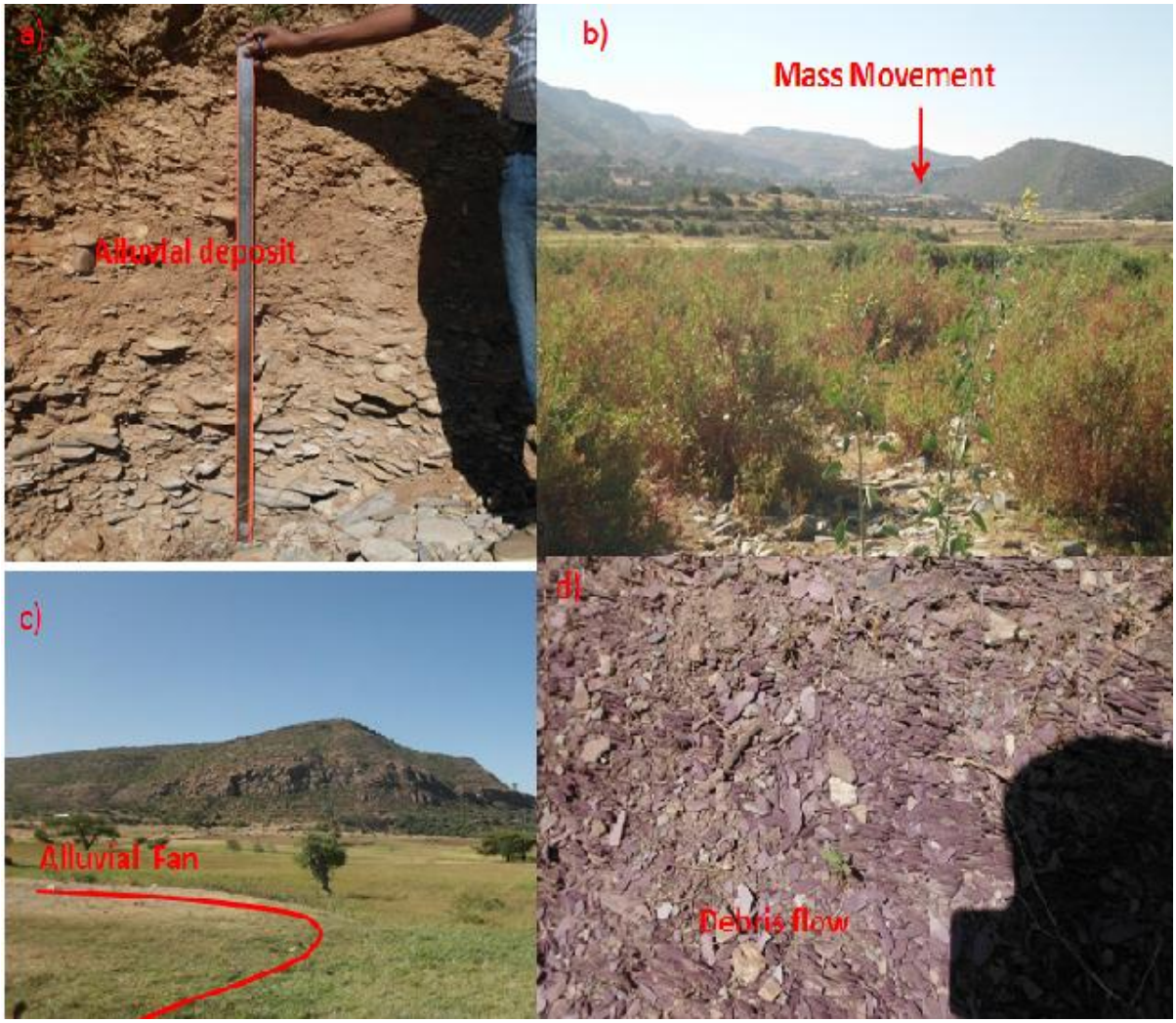

Figure 5-25: Geomorophological units of the Laelay Wukro test site: Alluvial deposit (a); mass movement (b); Alluvial fan (c); debris flow (d).

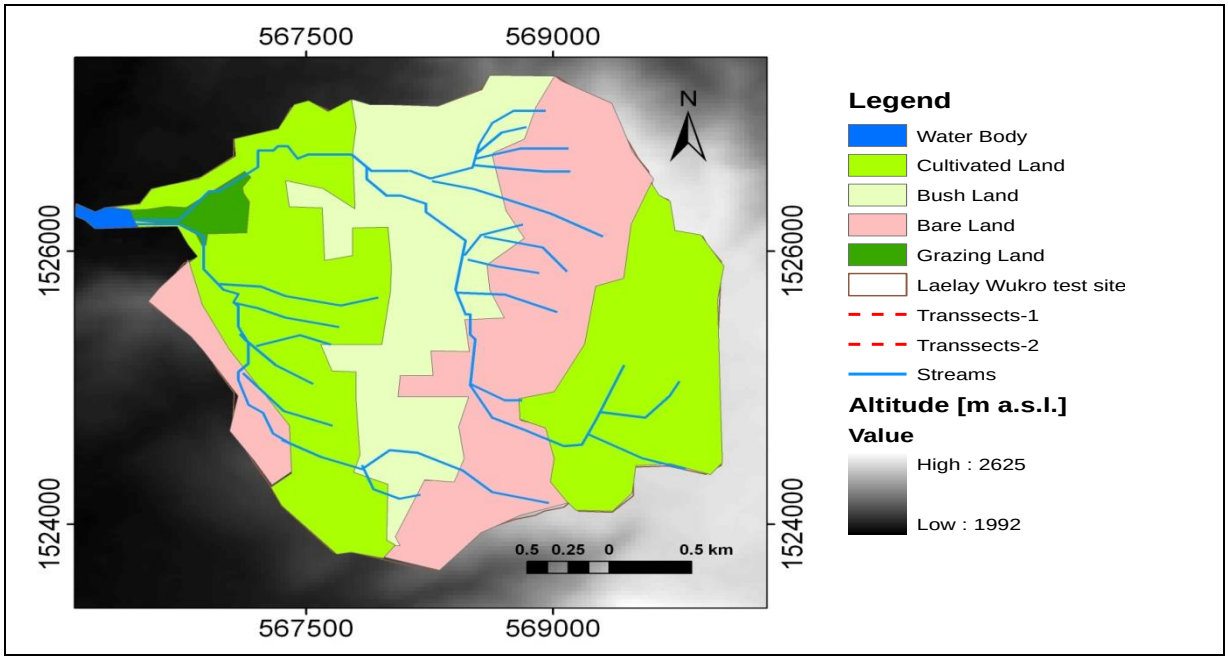

Figure 5-26: Geomorophological map of Laelay Wukro test site (Data base: Jarvis et al., 2008).

5.4 Abraha-We-Atsebha test site

The test site is located near Abraha-We-Atsebha village in Suluh sub-watershed. Geographically, it is located between 39°31′–39°33′ E and 13°49′–13°51′ N. It has an areal extent of 5.4 km^2. The Wukro meteorological station is the closest weather station for long time analysis of rainfall and temperature data. Mean annual rainfall is 615 mm (1969–2010). The average temperature is minimum 10.4°C and max. 26°C with a mean of 18.2°C

The predominaetly bedrock in the test site is the Adigrat sandstone. The Adigrat sandstone is friable, massive, and red to gray, porous in texture, mainly underlain by the Limestone units and meta-congromalite (Gebreyohannes et al., 2010). In the headwater area, limestones outcrop on the southeastern ridges while metaconglomerates dominate the northeastern ridges. Entecho sandstone forms the slopes northeast of the confluence in the Suluh River (Figure 5-27)

The soil map of the Abraha-We-Atsebeha test site is prepared based on FAO soil map (1998). The soils in the test site are dominated by very shallow Leptosols and Haplic Arenosols. The Abraha-We-Atsbeha test site is located in the highly dissected Genfel sub-basin. The test site is divided into mountainous area with plateau peaks, steep hill slopes, undulating plateau areas and in steep highly eroded west facing slopes.

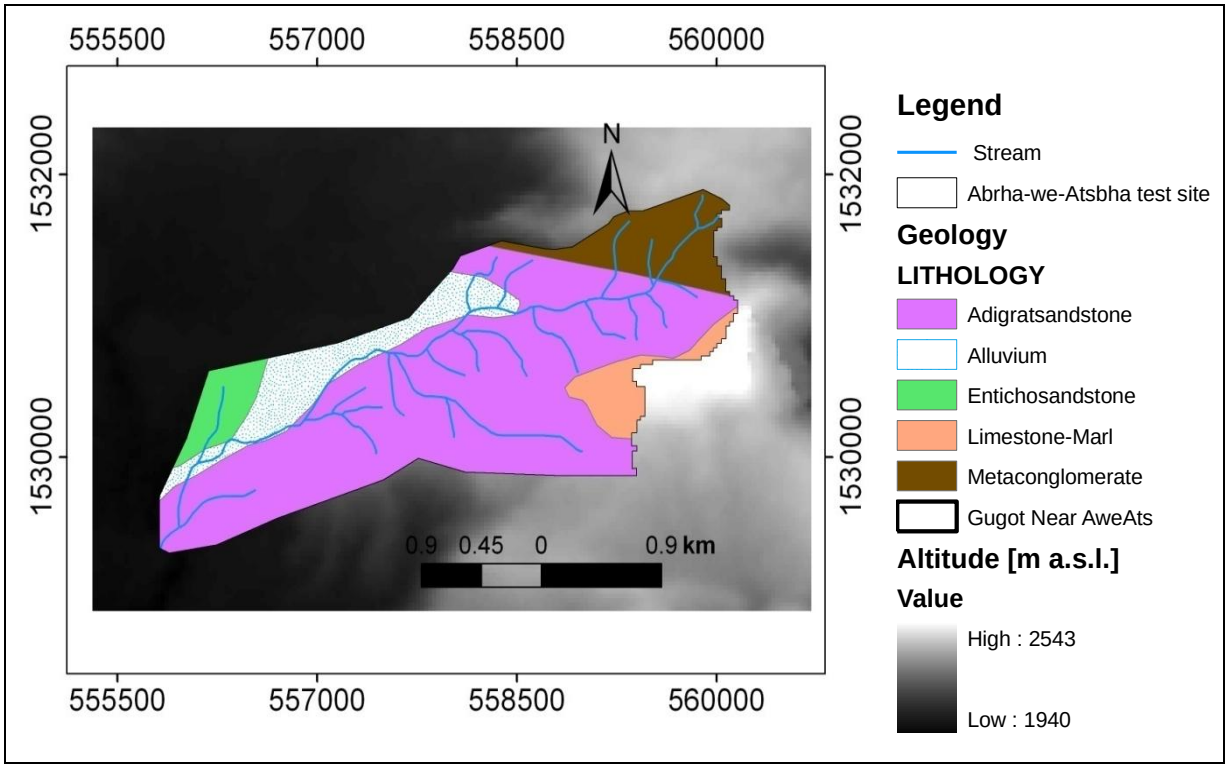

Figure 5-27: Geological map of Abraha-We-Atsebha test site (Data base: Jarvis et al., 2008).

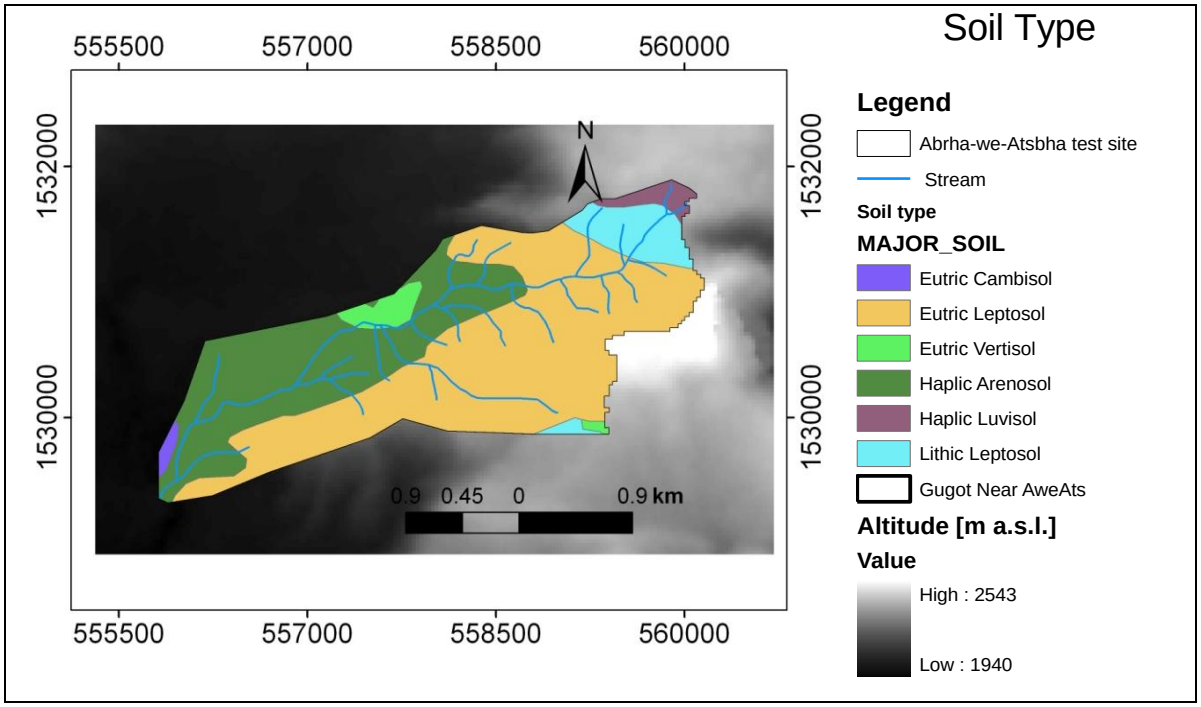

Figure 5-28: Soil map of the Abrah-We-Atsbeha Test site (Data base: Jarvis et al., 2008).

The relief of the area corresponds to a plateau followed bounded by dissected steep slopes in the middle part followed by flat flood plain in the footslope area. In this area soil erosion, weathering and masswasting is observed (Hunting Technical service, 1976). Due to the strong relief mass movements and intensive mass transport occurs. At the slope break from the steep slopes into the flat area, alluvial fans and colluvials are deposited.

5.5 Tsankanet test site

The Tsankanet test site is located near Senkata village in the Suluh sub-basin. Geographically it is located between 39°32′-39°34′ E and 14°00′–14°02′ N and has an areal extent of 19 km^2.The Tsankant test site is situated in the north-western part of the Suluh sub-basin. To the East the test site is demarcated by the Atsbi Horst.

The Senkata meteorological station is located in 5–6 km distance to the Tsankanet test site; the data of the Senkata metrological station are used for the Tsankanet test site. The mean annual rainfall is 715 mm (1973–2010). Temperature data from Senkata weather station were extrapolated to the study area using 0.6°C increment for 100 m depression. Resulting annual temperature average is minimum 9.4°C and max. 25°C (2000–2010) with a mean of 17.2°C.

The northern part and of the Tsankanet test site is entirely covered by the Enticho sandstones. The area is a very gently undulating plain and most of the area is used for agriculture. South of the Enticho sandstone Precambrian rocks outcrop, dominted by meta-volcanics, followed by meta-conglomerates (Gebreyohannes et al., 2010).

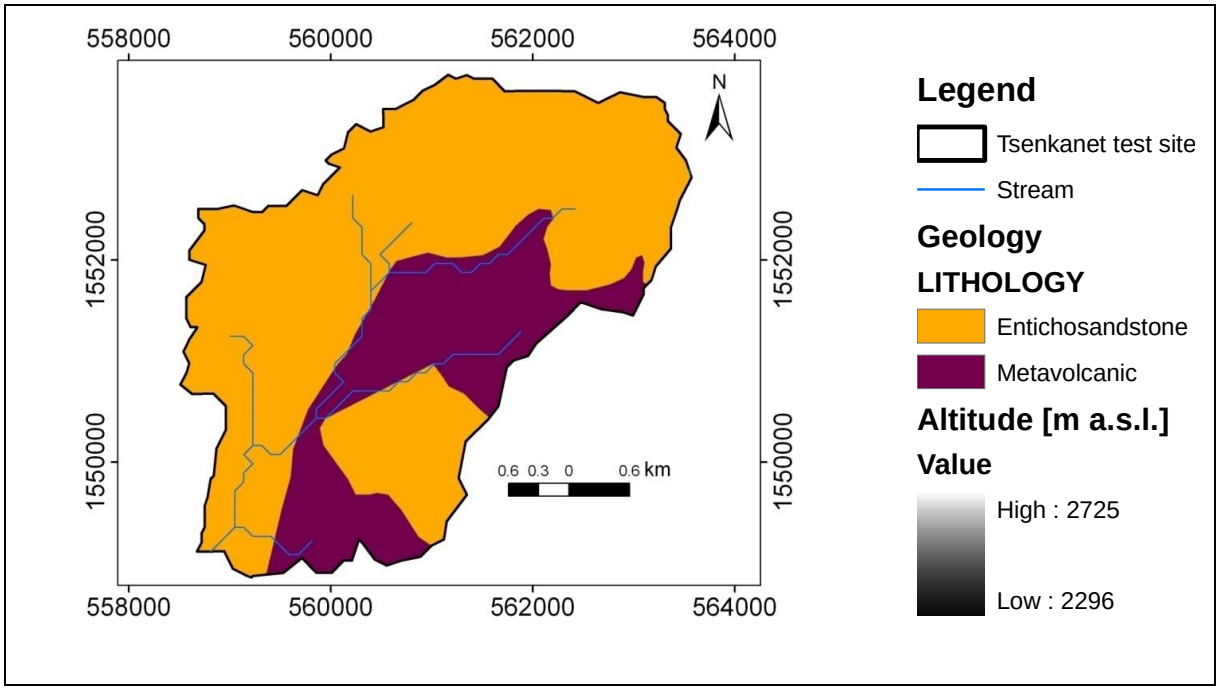

Figure 5-29: Geological map of the Tsankanet test site (Data base: Geology: Gebreyohanness et al., 2010; Jarvis et al., 2008).

The dominating soil type for Tsinkanet test site is Eutric cambisol; in the alluvial zone Vertisols dominate. Leaching of the weathered material and its accumulation in the depressions resulted in coarse textured and acidic soils on the higher locations and more fine textured and base saturated soils in the depressions.

The northern part of the test site is entirely covered by the Enticho sandstones. The area is a very gently undulating plain and most of the area is used as agricultural land. Virgo and Munro (1978) found a relatively high base saturation of the soils despite high quartz content which has its origin in the sandstone. The reason for this rather high base saturation was attributed to the calcitic cement in the sandstone (Virgo and Munro, 1978).

The Tsankanet test site corresponds to a gently undulating plain. The flat flood plain in the center of the main valley has very low relief. Adjoing colluvial deposits have a high permeability and low runoff coefficients. Where the texture of the alluvial and colluvial deposit is dominated by clays soils are mainly Vertisols. They show prominent cracking and sinkhole features during desiccation. Locally extensive deposition of sand and gravel has covered the Vertic Cambisols but cracking pattern is exposed. The valleys show a dendritic pattern. The central drainage lines are rarely incised more than one meter and in many cases a distinct channel is even missing.

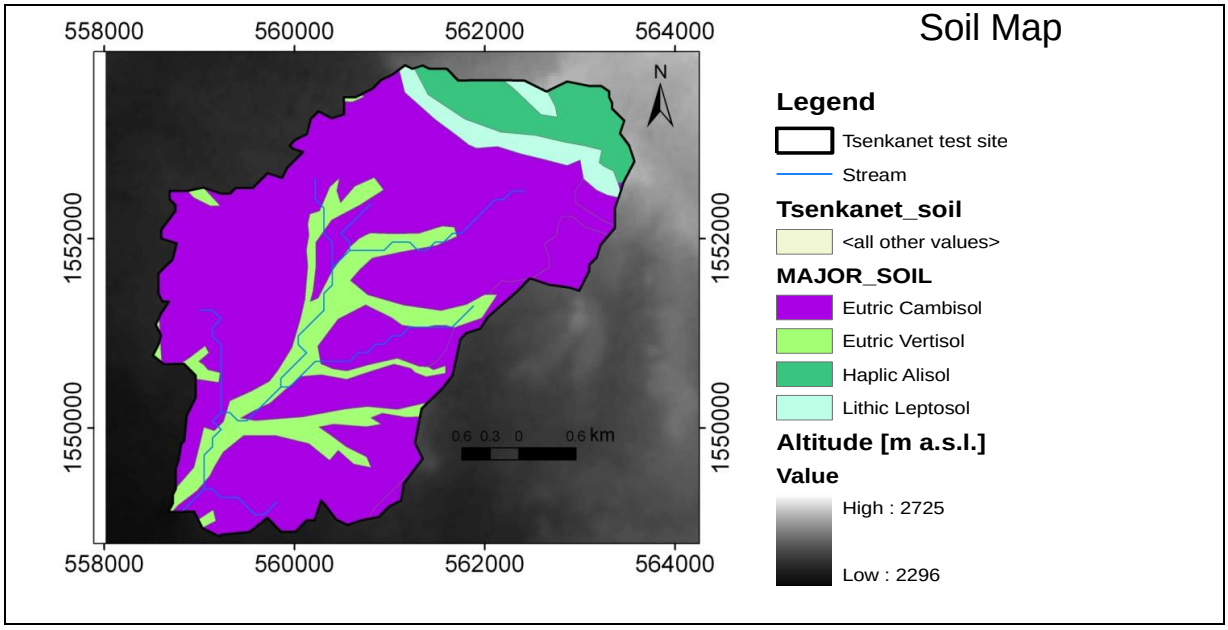

Figure 5-30: Soil Map of Tsankenet test site: (Data base: Jarvis et al., 2008).

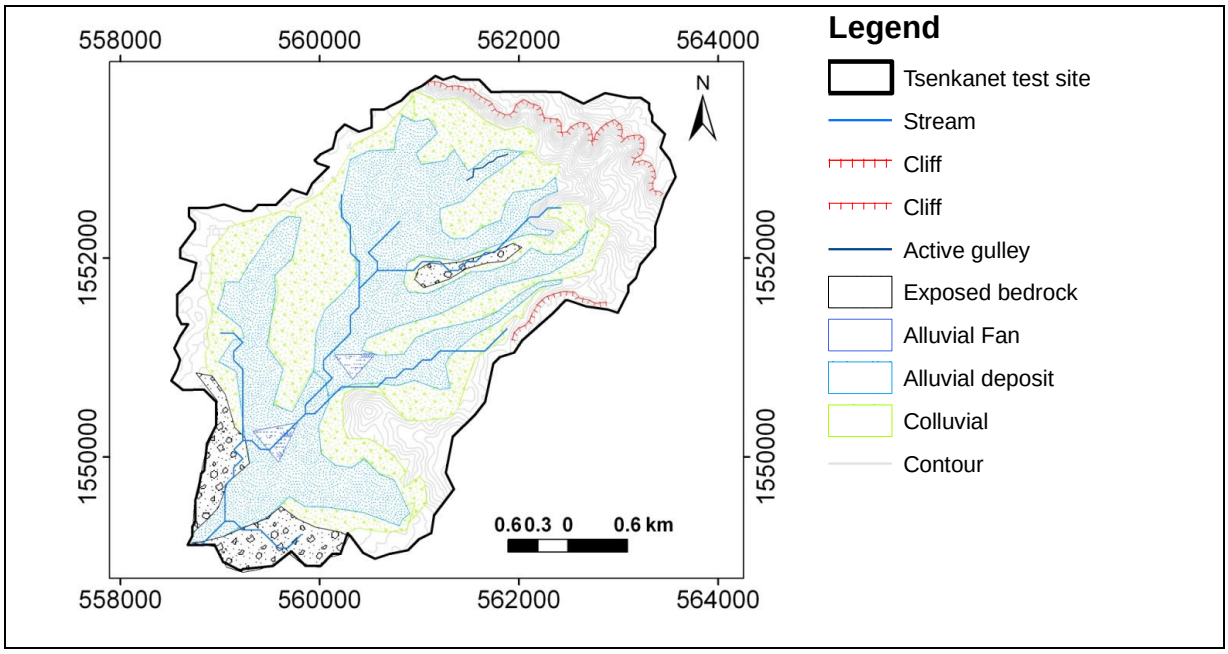

Figure 5-31: Geomorophological maps of the Tsananet test site (Data base: Jarvis et al., 2008).

5.6 Teghane test site

The Teghane test site is located near Atsbi village in the Genfel sub-basin. Geographically it is located between 39°44′–39°45′ E and 13°53′–13°54′ N and has an areal extent of about 6.32 km^2. The rainfall of Tegehane test site is interpolated from Wukro and Atsbi metrological stations. The mean annual rainfall in the area totals 636 mm (1973–2010). Similarly, temperature data is taken from the Wukro

meteorological station, and extrapolated to the study area using 0.6°C increment for 100 m depression. The annual temperature of the area averages 14°C (1991–2010).

Bedrock of Teghane test site is composed of Precambrian metavolcanics in the west Precambrian metasediment in the east and Enticho sandstone in the north (Gebereyohannes et al., 2010). In the central part of the area a large undulating plain occurs with rather deep soils developed which are used for cultivation (Hunting Technical Services, 1976). In the eastern, northern and locally in the central part outcrops of Enticho sandstone occur, forming mesas or smaller buttes (Hunting Technical Services, 1976). However, most of the area is covered by metavolcanic rocks.

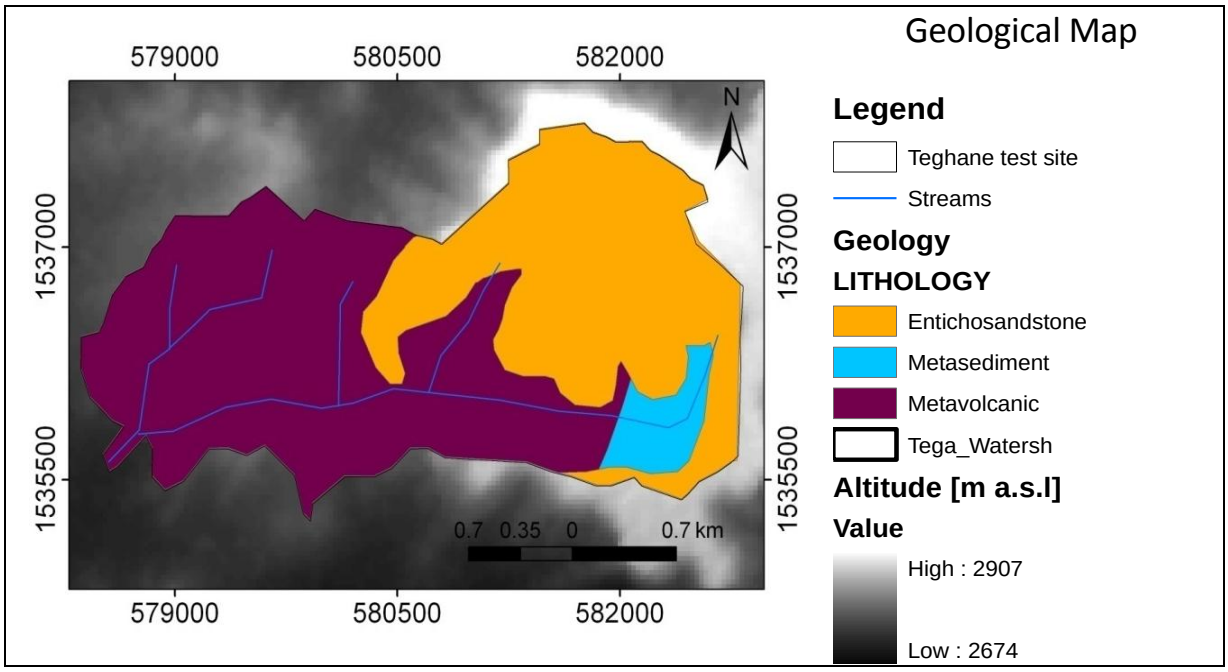

Figure 5-32: Geological map of the Teghane test site (Data base: Geology: Gebreyohanness et al., 2010; Jarvis et al., 2008).

On the undulating plains, moderately deep, fine textured Luvisols are found. In the alluvial and colluvial deposits, deep Cambisols and Luvisols are developed. In the northwestern part landforms are characterized by the prominent mesa of the Enticho sandstone with shallow Haplic Alisols and Luvisols are developed on the plateau (Hunting Technical Services, 1976). In the Teghane test site landforms are characterized by mesas of Enticho sandstone. The slopes of the mesa are very steep and rocky. At some areas landslides occur and material is deposited at the foot of the hills. The valley centers are alluvial deposits, which are used for grazing. Erosion is less apparent there, but sever erosion occurs on steeper land; these areas are often deeply dissected and have soils with shallow depth.

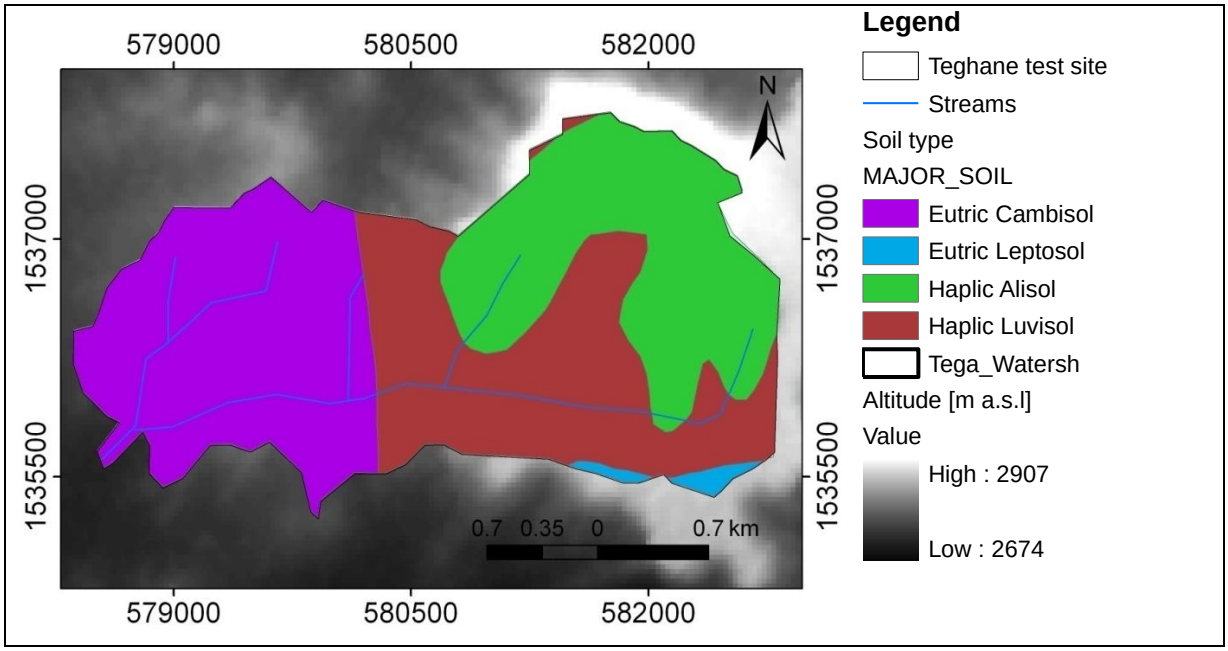

Figure 5-33: Soil Map of Teghane test site (Data base: Jarvis et al., 2008).

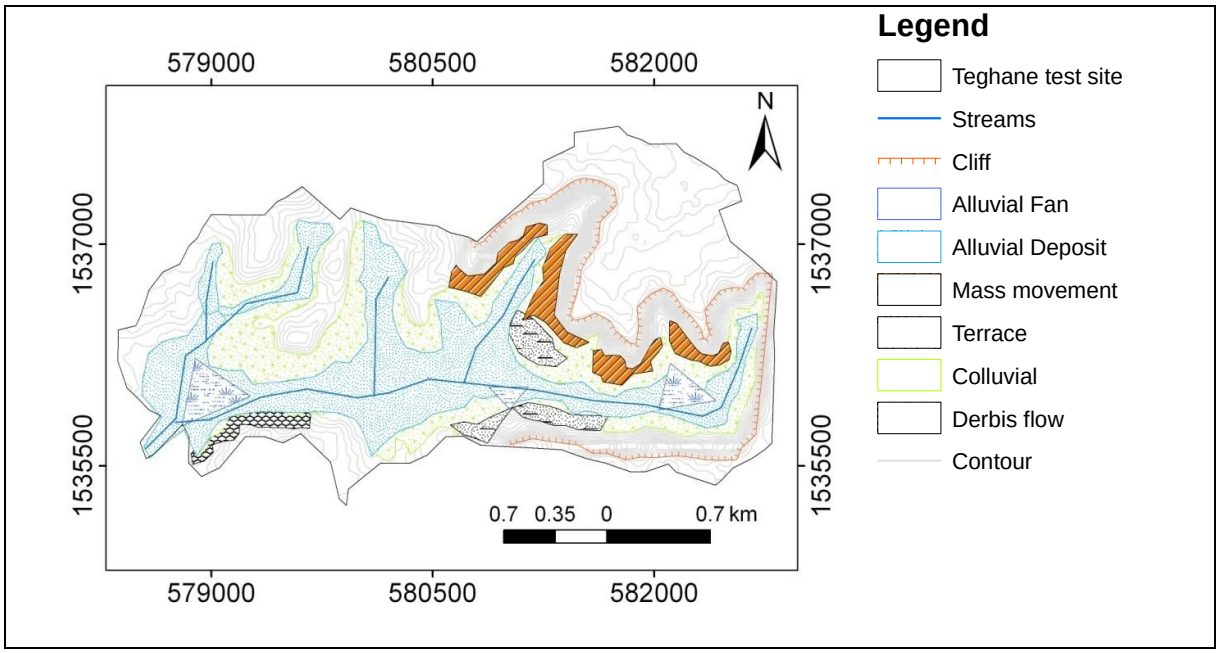

Figure 5-34: Geomorophological maps of the Teghane test site (Data base: Jarvis et al., 2008).

6 Land Cover and Climate Changes and Future Scenarios

6.1 Land Use and Land Cover Change Detection and Scenarios

Land use refers to directly human activities and serves to make land resources available. Land use interfers with the ecological processes that determine the functioning of land cover (Veldkamp and Fresco, 1996, cited in Niehoff et al., 2002). Land use is controlled by the potential of the land for different uses and is governed by multilevel economic and socio-cultural interactions. In contrast land cover refers to the surface appearance of the landscape, which is mainly affected by its use, its cultivation and the seasonal phenology (Jansen and Di Gregorio, 1997; Niehoff et al., 2002).

The Geba watershed is experiencing land cover changes for the last decades. Studies in the northern part of Ethiopia document this fact (Hadgu, 2008; Abraha, 2009). The need to provide food, water and shelter to the people has led to changes in land cover. The Ethiopian population has increased from approximately 6.6 million to 77 million between 1868 and 2008, i.e. the population density increased from 7 to 70 persons per km^2 (Nyssen et al., 2001). This population density is more pronounced in the study area. Based on the central statistics agency census data base of *woredas* (small districts) (CSA, 2008), the Geba basins population density is almost double of the average country level population density (Table 6-1).

Table 6-1: Area-weighted population density of Geba sub-watersheds (after Abraha, 2009).

Sub watersheds	Area (km^2)	Population density (persons km^{-2})
Suluh	969	142
Genfel	733	115
Agula	692	135
Average for upper Geba	2,440	130

This high population density creates environmental instability (Lu et al., 2004). Changes of land use are caused by modified biophysical or human demands that arise from changed natural, economic or political conditions (FAO, 1998). The consequences of the changes are either modification or conversion:

- A change between classes is a conversion of land cover from one category to a completely different category, for example through deforestation or urbanization.
- A change within classes is a modification of the conditions of the land-cover type within the same category, for example through selective logging.

To differentiate and quantifying these changes, change detection and quantification technique is applied for the images acquired in different times.

6.1.1 Change Detection and Quantification

Change detection is the process of identifying differences in the state of an object or phenomenon by observing it at different times (Singh, 1989). For this purpose from Global land cover facility website (www.landcover.org) satellite images were downloaded for the study area. Three land use and land cover maps from 1972, 1986 and 2000 were produced following the step-by-step detection and quantification procedures of satellite images. Landsat MSS (Multispectral Scanner) acquired on November 5, 1972, Landsat TM7 (Thematic Mapper seven) acquired on January 27, 1986 (path 168, row 51 and path 169, row 50), and ETM+ (Enhanced Thematic Mapper Plus) acquired on January 27, 2000 (path 168, row 51 and path 169, row 50) were used for this study.

A pixel based supervised image classification with maximum likelihood classification algorithm was used to map the land use and land cover classes (Lillesand and Kiefer, 2000). A total of 120 ground truth points collected from the field were used for image classification (59) and validation (61). The overall classification accuracies and accuracies of the single land use and land cover classes are shown in Table 7-3. Ongoing, the land use and land cover changes between the three periods (i.e., 1972, 1986 and 2000/2003) were quantified and a change detection matrix of 'from-to' change was derived to show land cover class conversion during the 31-year period by comparing the 1972 and 2003 images. Discussions with elders and leaders of the local population and development aid experts to understand the land cover dynamics and consequences of the changes. Subsequently, spatial analyses were carried out to describe land use and land cover pattern, overall land use changes over time, to evaluate the rate of change at watershed (detail results in chapter 7).

6.1.2 Land use and land cover scenarios development

Based on the land cover change detection different probable land use and land cover scenarios are developed for the impact studies. The scenario development is based on three main considerations (Niehoff et al., 2002)

1. Identifying observed land cover changes in the past and on this basis extrapolating the future changes with their spatial distribution.
2. Relating to the mechanism of runoff generation in the basin i.e Hortonina or saturation overland flow and how this runoff generation is affected by land covers changes.
3. The influence of land cover change on rainfall-runoff relations and its effect on characteristics of rainfall in space and time

The land cover scenarios are designed in a way to perform two tasks: One, based on the past changes and existing land cover and land uses future trends and change patterns are determined. Second, future spatial distribution is projected from the socio-economic conditions. For the impact study the neighborhood relations are not considered only the areal percentages of coverage change of land use types are considered (Niehoff et al., 2002).

Hence, this study utilizes spatially differentiated trends in land-use change derived from change detection between 1972 and 2000. The governmental climate-resilient green economy policy and strategies on the agricultural development and reforestation are included in the analysis. Particular

focus is also given to the internal and external analysis like improving management of the land together with the socio-economic factors.

1. Land use and land cover change sequence analysis in developing scenarios

In this analysis, typical land use patterns, the influence of infrastructural development, strategic plan and policy of the country and of the region are included. Among the many factors, the combination of above criteria is controlling the land cover changes (Niehoff et al., 2002). However, the conversion from one land cover to another is directed by the governmental strategies and policy on the environment and economy. In this study, the Ethiopian government policy on green economy is adopted. The policy clearly emphasized that agricultural sector gives higher rank in the future followed by settlement expansions, , afforestation and conservation work to sustain the green economy Ethiopian Climate Resilient Green Economy strategic plan (CRGE, 2011). Internal and external analysis was made on the land use and land cover types and its future conversion possibilities for the three major land use and land cover classes.

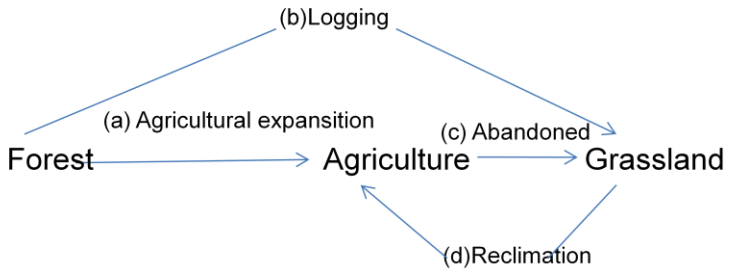

Land use conversion matrix

Future land use / Present land use	Forest	Agriculture	Grassland
Forest	+	+(a)	+(b)
Agriculture	-	+	+(c)
Grassland	-	+(d)	+

+ conversion possible
- conversion impossible

Figure 6-1: Example of land use change sequence within three land covers and its conversion matrix (after Verburg and Overmars, 2009).

2. Socio-economic and policy factors in developing Scenarios

The socio-economy and policy factor considered in the land use and land cover change analysis is manly related to the government's policy and strategies in the green economy. The Green Economy Plan of the country is based on four pillars (Ethiopian Climate Resilient Green Economy strategic plan (CRGE), 2011) including the:

- Extended agricultural expansion with improved crop production while reducing carbon emission
- Expanding afforestation and soil and water conservation works

Considering the above aspects, three scenarios were developed. Attempts were made to consider the ongoing trends of land use and land cover change within the study area related to the country's green economy policy. The scenarios mainly focus on the most likely changes that might occur in the near future. All of the scenarios focus on local issues to evaluate the consequences of different hypothetical

land management practices that could have impacts on stream flow and future agricultural production and overall green economy strategies. However, changes in soil management practices using soil and water conservation practices could have also impacts on stream flow but are not considered in this research.

Scenario 1: Continuation of Current Practices (No Interventions)

Scenario 1 assumes the continuation of existing traditional agricultural production and assumes there will be no intervention in any part of the watershed. Although this scenario is impractical due to the ongoing water supply development project for Mekelle city, irrigation development in the upstream area and intensive human activities in the watershed, it offers reference point/baseline data when interpreting the hydrological implications of other management scenarios. Therefore this scenario acts as a base when evaluating the performance of the other scenarios.

Scenario 2: Following the country recent track record in agricultural development

In scenario 2 the actual country records in achieving the economic development on the land management are considered. Refering to the report released from Ministry of Finance and Economy and the government policy and strategies on green economy (Ethiopian Climate Resilient Green Economy strategic plan (CRGE, 2011), a 15% expansion of agricultural land and 3% reforestation is accounted for the growth in the agricultural sector over the last five years. Therefore, in this scenario the ongoing invention of irrigation projects in the upper reach of the Geba watershed and the new irrigation projects are considered with the rate of the country level agricultural development strategies.

In scenario 2 partial grassland and bare land conversion into arable land and conversion of bush land and bare land into forest is considered. This scenario involves a reduction of grass land, bush land and bare land cover by 15% for agricultural expansion and a reduction of bush and bare land for forest development by 3%. It is assumed that, the implementation of new irrgation projects will create impact on downstream water users and causes water shortage. A decrease in water quantity will cause an effect on the Mekelle city water supply.

Scenarios 3: Allied with the Ethiopian Climate-Resilient Green Economy policy and strategie – Fast growth with food-focus scenario

In scenario 3 agricultural developments will continue with 10% by intensifying crop production without aerial extension. A relatively low rate of land transformation is assumed, leading to conversions of bare land, bush land and grass lands into agricultural land. The ground water potential and surface water are increasingly used to irrigate more land to intensify crop production based on food security policy. The irrigation projects consider the regional supply food as well as an export oriented agricultural policy. This requires the implementation of reserviours in the upstream area. To reduce reserviour siltation area closures will be implemented at slopes > 45% inclination. Slopes with inclination < 30% will be terraced. Additional 3% of the area will be afforested to protect and re-establish forests for their economic and ecosystem services. In scenario 3 most of the grasslands and some of the barelands will be replaced by forest land. Scenario 3 can be considered as good management practices. Generally, in this land use change scenario high focus is given to the small scale irrigation intervention with an objective to identify the impacts on the Mekelle water supply projects.

6.2 Trend analysis of hydro-meteorological data and climate changes scenarios

6.2.1 Trend analysis of hydro-meteorological data

The variation of climate and weather is controlled by macro scale pressure pattern and monsoon flows which create periodic variation in the weather system. The periodic nature of weather results seasonality of the hydro-meteorological time series (Githui, 2009). This seasonality is analyzed using Seasonality index, SI.The Seasonality Index (Walsh and Lawler, 1981) is applied to each rainfall station within the upper Geba basing:

$$SI = \frac{1}{Ri}\sum_{i=1}^{j=12}\left|Mij - \frac{Ri}{12}\right| \qquad \text{Equation 6-1}$$

Where Ri is the total annual precipitation for the year *i* under study and M_{ij} is the monthly precipitation for month *j*.

The long-term mean index for each station is calculated in two ways (Sumner et al., 2001; Celleri et al., 2007). SI_i was computed for all eight rain gauge sites within Geba watershed for each of forty-nine years provided by the data base. The long-term mean, SI_{mean}, for each site was derived by averaging the SI_i values computed for each year of the record over the study period.

$$SImean = \frac{1}{49}\sum_{i=1}^{j=49} SI\ i \qquad \text{Equation 6-2}$$

The alternative seasonality index SI_a, was computed for each station using mean monthly and annual rainfall data directly (Equation 6-2); the resulting index will possess a lower magnitude as a result of smoothening by averaging the noise in the year to year distribution of monthly precipitation values (Sumner et al., 2001).

With the replicablity index, RI, distribution of wetter periods in a year are indicated (Walsh and Lawler, 1981):

$$RI = \frac{SI_a}{SI_{mean}} \qquad \text{Equation 6-3}$$

Table 6-2: Seasonal and Replicability Index in the Geba basin (Data base: Ethiopian Meteorological Service Agency).

Station	SI_a	SI_{mean}	SI_{min}	Year	SI_{max}	Year	RI
Adigrat	0.81	1.0	0.7	1992	1.4	1999	0.82
Agulae	1.07	1.2	0.8	1993	1.5	1999	0.91
Edagahamus	0.80	1.0	0.7	2007	1.4	1999	0.80
Hagereselam	0.90	1.0	0.7	1993	1.3	1988	0.86
Hawzen	0.97	1.1	0.7	2009	1.5	2010	0.90
Mekelle	1.06	1.1	0.8	1993	1.5	1981	0.92
Senkata	0.74	1.0	0.5	1979	1.3	1974	0.75
Wukro	1.11	1.2	0.9	1993	1.6	1968	0.91

The values of SI_{mean} and RI, the periodicity and seasonality of the precipitation of the stations in Geba basin indicate that the wettest months of the year occurs within short periods due to its high value of replicablity index (RI) (Table 6-2). At the same time a stable long term annual distribution is observed due to its high value of SI_{mean}. In the Geba watershed increased values revealed for all stations attributed to concentration of precipitation to less than three months of the year.

Table 6-3: Seasonal precipitation regimes as classified by seasonality index (copied from Walsh and Lawler, 1981).

Seasonality Index (SI)	Precipitation regime
<0.19	Precipitation spread throughout the year
0.2-0.39	Precipitation spread throughout the year, but with a definite wet season
0.4-0.59	Rather seasonal with a short dry season
0.6-0.79	Seasonal
0.8-0.99	Markedly seasonal with a long dry season
1.00-1.19	Most precipitation in less than 3 months
>1.2	Extreme seasonality, with almost all precipitation in 1 to 2 months

Thresholds for the Seasonality Index SI document considerable degrees of precipitation seasonality at all rain gauge stations considered. Due to this seasonality, the trend analysis is made by incorporating the seasonal component applying the Mann-Kendall method (Helsel and Hirsch, 1992). Tau (τ) measures the strength of the monotonic relationship between input and output (Kendall, 1938 cited in Helsel and Hirsch, 1992). Since Tau (τ) is calculated based on the rank of the numbers due to its ranked procedures, it does not give consideration for small values and at the same time it will lead with wrong values with the data that contain outliers.

The non-parametric Seasonal Kendall test is used for trend analysis due to less underlying assumptions on the data, making it robust against departures from normality (Helsel and Hirsch, 1992). Outliers and

missing values are well treated by the Seasonal Kendel methods because it uses the rank of the values. This makes the test not sensitive to outliers and missing values. The test accounts for seasonality includes the calculation of the Mann-Kendall test values for each month separately and then adding all monthly values. These values are compared month by month or season by season with the measured values of temperature or rainfall. The number of times the rainfall or temperature increases above the calculated seasonality value and the number of times the rainfall and temperature decreases from seasonal value is calculated. Kendall's S statistics S_i and the overall total S_k were calculated following Hirsch et al. (1982).

To approximate the seasonality value S_k to normal distributions, the product of the number of seasons and number of years considered is the main criteria. If the product of the number of years and months exceeds 25 we can assume that the distribution is normal. In the case of the Geba drainage basin S_k is approximated as a normal distribution with the expectation (μS_k) equal to the expectation of the individual months considered under the null hypothesis, and variance equals the sum of each month varainces. S_k is calculated using Equation 6-4 and Z_{sk} is evaluated against the standared table of normal distribution:

$$Z_{Sk} = \begin{cases} \dfrac{S_k - 1}{\sigma_{Sk}} \; if S_k > 0 \\ 0 \; if S_k = 0 \\ \dfrac{S_k + 1}{\sigma_{Sk}} \; if S_k < 0 \end{cases} \qquad \text{Equation 6-4}$$

$$\text{where } \mu_{Sk} = 0$$

$$\sigma_{Sk} = \sqrt{\frac{\left[n(n-1)(2n+5) - \sum_{i=1}^{n} t_i(i)(i-1)(2i+5)\right]}{18}} \qquad \text{Equation 6-5}$$

Where N is the number of data in a given season and t_i is number of ties of extent i

The significant value (p-value) is estimated by considering the distribution of the test statstics of large samples as normal distributed. Then Z_{sk} can be approximated by the normal distribution data. The significant value (p-value) is rejected or accepted based on the Z_{crit} which is the value of the normal distribution data, with selected exceedence of probability $\alpha/2$. If the p-value is less than the significant value taken (Z_{crit} value), the null hypothesis is (Hirsch and Slack, 1984, cited in Helsel and Hirsch, 1992).

The Kendall slope between paired data, in this case rainfall and temperature of the Geba basin, is calculated by the median slope to check overall trends with seasonal trends.This slope β is given by:

$$\beta = Median\left[\frac{Y_j - Y_i}{T_j - T_i}\right] for\ all\ i < j \qquad \text{Equation 6-6}$$

Based on Equation 6-8, all slopes within each seasons and months are calculated and compared with the overall seasonal Kendall slope trend. The result shows that there is no cross slopes contribution to the overall slope trend.

6.2.2 Trend analysis of rainfall and temperature (1961–2010)

The monthly rainfall and temperature data for the period 1961–2010 were analyzed on their trends (Table 6-4)

Table 6-4: Slopes and trend for monthly rainfall and temperature using the Seasonal Kendall Method (1961–2010).

	Rainfall			Temperature		
Station	Slope	P-value	Z-Value	Slope	P-value	Z-Value
Mekelle Airport	-0.04	0.88	0.35	0.04	0	4.86
Senkata	-0.27	0.44	-0.49			
Hawzen	-0.05	0.5	-0.15			
Hagerselam	-0.15	0.33	-0.3			
Edagahamus	-0.30	0.01	-0.51			
Wukro	0.09	0.8	0.22			
Agulae	0.10	0.04	0.89			
Adigrat	-0.08	0.7	0.32			

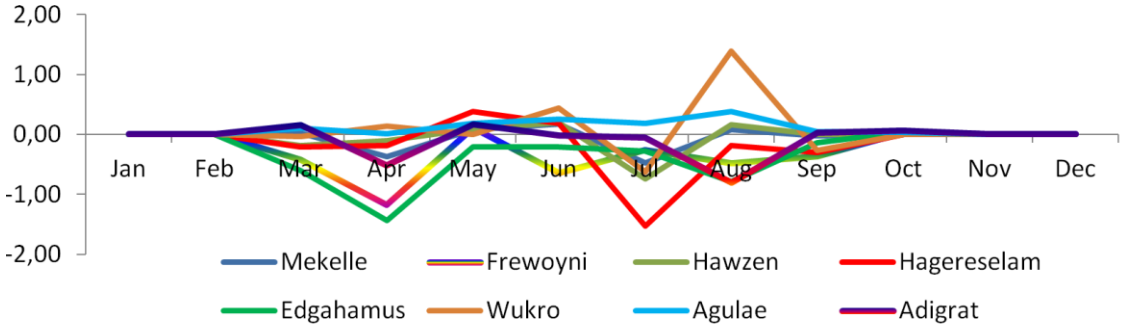

Figure 6-2**:** Slopes and trend for monthly rainfall

Trend analysis of the monthly data shows that out of a total of eight rainfall stations, two show significant trends $\alpha < 0.05$, increasing for the data from Agula station decreasing for those of the Edagahamus station. The two stations are located in the northern and southeast part of the basin. The trend analysis of temperature data tested is not statistically significant ($\alpha > 0.05$).

6.2.3 Trend analysis of stream flow (1962–2003)

The stream flow data from the outlet of Geba Nr. Mekelle station were trend analyzed using the monthly data of the period 1962–2003. The descripitive statistics (mean, standard deviation (SD), minimum, maximum, median, skewness, kurtosis and coefficient of variation (CV)) are given in Table 6-5. Determining the confidence intervals of the meadian slope, 5% significant level is considered in two sides of slope estimator. Based on the sample size Z at α=0.05 is determined from tables of normal distribution which determines the upper and lower ranks of the discharge slope l (Helsel and Hirsch, 1992). The value of Z at α=0.05 is 1.96. Using Eq. 6.7 and 6.8, M_l and M_u are calculated as (Hirsch and Slack, 1984, cited in Helsel and Hirsch, 1992):

$$M_l = \frac{N - 1.96 * \sqrt{\sigma_{Sk}}}{2}$$ Equation 6-7

$$M_u = \frac{N + 1.96 * \sqrt{\sigma_{Sk}}}{2}$$ Equation 6-8

Where: N is the total number of slope estimates and σsk as given in Equation 6.7. The lower and upper limits of the confidence interval of the slope are the M_l th and the $(M_{u+1})^{th}$ ranks of the N ordered slope estimates.

The slope estimator shows an annual decrease of 0.71 m^3/s for the Geba Nr.Mekelle station (Table 6-5). The p-values 0.5, for Geba Nr. Mekelle station, obtained against the null hypothesis of no trend show that there is no significant trend.

Table 6-5: Monthly and annual mean stream flow statistics for the Geba Nr. Mekelle station (1962–2003) (Units of flow: Mm^3) (Data base: Minstry of Water Resource of Ethiopia).

Month	Jan	Feb	Mar	Apr	May	Jun	Jul	Aug	Sep	Oct	Nov	Dec
Mean	0.43	0.64	2.86	5.50	4.21	4.21	94.83	218.41	25.27	2.29	1.46	0.26
Max	3.21	6.40	14.64	25.46	24.44	14.37	202.22	436.56	84.64	17.76	8.90	3.59
Min	0.10	0.10	0.10	0.01	0.10	0.10	3.60	15.20	0.10	0.10	0.10	0.10
STDEV	0.50	1.00	2.90	5.50	4.60	3.50	42.80	93.20	15.80	3.70	2.00	0.50
CV	1.90	2.10	0.90	0.90	1.00	0.90	0.40	0.40	0.70	2.30	2.20	2.50

Annual	Mean	Max	Min	STDEV	CV	Skeweness	Kurtosis
	360	693.48	36.8	131.8	0.24	1.24	2.28

Table 6-6: Kendall Slope of the annual stream flow with lower and upper limits at 95%.

		Confidence interval for slope		Seasonal Kendell	
	Slope(m^3/s)	Lower 95%	Upper 95%	P-Value	Z-Value
Geba Nr.Mekelle	-0.71	13.6	35.4	0.56	0.35

The Seasonal Kendall trend analysis performs on the monthly totals (Table 6-4). The annual Kendell slope of the Geba Nr. Mekelle station shows a negative slope with a decrease of 0.71 m^3/s per year and a p-value of 0.56. This is due to an increase temperature and resulting increase of evapotranspiration. Above, more water abstractions due to irrigation have to be expected, also reducing stream flow.

6.2.4 Future climate change scenarios

In climate change studies the widely used methods for generating climate change scenarios are General circulation models (GCMs), which are based on the physical interaction among the atmosphere-ocean and land surface on a global scale. The GCMs currently simulate the estimates of future greenhouse gas concentration on the atmosphere and its response on the global climate system and future variable (Bates et al., 2008). General circulation models show the climate in a three dimensional grid over the globe based on the physical laws governing the atmospheric physics with a resolution of between 250 and 600 km and in 10 to 20 vertical layers (Bates et al., 2008; Matondo et al., 2004).

The GCMs calculate weather parameters like wind speed, temperature and atmospheric moisture distribution. However, many physical processes, related with clouds which occur at smaller scales cannot be modeled other than averaging over a large scale. Averaging parameter values over large scales is a source of uncertainty in GCM simulations of future climate.With this uncertainity, future simulation for estimating future climate performs two simulation i.e equilibrium and transiet (Matondo et al., 2004).The equilibrium mode is subjected to doubling CO_2 emission while the transiet one is less emission relative to the base year 1961-1990.This is because the implication of future change is assed based on the present condition of the environment,demographic conditions and economy (IPCC, 1999; Setegn et al., 2010; Mengistu, 2009; Githui, 2009; Bates et al., 2008; Lin et al., 2007).

For this research the baseline period of 1961–2000 is considered to for the scenario construction in simulating the future climate. Climate change scenarios were taken from the two Special Reports on Emission Scenarios (SRES) using climate change scenarios A2 and B2 and the two general circulation models, HadCM3 and CGCM3. Models were selected due to the availability of a downscaling model with sufficient details on predictor files representing the study area. A set of scenarios was published by the IPCC with a projection period 2011–2100 (Bates et al., 2008). To reflect the current understanding and knowledge on the future developments of the global environment with the production of greenhouse gases, scenarios are developed to represent the range of driving forces and emission forces. The Special Report on Emission Scenario (SRES) team developed four “scenario families” labeled A1, A2, B1 and B2 to describe the forces driving greenhouse emission and aerosol emission and create relation between two Bates et al., 2008. The four story line families are based on the income differences among the world, technological advancement, demographic changes and economic development and energy consumptions (Bates et al., 2008; Annex-5).

7 Hydrological Modelling

7.1 Hydro-meteorological results

The soil and water assessment tool (SWAT) needs several annual and seasonal hydro-meteorological input data to generate spatially differentiated data, here displayed in 30 m x 30 m resolution.

7.1.1 Rainfall

The spatial distribution of the rain gauge stations in the Geba basin is sparse and heterogeneous. The variability and distribution of rainfall in the basin is studied based on the thirty-eight year monthly rainfall database, integreating eight stations within and nearby the basin. (Figure 7-1 to 7-3) displays the annual mean average rainfall distribution in the watershed.

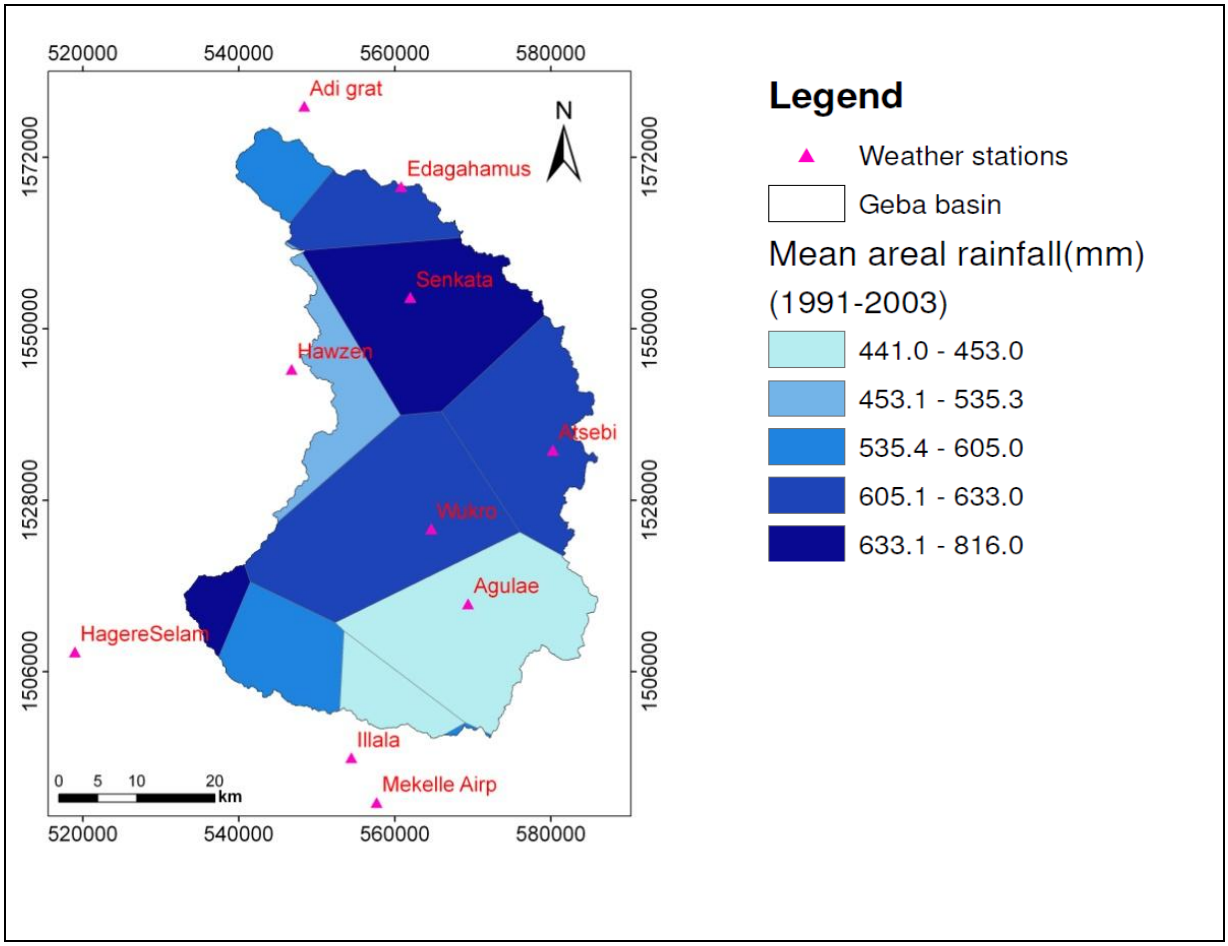

Figure 7-1: Computed annual rainfall distribution in the Geba basin using Thiessen polygon (Data base: Ethiopian National Meteorological Agency for rainfall data; Jarvis et al., 2008).

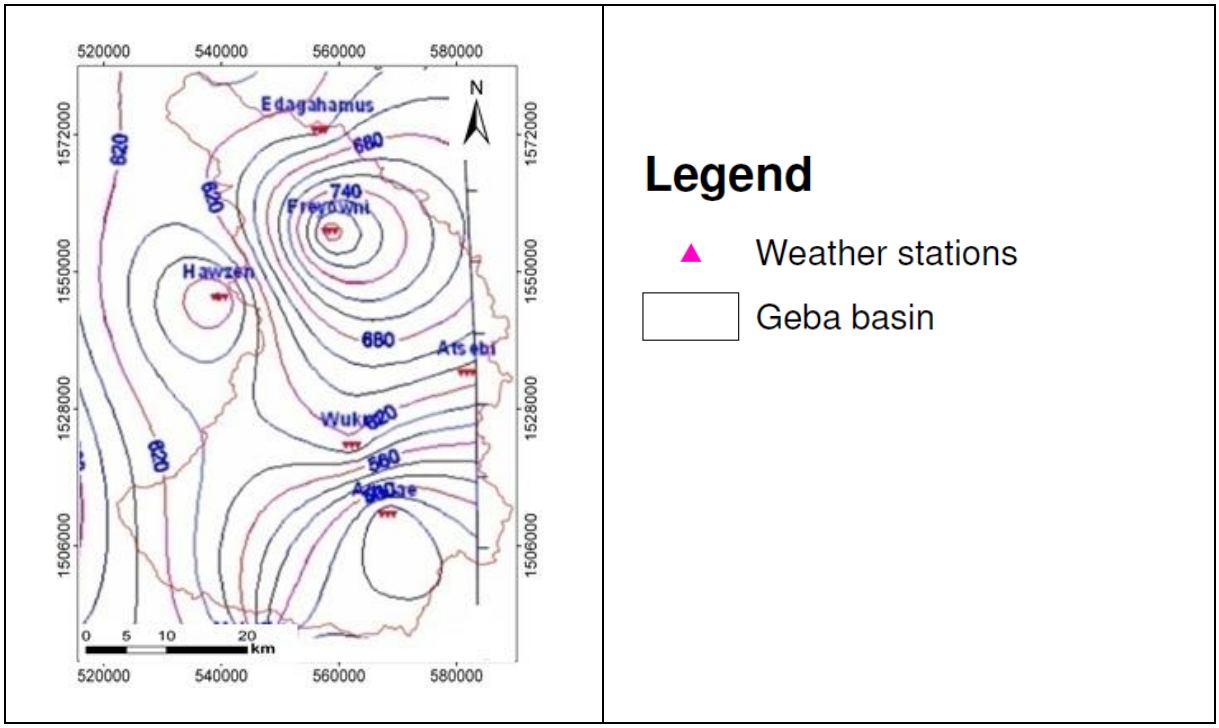

Figure 7-2: Computed annual rainfall distribution in the Geba basin applying isohytal method (Surfer 8) (Data base: Ethiopian National Meteorological Agency for rainfall data and Jarvis et al. 2008).

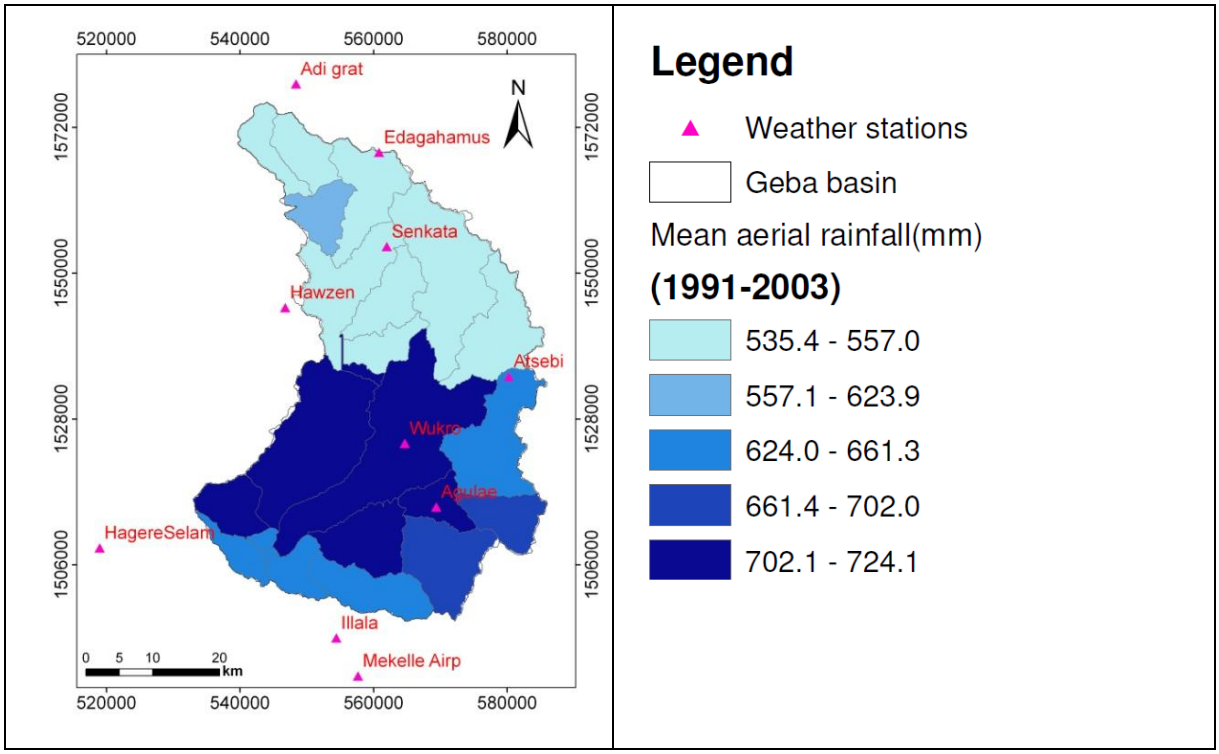

Figure 7-3: Computed annual rainfall distribution in the Geba basin using weather generator program (SWAT) (Data base: Ethiopian National Meteorological Agency for rainfall data and prepared using SURFER 8 softaware: Jarvis et al., 2008**).**

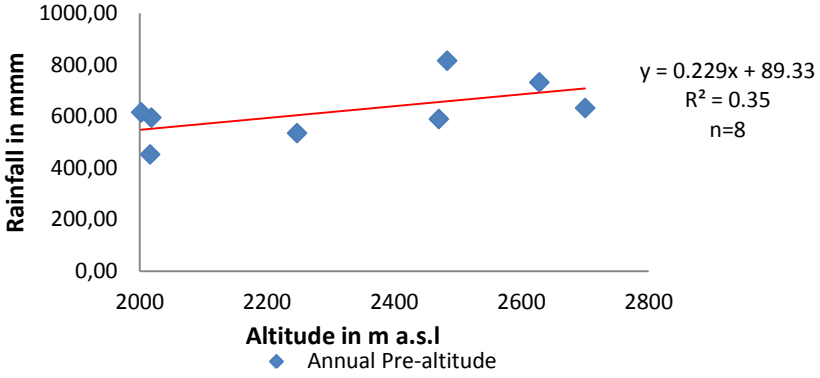

(a)

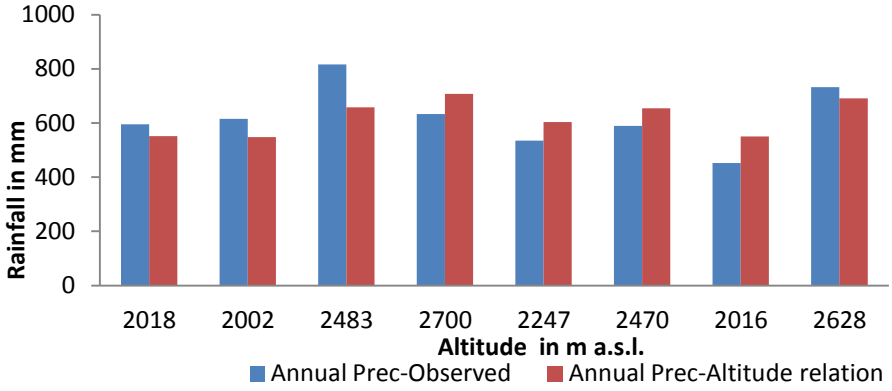

(b)

Figure 7-4: Precipitation-altitude relation of rain guage stations in and near by the Geba basin (Table 3-4) (a) observed versus calculated with altitude-reinfall relation (b) (Data source: National Meteorological Agency).

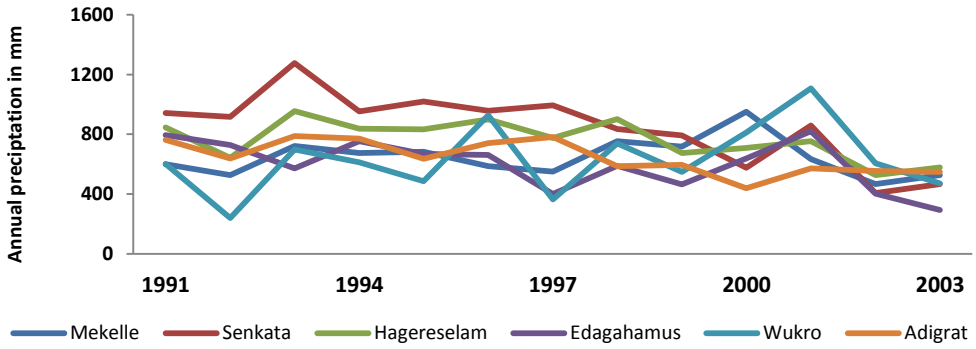

Figure 7-5: Annual and inter annual precipitation variability of selected meteorological stations.

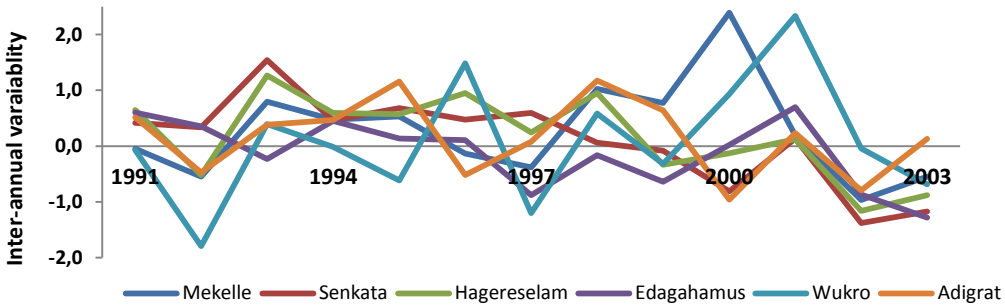

Figure 7-6: Station based annual precipitation variability of selected meteorological stations.

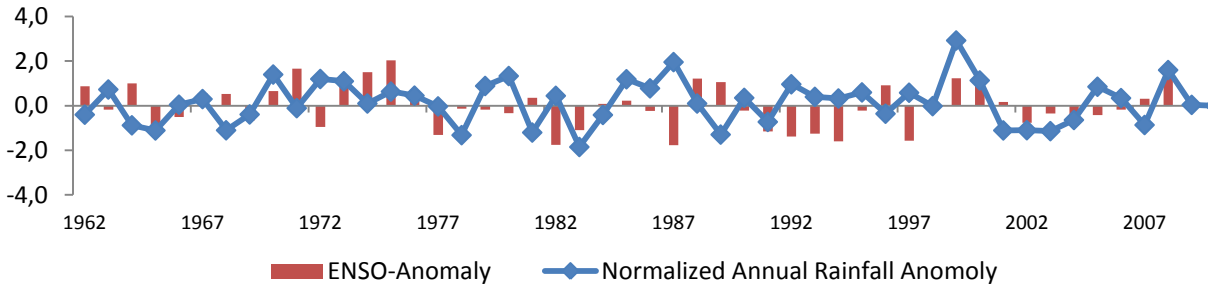

Figure 7-7: Mean areal normalized annual rainfall and ESO-anomaly (Data base: National Meteorological Agency).

The variation of climate and weather during the year is largely controlled by small scale effects. The main macro scale factor influencing weather are the overall pressure pattern, the position of inter tropical convergent zone, the position and intensity of Tropical Easterly Jet (WAPCOS, 2003). Figure 7-8 shows deviations of the mean from the annual areal mean in the Geba basin and El Nino and southern oscillation (ENSO) correspondence with the mean deviation.

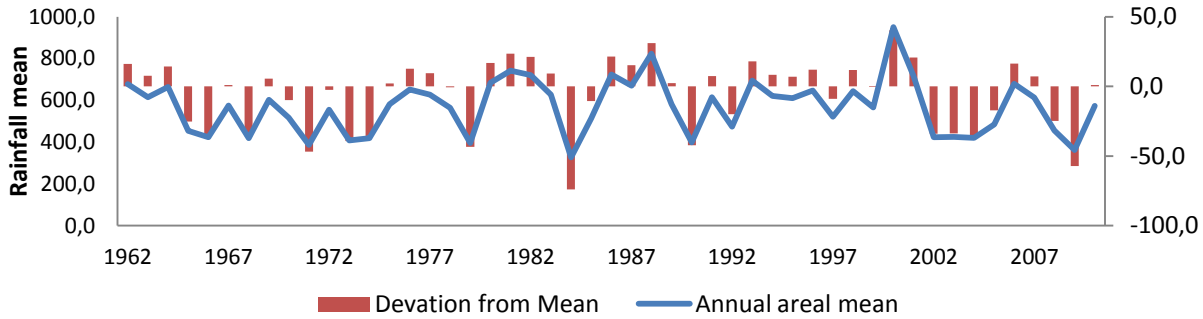

Figure 7-8: Rainfall mean versus deviation from mean for the Geba basin (1962–2010) (Data base: Nation Meteorological Service Agency).

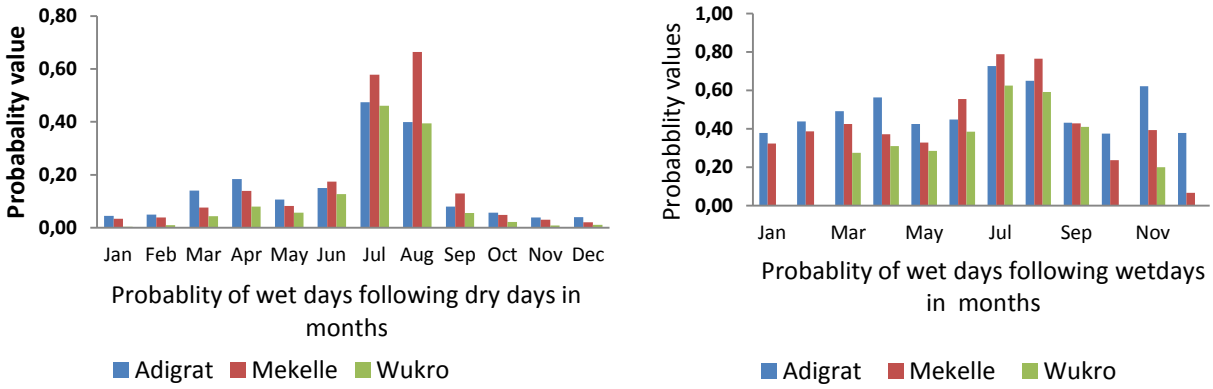

Figure 7-9: Probability of dry spell analysis (wet-dry days in a month) for the Geba basin (1991–2003): a) probability of wet days following dry days in months, b) probability of wet days following wet days in months. Wet spells defined as the number of consecutive days with at least 1 mm of rainfall, and dry days are with less than 1 mm rainfall (Data base: Ethiopian Meteorological Agency).

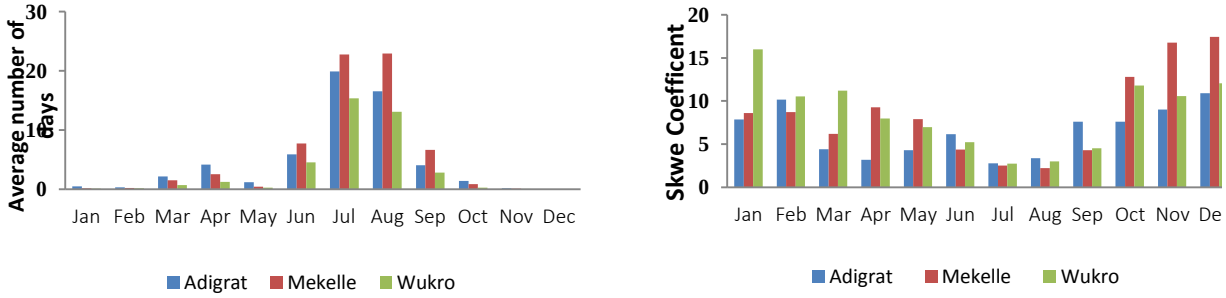

Figure 7-10: Average number of days of precipitation (a) and skew coefficient for daily precipitation in a month (b) for the Geba basin (1991–2003) (Data base: Ethiopian Meteorological Agency).

The El Nino and La Nina effects on the Geba basin are checked of the ENSO anomaly (Figure 7-7) by the rainfall annual deviation from mean (Figure 7-8). Following the analysis of El Nino and La Niña, in relation with dry years and wet years in the basin, the length of wet and dry days is studied by the SWAT2009 model using the weather generator program (Figure 7-9, Figure 7-10) to get an overview of the most relevant patterns of wet and dry spell lengths and their spatial and temporal description in relation to water availability.

7.1.2 Evapotranspiration

The soil and water assessment tool (Arnold et al., 2011) model calculates total evapotranspiration as a sum of evaporation of water intercepted by vegetation, transpiration of the vegetative cover and evaporation from bare soil and open water bodies (Figure 7-11).

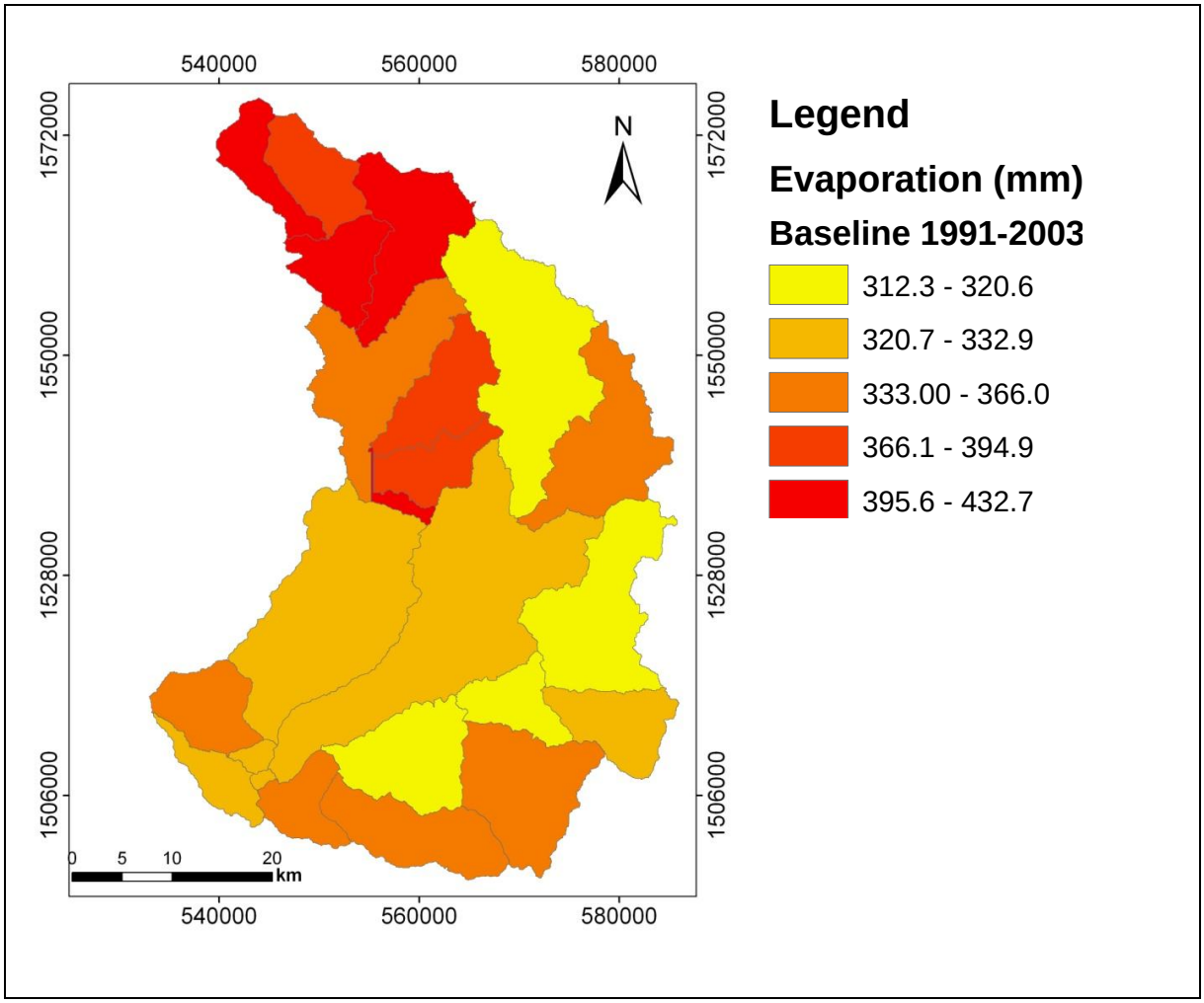

Figure 7-11: Actual Annual Evapotranspiration (mm) for the Geba basin (Data base: Jarvis, et al., 2008; Ethiopian Meteorological Agency).

7.1.1 Stream flow

The annual maximum, minimum and mean stream flows for the period 1991–2003 (Ministry of Water Resource) with some missed value (Figure 7-12).The high flows concentrate on the two months of the rainy season (July, August). A secondary peak occurs during the spring minor rainy season in April. The high seasonal variability of the Geba river's runoff is documented in Table 7-1.

Table 7-1: Variability of daily flows of Geba Nr Mekelle (Rainy months of 1981).

Date	3 Aug-80	4 Aug-80	5 Aug-80	6 Aug-80	7 Aug-80	8 Aug-80	9 Aug-80	10 Aug-80
Q(cms)	19	102	172	189	32	180	87	172
Date	11Aug-80	12Aug-80	13Aug-80	14Aug-80	15Aug-80	16Aug-80	17Aug-80	18Aug-80
Q(cms)	1445	523	97	12	60	23	13	42

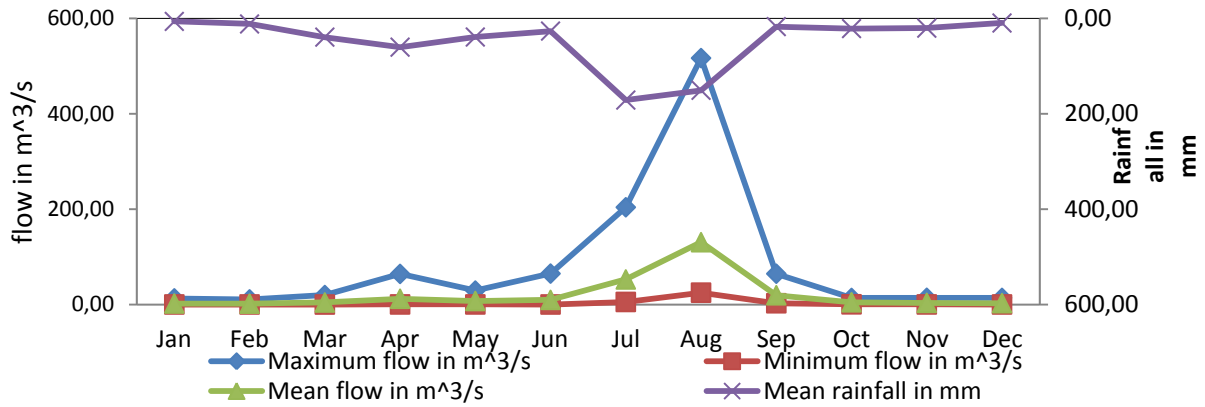

Figure 7-12: Annual mean monthly rainfall (mm) and stream flow (m^3/s) for the Geba basin (1991–2003) (Data base: Ethiopian Meteorological Agency).

7.2 Soil Texture Analysis

The physical properties and texture of the soils are the main input to models to predict runoff. The descriptive statistical analysis results are shown in Table 7-2. The detailed soil sample (Figure 7-13) analysis data base is attached in Annex-5.

Table 7-2 : Descriptive statistics of soil properties in the topsoils of the Geba basin (n= 112).

Parameter	Min.	Max.	Mean	STDEV	CV in%
Clay (%)	0.09	62.58	19.32	13.89	0.72
Silt (%)	0.18	81.35	42.32	21.71	0.51
Sand (%)	2.37	97.73	38.36	26.91	0.7
Bulk density	1	1.5	1.37	0.17	0.12
Avaliable moisture content (mm/mm)	0.05	0.15	0.12	0.02	0.19
Hydraulic conductivity (mm/hr)	0.09	17.24	8.2	7.94	0.97
Organic carbon (%wt)	0.1	3	1	0.5	0.5
Soil acidity	6.6	8.1	7.51	0.33	0.04
Cation exchange capacity(meq/100g)	7.23	74.5	32.4	18.43	56.91

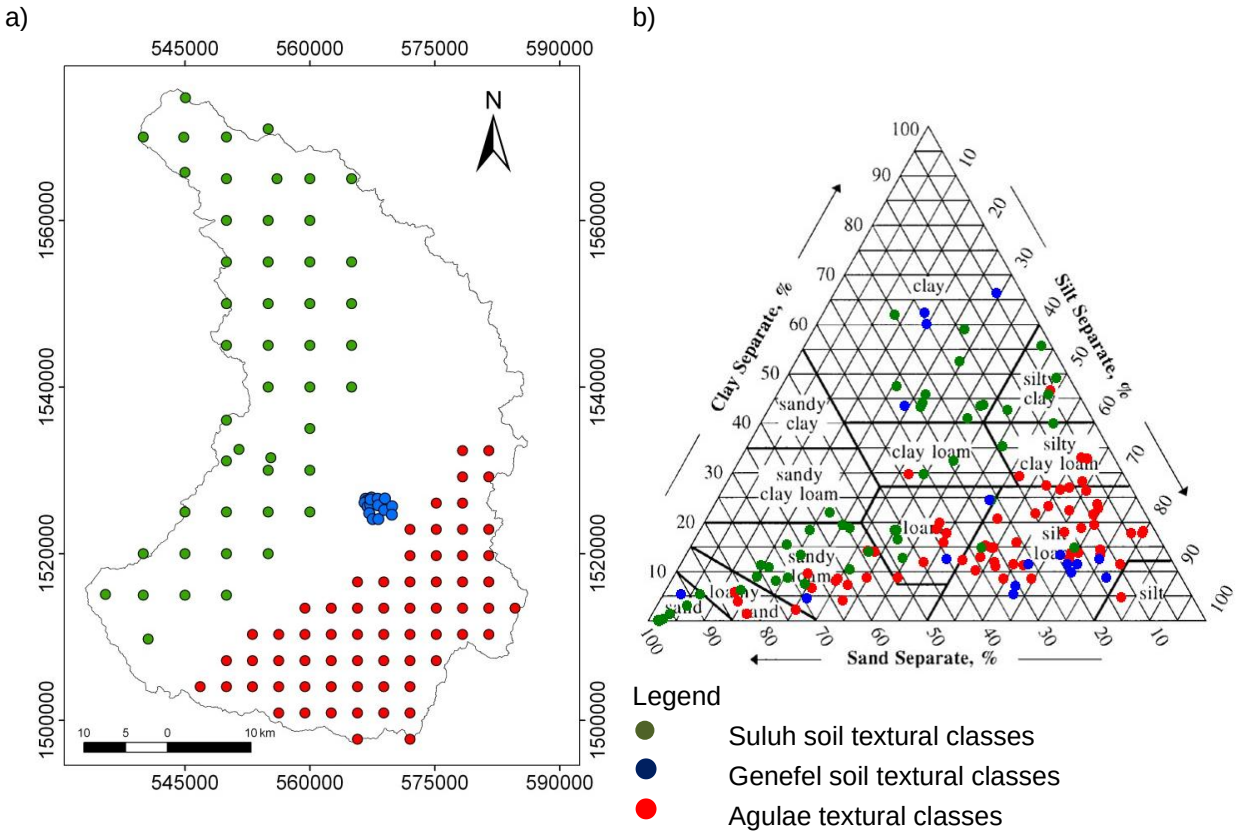

Figure 7-13: Soil sample distribution in the Geba basin a) and textural analysis b) (Data base: Jarvis et al., 2008).

7.3 Land use and land cover

Land use and land cover maps were generated for 1972, 1986 and 2000 following the step-by-step procedures (chapter 6) of satellite image analysis (Figure 7-14 to 7-16). Table 7-3 shows the classification accuracy assessment for the Landsat (ETM+) image from 2000. The land use and land cover map for 2003 is derived from data provided by the Ministry of Agriculture Woody mass Project (WBISPP, 2004) and used for verification of the 2000 Landsat (ETM+) image from January 2000 (paths 50 and 51, rows 168 and 169).

Using satellite image based classification and reference test data information, the accuracy of the classification was assessed by comparing two sources of information (Jensen, 1996). On the basis of field observations two sample sets were created for the Landsat (ETM+) training samples, one for classification, the other one for verification. Table 7-3 shows the accuracy of the different land cover classifications.

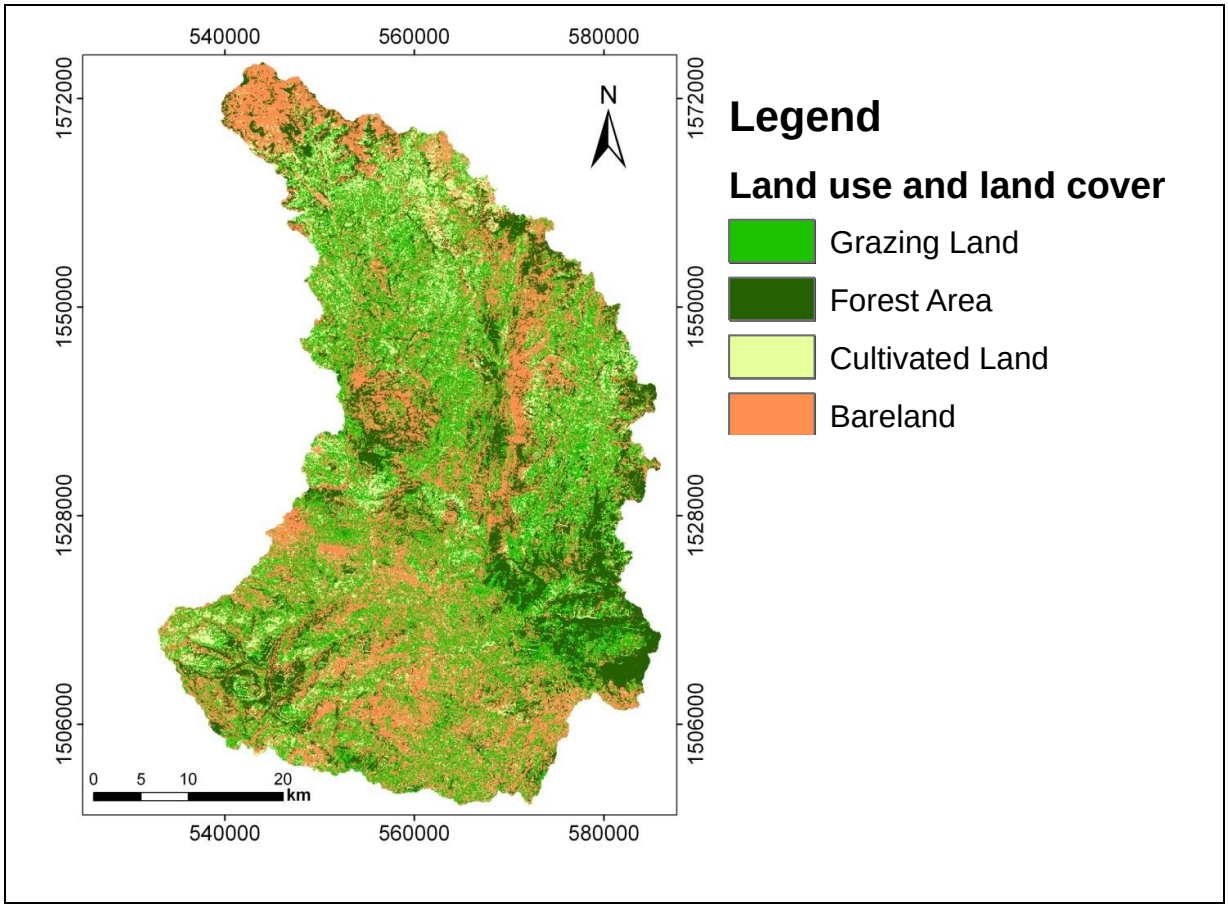

Figure 7-14: Land use and land cover of the Geba basin based on satellite image classification. 1972 land use and land cover (Data base: www.landcover.org; WBISPP, 2004; Jarvis et al., 2008).

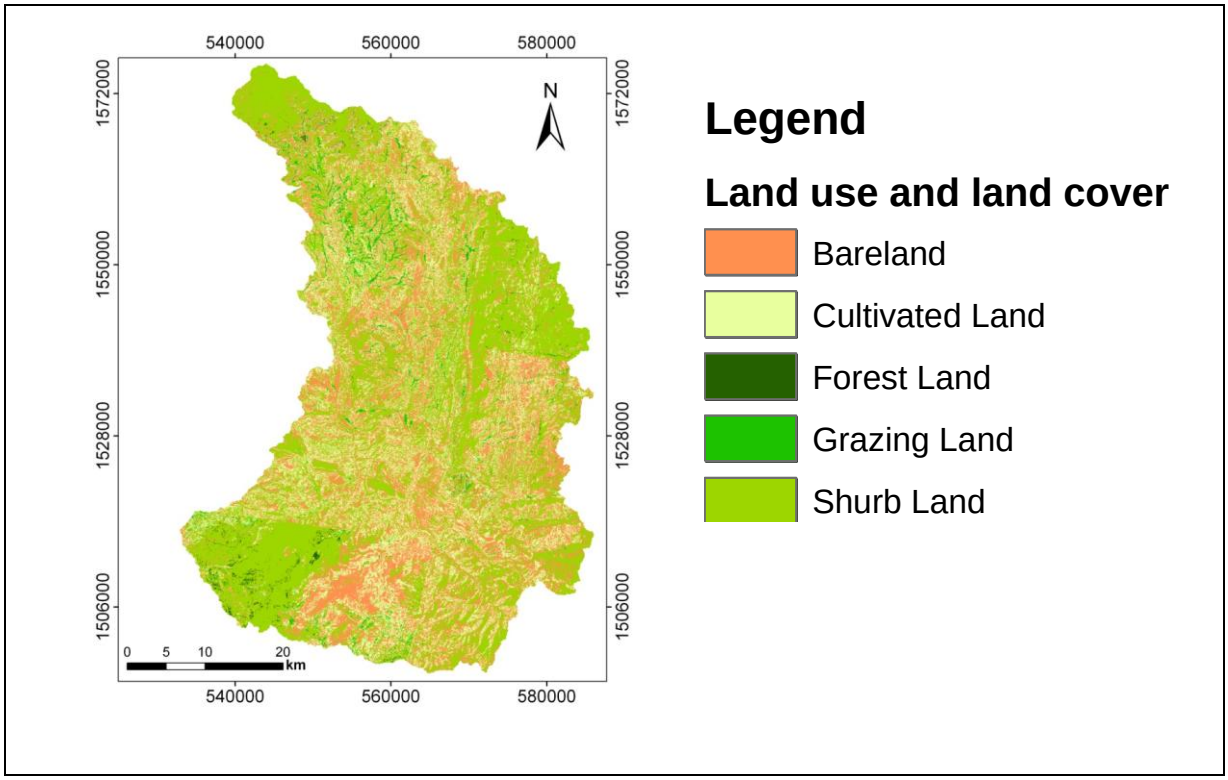

Figure 7-15: Land use and land cover of the Geba basin based on satellite image classification. 1986 land use and land cover (Data base: www.landcover.org; WBISPP, 2004; Jarvis et al., 2008).

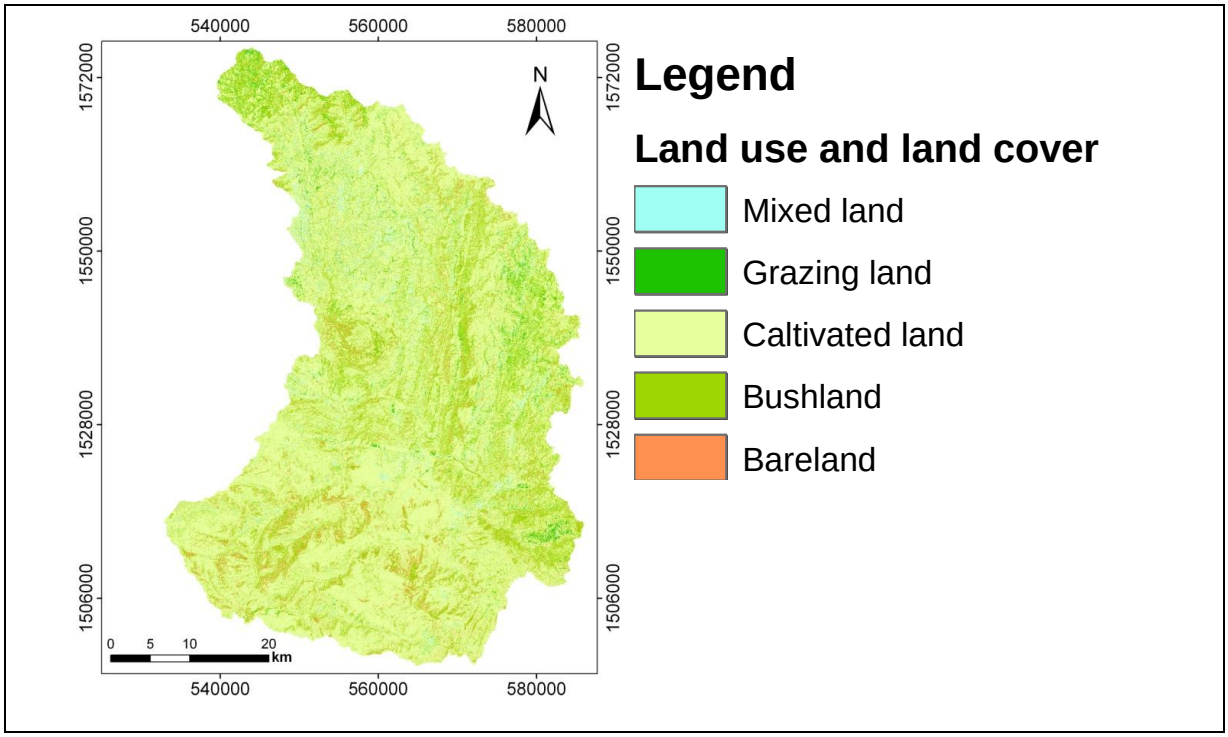

Figure 7-16: Land use and land cover of the Geba basin based on satellite image classification. 2000 land use and land cover (Data base: www.landcover.org; WBISPP, 2004; Jarvis et al., 2008).

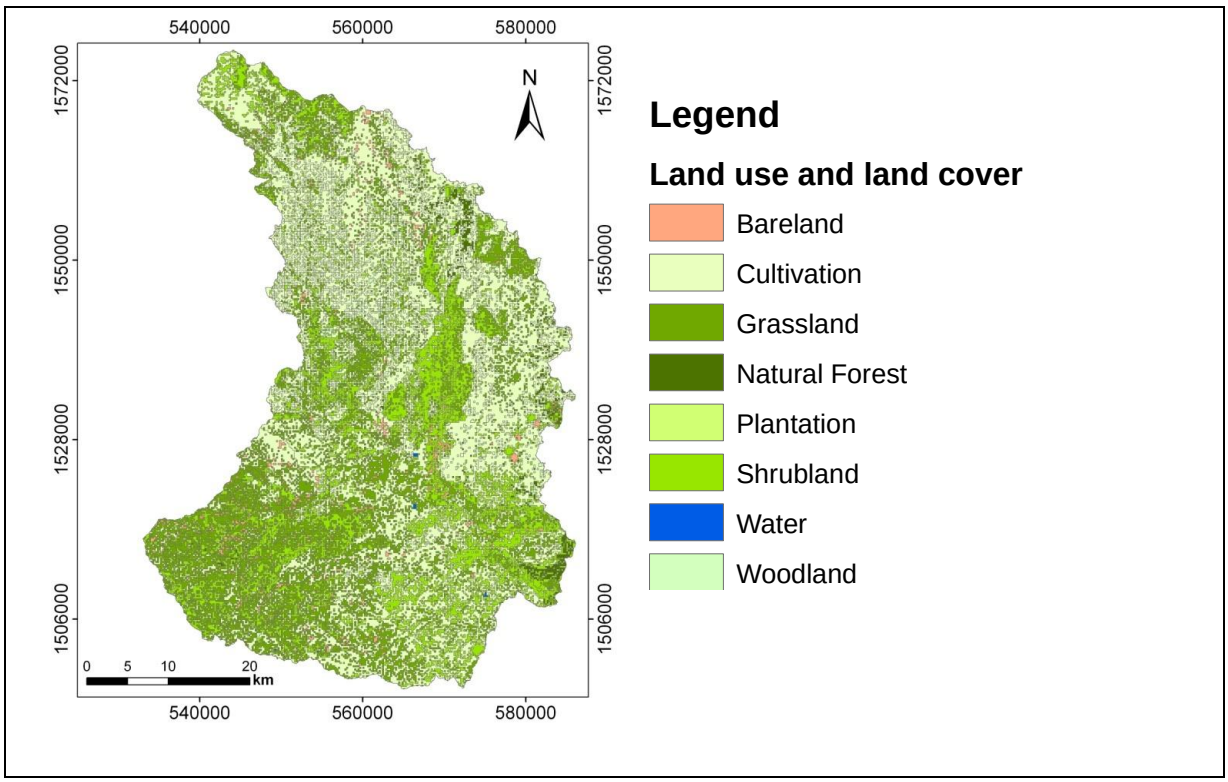

Figure 7-17: Land use and land cover of the Geba basin based on satellite image classification. 2003 land use land cover (Data base: WBISPP, 2004).

Table 7-3: Accuracy assessment report for land use and land cover classification of Landsat ETM^{+} from January/2000 (path 168/169, row 50/51).

CLASSIFICATION ACCURACY ASSESSMENT REPORT

ACCURACY TOTALS

Class Name	Reference Totals	Classified Totals	Number Correct	Producers Accuracy	Users Accuracy
Forest land	2	1	1	50.00%	100.00%
Grazing Land	5	6	5	100.00%	83.33%
Mixed landuse	7	6	5	71.43%	83.33%
Bareland	10	14	9	90.00%	64.29%
Bushland	9	10	8	88.89%	80.00%
Clutvated land	25	22	21	84.00%	95.45%
Totals	59	60	50		

Overall Classification Accuracy = 83.33%

----- End of Accuracy Totals -----

KAPPA (K^) STATISTICS

Overall Kappa Statistics = 0.7814

Conditional Kappa for each Category.

Class Name	Kappa
Forest land	1.0000
Grazing Land	0.8182
Mixed landuse	0.8113
Bareland	0.5714
Bushland	0.7647
Clutvated land	0.9221

----- End of Kappa Statistics -----

7.4 Model performance

The performance of the model is checked for the Geba watershed at the outlet near Mekelle and for the Laelay Wukro test site. The model performance of flow prediction for a specific application is evaluated through sensitivity analysis, calibration, validation and uncertainty analysis.

7.4.1 Sensitivity Analysis

Parameters identified by sensitivity analysis that influence predicted outputs are often used to calibrate a model (White and Chaubey, 2005; Van Griensven et al., 2006). In this research, a Latin hypercube-one factor at a time (LH-OAT) sensitivity analysis, which is incorporated in the soil and water assessment tool (SWAT2009), and sequential uncertainty fitting-two (SUFI-2) of SWATCUP2009, were used for sensitivity analysis. The analysis was carried out based on the objective function of the sum of the square of residual (SSQ) for all the 27 model parameters and 10 intervals of Latin hypercube (LH) sampling.

Table 7-4 : Sensitivity analysis result with, mean and category of the parameters.

Parameters	Sensitivity Rank	Mean	Sensitivity Category
SCS runoff curve number for moisture condition II (CN2)	1	3.31	Very High
Available water capacity of the soil layer (mm/mm soil) (Sol_AWC)	2	1.38	Very High
Base flow alpha factor(days) (Alpha_Bf)	3	0.924	High
Soil evaporation compensation factor (ESCO)	4	0.537	High
Threshold depth of water for return flow (Gwqmn)	5	0.4	High
Channel hydraulic conductivity (CH_K2)	6	0.294	High
Channe manning coefficent (CH_N2)	7	0.252	High
Groundwater delay (days) (GW_delay)	8	0.159	Medium
Groundwater ‘revap’ coefficient (GW_revap)	9	0.113	Medium
Soil conductivity (mm/h) (Sol_k)	10	0.0224	Small
Ground water recharge (Recharg_DP)	11	0.0213	Small

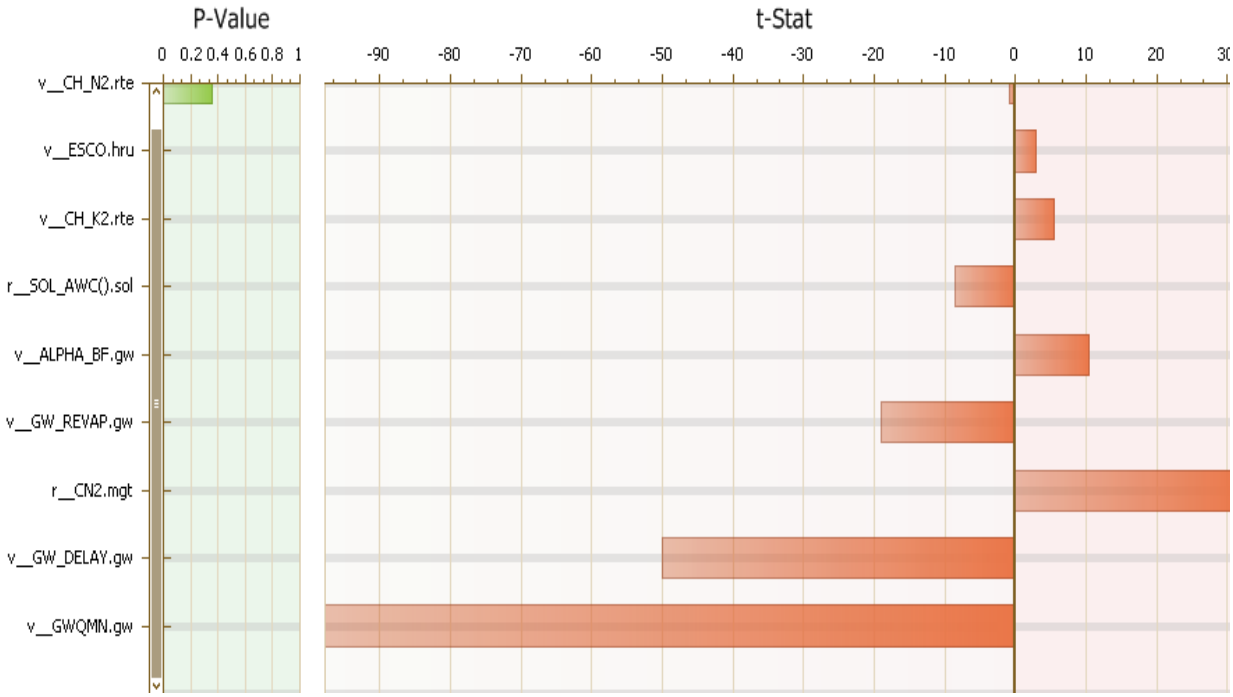

Figure 7-18: Ranks of sensitive parameters used for the flow calibaration.

The results of the analysis indicate that eleven parameters (Table 7-4) are most crucial for the Geba basin. The classes are based on mean relative coefficient index, as given by sensitivity classification of Lenhret et al. (2002).

7.4.2 Calibration

7.4.2.1 The SWAT2009 Model

The SWAT2009 model is tested in the Geba outlet and one of the test sites within the Geba.The model calibrated with the measured stream flow between 1994-1998 with the warm up period of 1991-1993 at Geba outlet.For the test sites the calibration is done with the measured data of 2001-2003 at Laelay Wukro test site.The simulated hydrograph at the two outlets (Figure7-19, Figure 7-22). To test model accuracy a statistical test and graphical representation is prepred to see how it fits with the measured data.The calibration is done based on the sensitive parameters that are identified (Table 7-4, Figure 7-18).The calibration is done with fine adjustement of the sensitive parameters in annual, monthly and daily basis with the stastical measures of R^2 (coefficient of determination) > 0.6 and E_{NS} (Nash Sutcliffe coefficient) >0.5 (Santhi et al., 2001; Moriasi et al., 2007).

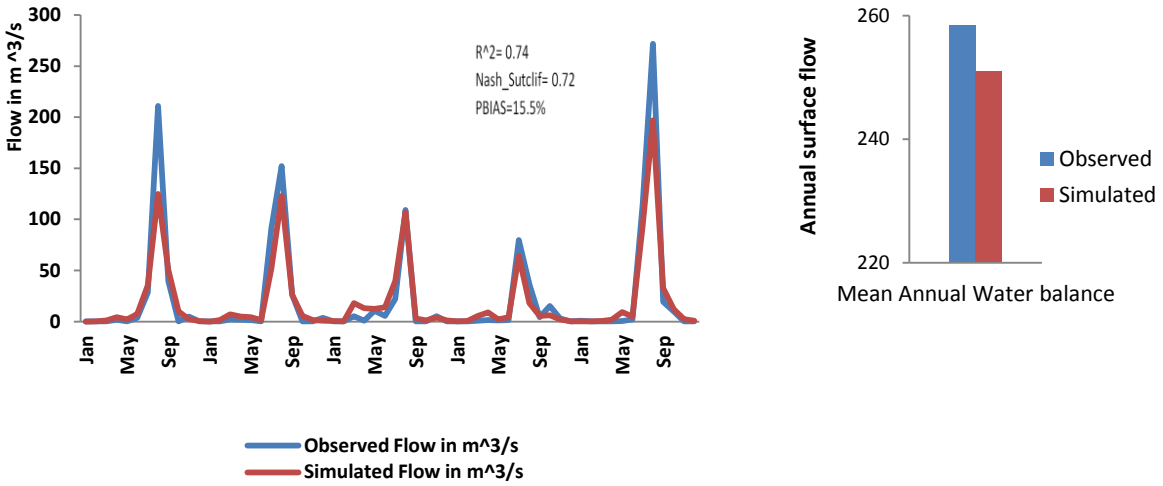

Figure 7-19: Monthly mean simulated versus observed, during calibration of the Geba river at Geba Nr. Mekelle station (1994-1998) (a) and corresponding mean annual average flow million meter cube (MCM) (b) (Data base: Ministry of Water resource and own processing).

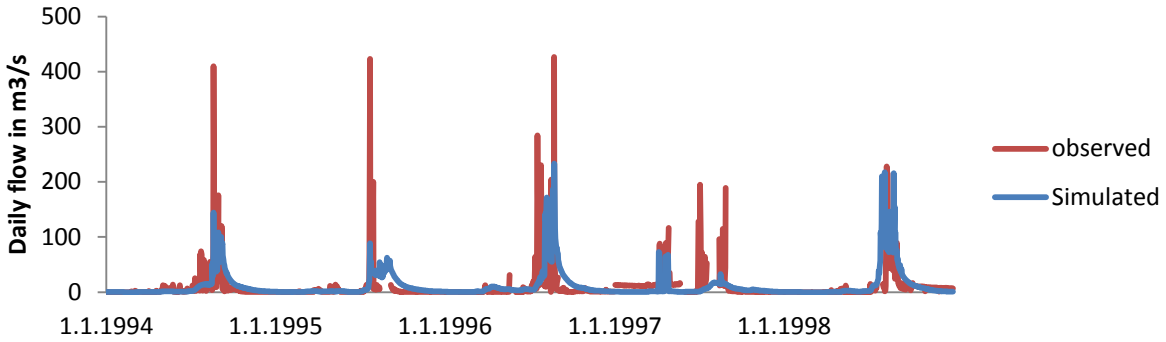

Figure 7-20: Simulated daily flow (m^3/s) versus observed daily flow (m^3/s) for Geba basin at Geba Nr.Mekelle station (Data base: Minstry of Water resource and own processing).

For the ground water delay estimation, well level fluctuations were considered as internal calibration (Figure 7-21). Water level changes of 2 wells all over from the Geba basin were considered for this assessment. For the Laelay Wukro test site modeled daily groundwater levels were compared to the observed groundwater levels and show a satisfying performance (Figure 7-22).

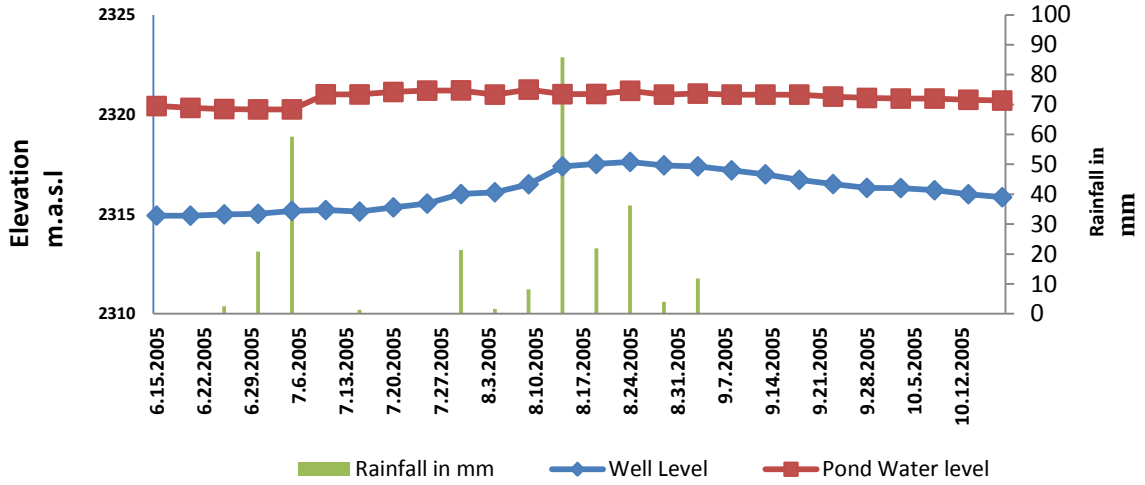

Figure 7-21: Rainfall (mm),well levels (m a.s.l) and pond water level (m a.s.l) of Tsankanet pond in Geba basin documenting ground water level (Data base: Gebreyohannes et al., 2010).

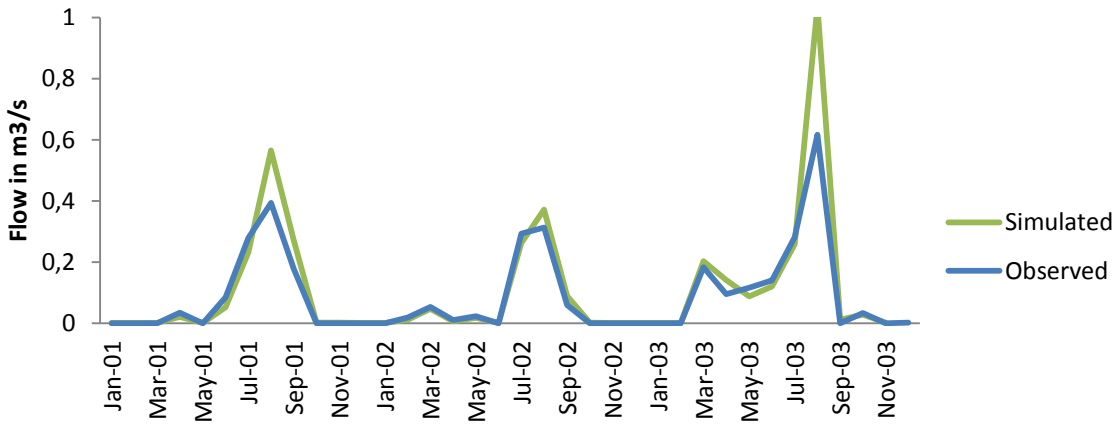

Figure 7-22: Simulating daily flow (m^3/s) versus observed daily flow (m^3/s) for the Laelay Wukro test site (Data base: Tigray Water Resource Bureau weather station data base).

The response of the sub-basins of the basin on the rainfall is documented by the runoff coefficient (Figure 7-23). This runoff coefficient map can be used for internal calibration of water availability in each sub basin. It can also be used for planning and managing the water resources.

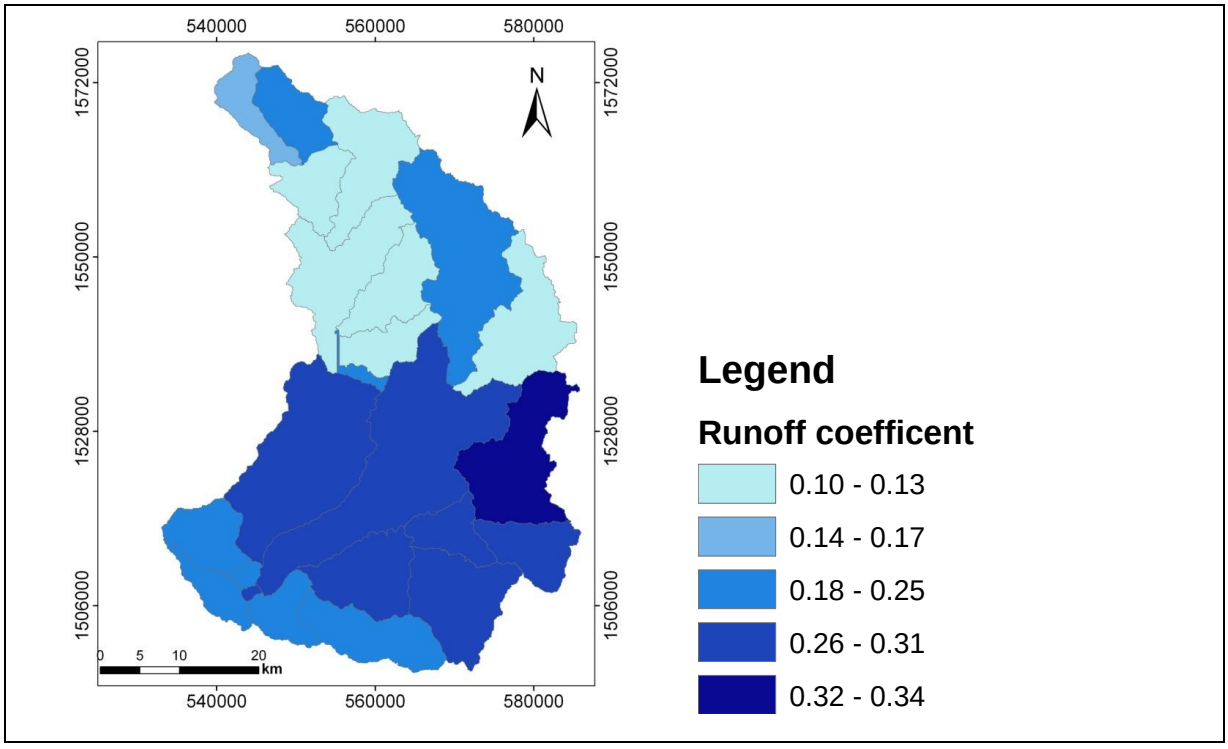

Figure 7-23: Runoff coefficient for the Geba basin in 2003 shown on sub-basin basis (Data base: Jarvis et al., 2008, National Meteorological Agency).

7.4.3 Validation

The validation is done after calibration with out any further changes in values of the sensitive parameters used in calibration.It is tested with the new separated data to determine wheather the onjective function is met or not.In similar way the model performance is checked with R^2 and E_{NS} recommended by Moriasi et al. (2007). Figure 7-24 to Figure 7-27 shows the validation result.

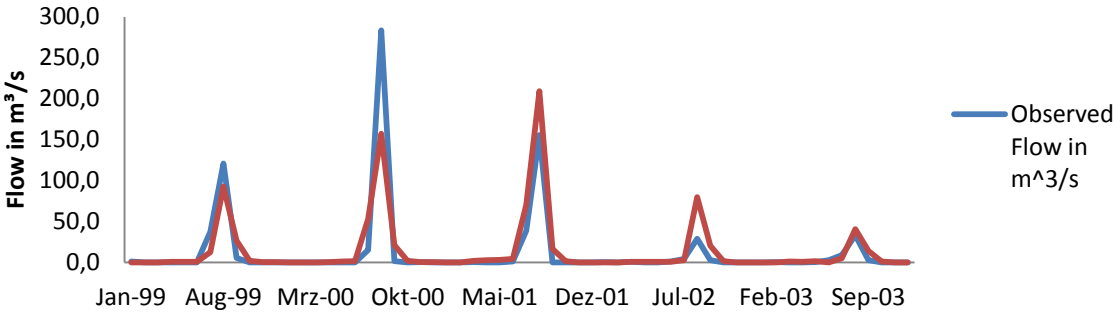

Figure 7-24: Validation of monthly simulated flow data of Geba river (m^3/s) referring to observed flow data at Geba river Nr.Mekelle station (January 1999–October 2003) (Data base: Ministry of Water Resources).

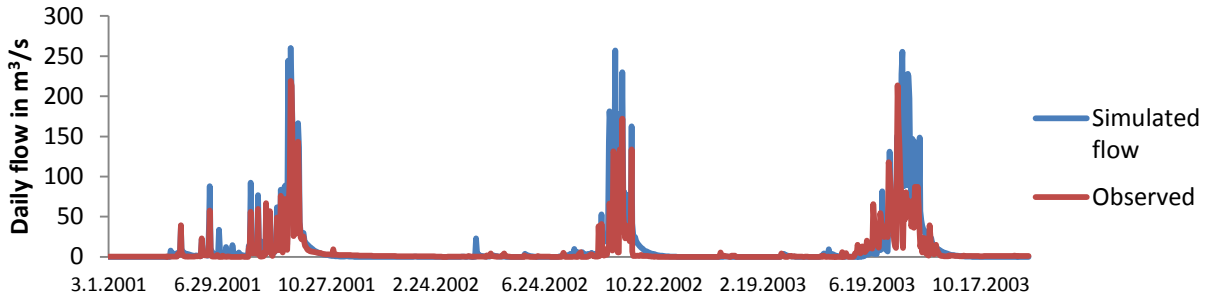

Figure 7-25: Validation of daily simulated flow data of Geba river (m3/s) referring to observed flow data at Geba river Nr.Mekelle station (2001–2003) (Data base: Ministry of Water Resources).

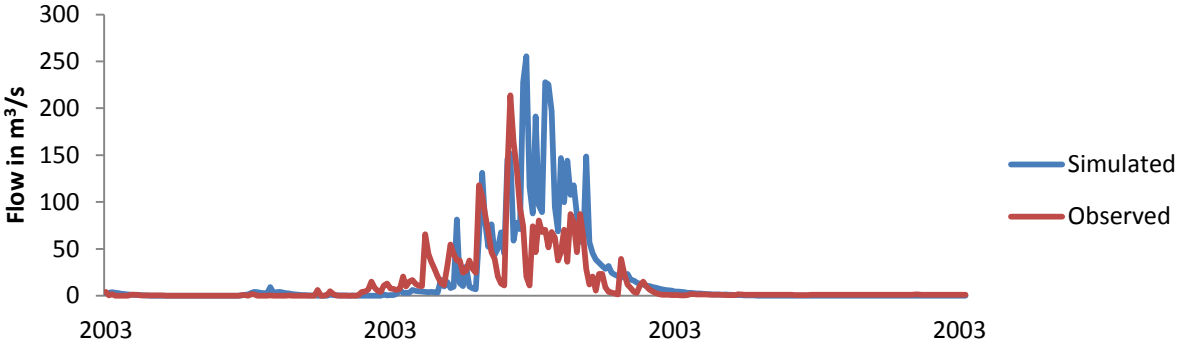

Figure 7-26: Validation of daily simulated flow data of Geba river (m3/s) referring to observed flow data at Geba river Nr. Mekelle station (2003) (Data base: Ministry of Water Resources).

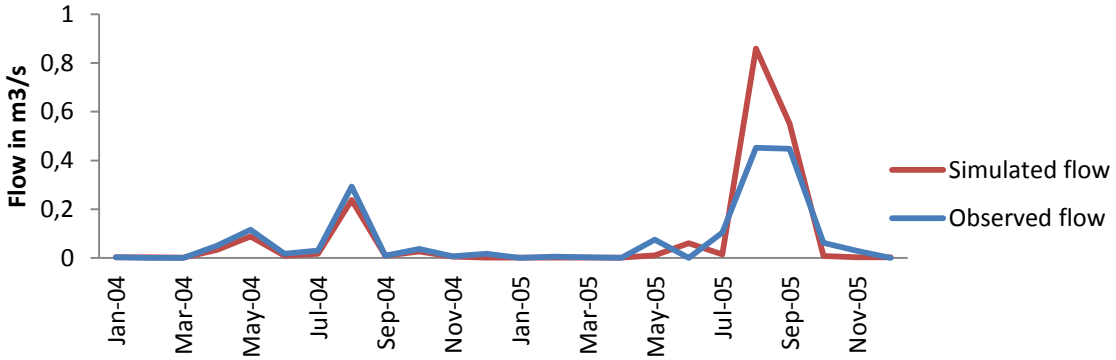

Figure 7-27: Validation of daily simulated flow data of Laelay Wukro test site (m³/s) referring to observed flow data at the outlet (2004–2005) (Data base: Tigray Bureau of Water Resources).

Table 7-5: Calibration parameter ranges used in calibration of the model at Geba Nr. Mekelle station and Laelay Wukro test site. Grouped as surface flow parameters, ground flow and hydraulic parameters.

Parameter	Description	Calibration range	L/ Wukro Test Site	Main Watershed (9 parameters)	Main Watershed (11parameters)
CN2	curve number	± 25%	±13%	±10%	±12.46%
ESCO	Soil evaporation Compensation	0-1	0.3	0.32	0.22
Sol_AWC	Available soil water capacity	± 25%	-16.7%	-13%	-16.7%
Sol_K	Soil hydraulic conductivity	± 25%	-12.3%		-15%
GW_REVAP	Ground water "revap" coefficient	±0.036	0.07	0.13	0.07
GWQMN	Threshold depths for return flow	0-5000	7.5	68.75	112
GW_DELAY	Ground water delay	0-500	37.9	37	20
ALPHA_BF	Base flow alpha factor	0-1	0.75	0.22	0.31
REVAPMN	Threshold depths for return flow	0.001-100	4.82		90
RECHARG_DP	GroundwaterRecharge		0.35	0.35	0.42
CH_K2	hydraulic conductivity	0-150	34	41.35	11
CH_N2	Channel roughness	0-1	0.05	0.08	0.05

Table 7-6: Model performance for the Geba basin: (PARSOL is parameter solution and SUFI-2 is sequential uncertainty fitting two).

Objective function		1972 Land cover map				2003 Land cover map			
		Calibration 1994-1998		Validation 2000-2003		Calibration 1994-1998		Validation 2000-2003	
		Daily	Mon.	Daily	Mon.	Daily	Mon.	Daily	Mon
Coefficient of Determination (R^2)	PARASOL	0.54	0.60	0.6	0.75	0.56	0.74	0.56	0.77
	SUFI-2	0.61	0.74	0.69	0.83	0.6	0.8	0.7	0.87
Nash-Scott ,E_{NS}	PARASOL	0.34	0.52	0.36	0.72	0.39	0.72	0.41	0.77
	SUFI-2	0.44	0.75	0.46	0.74	0.43	0.75	0.46	0.86
Percent Bias (PBAIS), in%	PARASOL	29.6	16.3	19	15	27	15.5	18.9	15.1
	SUFI-2	26.7	15.5	23	14	24	14	21.5	13.5

Table 7-6 indicates that the SWAT2009 model predicted the monthly and daily stream flows in acceptable performance. With this performance, the model simulates different hydrological component based on the 2003 land use and land cover conditions (Table 7-7).

Table 7-7: Simulation based on the monthly hydrological components for 1991-2003 using 2003 land cover map.

Hydrological componenets	Months												
	Jan	Feb	Mar	Apr	May	Jun	Jul	Aug	Sep	Oct	Nov	Dec	Total
Surface flow (mm)	0.01	0	0.6	0.68	0.32	0.8	18	34	1.24	0.2	0.04	0.04	55.9
Base flow (mm)	0.01	0	0.2	0.25	0.01	0.3	4	28	14	0.4	0.01	0.26	46.6
Lateral flow (mm)	0.26	0.3	1.36	2.19	2.02	2	11	18	4.7	1.1	0.54	0.03	43.5
Stream flow (mm)	0.28	0.3	1.96	2.87	2.34	2.8	34	79	19.9	1.7	0.59	0.33	146
Areal Rainfall (mm)	6.4	12	39.4	60.4	39.1	27	171	151	17.3	22	20.6	9.8	575

7.4.4 Uncertainty Analysis

Uncertainty analysis was implemented after sensitivity analysis, calibration and validation was finished, using the PARASOL methods of SWAT2009, and SUFI-2 methods of SWAT-CUP. Uncertainities associated with parameters are an issue in calibrating and predicting flow. The parameters are controlled by watershed conditions and are highly dependent on the spatial resolution of the watershed and its input parameters and the detailing of the data. The uncertainty is associated with parameters that are determined by different watershed attributes and are to be reduced corresponding to the spatial resolution of these attributes. Conversely, uncertainties of parameters that are not determined from those attributes are reduced with calibration procedure through a systematic range adjustment process.

Table 7-8: Explicit Calibrated parameters of major parameters.

Parameters	SWAT2009 default		Actually Used	Uncertainty ranges				Type of changes
				Parsol		SWATCUP-SUFI2		
	Lower bound	Upper bound		Min.	Max.	Min.	Max.	
Curve number(CN2)	25	98	51 to 91	-6.7	12.46	-0.05	0.23	*relative
Soil evaporation Compensation (ESCO)	0	1	0.22	0.12	0.45	0.11	0.5	*relative
Available soil water capacity(Sol_AWC)	0	1	0.03 to 0.12	-4.5	23	-0.01	0.27	*relative
Soil Hydraulic conductivity (Sol_K)	0	100	4 to 32	-0.6	0.35	-0.2	0.41	*relative
Base flow alpha factor (ALPHA_BF)	0	1	0.29	0.22	0.47	0.12	0.51	*relative

*Relative change in percentage

7.5 Impacts of land use and land cover change on hydrological process

7.5.1 Present conditions

Simulation analysis of the effect of land use and land cover change on the hydrological regime of Geba basin using SWAT2009 refers to the baseline data of the 2003 land use and land cover map. Same procedure was done including the 1972 land use and land cover map. Two independent simulation runs were conducted on a monthly basis using the 1972 and 2003 land use and land cover maps each considering climate data of the period 1991–2003, keeping other input parameters unchanged (Figure 7-29 to Figure 7-32). Comparisons were made for the contribution of surface runoff, lateral flow and ground water flow to stream flow (Table 7-9).

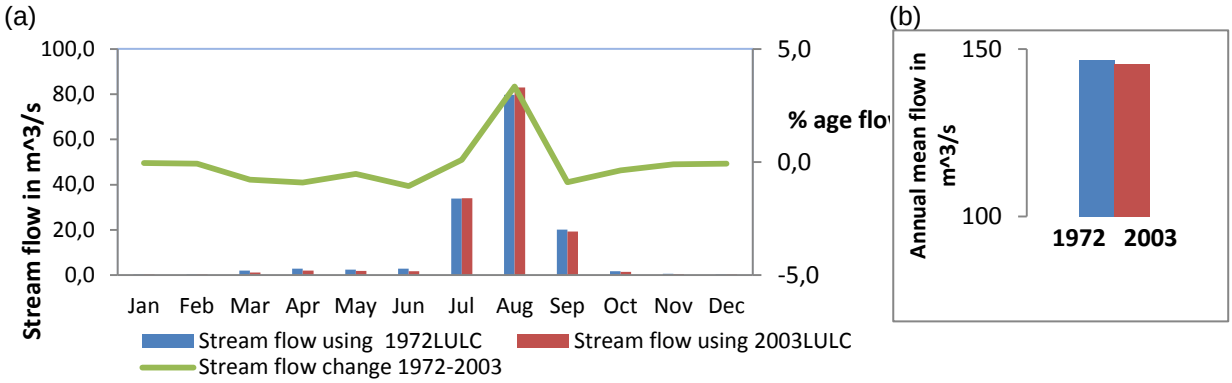

Figure 7-28: Land cover change impacts on monthly average stream flow (m^3/s) of the Geba river under the land use and land cover conditions of 1972 and 2003 using climate input parameters of the measuring period 1991–2003.The green graph shows the relative change of stream flow due to land use land cover change (a), effect on annual average stream flow is shown in diagram (b).

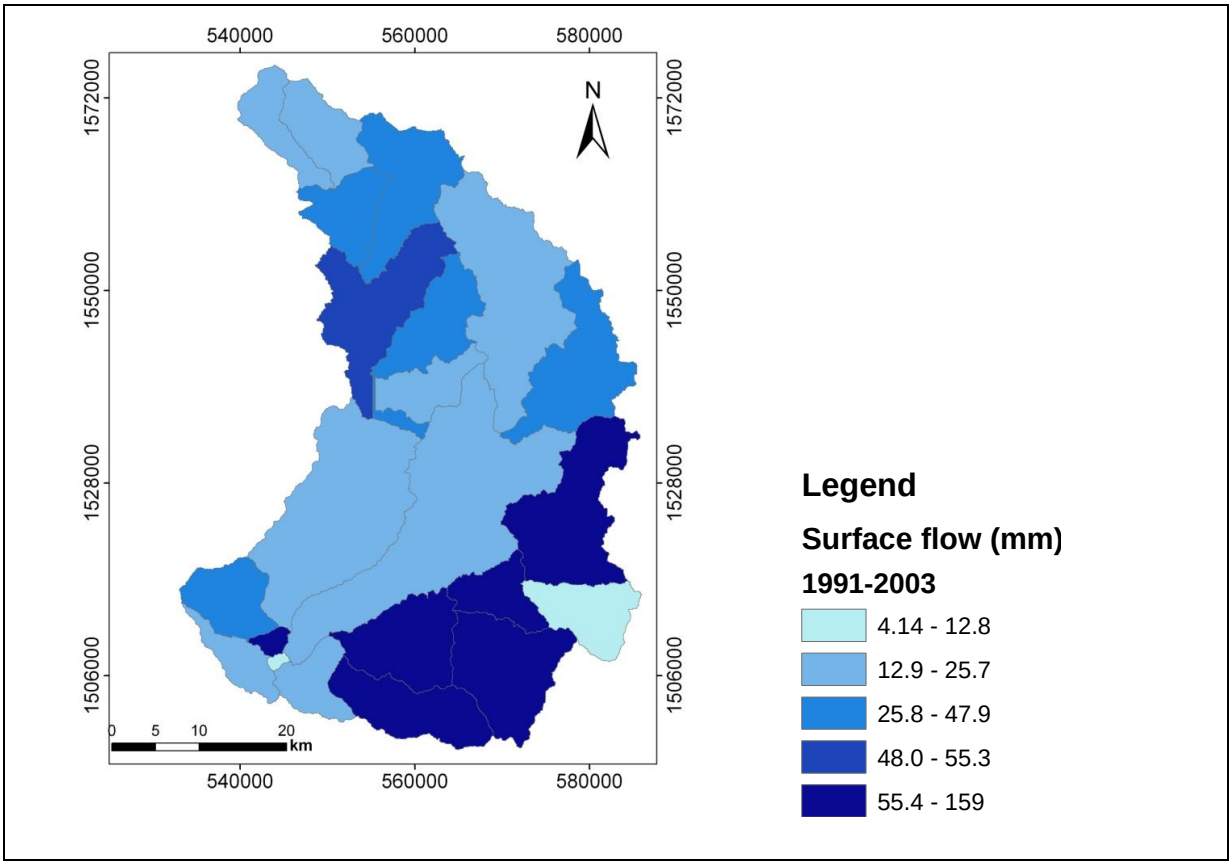

Figure 7-29: Spatial distribution of surface flow (mm) in the Geba basin modelled using 1972 land use and land cover.

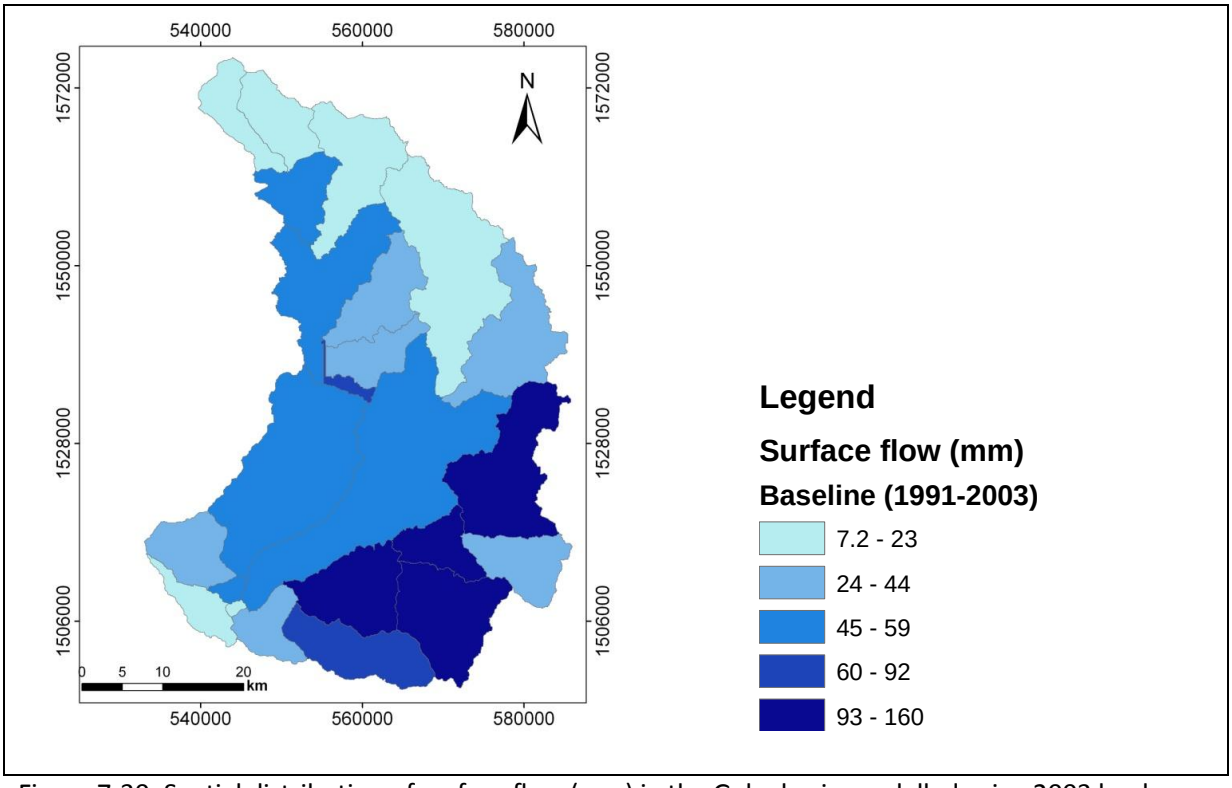

Figure 7-30: Spatial distribution of surface flow (mm) in the Geba basin modelled using 2003 land use and land cover.

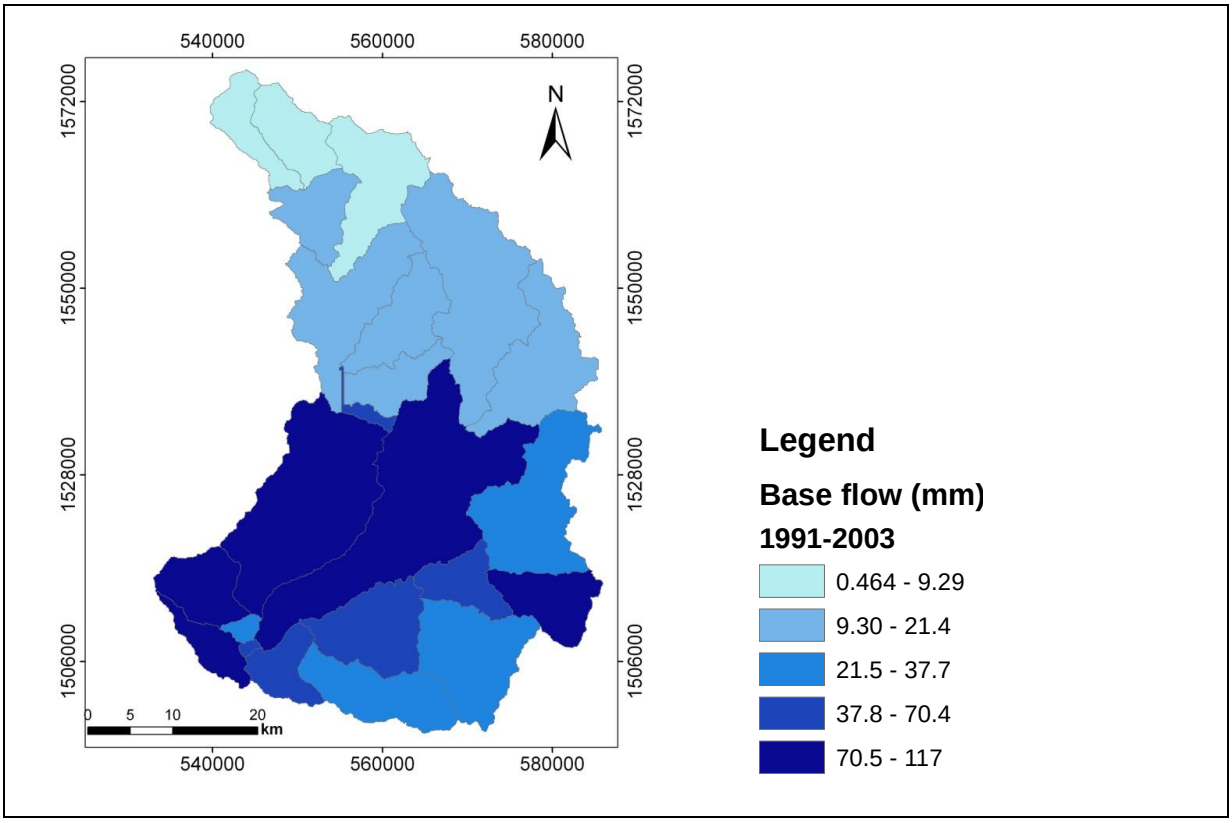

Figure 7-31: Spatial distribution of baseflow (mm) in the Geba basin modelled for land use and land cover conditions in 1972.

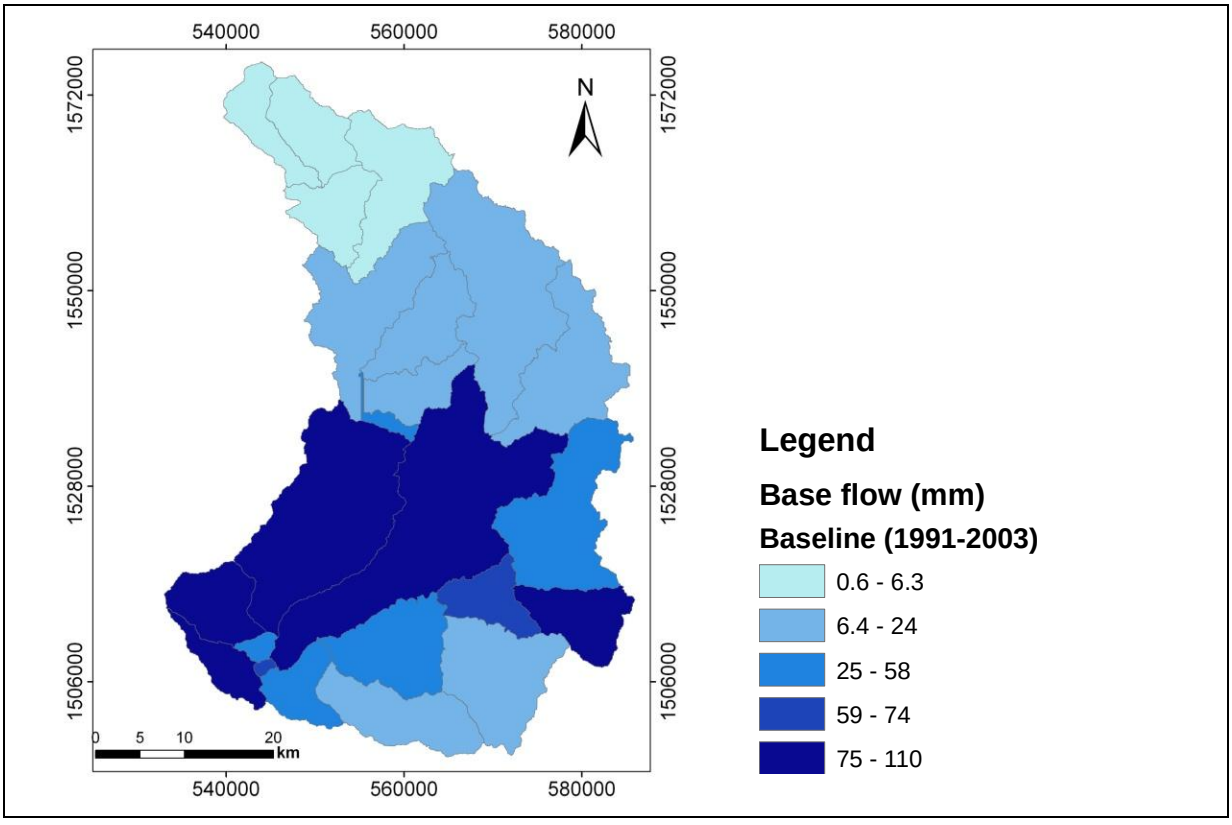

Figure 7-32: Spatial distribution of baseflow (mm) in the Geba basin modelled for land use and land cover conditions in 1972.

Table 7-9: Mean monthly wet (June to Septemer) and dry season (February to May) stream flow variability (1991–2003) of the Geba watershed and selected subbasins.

Selected sub-basins	Area in km²	Agricultural expansion in%		Mean wet periods flow (mm)		Mean dry periods flow (mm)	
		1972	2003	1972	2003	1972	2003
Sub-basin 12	53.872	8.64	56.71	35.85	53.6	0.8	0.52
Sub-basin 15	268.29	13.21	36.86	32.54	41.54	1.08	0.91
Sub-basin 17	356.03	10.85	23.1	34.01	48.86	2.28	1.43
Sub-basin 19	134.24	9.24	52.51	34.48	42.34	1.27	0.4
Entire watershed	2404	13.52	68.07	31.02	33.91	2.06	1.44

7.6 Simulating impacts of climate change on hydrological processes

The assesement of the implications of future climate changes on the hydrological regime were carried out by developing climate scenarios based on A2a and B2a scenarios of the Inter Governmental Panel Climate Council-Special Report on Emission Scenario (IPCC-SRES) (IPCC, 2008) generated from the HadCM3 and CGCM3 results. The climate change scenarios are used to generate future climatic data as input for the SWAT2009 model to determine the possible future watershed hydrological response to the changes in climate. Trend and statistical analysis based on the past climate data were made to get an insight on the trend of past climate change and variability to future changes (cf. Chapter 6).

The climate scenarios are generated by Statistical Downscaling Scaling model (SDSM) based on the data from National Center for Environmental Protection (NCEP) and observed data from Mekells station. The best correlated predictor variables from HadCM3 (A2a and B2a) and CGCM3A2a were selected for minimum temperature, maximum temperature and precipitation for Mekelle meteorological stations with a baseline of weather condition (1980–2000). The predictors are listed in Table 7-10.

Table 7-10: Selected predictor variables for the predictands for Mekelle weather station.

Model	Daily Rainfall	Daily min. and max. Temperature
Predictors	• Surface divergence • Relative humidity at 500hPa • 850 hpa meridian velocity • Mean sea level pressure	• Mean sea level pressure • 850hpa divergence • Relative humidity at 500hPa • Mean temperature at 2m • 850 hpa zonal velocity
Model type	• Daily • Fourth root transformation • Conditional process	• Daily • Linear model • Unconditional process

The performance of the SDSM models in comparison with the observed rainfall and temperature data were evaluated by downscaled time series data from. Each series was summarized by mean of accumulated monthly totals averaged over the twenty ensembles and then compared with the observed rainfall series. Comparison was performed over the period of SDSM calibration (1961–80) and the independent verification period (1980–2000) (Figure 7-33, Figure 7-34).

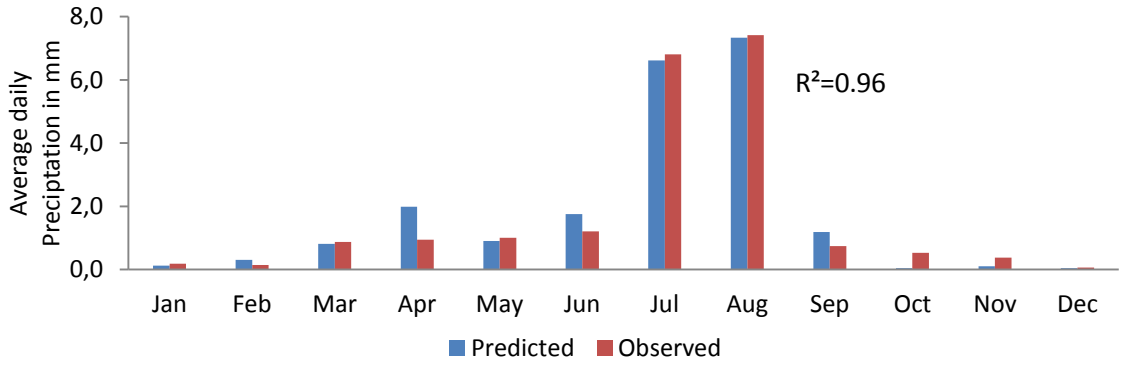

Figure 7-33: Comparison of observed and predicted mean monthly precipitation for the period 1991–2001 at Mekelle weather station.

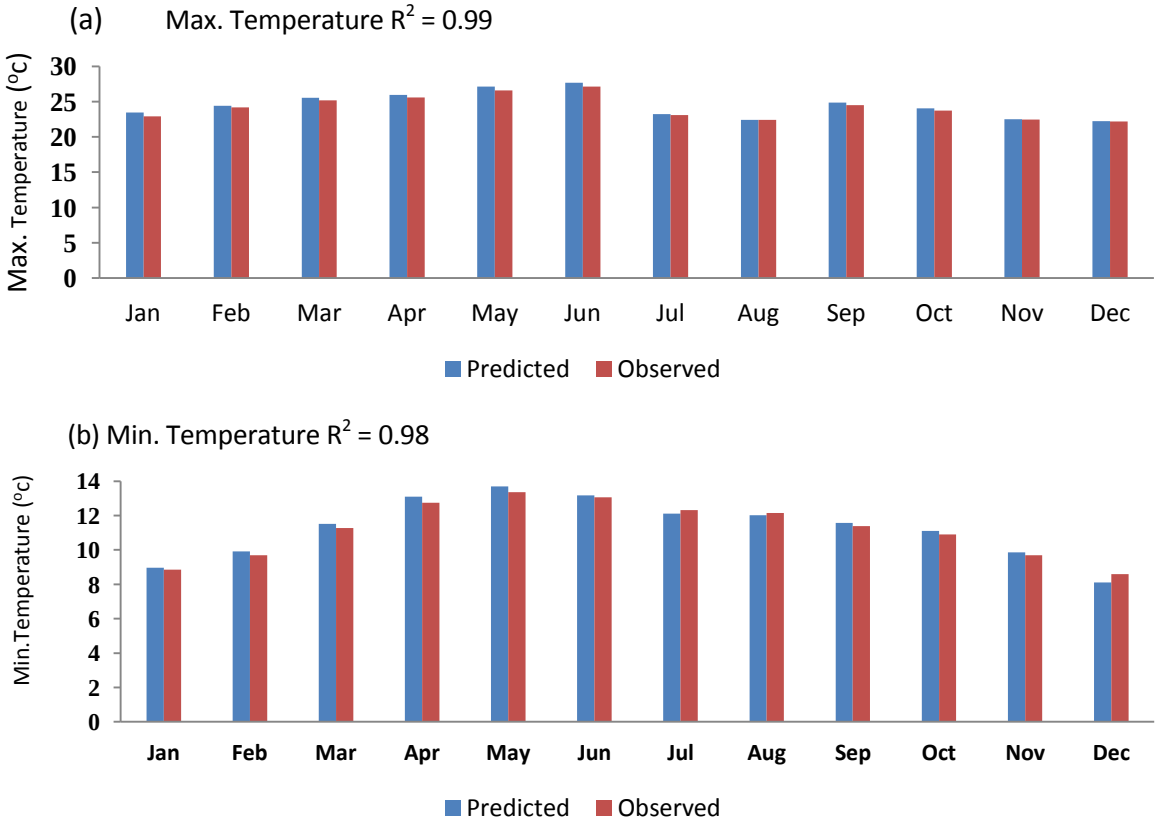

Figure 7-34: Comparison of observed and predicted mean (a) minimum and (b) maximum monthly temperatures for the period 1991–2001 at Mekelle weather station.

Following the results of observed and predicted model result for the baseline line period, the future scenarios for mean annual rainfall, maximum and minimum temperatures for Mekelle weather station are tabulated (Table 7-12 to 7-15). The mean annual data for Mekelle weather station show that an increase of rainfall within a range of 4% to 12% in the coming 90 years with different GCM and scenarios has to be expected (Table 7-12). A minimum percentage of change with 4% for the A2a scenario of the HadCM3 model relative to the baseline is predicted whereas a maximum change of 12% with for the A2a scenario of the CGCM3 model is predicted.

Table 7-11 Mean annual predicted values and relative changes of rainfall at Geba watershed (Mekelle Station).

GCM	Scenarios	Baseline 1981–2001	2011–2040 (mm)	2041–2070 (mm)	2071–2100 (mm)	Max.% change
HadCAM3	A2a	636.5	628.8	640.71	662.62	4.1
HadCAM3	B2a	636.5	641.3	652.88	677.84	6.4
CGCM3	A2a	636.5	579.5	639.49	714.98	12.3

Table 7-12: Mean annual predicted values and relative changes of maximum temperature at Geba Mekelle weather station.

GCM	Scenarios	Baseline 1981–2001	2011–2040 (°C)	2041–2070 (°C)	2071–2100 (°C)	Max. change (°C)
HadCAM3	A2a	24.1	24.8	25.1	25.5	1.4
HadCAM3	B2a	24.1	24.8	25.0	25.3	1.2
CGCM3	A2a	24.1	24.4	24.4	24.5	0.4

Table 7-13: Mean annual predicted values and relative changes of minimum temperature at Mekelle weather station.

GCM	Scenarios	Baseline 1981–2001	2011–2040 (°C)	2041–2070 (°C)	2071–2100 (°C)	Max. change (°C)
HadCAM3	A2a	9.7	11.35	11.61	11.9	2.2
HadCAM3	B2a	9.7	11.35	11.52	11.7	2.0
CGCM3	A2a	9.7	11.30	11.53	11.8	2.1

Table 7-14: Annual and monthly maximum average temperature change (°C) under various climate range scenarios (the future predicted value subtracted from the baseline).

	Month												
Scenarios	1	2	3	4	5	6	7	8	9	10	11	12	Max.
HadCM3A2a 2011-2040	0.01	0.26	0.70	0.91	0.61	0.99	1.41	1.20	0.51	0.98	0.31	-0.40	1.41
HadCM3B2a 2011-2040	0.02	0.10	0.60	0.87	0.66	1.03	1.65	1.13	0.52	0.85	0.40	-0.22	1.65
CGCM3A2 2011-2040	0.26	0.14	0.49	0.79	0.86	0.88	-0.91	-0.78	-1.56	1.35	1.27	0.25	-1.56
HadCM3A2a 2041-2070	0.54	0.96	0.97	1.01	0.80	1.54	1.69	1.44	0.35	1.26	0.85	0.13	1.54
HadCM3B2a 2041-2070	0.43	0.56	0.93	0.96	0.76	1.54	2.16	1.31	0.47	0.94	0.53	-0.08	2.16
CGCM3A2 2041-2070	0.75	0.61	0.70	0.93	0.94	0.80	-1.65	-1.35	-2.25	1.42	1.62	0.41	-2.25
HadCM3A2a 207-2099	1.20	1.53	1.40	1.19	0.95	2.45	2.28	1.56	0.12	1.76	1.39	0.11	2.28
HadCM3B2a 2071-2099	0.82	0.84	1.17	1.15	0.93	2.09	2.77	1.57	0.46	1.13	0.96	0.05	2.77
CGCM3A2a 2071-2099	1.27	1.32	10	1.23	1.23	0.69	-2.21	-1.99	-3.22	1.58	2.30	0.36	-2.21

Increasing maximum temperature shows high variations at the monthly time steps up to range 1.4°C to 1.5°C in 2011–2040, 1.7°C to 2.6°C in 2041–2070 and 2.6°C to 2.7°C in 2070–2099 for both A2a and B2a emission scenarios. Whereas a decrease in all period is observed in CGCM3A2a scenario (Figure 7-29, Table 7-14).

Monthly minimum temperature is also expected to increase, but with higher relative variations than the monthly maximum temperature. Increase of monthly minimum temperature at Mekelle weather station is expected to range between 0.5°C to 1.1°C in 2011–2040, 1.2°C to 4.3°C in 2041–2070 and 2.4°C to 5.5°C in 2070–2099 for both A2a and B2a emission scenarios (Table 7-15, Figure 7-29 b, d)

The expected future precipitation at Mekelle weather station for the time periods 2011–40, 2041–2070 and 2071–2099 is also predicted downscaling data of HadCM3A2a,HadCM3B2a and CGCM3A2a scenarios (Figure 7-36).

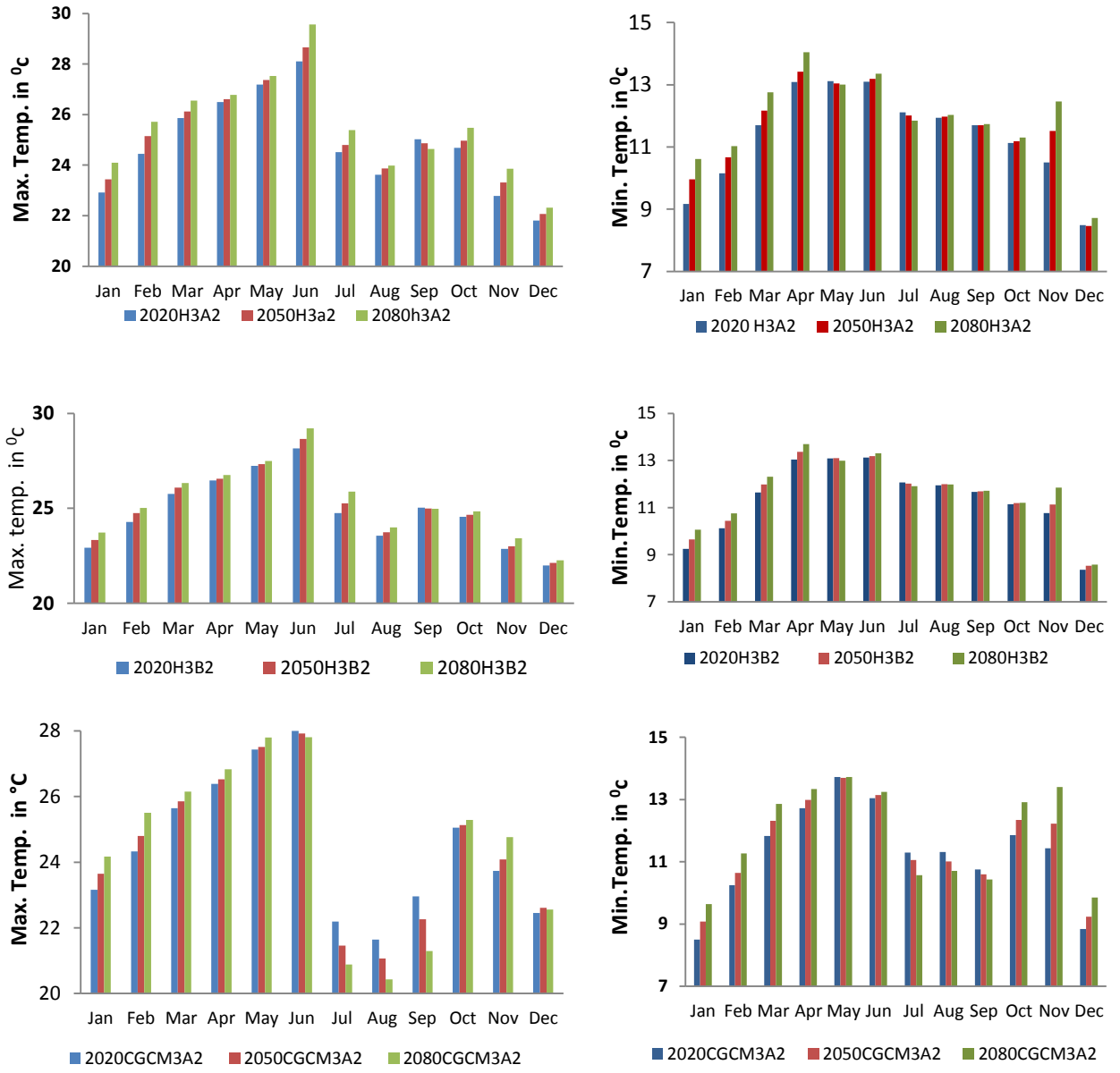

Figure 7-35: Monthly mean maximum and minimum temperatures projected by the Global circulation model for the periods 2011–2040 (blue), 2041–2070 (red) and 2071–2099 (green) for HadCM3A2 emmission scenario (a,b), the HadCM3B2 emmission scenarios (c,d) and CGCM3A2 scenarios (e,f).

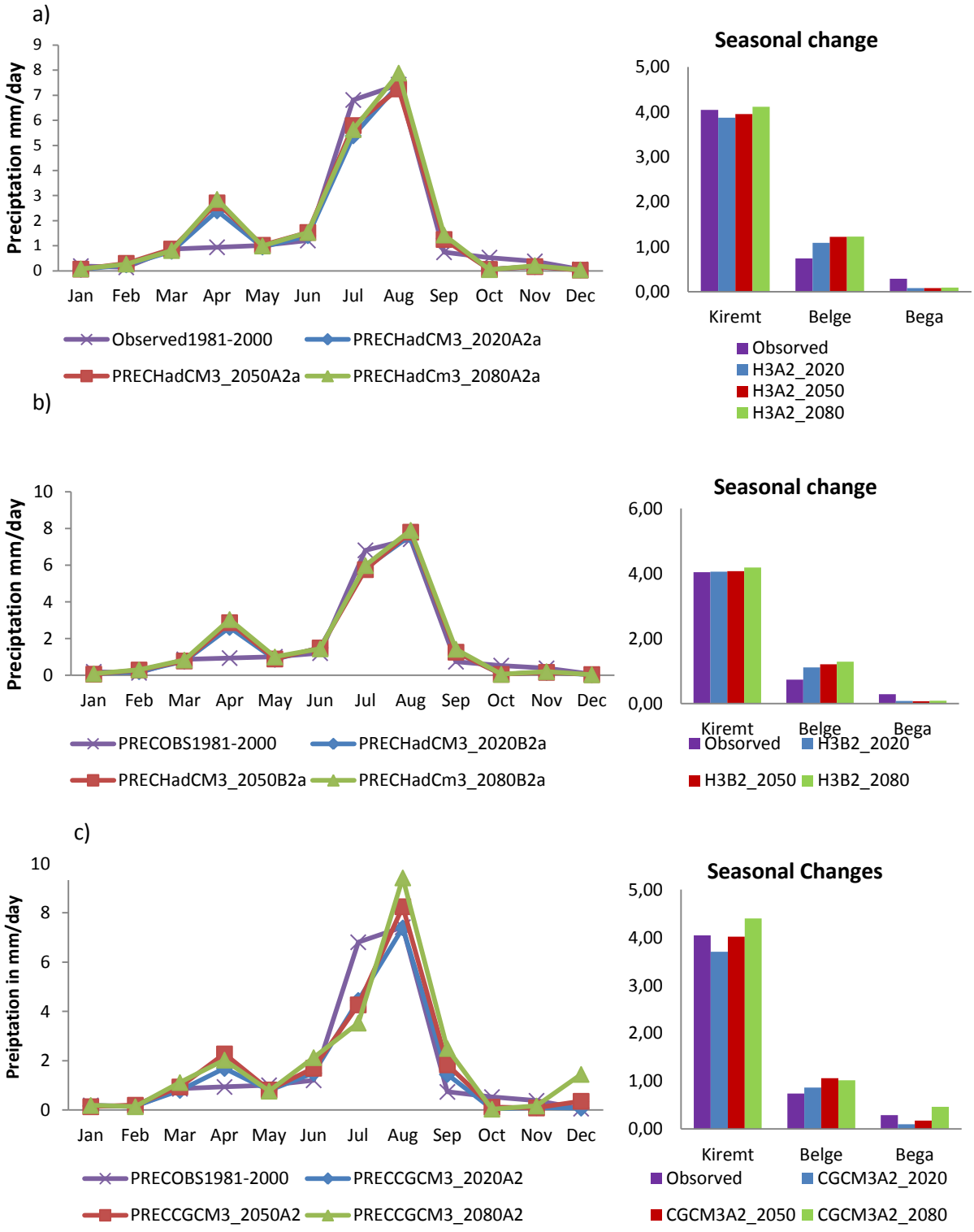

Figure 7-36: Average change in daily rainfall on monthly based on the different global circulation model sceenarios (a) HadCM3A2a, (b) HadCM3B2a and (c) CGCM3A2a for observed data and the time periods 2011-2040,2041-2070 and 2071-2099) (Data base: Canadian Institute for climate studies).

Table 7-14: Annual and monthly minimum average temperature change (°C) under various scenarios (the future predicted value subtracted from the baseline).

	Month												
Scenarios	1	2	3	4	5	6	7	8	9	10	11	12	Max
HadCM3A2a 2011-2040	0.33	0.46	0.42	0.34	-0.25	0.02	-0.21	-0.22	0.30	0.23	0.81	-0.11	0.46
HadCM3B2a 2011-2040	0.40	0.43	0.36	0.30	-0.27	0.06	-0.27	-0.22	0.27	0.25	1.07	-0.25	1.07
CGCM3A22011-2040	-0.34	0.55	0.55	-0.02	0.36	-0.03	-1.03	-0.84	-0.63	0.97	1.74	0.25	0.97
HadCM3A2a 2041-2070	1.11	0.98	0.89	0.67	-0.32	0.11	-0.31	-0.19	0.31	0.29	1.82	-0.13	1.11
HadCM3B2a 2041-2070	0.80	0.74	0.70	0.62	-0.26	0.11	-0.31	-0.16	0.30	0.29	1.44	-0.08	0.8
CGCM3A22041-2070	0.23	0.95	1.04	0.25	0.33	0.07	-1.27	-1.15	-0.79	1.45	2.53	0.64	-1.27
HadCM3A2a 207-2099	1.77	1.33	1.47	1.31	-0.36	0.28	-0.48	-0.13	0.34	0.41	2.77	0.12	2.77
HadCM3B2a 2071-2099	1.21	1.06	1.04	0.96	-0.38	0.24	-0.42	-0.18	0.32	0.31	2.15	-0.02	2.15
CGCM3A2a2071-2099	0.80	1.57	1.58	0.60	0.36	0.18	-1.75	-1.45	-0.96	2.02	3.71	1.26	3.71

7.7 Impact of future land useand land cover on the hydrology

The assessment of impacts of future land use and cover changes on the hydrological regime is carried out for the three land use and land cover scenarios (cf. chapter 6). Mean monthly water balance of the Geba river is calculated for each land use and land cover scenarios for the time period 2011–2040 applying SWAT2009. While differences do not occur during the minor rainy season in March/April, distinct differences occur for the major rainy season and following dry season (June–October) (Figure 7-37).

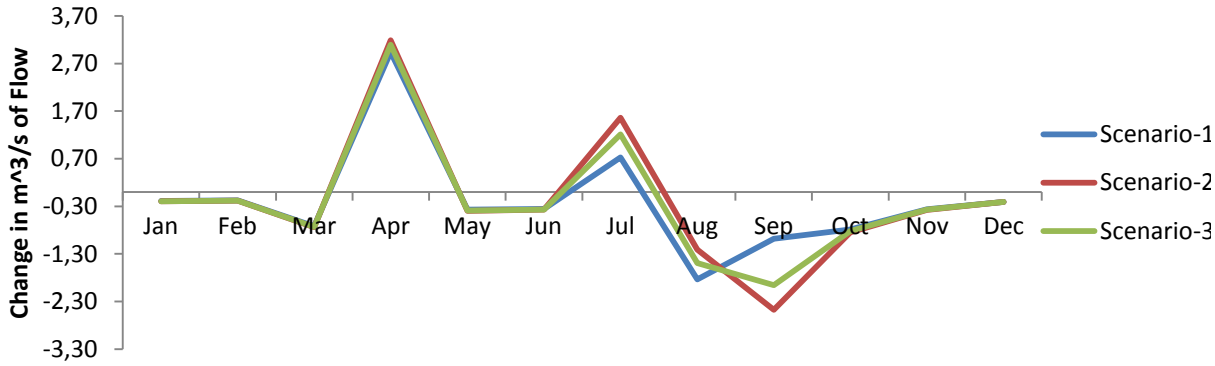

Figure 7-37: Change in mean monthly discharge (m^3/s) for Geba river calculates the three scenarios for the period 2011-2040 as compared to the base line (1991–2003).

7.7.1 Hydrological responses to changes in land cover and climate

The hydrological response of the Geba watershed to changes in land cover and climate were separately analyzed in chapters 7.6 and 7.7. The combined impacts on hydrological processes of the Geba basin were analyzed. Outputs of climate change scenario analysis in the previous section (7.6) were utilized as weather data in simulating the SWAT2009 model for future 2030 scenarios.

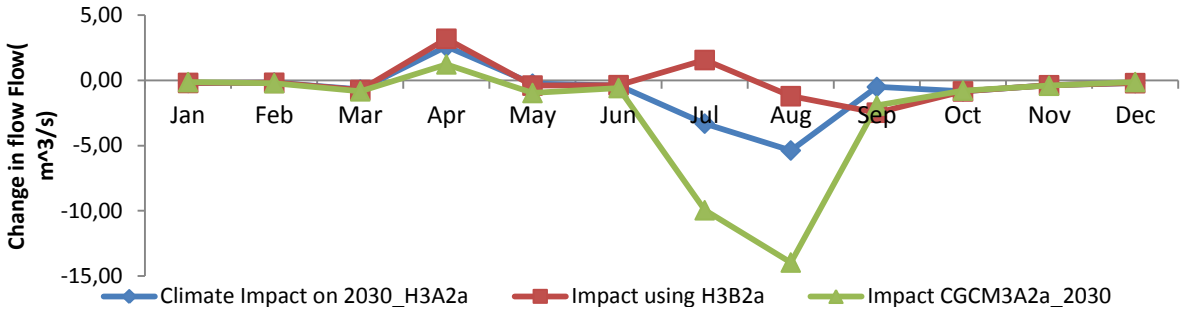

Figure 7-38: Combined impact of land cover and land use and climate change in the Geba river flow for the period 2011–2040

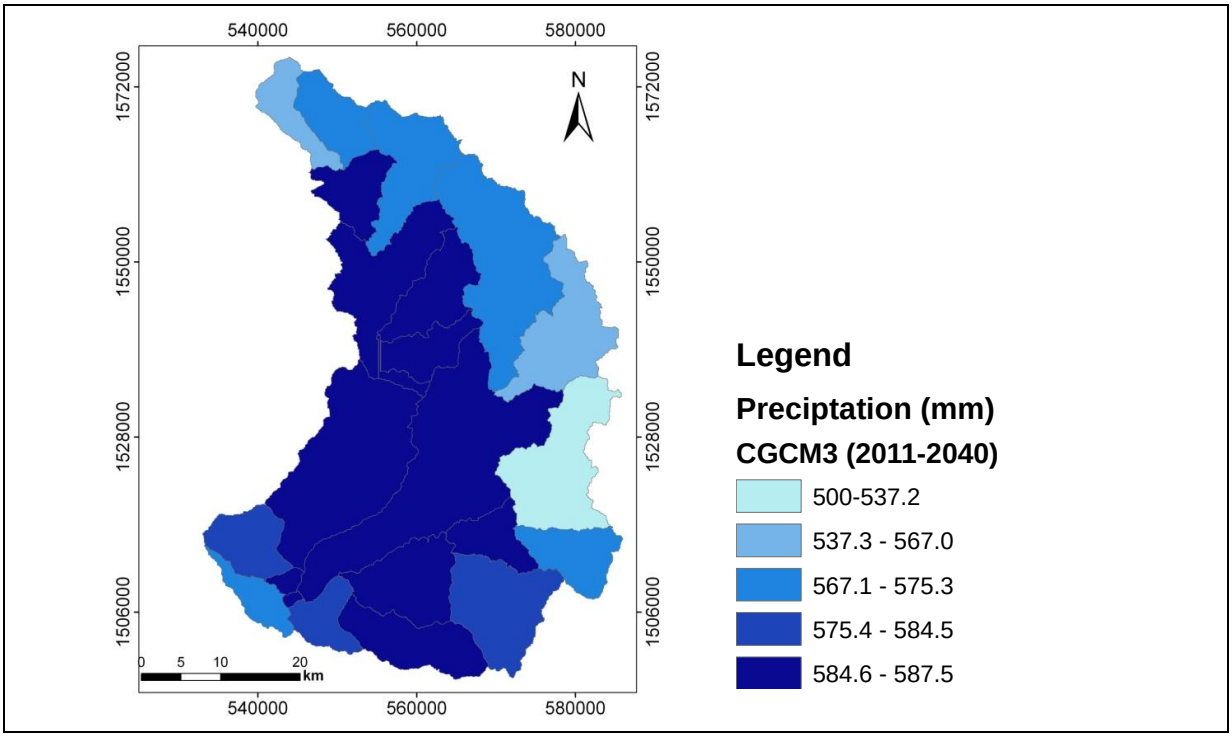

Figure 7-39: Model predicted results of Geba precipitation (2011–2040) by CGCM3 (Data base: Canadian Institute for climate studies).

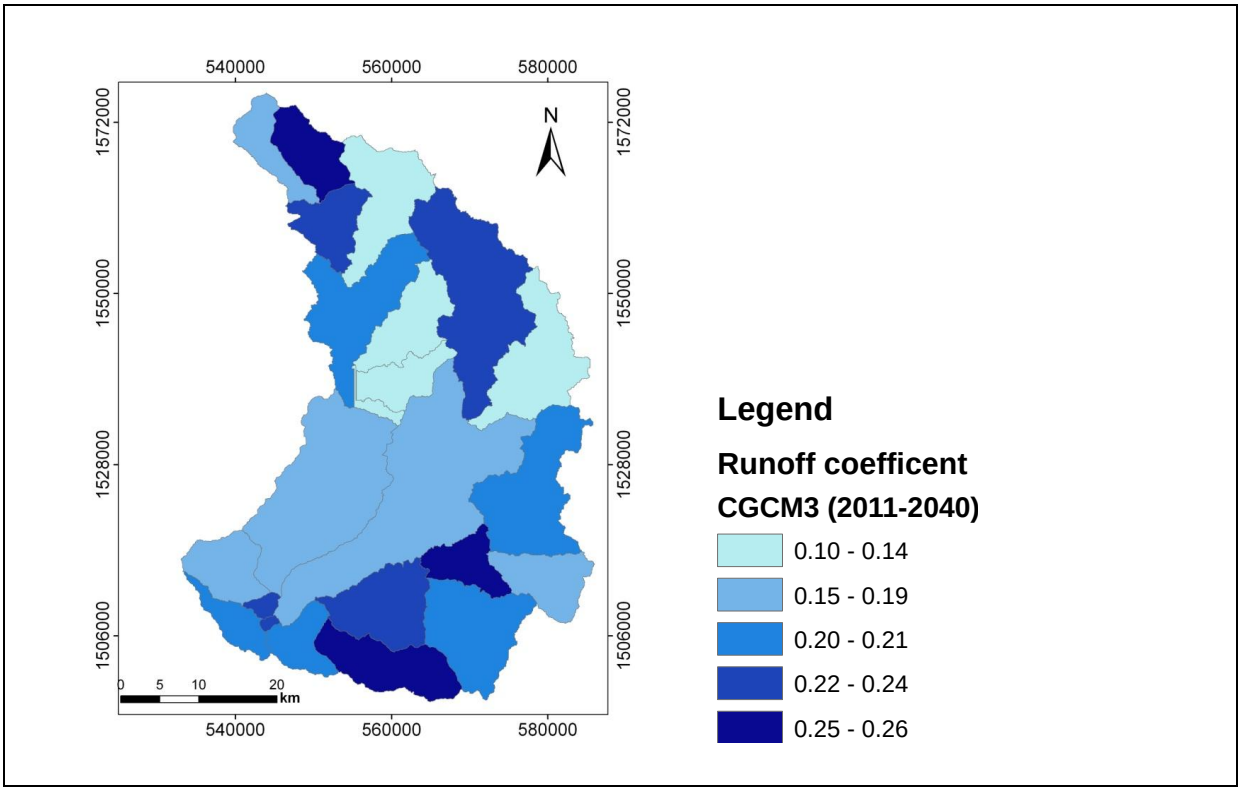

Figure 7-40: Model predicted results of Geba runoff coefficient (2011–2040) (Data base: Canadian Institute for Climate Studies).

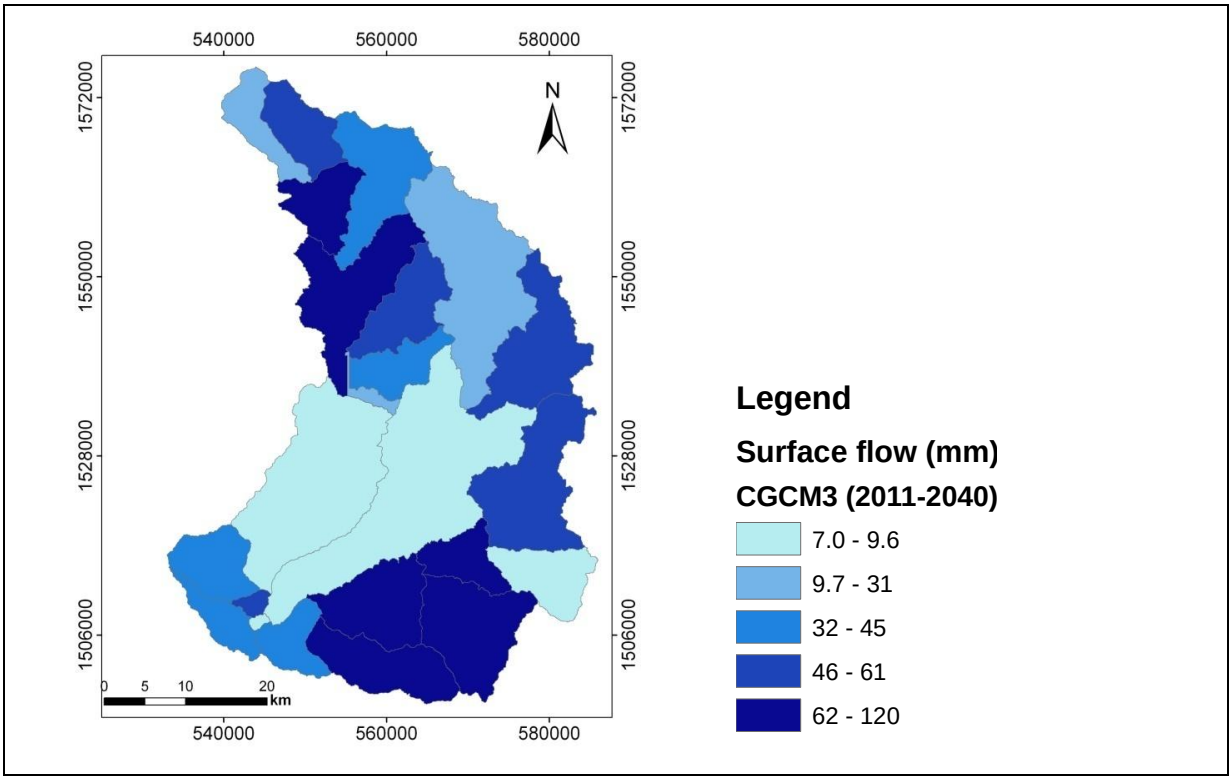

Figure 7-41: Model predicted results of Geba surface runoff (2011–2040) (Data base: Canadian Institute for Climate Studies).

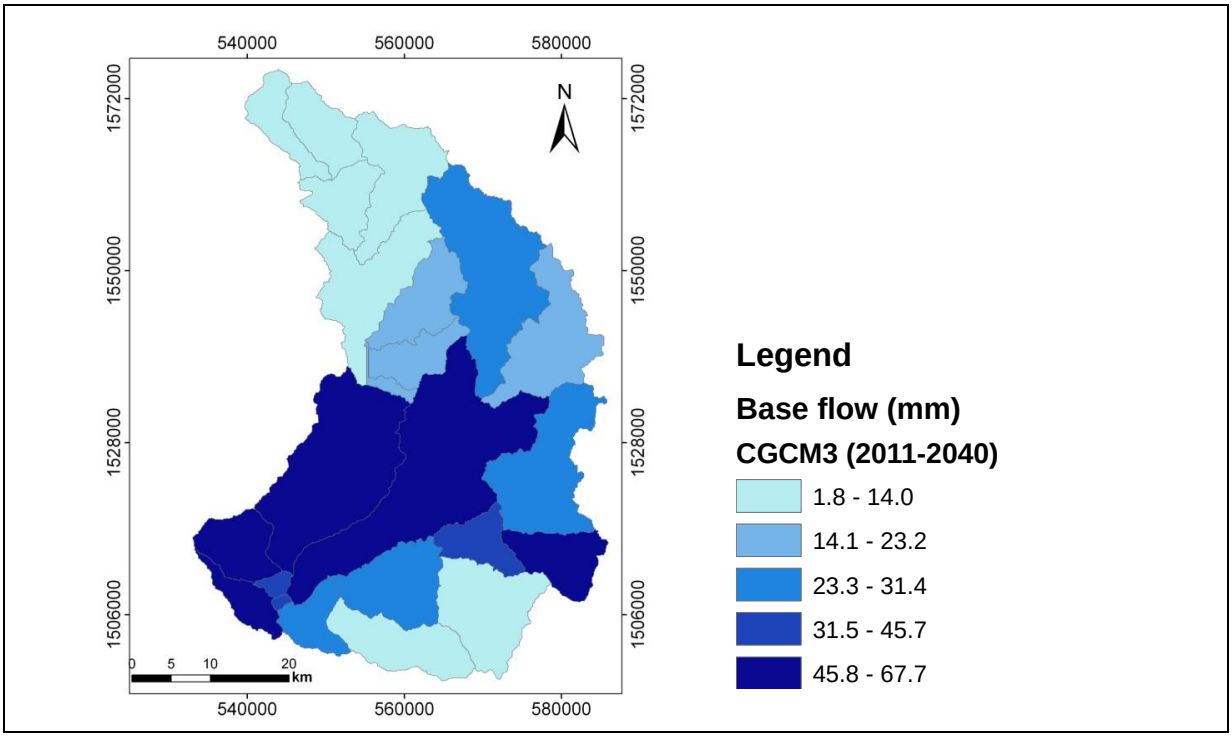

Figure 7-42: Model predicted results of Geba baseflow (2011-2040) (Data base: Canadian Institute for climate studies).

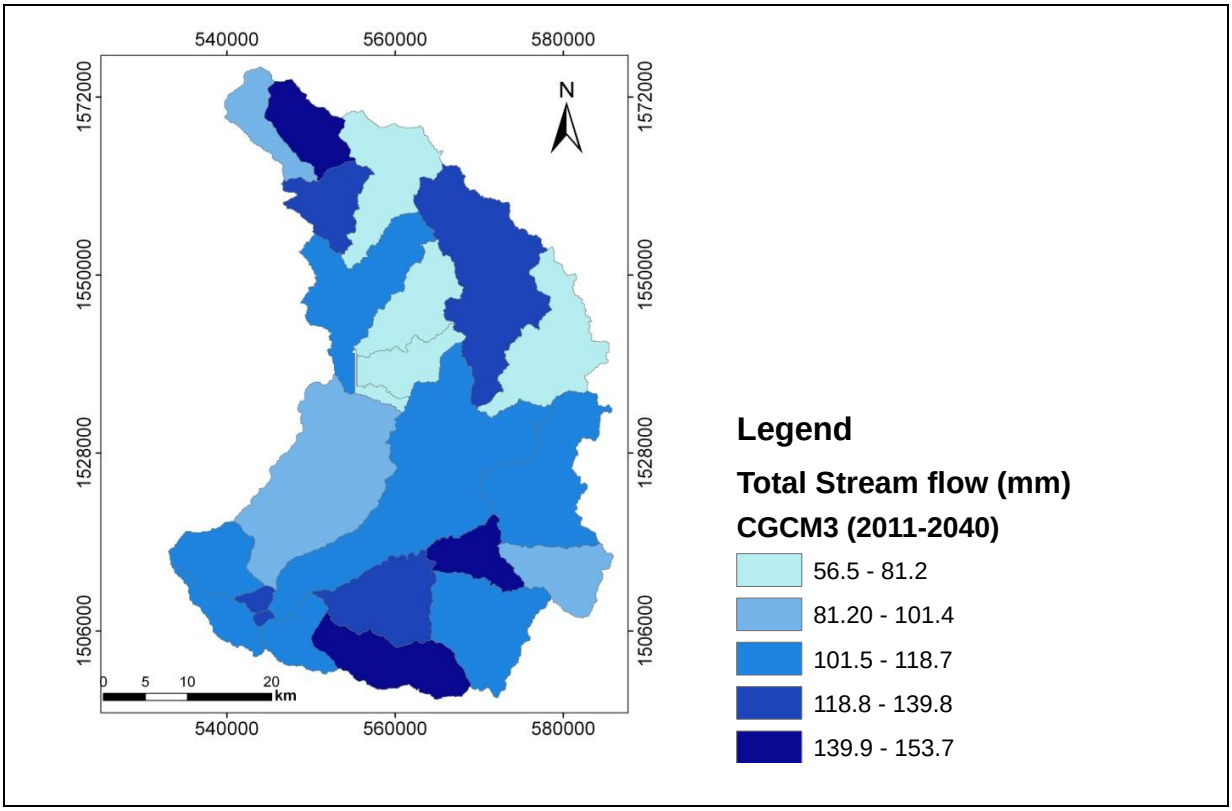

Figure 7-43: Model predicted results of Geba total stream flow (2011-2040). (Data base: Canadian Institute for Climate Studies).

Table 7-16: Land cover change impact on water balance in million cubic meter (MCM) and percent changes considering land use Scenario-2 with different GCM climate model.

	1972	2003	2030 H3A2a	2030 H3B2a	2030 CGCM3A2a
Annual mean Precitation in mm	636	636	629	641	589
Surface flow (SURQ) in MCM	147.86	136.51	124.42	142.37	126.16
Base flow(GWQ) in MCM	122.44	112.04	95.46	99.23	75.44
Interflow(LATQ) in MCM	115.65	97.54	100.68	98.17	69.25
Total water Yield(WYLD)in MCM	385.95	346.08	320.57	339.77	270.85
From 1972 in%		-10.33	-16.94	-11.97	-29.82
From 2003 in%			-7.37	-1.82	-21.74

*MCM-million meter cube

Future water demand in the Geba basin for aricultural use and domestic water supply shows higher values between January–May when the flow in the Geba river is low. At the same time the Geba flow during rainy season, June –September, shows excess flows (Figure 7-34).

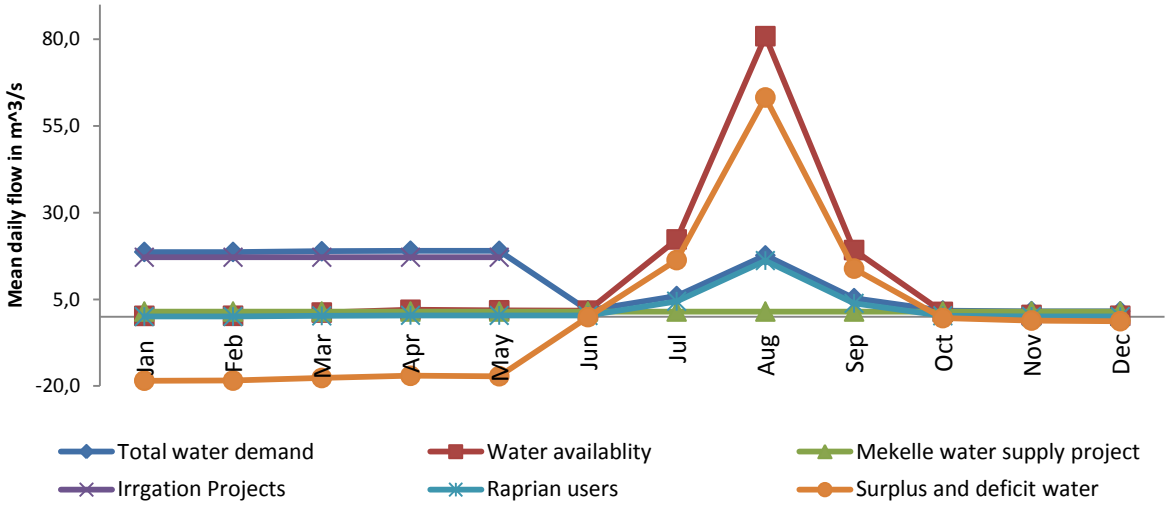

Figure 7-44: Future water demand and supply in Geba river at Nr.Mekell station outlet. Irrigation water demand in the Geba basin, domestic water supply for Mekelle city and raprian users.

7.8 Water balance in the watershed for future time (2030)

The annual water balance is predicted applying the global climate model as input data for the Soil and Water Assessment Tool (SWAT2009). The results are shown in Figure 7-45.

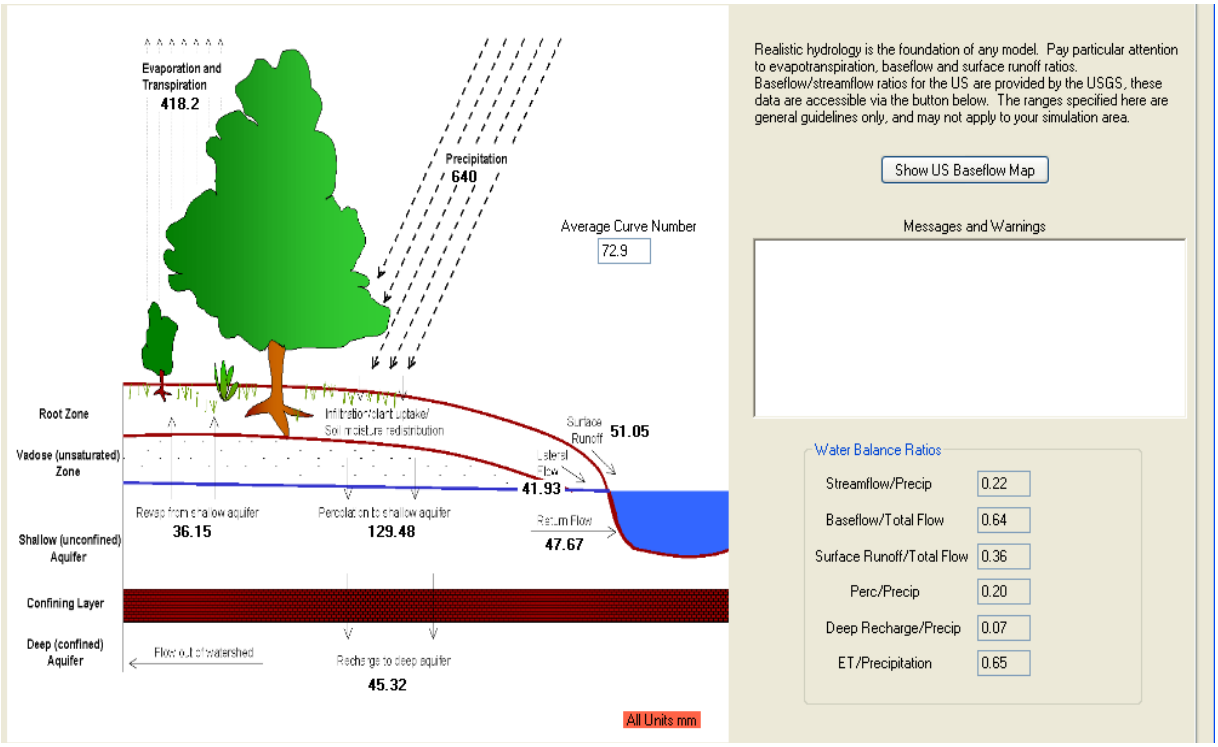

Figure 7-45: Hydrological response of Geba basin in 2030 based on predicted climate variables (Neitsch et al., 2005).

8 Discussion

8.1 Hydrometeorology

8.1.1 Rainfall

The soil and water assessment tool (SWAT) sets rainfall amounts from the weather station that is closest as the centroid of each sub-basin. The model does not interpolate the point rainfall to areal rainfall. It needs independent separate tools as it is shown in Figure 7-1 to 7-3. The variability and distribution of rainfall in the study area were evaluated using the 38 years monthly rainfall database available for eight stations within and nearby the Geba basin (1972–2010). Figure 7-1 to 7-3 and Figure 7-4 results indicate that there is a high variability of rainfall with altitude and latitude due to topographic influences. The statistics result of variability with elevation shows weak relations even considering that the number of samples is small. Verification was made with observed station based on the relation created (Figure 7-4).

Mean annual rainfall differs between ~550 to 650 mm/year in the southern part of the basin and a maximum of ~560 to 700 mm/year in the northern part of the basin. However, the result (Figure 7-1) differs depending on the interpolation methods applied (Figure 7-1 to 7-3). These are basically due to the topographic nature of the area, the assumption within the method and number and distribution of gauge in the basin. Similar results were pointed out in Nyssen et al. (2004), who indicate that the rainfall in northern Ethiopia is highly variable with elevation. Interestingly, at a given altitude precipitation decreases and seasonality increases with latitude and, thus, documents shows how the rainfall varies in the area. Above, Nyssen et al., (2005) observes for an area of 80 km^2 equipped with 60 rain gauges that due to topographic barriers of the overriding winds the spatial variation of the rainfall is strained by orographic effects. Amare (1996) points out that the altitude-rainfall relationship is highly influenced by orographic and agro-ecologic niches or micro-climate. This is strengthened by Humphreys et al. (1997), who studied the orographic effect on annual rainfall for selected locations in Ethiopia and Eritrea. Their results show that the yearly rainfall pattern is dictated by the orography and the position of the various mountain ranges with respect to the moisture laden winds. Again, Abraha (2009) draws the conclusion that topographical aspects control the spatial distribution of annual rain depth rather than altitude and that annual precipitation is mainly controlled by flow paths of air masses. Therefore, the interpolated results as provided by the weather generator WGNmaker4.xlsm (Gabrielle, 2011) were used for the modeling as this interpolation tool gives better result than Thiessen polygon. It also provides an isohytal interpolation due to its consideration of orographic effects and effects of other meteorological parameters on rainfall variability. This method classifies the rainfall with elevation bands to accounts orographic effects on the area (Gabrielle, 2011).

The analysis of the inter- as well as intra-annually variability of the rainfall in the Geba basin clearly shows that rainfall is highly variable ,both, in time and space as well as inter- and intera-annually (Figures 7-5–7-7). Nyssen et al. (2005) highlight similar result for Tigray, northern Ethiopia. Similar results by Belete (2007) on the Tekeze basin show that the coefficients of variation in annual rainfall range from 20% in the highlands to 40% in eastern lowlands, which is much higher compared to 8% for the whole country as studied by Amare (1996). The high rainfall variability in norther Ethiopia is documented by numerous authors (Troll, 1970 cited in Abraha, 2009; Amare, 1996; Humphreys et al.,

1997; Nyssen et al., 2004; Asfaw, 2005; Nyssen et. al., 2005; Yazew, 2005; Abraha, 2009; Abdurahman, 2009; Gebreyohannes, 2009; Tulu, 2010).

There are studies for different parts of the country that show the dependency of precipitation and altitude. However, as the precipitation in Ethiopia is strongly linked to the movement of the inter tropical convergence zone (ITCZ) and the influence of the Indian Monsoon sea-surface temperatures of the Pacific, comparing results from one part of the country to other and adopting the methods misleads to erroneous results. In addition, the dry spell analysis i.e. wet and dry spells lengths (durations) shows their spatial and temporal distribution in relation to water availability and future water balances (Figures 7-9 and 7-10). The number of rainy days in a month, the probability of wet days following wet days and the probability of wet days following dry days gives clear indications for the water balance study. However, there are some uncertainties observed. The duration of wet days in July (Figure 7-10) is around 24 days. On the other hand, the probability of wet days following wet days in the same month amounts 60% compared to wet days following dry days with a probability of 80%. This underestimates the probability of wet days in that month has a direct influence in antecedent moisture content and runoff generation.

Likewise, the El Niño and La Niña related patterns affect the weather patterns. This was verified using the ENSO anomaly and rainfall annual deviation from the mean (Figure 7-7). It gets obvious that some of the drought years coincide with this anomaly and some do not. This observation gives an indication that there is variability of weather in the watershed which might not be an effect of global warming.

8.1.2 Evapotranspiration

The annual evapotranspiration in the Geba basin shows in average 61% of the total precipitation (386 mm). Gebreyohannes (2009) studies climate of the Geba basin using the WetSpass model and comes up with a total evapotranspiration of 462 mm, thus, being a slighter higher amount of annual evapotranspiration than the presented in this study. However, the areal distributions of high and low values are similar in both studies due to the underling algorithms. In addition, proper simulation of land cover, crop parameters and land cover representation in the model are very crucial in determining evapotranspiration. Without this information, comparing the model results may lead to wrong conclusions.

The vegetation cover causes, due to its topography, friction for the horizontal wind fluxes. The lower the vegetation cover, the higher the wind speed. The moist air from land surface is replaced by dry air and reduces the relative humidity of the area finally result in high evaporation rates. About ~80% of the annual evapotranspiration takes place during the summer. This is due to short rainfall duration in the area and inferring warm air condition in between the rainfall events (WAPCOS, 2003; Tulu, 2010).

8.1.3 Runoff

The runoff analysis for the Geba River (Figure 7-12) focuses on the time span 1991–2003 because of poor data availability and data quality. The observed discharges at the river gauging station document

an intra-annual bimodal distribution with a small peak discharges in April and a large peak during the rainy seasons in July and August. Most runoff occurs during the rainy season, more than 70% of the total annual runoff. Like rainfall, runoff is highly variable in the Geba basin. A study by Abraha (2009) on the runoff variability in the area based on a network of eight gauging stations and an observation period of four years shows that during the rainy season 72–82% of annual rainfalls generating 70% of the annual runoff. He tries to develop a runoff coefficient for the basin during the period and shows its high spatial and temporal variability.

In semi-arid regions runoff generation is dominated by Hortonian overland flow (Smith and Goodrich, 2005). On the other hand, in semi-arid regions, convective rainfall (high rainfall within short period) can be expected which generates flash floods without satisfying the infiltration demand of the soil. This nature of the runoff in semi-arid regions affects the runoff generation analysis and runoff coefficient unless these events are identified. SWAT2009 allowed a spatially differentiated display of the highly variable runoff coefficients (Figure 7-23).

The inter-annual monthly maximum discharge volumes always occur in July and August, the minimum discharge volumes in May. The runoff depends on total precipitation, evaporation and soil water storage. It is clearly seen that for high potential of evapotranspiration (Figure 7-11), there is corresponding low runoff coefficient (Figure 7-23) indicating the effect of evapotranspiration on runoff.

The daily stream flow (Table 7-1) shows high variable flows in the Geba River. In August 1980 the daily flow averaged 119 m^3/s on August 10, 1980 and peaked next day to 1445 m^3/s, dropping to 523 m^3/s in August 12, further dropping to 97 m^3/s. This hydrograph indicates the flashy nature of the runoff. However, it is suspected that the peak discharge of 1445 m^3/s is overestimated. As per the information from elder local peoples the bridge at the gauging station has not been overflown and the capacity of the bridge is estimated 1000 m^3/s. However, even with this overestimation, the flow still shows the high variability within a month.

Very high floods within short time are also depending on the land cover and population density. The area is predominantly cropped corresponding to bare land except during the rainy seasons when the agricultural lands are covered by crops. This lack of vegetation cover reinforces the splash effect Tulu (2010) which, together with soil compaction by the movement of people and cattle (Descheemaker et al., 2006), leads to a large reduction of infiltration rate and produces extensive overland flow (Descheemaker et al., 2006; Abraha, 2009; Tulu, 2010).

Base flow separation (Figure3-4) indicates the discharge data collected by the Ministry of Water Resources almost neglect the base flows. As the gauging instruments are installed at one side of the river banks and as the dry weather flows mostly occur concentrated in the deep section of the river these flows are not captured. However, manual flow depth measurements were conducted during the field work and show significant amounts of flow, parallel not recorded by Ministry of Water Resources.

Similarly, Gebreyohannes (2009), in his study on groundwater modeling, tries to compare accumulated base flow measurements of the Ministry of Water Resources made in January and February with measured groundwater recharge amounts. They found out that the observed base flow as indicated by the data base of the Ministry of Water Resource highly devates from measured base flow as checked by current meter at 15 different points in the basin. In addition, the rating curve is not updated frequently, leading to erroneous results. NEDECO (1996) developed a rating curve as part of Tekeze

master plan study which is significant different than that of the Ministry of Water Resources. This problem was also been addressed by the Hunting technical service (1976) who approximated a rating curve based on the Manning equation.

8.1.4 Soil type and soil texture

Soil texture is a major input parameter for modeling withSWAT2009.The Hunting Technical Service (1976) developed a soil map 1:50,000 for the study area based on the FAO (1986) soil map. Additionally on country level, the Ministry of Agriculture, (2008) developed a soil map of 1:1,000,000 referring to the FAO (1998) soil map. Sander (2012) developed a bench marking soil map in scale of 1:50,000 based on the soil map of Hunting Technical Service (1976). The soil texture analysis (Figure 7-13, Table 7-2) indicates that topsoils in the Geba basin are overall of loamy character.

Complementary, soil maps by Sander (2012) indicates that on the steep slopes (>40%) shallow Leptosols and bare rock dominate. On slopes with 20–40% inclinations shallow, strong Cambisols, Regosols besides Leptosols are found. On flat slopes (10–20%) young soils like Cambisols and Regosols occur. In contrast, on the flat slopes of the plateaus, soil depth is also often shallow and parent material crops out.

Modelling result shows that Haplic Lixisols soils as the predominating contributed the least surface runoff while basins with Humic Alisols and Eutric Regosols predominating generate more surface runoff. This is due to Haplic Lixisols' generally low clay contents and their high saturated hydraulic conductivity with 11 mm/hr. In contrast, Humic Alisols and Eutric Regosols have low hydraulic conductivities less than 5 mm/hr (Mengistu, 2009).

8.1.5 Land cover analysis

Land cover has a great impact in runoff generation (Githui, 2009). The land cover change in the Geba basin is due to high population and socio-economic development of the area. Hadgu (2008) mentioned that natural vegetation depletion due to population pressure and land expansion of agricultural was the major driver for land cover changes. Agriculture has gradually expanded from gently sloping land into the steeper slopes. The most significant period of expansion of agriculture and settlements was in the period 1986–2003, due to high population resettlement after the end of a civil war in the area in 1991 (Abraha, 2009).

8.2 Model performance

8.2.1 Sensitivity analysis

Sensitivity analysis (Table 7-4) indicates that eleven parameters determine the stream flow in the Geba basin, highlighting curve number, available water capacity of the soil and base flow separation factor. Similarly, the sequential uncertainty fitting two (SUFI-2) model result (Figure 7-18) shows the same parameters with different ranks are sensitive.

All the eleven parameters generally govern the surface and subsurface hydrological processes and stream routing. It is important to note that each of these parameters was treated identically across different sub-watersheds or hydrological response units for calibration and validation processes. The results illustrate that the parameter sensitivity is highly site specific and depends on land use, topography and soil types. However, parameters CN2, Sol_AWC, and Alpha_BF are identified as sensitive parameters in different ranks (Setegn et al., 2009a; Mekonnen et al., 2009; Dilnesaw, 2009; Githui, 2009; White, 2009; Mengistu, 2009).

8.2.2 Calibration and validation (Fit-to-observation)

The performance efficiency values in both the calibration and validation phases prove that SWAT2009 predicted measured stream flow satisfactorily for monthly flows and poor but acceptable for daily flows. This is mainly due to the bad quality of the data. Table 7-6 summarizes different coefficient for quality control. The Nash-Suttcliffe (E_{NS}) varies from 0.34 to 0.46 for daily and 0.52 to 0.86 for monthly calibrations and validations with the highest R^2 and E_{NS} values being during the calibration of the model for the 2003 land cover condition. A similar study performance in the Choke Mountain (Nile basin of Ethiopia) by Koch et al. (2012) stresses the bad data quality of the region and pointing out that a E_{NS} of 0.39 is acceptable for the daily basis. This considers that the E_{NS} statistics is strongly influenced by peak values of the rainy seasons. Besides, it is documented that if rainfalls exceed 100 mm SWAT seems to significantly overestimate flows and the E_{NS} coefficient is highly sensitive to the peaks (McCuen et al., 2006).

Different applications of SWAT in Upper Nile and in Ethiopia also recognize the lack of data as a problem. At the same time, the model performs well in daily time steps. It was tried to compare the results with this study in relation to parameters range and values used for the calibration of the model. In some of the studies some parameters were ignored or not considered by their own physical meanings and parameter range values. Some examples are given in the following: The Awash river is perennial with high flow all over the year. However the GWQMN parameter value used by Dilnesaw (2009) seems a bit high for the river whose groundwater level is above the bed. Setegn et al. (2009a) report an out of range value for “GW_REVAP” in the Nile basin. Easton et al., (2010) compute a base flow factor of more than 90% for the Nile basin. Nodma et al. (2008) and Mulungu et al. (2007) use very high groundwater recharge values for “RECHG_DP” of 90% which results that 90% of the water is lost to groundwater recharge. Besides these unrealistic parameter values Griensven et al. (2012) evaluated hydrological mass balances contained losses that are not justified.

Figures 7-19–7-22 and Figure 7-24-7-27 displays measured and simulated data and allows the identification of general trends in the data and differences between model simulations. This graphical interpretation together with the numerical analysis given in Table 7-6 gives a comprehensive measure of the agreement between measured and simulated data and shows how the model performance fits with its observation data. However, the monthly peak flows are underestimated whereas the daily flows are overestimated even when the water balances are in good agreement. This may be due to transmission losses in the channel bed and bank that affecting the peak discharges. Geology of the area favors for this loss as bedrock is highly fractured. Lang (2005) indicates that transmission loss is higher during peak discharge periods and lower in medium to low flows. Transmission loss is also proportional to upstream inputs Jordan, (1977). In contrast, Leistert (2005) indicates that total loss depends on the texture of the alluvial material. For the Geba river geological and geomorphological channel characters were considered as input parameters. On this basis an appropriate value for the loss coefficient is provided and calibrated. Generally, it is observed that the model has a problem in predicting the high flows or outliers but good agreement with the water balance.

Similarly, the daily flow simulated for the beginning of the rainy season is higher than the observed flow. This may be due to the temporal soil conditions, as most of the times the first flow disappears in the soil cracks and gets stored there or creates interflow. Abraha (2009) evaluates the rainfall and runoff throughout the rainy season by comparing runoff depth (total measured discharge divided by the watershed area) with rainfall depth and draws a conclusion that in many cases runoff tends to increase at the end of the rainy season, which is probably due to the increased base flow.

Runoff in the dry season (December to May) is mainly fed from ground water. Table 7-7 shows that a large contribution of lateral flows is indicated in the monthly simulation results, also for months during dry season. A reasons for this may the assumption made in the model that *sine of angle* of inclination of hill is equivalent with the *tan angle* (cf. chapter 8.2.4). Above, the simulated runoff produced after a heavy storm during the dry season is less than the observed one. The flashy nature of rainfall and high response of basins are among the reasons. The high intensive rainfalls will not give time to infiltrate the soil and flows as runoff forming Hortonian overland flow. Similar observation is made by Tulu (2010) in his study on one of the Geba tributaries. Also response of the rocky and very shallow steep nature of the basin has to be considered causing low infiltration rate.

The annual average areal rainfall and other hydrological components were compared for each year of the calibration periods (Table 7-6). The simulated water fluxes indicate that in a wet year surface runoff dominates water yield. However, in a dry year, contribution of lateral flow is significant which seems a bit exaggerated because in dry years lateral flow is much less than baseflow. The model can better predict the surface runoff than groundwater flow during wet season. This might be due to the soil data quality and estimation of the curve number at dry moisture conditions. Since the curve number is a function of the soil's permeability, land use and antecedent soil water conditions the estimation of the curve number under dry soil moisture conditions (wilting point) might not be efficient. On an annual basis, the observed baseflow totals 34% of the total runoff over the calibration period. In contrast, the simulated baseflow totals 31% (46.6 mm out of 146 mm stream flow) of the total runoff over the calibration period (Table 7-7) Values which correspond to the data are documented by Gebreyohannes (2009).

8.2.3 Model parameter evaluation (Fit-to-reality)

Van Griensven et al. (2012) recommended that during calibration the sensitive parameters are checked on their physical meanings and comparing the range of their calibrated values with the other system parameter (Table 7-5). The following table summarizes parameters that control surface water loss to shallow and deep aquifer in reviewed papers.

Table 8-1: Parameters that are controlling losses to shallow and deep aquifer (after Van Griensven et al., 2012).

Parameters	Parameter range	Reported values	Used in this study	Reviewed papers
Channel hydraulic conductivity (CH_K)	0–150	0.7–150	11	1. Mengistu, 2009 2. Setegn et al., 2009a 3. Setegn et al., 2009b 4. Mekonnen et al., 2009 5. Bitew and Gebremicheal, 2011 6. Githui, 2009 7. Dargahi and Setegn, 2011 8. Ndomba and Berhanu, 2008 9. Mulungu and Munishi, 2007
Threshold depth of water for return flow (GWQMN)	0–5000	0–1500	108	
Deep groundwater recharge (RCHRG_DP)	0–1	0–1.1	0.4	
Loss from shallow ground water (GW_REVAP)	0.02–0.2	0–50	0.13	
Base flow (ALPHA_BF)	0–1	0–0.8	0.22	

In comparison to the reviewed papers, the value taken for this research belongs to the lower ranges. This is due to the physical meanings behind the parameters and the real hydrological representations in the basin.

In the parameter evaluation high focus is given to the subsurface parameters that are highly sensitive to the model and related to water losses from the system. Beside this, baseflow factor (ALPHA_BF) of the subsurface parameter is given attention due to its high sensitivity ranks in the model. This parameter influences the mix of groundwater and other flow (overland runoff and lateral flow) in the channel. Over an annual water-cycle under equilibrated conditions, baseflow factor ALPHA_BF does not give any information the total quantity of base flow, moreover the total quantity of base flow will be controlled by the net infiltration that eventually recharges the aquifer. However, baseflow factor ALPHA_BF controls the rate of groundwater release from the shallow aquifer. If its value is too large, the shallow aquifer cannot hold enough water, causing the loss the aquifer characteristics. These conditions are considered based on the geological map (Gebreyohannes et al., 2010).

Channel hydraulic conductivity (CH_K) represents infiltration in the riverbed where the riverbed is higher than the groundwater level and contributes partially to the aquifer recharge. This parameter should only get a value > 0 for channels where the groundwater level is below riverbed. Groundwater level around the outlet is below the river bed during dry seasons while it might increase about river bed during rainy season. Deep groundwater recharge (RCHRG DP) simulates the ground water recharge that is going to deep water storage and will not discharge towards the river. This will have more significant impact on the water balance of small basins than in larger ones. For big watershed RCHRG DP will not be high value as groundwater springs off somewhere in the watershed. Considering the slopes of the basin and its size an appropriate value is calibrated. However, for small basins RCHRG

DP highly affects the flow since it is a water loss from the system. Loss from shallow ground water (GW REVAP) is the water that flows to the soil above the aquifer by the process of capillary rise. These losses describe evapotranspiration from the shallow aquifer which is controlled by the potential evapotranspiration and lost from the system. This loss is high in arid and semi arid areas and shallow depths of the aquifer. GWQMN is a threshold depth of water in the shallow aquifer that controls the recharge of groundwater when the aquifer level is higher than GWQMN recharge will occur. If this value is too large, the model will build up water in the shallow aquifer whereby the input (rainfall) might not equal the output. Considering all these facts, the parameters defined for the research area differ from other studies in the Nile basin.

8.2.4 Process representation in the model performance (Fit-to-reality)

Interflow is a major hydrological process, having a direct impact on surface flow calculation. The kinematic wave approximation of saturated subsurface/lateral flow assumes that the lines of flow in the saturated zone are parallel to the impermeable boundary and the hydraulic gradient equals the slope of the bed assuming that sine is approximately equal to tan of the hillslope angle (SWAT2009 user manual; Arnold, 2009).

The above assumption of dependency of slope with lateral flow is highly significant in a steep basin like this study area and results a considerable error in the lateral flow predictions, affecting the other component results. Contribution of lateral flow to total runoff increases with increasing slope inclination of the drainage basin (Equation 3-10). The estimation of interflow might work for slopes of less than 5° inclination. For higher inclinations, lateral flow gets exaggerated and surface flow gets underestimated.

8.2.5 Hydrological response of the watershed

The responses of the watershed were checked for different hydrological components and were compared for each year of the calibration and validation periods (Table 7-7). In the Geba watershed around 35% of the area has slopes with more than 15° inclination; therefore, the overestimated lateral flow significantly affects other components. In the reviewed papers and journals, no one reports the effect of slope on the lateral flow.

The baseflow was evaluated on an annual basis for the Geba basin. The baseflow filter program (Arnold and Allen, 1999) generates a range of predicted baseflow volumes and results. The resulting values highly differ from the observed flows and mostly are overestimated. On an annual basis, the measured flow at Geba Nr. Mekelle gauge station is estimated as 34% baseflow over the calibration period. In comparison, the simulated flow is estimated as 45% baseflow over the calibration period. In consequence, the calibrated model was considered to generate acceptable predictions of baseflow. However, the model can better predict the surface runoff than the groundwater contribution during dry season. This may be due to bad soil data quality and insufficient estimation of the curve number since it is a function of soil permeability, land use and antecedent soil water conditions.

8.2.6 Uncertainty

The Sequential Uncertainty Fitting version two (SUFI-2) shows a much larger uncertainty bounds than the Parameter Solution method (PARASOLl) indicateing that other causes of uncertainty are involved including the in accuracy in the data set to identify the important processes, model structural errors, and model discretization errors. Unlike the PARASOLl provides only parameter uncertainty analysis, while SUFI-2 assesses the total uncertainty that might be used in comprehensive decision making. Uncertainty analysis from these methods leads to more selections of parameter combinations and much wider uncertainty ranges and thus enables to assess predictive uncertainty that helps decision makers to understand how uncertain their models in consequence they will be able to put the proper level of trust in computational models of the environment. The results indicate that concern should be given to both the uncertainty associated with model structural errors and model parametric uncertainty. However, since the underlying assumptions of the parameter uncertainty method assumed to be correct the datasets used in SWAT2009 are adequate to translate the variability of the system into a model and the results of the SUFI-2 uncertainty analysis do not cause larger uncertainty bounds for the model outputs compared to PARASOL.

8.3 Impacts of land use land cover change on hydrological regimes

The analysis of the effects of land cover change on the streamflow variability in the period 1991–2003 (Figure 7-28, Table 7-9) shows that mean monthly discharge in wet months has increased by 9% while in the dry months decreased by 30%. Where high agricultural land expansions observed (Table 7-9, sub basins 12, 15, 17 and 19) mean monthly flow totals up to 50% in wet months. Moreover, the analysis shows that the dry period flow is highly sensitive to land cover changes as less vegetation cover initiates groundwater recharge during the dry season (Mengistu, 2009).

The impact of land covers change between 1972 and 2003 considering similar meteorological parameters shows (Figure 7-29-7-32), relatively higher stream flow as a result of resulting surface runoff. Several studies confirm (that forests have the effect of reducing surface runoff and increasing the infiltration into the shallow aquifer whereas the agricultural expansion results in the reduction of infiltration (Githui, 2009; Mengistu, 2009; Trimble et al., 1987; , Swank et al., 1988). In contrast, other studies show that when agricultural land is plowed, compaction of the lower soil horizons occurs which causing a decrease of infiltration capacity and finally producing more runoff (Ankeny et al., 1990; Logsdon et al., 1990; Abu Hamdeh, 2003).

Surface runoff has increased from 68% in 1972 to 72% in 2003 of the total runoff due to the agricultural expansion in this period. On the other hand, ground water flow has decreased from 32% to 28% due to the reduction of vegetation cover that supports aquifer recharge (Mengistu, 2009).

The expansion of agricultural land displacing forest and bush land results in an increase of surface runoff generation following rainfall events and causes changes in soil moisture conditions and groundwater storage.The expansion of agricultural land also results in a compaction of the top soil, aggravating infiltration into the shallow aquifer layer (Githui, 2009). These factors together with the

very steep nature of the area favor surface runoff and floods during the wet months and reduce dry weather flows during dry season which is fed from the shallow aquifer as return flow or base flow. The analysis of land cover changes between 1972 and 2003 confirms these effects of land use change runoff generation. In addition, change in land use and land cover affects the water retation capacity of the soil and sub-surface transmisstivity (Githui, 2009).

The results also indicate that changes of land use and land cover influenced the rainfall-runoff relationship and contributed to an increase in runoff in the wet months. However, the impact study presented indicates that hydrological response to the land cover change in the basin is not significant. This insignificance values do not mean there is no impact in the watershed rather it shows that the spatial dimensions of land use effects on the hydrological cycle is not simulated well due to the watershed size. Kiersch (2001) and Archer (2003) studied different watersheds and pointed out that, the watershed area should not be more than 100 km^2 to study the effect of land cover on average flow, base flow, groundwater recharge and peak flow.

8.4 Impacts of climate change on hydrological regimes

8.4.1 Baseline period

Impact of climate change on the hydrological regime requires climate downscaling to create the relationship between the predictor and the predictand. The predictor represents large scale atmospheric variables whereas the predictand represents local surface variables such as temperature and precipitation. Appropriate downscaling predictor variables were selected through seasonal correlation analysis, partial correlation analysis and scatter plots and used with Mekelle station predictands to all statistical downscaling (cf. Table 7-10) corresponding to those of different studies conducted in Ethiopia (Goitom et al., 2012 in northern Ethiopia; Mengistu, 2009 in southern Ethiopia; Setegn, 2009 Nile basin; Taddele, 2009 in Lake Tana among others).

The downscaled observed variables for the baseline period indicate that the model replicates observed inter-monthly and inter-annual variability are highly significant (Figure 7-33, Figure 7-34). The performance of the statistical downscaling model is almost as better over the verification period than calibration period, indicating that the empirical model has not been over-fit to the data.

8.4.2 Climate scenarios based on Global Climate Model (GCM)

The climate scenario for future periods was developed from statistical downscaling using the GCM predictor variables for the two Special Report on Emission Scenario (SRES) A2a (large population and regionally oriented economic development) and B2a (less population growth and local economical development) emission scenarios (HadCM3A2a, HadCM3B2a, and CGCM3A2a) for 90 years based on the mean of 20 ensembles. The analysis was done based on the three 30-year periods (2011–2040, 2041–2070 and 2071–2099).

In contrast to the result presented the study in the basin by Goitom et al., 2012 using HadCM3 indicates that overall annual change in precipitation will experience a decreasing trend in the future. The decrease in precipitation will be predominantly significant in the rainy season, while there may be less difference in precipitation during dry periods. Similarly for the Nile basin region by Setegn, 2009; Mengistu, 2009; Legesse et al., 2003, Kingston and Taylor, 2010 studied climate change on water resource in the upper Blue Nile and found that due to the increase in temperature groundwater flow will decrease and evapotranspiration increase. A similarly studies from Kenya (Githui, 2009) indicates that temperature and precipitation will increase in the future. Mango et al. (2011) predict an increase of annual precipitation by 7% in 2099 with the projections ranging between -3 to 25%.

8.5 Future land use land cover scenario analysis on hydrological processes

Three land cover scenarios are developed to analyze the impact of land cover changes to the hydrological regime.

Scenario 1: Continuation of current practices

This scenario speculates the continuation of existing agricultural production and assumes there will not be any intervention in any part of the watershed. Although this scenario is impractical due to the ongoing water supply development project for the Mekelle city, irrigation development in upstream areas and intensive human activities in the watershed, it offers a reference point/baseline data when interpreting the hydrological implications of other management scenarios. The analyzed result of this scenario Figure 7-37 shown that, the change in stream flow fluctuates is between decreases by 1.8 m^3/s to an increase of up to 3 m^3/s. However, the decrease of flow is observed for the rainy period around August and September. This will have an impact in supplying the demand for dry period's agricultural practice and other water supply purposes.

Scenario 2: Following the country recent track record in agricultural development

In this scenario the actual country records in achieving the economic development on the land management is considered. The report released from the Ministry of Finance and Economy and the government policy and strategies on green economy (Ethiopian Climate Resilient Green Economy strategic plan (CRGE, 2011), shows a 15% expansion of agricultural land and 3% re-forestation work accounts for growth in the agricultural sector over the last five years. Partial grass land and bare land conversion to agricultural practices and part of bush land and bare land conversion to forest land is considered. This scenario includes grass land, bush land and bare land cover reduction it by 15% for agricultural expansion and 3% of bush and bare land for forest development.

The results for scenarios 1 and 2 the changes in stream flow fluctuations do not significantly differ from the first scenario ranging between a decrease of 2.8 m^3/s to an increase up to 3.2 m^3/s. A significant flow reduction can be observed for August and September for the second scenario. The range indicates further reduction during the dry season compared to scenario 1 due to the agricultural expansion. However, the trends of the two graphs are similar despite the value difference at each month. The reduction in stream flow during the dry season can be explained by considering the increase of

irrigation agriculture and water supply for domestic use. The flow reduction in August and September will affect not only the agricultural development but also the cattle farming.

Scenarios 3: Allied with the future Ethiopian Climate-Resilient Green Economy (ECRG) policy and strategies – fast growth with food-focus scenario

In this scenario agricultural use will increase by 10% giving more attention to improving crop production than area coverage. A relatively low rate of land transformation is assumed, leading to conversions of bare land, bush land and grass lands into agricultural land using the groundwater potential and surface water to irrigate more land. The irrigation projects focuses on food supply and an export oriented agricultural policy and includes the constructing of dams and reservoirs in the upstream area. Soil conservation measures are widely used to prevent the reservoirs from siltation. Grass land and some bare land will be replaced by forest land. This scenario can be considered as good management practices. Generally, in this land use change scenario more focus is given to the small scale irrigation intervention with an objective to identify the impacts on the Mekelle water supply projects.

The results of this scenario (Figure 7-37) indicate that the scenario had a pattern different from the first two scenarios. The change of stream flow, when compared to the base period, increases to 3 m^3/s during the dry season while decreases to 2 m^3/s during the wet season. This could be due the integrated impacts of the abstraction of water for irrigation in the upper and middle reach, the reduced slopes due to soil conservation measures and afforestation.

In general, the impact of future land cover change on hydrological regime is not quantified well due to the size of the watershed. However, from the physical observation in the watershed, land management practices will have a great impact in very steep basin like the Geba basin. This is due to the existing conventional tillage system (Amharic *maresha*) and steep slopes of cropland facilitating soil erosion and silitation (Chekol, 2006). Resulting land degradation causes land cover changes. Again consolidation of small fields into larger ones often results in longer slope lengths with increased erosion potential, due to increased velocity of water which permits a greater degree of scouring (Chekol, 2006). Therefore, with agricultural expansion and human interaction, hydrological responses are expected to be modified or changed. Study conducted in the Awash basin by Chekol (2006) confirms this fact.

8.6 Hydrological responses to changes in land cover and climate

The combined effect of land cover and climate changes (Figure 7-38) shows that a runoff reduction of up to 5% and 15% during rainy season observed in Hadley climate model (HadCM3A2a) and Canadian Global Climate Change Model 3 (CGCM3_A2a). However, in the Hadley climate model (HadCM3B2a) a flow increase occurs in July and a reduction in September. Looking for the base flow results, again all the models show consistency for the period 2011–2040 with the exception of CGCM3A2a. In the other periods, except for scenario HadCM3B2a, all the other models showed decrease in base flow. CGCM3 has the lowest annual rainfall compared to the other models. All the model results for 2011–2040 show consistent result with respect to changes in both runoff and base flow with the exception of HadCM3B2a. The lowest (124 mm) and highest (142 mm) mean annual runoff depth corresponds to

scenarios HadCM3B2a and HadCM3A2a. The lowest (75 mm) and highest (99mm) mean annual base flow corresponds to scenarios CGCM3 A2a and HadCM3B2a (Table 7-16).

In 2011–2040 HadCM3A2a and CGCM3A2a is a warmer scenario than B2 and this could cause more evaporation, giving rise to less surface runoff. The evapotranspiration amounts in the 2011–2040 show very little variability between the models, corresponding to low temperature variation. In the 2041–2070 and 2070–2099 temperatures are higher and more variable than in the 2011–2040, leading to higher and a wider range of evapotranspiration estimates.

8.7 Implication of landover change and climate on water availability

The results from the climate models were used to derive relationships between changes in rainfall and runoff. Evapotranspiration is about 68% of the annual rainfall and is highest in the rainfall seasons but lags the rainfall peak by about one month. In certain months (November–February) the evapotranspiration exceeds rainfall. This can affect the relationship between rainfall and stream flow due to changes in soil moisture and the evaporative demand of the vegetation and soil surfaces (Mengistu, 2009). The change in annual evapotranspiration due to the climate change scenarios was in the range 15 to 18% (156–179 mm). In contrast Githui (2009) indicate in their study in the Nzoia watershed in Kenya that the stream flow is not sensitive to temperature changes. Miller et al., (2003) documented that temperature changes are known to have a significant effect in regions with snowmelt conditions. On the other hand Mengistu, 2009; Kingston and Tylor, 2010 and Mango et al., 2011) confirms that increasing temperatures lead to increases in evaporation and, hence, to decreasing stream flow.

Land cover effects on hydrology can largely be attributed to changes in water use throughout the year, and specifically during the dry seasons where irrigation water demands are at their peaks. Under the current set of model parameters, the result of the simulation demonstrates that that increased croplands in the upper watershed caused a reduction on dry-season flows having direct relation to the water demand during this period. Figure 7-44 presents water demand of the downstream project and water availability.

Higher stream flow occurs as a result of increased agricultural and decreased forest areas (Githui, 2009). Forests have the effect to reducing runoff (Githui, 2009), thus the smaller the area the more the runoff. A similar explanation applies to Scenario 2 where less agricultural area and more forest cover have the overall effect of reduced runoff. Studies by Trimble et al. (1987) and Swank et al. (1988) indicate reduced stream flow as a result of afforestation. Various studies have shown that when agricultural land is tilled, compaction of lower soil horizons occurs, lowering infiltration capacity and increasing bulk density (Ankeny et al., 1990; Logsdon et al., 1990; Abu Hamdeh, 2003). As under this condition rainfall saturates the soil profile quicker in agricultural lands than in the forested areas more runoff is produced (Ankeny et al., 1990; Logsdon et al., 1990; Abu Hamdeh, 2003). In the study area the bulk density of the top soil layer interacts is in average higher for agricultural lands (1.22 Mg/m^3) than in forested (1.19 Mg/m^3) areas. Runoff is dependent on the antecedent soil water conditions, which is a function of bulk density. The bulk density affects percolation as saturated flow occurs when the water content of a soil layer exceeds the field capacity for the layer (Ankeny et al., 1990; Logsdon et al., 1990; Abu Hamdeh, 2003).

The upper part and middle reach of the watershed were predominantly affected by the land cover change during the 1975 to 2003 period. This was due to population growth, resulting in an increase of farmland and settlement area and uncontrolled use of firewood from the lower part of the watershed. Based on figures published by the Central Statistical Agency (2008), the districts in the watershed have an estimated population density of 142 people per km^2 (Hawzen woreda), 135 people per square kilometer (Agulae area) and 115 people per km^2 (Wukro woreda). Regional average totals 90 people per km^2 , which in turn is higher than the national average of 70 people per km^2 (CSA, 2008). The reduction of vegetation cover in the study area decreases infiltration and increases surface runoff and consequently alters the whole hydrological regime (Tulu, 2010). However, the predominant change in land use and land cover during the whole period is the increase in farmland and settlement areas, particularly in the upper part of the watershed, and the overall decline in forest, grasslands and woodlands. Though considerable conversion of other land use and land covers to farmlands may not be anticipated due to the reason that land occupation of arable areas has reached its limit in the watershed, modification of farmlands (rain-fed to small scale irrigations) are expected in the near future.

8.8 Water balance in the watershed

The main water balance components of the basin includes: the total amount of precipitation reaching a sub basin during the time step, actual evapotranspiration from the basin and the net amount of water that leaves the basin and contributes to stream flow in the reach (water yield). The water yield includes surface runoff contribution to stream flow, lateral flow contribution to stream flow; groundwater contributes to stream flow minus the transmission losses.

The simulated annual water balance components for the basin (Figure 7-45) indicate that 66% of the annual precipitation is lost by evapotranspiration in the basin during calibration period as compared to 61% during validation period. Surface runoff contributes 31% of the water yield during calibration period and 25% of the water yield during validation period. Whereas the ground water contributes 45% and 54% of the water yield during calibration and validation period respectively.

The analysis of Geba basin water balance indicates that the estimated annual precipitation falling on the basin is 640 mm and the evaporation loss from the basin is about 418 mm. The total water requirement (Figure 7-33) shows that there is a high water demand during dry periods and surplus during the wet season. In addition, considerable water demand is expected due to the irrigation development and water supply for domestic purposes. Therefore, optimized water allocation tool is needed to balance the demand versus supply in the basin.

9 Conclusions and Recommendations

9.1 Conclusions

The main subject of this thesis is to identify the impact of changes in climate and land use and land cover on the water balance of the Geba basin.

Land cover change detection analysis grants that for the last forty years there were a progressive land cover changes in Geba watershed. From the analysis of processed satellite images, it is evident that land cover changes have occurred between 1972 and 2003. Forest cover has decreased from 19% to almost zero%, attributable to logging for timber, firewood, and clearing for agricultural purposes. In contrast, the agricultural area increased over the years from 14% to 60%. Similarly grasslands and bushes have also been converted to agricultural areas.

It can be presumed that agricultural expansion occurred due to the rapid increase of population. The basin is under high demographical pressure with a population density of around 132 people per square kilometer which in turn is higher than the national with 70 people per km^2. Moreover, the extreme poverty and poor resource management result in an overexploitation of natural resources, which seriously affects the sustainable development of the area. These land cover conversions have caused land degradation and have interfered with biodiversity and ecosystems and causes the water stress in the area.

The Soil and Water Assessment Tool (SWAT) was calibrated and validated against the 1991–2003 stream flow. Parameters were adjusted based on the sensitivity analysis keeping the model parameters at reasonable ranges and minimized the uncertainty in the simulations before they are further used for scenario analysis. The application of this distributed hydrological model uses different spatial, temporal, time series data to predict flow components and hydrologic characteristics over the watershed. This is facilitated by use of ArcGIS processing of digital elevation model (DEM), land use and land cover, soil data and varies topographic attributes. Model results are spatially displayed so that it becomes possible to capture local complexities of the basin.

It can be concluded that good agreement between measured and simulated with daily stream flow and monthly runoff for the calibration as well as for the validation period occurs. However, the daily flow predictions were not as good as monthly flow predictions. This is due to the poor quality of the daily data; there are often large amounts of missing data. The simulation of base flow is over simulated, but overall, the agreement between the observed and simulated stream flow is acceptable for the monthly data. The daily as well as monthly peak flows were not adequately simulated, which can be attributed to inadequate representation of the spatial variability of rainfall and poor model responses to high rainfall amount.

Following calibration, validation and uncertainty analysis, impacts of past and present land cover on hydrological regime was carried out. Land cover is recognized to have major impacts on series of hydrological processes, such as runoff, evapotranspiration and groundwater flow. As a result of the land cover change in the area, stream flow decreased by ~10% during the wet season and by ~30% during the dry season between the years 1991–2003. Above, in the upper sub-watershed areas in surface runoff generation is disproportionally higher compared to middle reach and lower part of the basin.

The climate scenarios were generated from global circulation models and two models were selected (CGCM3 and HADCM3). The climate change socioeconomic and emission scenarios A2 and B2 were considered for the periods 2011–2040, 2041–2070, and 2071–2100. Scenario A2 puts emphasis on self reliance and economic development that is primarily regionally oriented. Scenario B2 puts emphasis on local solutions to economic, social, and environmental sustainability. The changes in rainfall and temperature were used to perturbe the historical time series for application in the hydrological model. In general, scenario A2 gives more increases in rainfall than B2 for each time period. According to the scenarios, more rainfall will be experienced in the 2041–2070 than in the 2011–2040. B2 is a warmer scenario than A2, with a much warmer climate indicated 2041–2070 than for 2011–2040. An increase in rainfall is expected for the months August and September and a relatively small increase in temperature compared to the months of May to July, which show a higher increase in temperatures and a decrease in rainfall. A distinct increase in rainfall is expected for the months March and April. These months are presently considered as the dry season. In general, the least increase in rainfall is seen in the July months, while the drier months have larger increases. Even with this pattern, the seasonality of rainfall is still maintained, though with varied total amounts.

Looking at the three different land cover scenarios basing scenario one, scenario two yields more surface runoff, base flow and total stream flow while scenario three yields reduced amounts. On the other hand, scenario three gives higher mean evapotranspiration than scenario two due to more vegetative cover than the former. Thus, there is an increase/decrease in water yield with a decrease/increase in evaporation. Without land cover change, climate change accounts for a decrease of about 20% in surface runoff. These results show that for this study region and for the considered period, land cover changes have contributed to less runoff changes than climate change. From the statistical trend analysis, rainfall is seen to be increasing, especially head water area. On the other hand, GCMs also project increasing rainfall for the region. This means that extreme wet events may be expected and thus, environmental conservation needs to be emphasized. Also, water harvesting techniques need to be explored to minimize the effects of droughts which occur especially after high flow has occurred.

Several outcomes of this research can be highlighted:

i. A great amount of spatial and temporal data describing the hydro-meteorology, soil and land use in the study area has been acquired, processed and organized in a consistent way. These data base were obtained from field work and were collected from different institutions and organizations. A complete hydrologic data set for the Geba basin is provided.

ii. The maps produced in this research will be provided to to local and regional governments and stakeholders to be implemented to development strategies. This will assist planning, e.g. directing where water harvesting schemes are needed for further developments.

iii. The use of scenarios in this study helps to better understand and visualize how land cover and climate change act together to alter watershed hydrologic response. This will also support stakeholders and policy-makers to assess the impacts of several alternative sets of future.

iv. The study demonstrats the general potential of integrating spatial data and distributed modeling in impact assessment. It examines the direction and relative magnitude of changes in the future water balance associated land cover and climate change.

9.2 Recommendations and further studies

- Availability of in adequate data with good quality may be a far away dream in the developing countries and more sever in the study area. Interestingly, the quality of collected data especially from home institutions is always questionable. The use of new data gathering techniques and dissemination process should be envisaged so that local and regional authorities can be involved in integrated and coordinated data way for compilation.
- Further researches and structural change in some assumption of the model is needed to simulate processes like base flow and lateral flows. The existing base flow filter program provided by USGS exaggerates the base flow. Definite relationships between base flow and rainfall could not be established. It is obvious that this is a field where further research is needed. Similarly, the lateral flow assumes that the lines of flow in the saturated zone are parallel to the impermeable boundary and the hydraulic gradient equals the slope of the bed assuming that sine angle is approximately equal to tan angle of inclination of hill and sine angle is not equal to tan angle if the hillslope is more than 5°.
- The dry spell analysis shows that the probability of wet days following dry days is high during the rainy season and some of the rainfalls will not generate runoff. Therefore, hydrological water balance based on a seasonal and yearly basis leads to wrong results and is not recommended for this area.

10 References

Abate, S. (1994). Land use dynamics, soil degradation and potential for sustainable use in Metu area, Illubabor Region, Ethiopia. PhD thesis, Universität Bern, Switzerland.

Abbaspour, K. C. (2007). SWAT-CUP, SWAT calibration and uncertainty programs. A User manual. Swiss Federal Institute for Aquatic Science and Technology, Zurich, Switzerland.

Abbott, M. B. and Refsgaard, C. (1996). Distributed Hydrological modeling. Dordrecht, The Netherlands.

Abdurahman, M. A. (2009)**.** Assessment of micro-dam irrigation projects and runoff predictions for ungauged catchments in Northern Ethiopia. PhD thesis, Westfälische Wilhelms-Universität, Münster, Germany.

Abraha, A. Z. (2009). Assessment of spatial and temporal variability of river discharge, sediment yield and sediment-fixed nutrient export in Geba River catchment, northern Ethiopia. PhD thesis, Katholieke Universiteit Leuven, Belgium.

Abu-Hamdeh, N. H. (2003). Compaction and Subsoiling Effects on Corn Growth and Soil Bulk Density. *Soil Science Society of America Journal* **67**: pp. 1213–1219.

Aggarwal, S. P., Garg, V., Gupta, P. K., Nikam, B. R. and Thakur, P. K. (2012). Climate and lULC change scenarios to study its impact on hydrological regime. XXII ISPRS Congress, 25 August – 01 September 2012, Melbourne, Australia. *International Archives of the Photogrammetry, Remote Sensing and Spatial Information Sciences* **XXXIX-B8**: pp. 147–152.

Ahmed, K. F. (2011). Bias Correction and Downscaling of Climate Model Outputs Required for Impact Assessments of Climate Change in the U.S. Northeast. Unpublished Master's thesis, University of Connecticut, Sterrs, USA.

Allen, R. G., Pereira, L. S., Raes, D. and Smith, M. (1998). Crop Evapotranspiration – Guidelines for Computing Crop Water Requirements [Irrigation and Drainage Paper; 56]. Food and Agriculture Organization of the United Nations (FAO), Rome, Italy.

Amare, B. (1996). Climatic resources, agro-ecological zones and farming systems in Tigray. Paper presented at the Extension Intervention Program workshop, Mekele.

Andréassian, V. (2004). Waters and forests; from historical controversy to scientific debate. *Journal of Hydrology* **291**(1–2): pp. 1–27.

Ankeny, M. D., Kaspar, T. C. and Horton, R. (1990). Characterization of tillage and traffic effects on unconfined infiltration measurements. *Soil Science Society of America Journal* **54**: pp. 837–840.

Archer, D. (2003). Scale effects on the hydrological impact of upland afforestation and drainage using indices of flowvariability: the River Irthing, England. *Hydrology and Earth System Sciences* **7**(3): pp. 325–338.

Argaw Denboda, M. (2005). Forest conversion – soil degradation – farmers' perception nexus: Implication for sustainable land use in the southwest of Ethiopia [Ecology and Development Series; 26]. Göttingen, Germany and PhD thesis, Rheinische Friedrichs-Wilhelms-Universität, Bonn, Germany.

Arnold, J. G. and Williams, J. R. (1987). Validation of SWRRB: Simulator for water resources in rural basins. *Journal of Water Resources Planning and Management* **113**(2): pp. 243–256.

Arnold, J.G. and Allen, P.M. (1996). Estimating hydrologic budgets for three Illinois watersheds. *Journal of Hydrology* **176**(1–4): pp. 57–77.

Arnold, J. G., and Allen, P. M. (1999). Automated Method for Estimating Base flow and Groundwater Recharge from Stream Flow Records. *Journal of the American Water Resources Association* **35**(2): pp. 411–424.

Arnold, J. G., Allen, P. M. and Bernhardt, G. (1993). A comprehensive surface-groundwater flow model. *Journal of Hydrology* **142**(1–4): pp. 47–69.

Arnold, J. G., Srinivasan, R., Muttiah, R. S. and Williams, J. R. (1998). Large area hydrologic modelling and assessment; part I: model development. *Journal of the American Water Resources Association* **34**(1): pp. 73–89.

Arnold, J. G., Muttiah, R. S., Srinivasan, R. and Allen, P. M. (2000). Regional estimation of base flow and groundwater recharge in the Upper Mississippi river basin. Journal of Hydrology 227(1–4): pp. 21–40.

Asfaw, M. G. (2005). Groundwater recharge and water balance assessment in Geba Basin, Tigray, Ethiopia. Unpublished Master's thesis, Vrije Universiteit Brussel, Belgium and Katholieke Universiteit Leuven, Belgium.

ASTM, American Society for Testing and Materials (1998). Designation: D 422 – 63 (Reapproved 1998). Standard Test Method for Particle-Size Analysis of Soils. West Conshohocken, PA, USA.

Awulachew, S. B. (2010). Improved water and land management in the Ethiopian highlands and its impact on downstream stakeholders dependent on the Blue Nile. CPWF Project Number 19. URL: http://cgspace.cgiar.org/bitstream/handle/10568/3908/PN19_IWMI_Project%20Report_May10_final.pdf?sequence=1)

Awulachew, S. B, Merrey, D. J., Kamara, A. B., van Koppen, B., Penning de Vries, F., Boelee, E. and Makombe, G. (2005). Experiences and opportunities for promoting small-scale/micro irrigation and rainwater harvesting for food security in Ethiopia [IWMI Working paper; 98]. Colombo, Sri Lanka.

Awulachew, S. B.; McCartney, M.; Steenhuis, T. S; Ahmed, A. A. (2008). A review of hydrology, sediment and water resource use in the Blue Nile basin [IWMI Working paper; 131]. Colombo, Sri Lanka.

Bates, B. C., Kundzewicz, Z. , Wu, W. S. and Palutikof, J. P. (eds.) (2008). Climate Change and Water. Technical Paper of the Intergovernmental Panel on Climate Change. IPCC Secretariat, Geneva, Switzerland.

Bauer, S. W. (1974). A modified Horton equation for infiltration during intermittent rainfall. *Hydrological Science Bulletin* **19**(2): pp. 219–225.

Bekele, E. (2004). Markov chain modeling and ENSO influences on the rainfall seasons of Ethiopia. In: World Meteorological Organization (ed.). Application of Climate Forecasts for Agriculture. Proceedings of an Expert Group Meeting for Regional Association I (Africa) (9 - 13 December 2002, Banjul, Gambia). Geneva, Switzerland.

Belay, T. (2002). Land cover/land-use changes in the Derekolli catchment of the South Welo Zone of Amhara Region, Ethiopia. *Eastern Africa Social Science Research Review* **18**(1): pp. 1–20.

Belete, K. (2007). Sedimentation and Sediment Handling at Dams in Tekeze River Basin, Ethiopia. PhD thesis, Norges teknisk-naturvitenskapelige universite, Trondheim, Norway.

Beven, K. J. (2001). Rainfall-Runoff Modelling: The Primer. New York City, NY, USA.

Beven, K. J. (2006). A manifesto for the equifinality thesis. *Journal of Hydrology* **320**(1–2): pp. 18–36.

Beven, K. J. and Binley, A. (1992). The Future of Distributed Models: Model Calibration and Uncertainty Prediction. *Hydrological Processes* **6**(3): pp. 279–298.

Beven, K. J. and Young, P. (2003). Comment on "Bayesian recursive parameter estimation for hydrologic models" by M. Thiemann, M. Trosset, H. Gupta, and S. Sorooshian. *Water Resources Research* **39**(5): p. 1116.

Bewket, W. (2003). Towards integrated watershed management in highland Ethiopia: the Chemoga watershed case study. PhD thesis, Wageningen Universiteit, The Netherlands.

Bewket, W. and Sterk, G. (2005). Dynamics in land cover and its effect on stream flow in the Chemoga watershed, Blue Nile basin. Ethiopia. *Hydrological Processes* **19**(2): pp. 445–458.

Birhanu, B. Z., Ndomba, P. M. and Mtalo, F. W. (2006). Application of SWAT Model for Mountainous Catchment [FWU Water Resources Publications; 6]. Siegen, Germany.

Bitew, M. M. and Gebremichael, M. (2011). Evaluation of satellite rainfall products through hydrologic simulation in a fully distributed hydrologic model. *Water Resources Research* **47**(6): W06526.

Bogale, G. (2007). Basin scale sedimentary and water quality responses to external forcing in Lake Abaya, southern Ethiopia rift valley. PhD thesis, Freie Universität Berlin, Germany.

Bormann, H. and Diekkrüger, B. (2003). Possibilities and limitations of regional hydrological models applied within an environmental change study in Benin (West Africa). *Physics and Chemistry of the Earth* **28**(33–36): pp. 1323–1332.

Bosellini A., Russo, A., Fantozzi, P. L., Getaneh, A. and Tadesse, S. (1997). The Mesozoic succession of the Mekele outlier (Tigre province, Ethiopia). *Memorie di Scienze Geologiche* **49**: pp. 95–116.

Boukhris, O. F. (2008). Climate change impact on hydrological extremes along rivers in Flanders. PhD thesis, Katholieke Universiteit Leuven, Belgium.

Bracken, L. J. and Croke, J. (2007). The concept of hydrological connectivity and its contribution to understanding runoff-dominated geomorphic systems. *Hydrological processes* **21**(13): pp. 1749–1763.

Brown, A. E., Zhang, L., McMahon, T. A., Western, A. W. and Vertessy, R. A. (2005). A review of paired catchment studies for determining changes in water yield resulting from alterations in vegetation. *Journal of Hydrology* **310**(1): pp. 28–61.

Bruijnzeel, L. A. (2004). Hydrological functions of tropical forests: not seeing the soil for the trees? *Agriculture, Ecosystems & Environment* **104**: pp. 185–228.

Bryant, R. B., Gburek, W. J., Veith, T. L. and Hively, W. D. (2006). Perspectives on the potential for hydropedology to improve watershed modeling of phosphorus loss. *Geoderma* **131**(3–4): pp. 299–307.

Bull, L. J. and Kirkby, M. J. (2002²). Dryland rivers: Hydrology and geomorphology of semi-arid channels. Chichester, UK.

Burn, D. H. and Hag Elnur, M.A. (2002). Detection of Hydrologic Trends and Variability. *Journal of Hydrology* **255**(1–4): pp. 107–122.

Celleri, R., Willem, P., Buytaert, W. and Feyen, J. (2007). Space – time rainfall variability in the Paute Basin, Ecuadorian Andes. *Hydrological Processes* **21**: pp. 3316–3327.

Central Statistical Agency (CSA) (2008). Ethiopia national statistics.

Chekol, D. A. (2006). Modeling of hydrology and soil erosion of upper Awash River basin. PhD thesis, Rheinische Friedrich-Wilhelms-Universität Bonn, Germany.

Daniel E. B., Camp, J. V., LeBoeuf, E. J., Penrod, J. R., Dobbins, J. P. and Abkowitz, M. D. (2011). Watershed Modeling and its Applications: A State-of-the-Art Review. *The Open Hydrology Journal* **5**: pp. 26–50.

Dargahi, B. and Setegn, S. G. (2011). Combined 3D hydrodynamic andwatershed modeling of Lake Tana, Ethiopia. *Journal of Hydrology* **398**(1–2): pp. 44–64.

DeFries, R. and Eshleman, K. N. (2004). Land-use change and hydrologic processes: a major focus for the future. *Hydrological processes* **18**: pp. 2183–2186.

Descheemaeker, K., Nyssen, J., Poesen J., Raes, D., Haile, M., Muys, B. and Deckers, S. (2006). Runoff on slopes with restoring vegetation: A case study from the Tigray highlands, Ethiopia. *Journal of Hydrology* **331**(1–2): pp 219–241.

DEVECON. (1992) Five towns water supply and sanitation study. Addis Ababa, Ethiopia.

Dewis, J. and Freitas, F. (1970). Physical and chemical methods of soil and water analysis. *Food and Agricultural Organization Soils Bulletin* **10**, Rome, Italy.

Dibike, Y. and Solomatine, D. P. (1999). River flow forecasting using artificial neural networks, European Geophysical Society, XXIV general assembly, The Hague, The Netherlands.

Dingman, S. L. (2002). Physical Hydrology. Upper Saddle River, NJ, USA.

Easton, Z. M., Fuka, D. R., White, E. D., Collick, A. S., Biruk Ashagre, B., McCartney, M., Awulachew, S. B., Ahmed, A. A., and Steenhuis, T. S. (2010). A multi basin SWAT model analysis of runoff and sedimentation in the Blue Nile, Ethiopia. *Hydrology and Earth System Sciences Discussions* **7**: pp. 3878–3878.

FAO (1970). Physical and chemical methods of soil and water analysis [Soil bulletin, 10]. Rome, Italy.

FAO (1986). Highlands Reclamation Study Ethiopia. Final Report. Vol. I & II. Rome, Italy.

FAO, United Nations Food and Agriculture Organization (1998). Soil and Terrain Database for Northeastern Africa: Crop Production System Zones of the IGAD Subregion. [CD ROM]. FAO Land and Water Digital Media Series 2.

FAO, United Nations Food and Agriculture Organization (2000). New Dimensions in Water Security – Water, Society and Ecosystem Services in the 21st Century. Rome, Italy.

Federal Democratic Republic of Ethiopia (2011). Ethiopia's Climate-Resilient Green Economy – Green economy strategy. n.p.

Fekadu, M. (1999). Runoff models for different time steps with special consideration for semi-arid and arid catchments. PhD thesis, Vrije Universiteit Brussel, Belgium.

Ferriz, H. and Gebeyehu, B. (2002). Development and Management of Water resource in Ethiopia. Proceedings of Ethioforum 2002 – A conference on alleviation of poverty, Addis Ababa, Ethiopia.

Finlayson, B. L. and McMahon, T. A. (1988). Australian vs the world: a comparative analysis of stream flow characteristics. In: Warner, R. F. (ed.). Fluvial geomorphology of Australia. Sydney, Australia: pp. 17–40.

Fohrer, N., Haverkamp, S. and Frede, H.-G. (2005). Assessment of the effects of land use patterns on hydrologic landscape functions: development of sustainable land use concepts for low mountain range areas. Hydrological Processes 19(3): 659–672.

Freese, C., Lorentz, S., le Roux, P., van Tol, J. and Vermeulen, D. (2010). A description and quantification of hillslope hydrological processes in the Necy,Weatherly catchment.
URL: http://www.ru.ac.za/static/institutes/iwr/SANCIAHS/2011/the.pdffiles/C_Freese_Paper.pdf

Freese, C., Lorentz, S., le Roux, P., van Tol, J. and Vermeulen, D. (2010). A description and quantification of hillslope hydrological processes in the Necy,Weatherly catchment.
URL: http://www.ru.ac.za/static/institutes/iwr/SANCIAHS/2011/the.pdffiles/C_Freese_Paper.pdf

Gebreyohannes, T. (2009). Regional Groundwater Flow Modeling of the Geba basin, northern Ethiopia. PhD thesis, Vrije Universiteit Brussel, Belgium.

Gebreyohannes, T., de Smedt, F., Miruts Hagos, Gebresilassie, S. Amare, K., Kabeto, K., Hussein, A. Nyssen, J., Hauer, H. and Moeyersons, J. (2010). Large-scale geological mapping of the Geba basin, northern Ethiopia [Tigray Livelihood Papers; 9]. n. p.

Gebrielle, B. (2011). Weather generator software (WGNmaker4.xlam) URL: http://swat.tamu.edu/software/links-to-related-software [accessed and downloaded on Feburary, 2012].

Giertz, S. and Diekkrüger, B. (2003). Analysis of the hydrological processes in a small headwater catchment in Benin (West Africa). *Physics and Chemistry of the Earth* **28**(33–36): pp. 1333–1341.

Githui, F. W. (2009). Assessing the impacts of environmental change on the hydrology of the Nzoia catchment, in the Lake Victoria. PhD thesis, Vrije Universiteit Brussel, Brussels, Belgium.

Global Land covers facility (GLCF). University of Maryland, College Park, USA. URL: http://www.landcover.org [last visit: October 21, 2012].

Global water partners (2012). Water resource management. URL: http://www.gwp.org/ [accessed on September 3, 2012

Goitom, H., de Smedt, F., Yohannes, T. G., Walraevens, K., Gebrehiwot, K., Bauer, H., Deckers, J. (2012). Modeling Climate Change Impact in the Geba Basin, Ethiopia. Proceddings of the 2012 International Conference on Environmental, Biomedical and Biotechnology. *International Proceedings of Chemical, Biological and Environmental Engineering* **41**: pp. 240–244.

Gonfa, L. (1996). Climate classification of Ethiopia. Addis Ababa, Ethiopia.

Gosain, A. K., Rao, S. and Basuray, D. (2006). Climate change impact assessment on hydrology of Indian River basins. *Current Science* **90**(3): pp. 346–353.

Govender, M. and Everson, C. S. (2005). Modelling streamflow from two small South African experimental catchments using the SWAT model. Hydrological Processes 19(3): pp. 683–692.

Green, C. H. and van Griensven, A. (2007). Auto calibration in hydrologic modeling: Using SWAT2005 in small-scale watersheds. *Environmental Modelling & Software* **23**(4): pp. 422–434.

Grigg, N. S. (2005). Water Resources Management. Water Encyclopedia 2: pp. 586–587.

Hadgu, K. M. (2008). Temporal and spatial changes in land use patterns and biodiversity in relation to farm productivity at multiple scales in Tigray, Ethiopia. PhD thesis, Wageningen Universiteit, The Netherlands.

Helsel, D. R. and Hirsch, R.M. (1992). Statistical Methods in Water Resources [USDA Techniques of Water-Resources Investigations Reports; Book 4, Chapter A3]. URL: http://pubs.usgs.gov/twri/twri4a3/

Henricksen, B. L., Ross, S., Tilimo, S. and Wijntje-Bruggeman, H.Y. (1984). Assistance to Land Use Planning, Geomorphology and Soils of Ethiopia, Scale 1:1,000,000, AGOA: ETH/ 78/003 Field Document 3. Technical Report. Food and Agriculture Organization of the United Nations, Rome, Italy.

Hirsch, R. M., Slack, J. R. and Smith, R. A. (1982). Techniques of trend analysis for monthly water quality data. *Water Resources Research* **18**(1): pp. 107–121.

Huang, M. B. and Zhang, L. (2004). Hydrological responses to conservation practices in a catch-ment of the Loess Plateau, China. *Hydrological Processes* **18**(10): pp. 1885–1898.

Huggett, R. J. (2007[2]). Fundamentals of Geomorphology. Routledge Fundamentals of Physcial Geography. London, UK, and New York City, NY, USA.

Hughes, D. A. (2009). Modelling semi-arid and arid hydrology and water resources: the south African experience. In: Wheater, H., Sorooshian, S. and Sharma, K. D. (eds.). Hydrological Modelling in Arid and Semi-Arid Areas. Cambridge, UK: pp. 29–40.
URL: http://dx.doi.org/10.1017/CBO9780511535734.004

Humphreys, H., Bellier, C., Kennedy, R., Donkin, K. (1997). Tekeze Medium Hydropower report. Annex B – hydrology report. Ministry of Water Resources, Addis Ababa, Ethiopia.

Hunting Technical Service (HTS) (1976). Tigray Rural Development Study, Annex 2: Water Resources. Hunting Technical Services ltd., Hemel Hempstead, UK.

IPCC, Intergovernmental Panel on Climate Change (2001). Climate Change 2001. The Scientific Basis. Contribution of Working Group I to the Third Assessment Report of the Intergovernmental Panel on Climate Change. Houghton, J. T., Ding, Y., Griggs, D. J., Noguer, M., van der Linden, P. J. Dai, X., Maskell, K. and Johnson, C. A. (eds.). Cambridge, United Kingdom and New York City, NY, USA.

IPCC, Intergovernmental Panel on Climate Change (2007). Climate Change 2007: The Physical Science Basis. Contribution of Working Group I to the Fourth Assessment Report of the Intergovernmental Panel on Climate Change. Solomon, S., Qin, D., Manning, M., Chen, Z., Marquis, M., Averyt, K. B., Tignor, M. and Miller, H. L. (eds.). Cambridge, United Kingdom and New York City, NY, USA.

IUSS Working Group WRB (2007). World Reference Base for Soil Resources 2006, first update 2007. World Soil Resources Reports **103**. Food and Agriculture Organization of the United Nations, Rome, Italy.

Jansen, L. J. M. and Di Gregorio, A. (1997). Problems of current classifications: development of a new approach. Proceedings of the Eurostat Seminar on Land Cover and Land Use Information Systems for European Policy Needs, Luxembourg, 21–23 January 1998.

Jarvis, A., Reuter, H. I., Nelson, A., Guevara, E. (2008). Hole-filled SRTM for the globe, Version 4. URL: http://srtm.csi.cgiar.org [accessed on November, 2010].

Jayakrishnan, R., Srinivasan, R., Santhi, C. and Arnold, J.G. (2005). Advances in the application of the SWAT model for water resources management. *Hydrological Processes* **19**(3): pp. 749–762.

Jembere, A. A. (2004). Information theory and artificial intelligence to management uncertainty in hydrodynamics and hydrological models. PhD thesis, UNESCO-IHE, The Netherlands.

Jensco, K. G., McGlynn, B. L., Gooseff, M. N., Wondzell, S. M., Bencala, K. E. and Marshall, L. A. (2009). Hydrologic connectivity between landscapes and streams: Transferring reach- and plot-scale understanding to the catchment scale. *Water Resources Research* **45**(4): W04428.

Jensen, J. R. (1996). Introductory digital image processing: a remote sensing perspective. Upper Saddle River, NJ, USA.

Jensen, J. R. (2005[3]). Introductory Digital Image Processing: A Remote Sensing Perspective. Upper Saddle River, NJ, USA.

Johansson, B. and Chen, D. (2003).The influence of wind and topography on preciptation distribution in Sweden: statistical analysis and modelling. *International Journal of Climatology* **23**(12): pp. 1523–1535.

Jordan P. R. (1977). Streamflow transmission losses in western Kansas. *Journal of the Hydraulics Division* **103**(8): pp. 905–919.

Kalin, L. and Hantush, M. H. (2006). Hydrologic modeling of an eastern Pennsylvania watershed with NEXRAD and rain gauge data. *Journal of Hydrologic Engineering* **11**(6): pp. 555–569.

Kassa, G. (2003). GIS based analysis of landuse and land cover, land degradation and population changes: A study of Boru Metero area of south Wello, Amhara Region. Unpublished Master's thesis, Addis Ababa University, Ehtopia.

Kiersch, B. (2001). Land use impacts on water resources: A literature review. Land-water linkages in rural watersheds, Electronic Workshop (Discussion Paper 1). FAO, Rome, Italy.

Kingston, D. G. and Taylor, R. G. (2010). Sources of uncertainty in climate change impacts on river discharge and groundwater in a headwater catchment of the Upper Nile Basin, Uganda. *Hydrology and Earth System Sciences* **14**: pp. 1297–1308.

Koch, F. J., van Griensven, A., Uhlenbrook, S., Tekleab, S., Teferi, E. (2012). The Effects of Land use Change on Hydrological Responses in the Choke Mountain Range (Ethiopia) – A new Approach Addressing Land Use Dynamics in the Model SWAT. In: Seppelt, R., Voinov, A. A., Lange, S. Bankamp, D. (eds.). 2012 International Congress on Environmental Modelling and Software Managing Resources of a Limited Planet. International Environmental Modelling and Software Society, proceedings of the Sixth Biennial Meeting, Leipzig, Germany.

Koning, G. H. J. de, Verburg, P.H., Veldkamp, A. and Fresco, L. O. (1999). Multi-scale modelling of land use change dynamics in Ecuador. *Agricultural Systems* **61**(2): pp. 77–93.

Lahmer, W., Pfützner, B. and Becker, A. (2001). Assessment of Land Use and Climate Change Impacts on the Mesoscale. *Physics and Chemistry of the Earth, Part B: Hydrology, Oceans and Atmosphere* ***26*** (7–8): pp. 565–575.

Lambin, E. F., Geist H. J., and Lepers E. (2003). Dynamics of land use and land cover change in tropical regions. *Annual Review of Environment and Resources* **28**: pp. 205–241.

Lambin, E. F., Geist, H. and Rindfuss, R. R. (2006). Introduction: local processes with global impacts. In: Lambin, E. F. and Geist, H. (eds.). Land-use and land-cover change: local processes and global impacts. Berlin, Germany.

Lange J. (2005). Dynamics of transmission losses in a large arid stream channel. *Journal of Hydrology* **306**: pp. 112–126.

Larsson, H. (2002). Analysis of variations in land cover between 1972 and 1990, Kassala Province, Eastern Sudan, using Landsat MSS data*. International Journal of Remote Sensing*, **23**(2): pp. 325–333.

Laurance, W. F. (1998). A crisis in the making: responses of Amazonian forests to land use and climate change. *Trends in Ecology & Evolution* **13**(10): pp. 411–415.

Legesse, D., Vallet-Coulomb, C. and Gasse, F. (2003). Hydrological response of a catchment to climate and landuse changes in tropical Africa: case study South Central Ethiopia. *Journal of Hydrology* **275**(1–2): pp. 67–85.

Leistert, H. (2005). Modelling transimission losses; Applications in the Wadi Kuiseb and Nahal Zin. Master's thesis, Albert-Ludwigs-Universität Freiburg, Germany.

Lenhart, T., Eckhardt, K., Fohrer, N. and Frede, H. G. (2002). Comparison of two different approaches of sensitivity analysis. *Physics and Chemistry of the Earth* **27**: pp. 645–654.

Leul, K. (1994). Need, potentials and limitations for irrigation development in Tigray. Commission for Sustainable Agriculture and Environmental Rehabilitation in Tigray, Mekelle, Ethiopia.

Leul K. (2003). Design and performance of community-based irrigation in Tigray. Paper presented at the workshop for research project for community based irrigation management in Ethiopia. ILRI. Addis Ababa. Ethiopia

Lillesand T. M. & Kiefer R. W. (2000[4]). Remote Sensing and Image Interpretation. Hoboken, NJ, USA.

Lin, Y.-P., Hong, N.-M., Wu, P.-J. and Lin, C.-J. (2007). Modeling and assessing land-use and hydrological processes to future land-use and climate change scenarios in watershed land-use planning. *Environmental Geology* **53**(3): pp. 623–634.

Linsely, R. K., Kohler, M. A. and Paulhus, J. L. H. (1982). Hydrology for engineers. New York City, NY, USA.

Liu, B. M., Collick, A. S., Zeleke, G., Adgo, E., Easton, Z. M., and Steenhuis, T. S. (2008). Rainfall-discharge relationships for a monsoonal climate in the Ethiopian highlands. *Hydrological Processes* **22**(7): pp. 1059–1067.

Liu, H. and Zhou, Q. (2004). Accuracy analysis of remote sensing change detection by rule based rationality evaluation with post-classification comparison. *International Journal of Remote Sensing* **25**(5): pp. 1037–1050.

Logsdon, S. D., Allmares, R. R., Wu, L., Swan, J. B. and Randall, G. W. (1990). Macroporosity and its relation to saturated hydraulic conductivity under different tillage practices. *Soil Science Society of America Journal* **54**(4): pp. 1096–1101.

Lu, D., Mausel, P., Brondízio, E. and Moran, E. (2004). Change detection techniques. *International Journal of Remote Sensing* **25**(12): pp. 2365–2401.

Lunetta, R. L., Knight, F. K, Ediriwickrema, J., Lyon, J. G., and Worthy, L. D. (2006). Land cover change detection using multi-temporal MODIS NDVI data. *Remote Sensing of Environment* **105**(2): pp. 142–154.

Makin, M., Kingham, T. J., Wadams, A. E., Birchal, C. J. and Teferra, T. (1975). Development Prospects in the Southern Rift Valley, Ethiopia [Land resources study; 21]. Land Resources Division, Ministry of Overseas Development Survey, Surbiton, UK.

Mango, L. M. , Melesse, A. M., McClain, M. E., Gann, D. and Setegn, S. G. (2011). Land use and climate change impacts on the hydrology of the upper Mara River Basin, Kenya: results of a modeling study to support better resource management. *Hydrology and Earth System Sciences* **15**: pp. 2245–2258.

Matondo J. I., Peter, G and Msibi, K. M. (2004). Evaluation of the impact of climate change on hydrology and water resources in Swaziland: Part I. *Physics and Chemistry of the Earth, Parts A/B/C* **29**(15–18): pp. 15–18.

Mausbach, M. J., and Dedrick, A. R. (2004). The length we go: Measuring environmental benefits of conservation practices. *Journal of Soil and Water Conservatinon* **59**(5): pp.96A–103A.

McCuen, R., Knight, Z., and Cutter, A. (2006). Evaluation of the Nash–Sutcliffe Efficiency Index. *Journal of Hydrologic Engineering* **11**(6): pp. 597–602.

McDonnell, J. J. (2003). Where does water go when it rains? Moving beyond the variable source area concept of rainfall-runoff response. *Hydrological Processes* **17**(9): pp. 1869–1875.

McGuire, K. J. and McDonnell, J. J. (2010). Hydrological connectivity of hillslopes and streams: Characteristic time scales and nonlinearities. *Water Resources Research* **46**(10): W10543.

McGuire, K. J., McDonnell, J. J., Weiler, M., Kendall, C., McGlynn, B. L., Welker, J. M., Seibert, J. (2005).The role of topography on catchment-scale water residence time. *Water Resources Research* **41**(5): W05002.

Mekonnen, M. A., Wörman, A., Dargahi, B., and Gebeyehu, A. (2009). Hydrological modelling of Ethiopian catchments using limited data. *Hydrological Processes* **23**(23): pp. 3401–3408.

Mekuria, A. D. (2005). Forest conversion – soil degradation – farmers' perception nexus: Implication for sustainable land use in the southwest of Ethiopia. Center for Development Research, University of

Bonn, Ecological and Development Series 26 and PhD thesis Rheinische Friedrich-Wilhelms-Universität, Bonn, Germany.

Mengistu, K. T. (2009).Watershed Hydrological Response to Changes in Land Use and Land Cover, and Management Practice at Hare Watershed, Ethiopia. PhD thesis, Universität Siegen, Germany.

Mengistu, K. T. and Förch, G. (2007). Impact of Landuse/ Land Cover change on streamflow: Acase study of Hare watershed, Ethiopia [FWU Water Resources Publications; 6]. Siegen, Germany: pp. 80–84.

Miller, N. L., Bashford, K.E. and Strem, E. (2003). Potential Impacts of Climate Change on California Hydrology. *Journal of the American Water Resources Association* **39**(4): 771–784.

Ministry of Water Resources (2001). Ethiopian Water Sector Policy. URL: http://www.mowr.gov.et [last visit: Sep. 2012]

Ministry of Water Resources (2002). Ethiopian Water Sector Policy. Ethiopian Ministry of Water Resources. URL: http://www.mowr.gov.et [retrieved on March, 2013

Minstry of Water Resourcse (2008). Tekeze River Basin – Physiography and Climate. Addis Ababa, Ethiopia. URL: http://www.mowr.gov.et [Retrieved on March, 2013]

Monteith, J. L. (1965). Evaporation and environment. Harpenden, UK.

Moriasi, D. N., Arnold, J. G., van Liew, M. W., Bingner, R. L. , Harmel, R. D. and Veith, T. L. (2007). Model evaluation guidelines for systematic quantification of accuracy in watershed simulations. *American Society of Agricultural and Biological Engineers* **50**(3): pp. 885–900.

Mulungu, D. M. M. and Munishi, S. E. (2007). Simiyu river catchment parameterization using SWAT model. *Physics and Chemistry of the Earth, Parts A/B/C* **32**(15–18): pp. 1032–1039.

Muttiah, R. S. and Wurbs, R. A. (2002). Scale-dependent soil and climate variability effects on watershed water balance of the SWAT model. *Journal of Hydrology* **256**(3–4): pp. 264–285.

Nash, J. E. and Sutcliffe, J. V. (1970). River flow forecasting through conceptual models part I – a discussion of principles. *Journal of Hydrology* **10**(3): pp. 282–290.

Ndomba, P. M. and Birhanu, B. Z. (2008). Problems and Prospects of SWAT Model Applications in NILOTIC Catchments: A Review. *Nile Basin Water Engineering Scientific Magazine* **1**: pp. 41–52.

Ndomba, P.M., Mtalo, F.W. and Killingtveit, A. (2008). SWAT model application in a data scarce tropical complex catchment in Tanzania. *Physics and Chemistry of the Earth, Parts A/B/C* **33**(8–13): pp. 626–632.

NEDECO (1997a). Tekeze River Basin Mater Plan Integrated Project, Land Degradation and Soil Conservation. Second Phase Report, Volume-ENV1. Consultant's report to the Commission for Sustainable Agriculture and Environmental Rehabilitation for Amhara Region (CoSAERAR). Bahir Dar, Ethiopia.

NEDECO (1997b). Tekeze River Basin Master Plan Study Report (TRMSR). Sectoral report volume III. Addis Ababa, Ethiopia.

Neitsch, S. L., Arnold, J. G. , Kiniry, J. R., Srinivasan, R. and Williams J. R. (2004). Soil and Water Assessment Tool Input/output File Documentation – Version 2005. Grassland, Soil & Water Research Laboratory, Agricultural Research Service and Blackland Agricultural Research Station, Temple, Texas. URL: http://swat.tamu.edu/media/1291/swat2005io.pdf

Neitsch, S. L., Arnold, J. G., Kiniry, J. R. and Williams, J. R. (2005). Soil and Water Assessment Tool Theoretical Documentation – Version 2005. Grassland, Soil & Water Research Laboratory, Agricultural Research Service and Blackland Agricultural Research Station, Temple, Texas. URL: http://swat.tamu.edu/media/1292/swat2005theory.pdf

Niehoff, D., Fritsch, U. and Bronstert, A.(2002). Land-use impacts on storm-runoff generation: scenarios of land-use change and simulation of hydrological response in a meso-scale catchment in SW-Germany 2002. *Journal of Hydrology* **267**(1–2): pp. 80–93.

Nyssen, J. (2001). Erosion processes and soil conservation in tropical mountain catchment under threat of anthropogenic desertification – a case study from Northern Ethiopia. PhD thesis, Katholieke Universiteit Leuven, Belgium.

Nyssen, J., Poesen, J., Moeyersons, J., Deckers, J., Haile, M. and Lang, A. (2004). Human impact on the environment in the Ethiopian and Eritrian highlands – a state of the art. *Earth-Science Reviews* **64**(3–4): pp. 273–320.

Nyssen, J., Vandenreyken, H., Poesen, J., Moeyersons, J., Deckers, J., Haile, M., Salles, C., Govers, G. (2005). Rainfall erosivity and variability in the Northern Ethiopian Highlands. *Journal of Hydrology* **311**(1–4): pp. 172–187.

Olivera, F., Valenzuela, M., Srinivasan, R., Choi, J. Cho, H., Koka, K. and Agrawal, A. (2006). ArcGIS-SWAT: A geodata model and GIS interface for SWOT. *Journal of the American Water Resources Association* **04087**: pp. 295–309.

Pilgrim, D. H., Chapman, T. G. and Doran, D.G. (1988). Problems of rainfall-runoff modeling in arid and semi arid regions. *Hydrological Sciences Journal* **33**(4): pp. 379–400.

Price, R. K. (2001). Mathematical modeling reference book. Unpublished reference book for MSc students. UNESCO-IHE, The Netherlands.

Refsgaard, J. C. (1996). Terminology, modeling protocol and classification of hydrological model codes. In: Abbott, M. B. and Refsgaard, J. C. (eds.). Distributed Hydrological Modelling. Dordrecht, The Netherlands, et al.: pp. 17–39.

Renard, K. G and Keppel, R. V. (1967). Hydrographs of ephemerals streams in the southwest. *Journal of the Hydraulics Division, Proceedings of the American Society of Civil Engineers* **92**(2): pp. 33–52.

Richards, J. A.(1995[2]). Remote Sensing Digital Image Analysis. Berlin, Germany, et al.

Richey, J. E., Nobre, C., Deser, C. (1989). Amazon River discharge and climate variability: 1903 to 1985. *Science* **246**: pp. 101–103.

Ringius, L., Downing, T. E., Hulme M., Waughray D. and Selrod R. (1996). Climate change in Africa: issues and challenges in agriculture and water for sustainable development [Center for International Climate and Environmental Research – Oslo, Report 8]. Oslo, Norway.

Rosenberg, N. J., Brown, R. A. Izaurralde, R. C., and Thomson, A. M. (2003). Integrated assessment of Hadley Centre (HadCM2) climate change projections in agricultural productivity and irrigation water supply in the conterminous United States: I. climate change scenarios and impacts on irrigation water supply simulated with the HUMUS model. *Agricultural and Forest Meteorology* **117**: pp. 73–96.

Russo, A., Fantozzi, P. L., Solomon, T., Getaneh, A., Neri, C., Russo, F., Asfwossen, A., Peccerillo, A. and Valera, P. (1996). Geological map of the Mekele outlier (western sheet). Addis Ababa, Ethiopia.

Saleh, A., Arnold, J. G., Gassman, P. W., Hauck, L. M., Rosenthal, W. D., Williams, J. R. and McFarland, A. M. S. (2000). Application of SWAT for the Upper North Bosque River Watershed. *Transactions of the American Society of Agricultural and Biological Engineers* **43**(5): pp. 1077–1087.

Sander, T. (2012). Towards a soil map of the Geba catchement using Bench mark soils. Unpublished Master's thesis, Katholieke Universiteit Leuven and Vrije Universiteit Brussel, Belgium.

Sang, J.K. (2005). Modelling the impact of changes in land use,climate and reserviour storage on flooding in the Nyando basin. Master's thesis, Jomo Kenyatta University of Agriculture and Technology, Juja, Kenya.

Santhi, C., Arnold, J. G., Williams, J. R., Dugas, W. A., Srinivasn R. and Hauck L. M. (2001). Validation of the SWAT model on a large river basin with point and nonpoint sources. *Journal of the American Water Resources Association* **37**(5): pp. 1169–1188.

Schulze, R. E. (2000). Modelling Hydrological Responses to Land Use and Climate Change: A Southern African Perspective. *Ambio* **29**(1): pp. 12–22.

Schütt, B. and Thiemann, S. (2001). Assessment and Monitoring of Erosion and Sedimentation Problems in Ethiopia. Investigation of Erosion Processes in eight selected Watersheds. Trier, Germany.

Setegn, S. G. (2010). Modelling hydrological and hydrodynamic processes in lake Tana basin, Ethiopia. PhD thesis, Royal Institute of Technology, Stockholm, Sweden.

Setegn, S. G., Srinivasan, R., and Dargahi, B. (2009a). Hydrological Modelling in the Lake Tana Basin, Ethiopia Using SWAT Model. *The Open Hydrology Journal* **2:** pp. 49–62.

Setegn, S. G., Srinivasan, R., Dargahi, B., and Melesse, A.M. (2009b): Spatial delineation of soil erosion vulnerability in the Lake Tana Basin, Ethiopia. *Hydrological Processes* **23:** pp. 3738–3750.

Silberstein, R. P. (2006). Hydrological models are so good, do we still need data? *Environmental Modeling & Software* **21**(9): pp. 1340–1352.

Singh, A. (1989). Digital change detection techniques using remotely sensed data. *International Journal of Remote Sensing* **10**(6): pp. 989–1003.

Singh, V. P. (1995). Computer models of watershed hydrology. Littleton, CO.

Singh, V. P. and Woolhiser, D. A. (2002). Mathematical modelling of watershed hydrology. *J Journal of Hydrologic Engineering* **7**(4): pp. 270–292.

Singh, J., Knapp, H. V.,Arnold, J. G. and Demissie, M. (2005). Hydrologic modeling of the Iroquois River watershed using HSPF and SWAT. *Journal of the American Water Resources Association* **41**(2): pp. 343–360.

Sleeter, B. M., Sohl, T. L., Bouchard, M. A., Reker, R. R., Soulard C. E., Acevedo, W., Griffith, G. E., Sleeter, R. R., Auch, R. F., Sayler, K. L., Prisley, S. and Zhu., Z. (2009). Scenarios of land use and land cover change in the conterminous United States: Utilizing the special report on emission scenarios at ecoregional scales. *Global Environmental Change* **22**(4): pp. 896–914.

Smith, R. E. and Goodrich, D. C. (2005). 111 Rainfall excess overland flow. In: Anderson, M. G. and McDonnell, J. J. (eds.). Encyclopedia of Hydrological Sciences. Hoboken, NJ, USA.

Srinivasan, R., and Arnold, J. G. (1994). Integration of a basin-scale water quality model with GIS. Journal of the American Water Resources Association 30(3): pp. 453–462.

Stednick, J. D. (1996). Monitoring the effects of timber harvest on annual water yield. *Journal of Hydrology* **176**(1–4): pp. 79–95.

Sumner, G., Homar, V. and Ramis, C. (2001). Precipitation seasonality in eastern and southern coastal Spain. *International Journal of Climatology* **21**(2): pp. 219–247.

Swank, W. T., Swift, L. W. and Douglass, J. E. (1988). Stream flow changes associated with forest cutting, species conversions, and natural disturbances. In: Swankand, W. T. and Crossley, D. A. (eds.). Forest hydrology and ecology at Coweeta. Ecological Studies **66**. New York City, NY, USA, et al.

Taddele, Y.D. (2009). Hydrological Modelling to Assess the Impact of Climate Change at Gilgel Abay River, Lake Tana Basin – Ethiopia. Master's thesis, Lunds Universitet, Sweden.

Taylor, J. C., Brewer, T. R. and Bird, A. C. (2000). Monitoring landscape change in the National Parks of England and Wales using aerial photo interpretation and GIS. *International Journal of Remote Sensing* **21**(13–14): pp. 2737–2752.

Tekeab, S., Uhlenbrook, S., Mohamed, Y., Savenije, H. H. G,, Temesgen, M. and Wenninger, J. (2011). Water balance modeling of Upper blue Nile Catchments. *Hydrology and Earth System Sciences* **15**: pp. 2179–2193.

Thiemann, S. (2006). Detection and assessment of erosion and soil erosion risk in the wetland of the Bilate River – South Ethiopian Rift Valley. PhD thesis, Freie Universität Berlin, Germany.

Trimble, S. W., Weirich, F. H. and Hoag, B.L. (1987). Reforestation and the reduction ofwater yield on the Southern Piedmont since circa 1940. *Water Resources Research* **23**(3): pp. 425–437.

Tulu, M. D. (2010). Event based rainfall-runoff modeling in semi-arid regions. PhD thesis. Universität für Bodenkultur Wien, Vienna, Austria.

UNCCD (1999). National report on the implementation of the United Nations Convention to combat Desertification (UNCCD). Addis Ababa, Ethiopia.

UNESCO-WWAP, United Nations Educational, Scientific, and Cultural Organization (UNESCO). World Water Assessment Program (2004). National Water Development Report for Ethiopia. Addis Ababa, Ethiopia.

UNFCCC, United Nations Framework Convention on Climate Change (2006). Handbook. Bonn, Germany.

USDA, Soil Conservation Service (1972). National Engineering Handbook, Section 4: Hydrology. Washington, D.C., USA.

USDA, Soil Conservation Service (1985). National Engineering Handbook, Section 4: Hydrology. Washington, D.C., USA.

Van Griensven, A., Francos, A. and Bauwens, W. (2002). Sensitivity analysis and auto-calibration of an integral dynamic model for river water quality. *Water Science and Technology* **45**(5): pp. 321–328.

Van Griensven, A., Breuer, L., Di Luzio M., Vandenberghe, V., Goethals, P., Meixner, T., Arnold, J. and Srinivasan. R. (2006). Environmental and ecological hydroinformatics to support the implementation of the European Water Framework Directive for river basin management. *Journal of Hydroinformatics* **8**(4): pp. 239–252.

Van Griensven, A., Meixner, T., Grunwald, S., Bishop, T., Diluzio, M. and Srinivasan, R. (2006). A global sensitivity analysis tool for the parameters of multi-variable catchment models. *Journal of Hydrology* **324**(1–4): pp. 10–23.

Van Griensven A. and Meixner, T. (2007). A global and efficient multi-objective autocalibration and uncertainty method for water quality catchment models. *Journal of Hydroinformatics* **9**(4): pp. 277–291.

Van Griensven, A, Ndomba, P., Yalew, S. and Kilonzo, F. (2012). Critical review of SWAT applications in the upper Nile basin countries. *Hydrology and Earth System Sciences* **16**: pp. 3371– 3381.

Van Liew, M. W., and Garbrecht, J. (2003). Hydrologic simulation of the Little Washita River experimental watershed using SWAT. *J.American Water Resour. Assoc.* 39(2): 413-426.

Van Tol, J. J., le Roux, P. A. L., Henseley, M. and Lorentz, S. A. L. (2010). Soil as an indicator of hillslope hydrological behaviour in the Weatherley Catchment, Eastern Cape, SouthAfrica. Water SA 36(5): pp. 513–520.

Veldkamp, A., and Verburg, P. H.(2004). Modelling land use change and environmental impact. *Journal of Environmental Management* **72**(1–2): pp. 1–3.

Verburg, P. H. and Overmars, K. P. (2009). Combining top-down and bottom-up dynamics in land use modeling: exploring the future of abandoned farmlands in Europe with the Dyna-CLUE model. *Landscape Ecology* **24**(9): pp. 1167–1181.

Virgo, K. J. & Munro, R. N. (1978). Soil and erosion features of the central plateau region of Tigrai, Ethiopia. *Geoderma* **20**(2): pp. 131–187.

Wagner, P. D. (2013). Impact of climate change and landuse change on the water resource of the Mula and Mutha rivers catchement upstream of Pune, India. PhD thesis, Universität zu Köln, Germany.

Walsh, P. D., and Lawler, D. M (1981). Rainfall seasonality: description, spatial patterns,and change through time. *Weather* **36**: pp: 201–208.

Walter, M. T., Mehta, K., Marrone, A. M., Boll, J., Gerard-Merchant, P., Steenhuis, T. S., and Walter, M. F. (2003). A Simple estimation of theprevalence of hortonian flow in New York City's watersheds. *Journal of Hydrologic Engineering* **8**(4): pp. 214–218.

Wang, S., Zhang, Z., Sun, G., McNulty, S. G. and Zhang, M., (2009). Detecting water yield variability due to the small proportional land use and land cover changes in a watershed on the Loess Plateau, China. *Hydrological Processes* **23**(21): pp. 3083–3092.

WAPCOS & Continental Consult. Commission for Sustainable Agriculture and Environmental Rehabilitation in Tigray and Water and Power Consultancy Services (India) Limited (2003). Suluh Valley Integrated Rural, Agricultural and Water Resources Development Study. Identification and Reconnaissance Report. Mekele, Ethiopia.

WBISPP, Woody Biomass Inventory and Strategic Planning Project in Ethiopia (2004). Land use and land cover database. Addis Ababa, Ethiopia.

Weismiller, R. A., Kristof, S. J., Scholtz, D. K., Anulta, P. E., and Momin, S. A. (1977). Change detection in coastal zone environments. *Photogrammetric Engineering and RemoteSensing* **43**(12): pp. 1533–1539.

Wheater, H., Sorooshian, S. and Sharma, K.D (2008). Hydrological modeling in arid and semi arid areas. Cambridge, UK.

White, E. D. (2009). Development and application of a physically based landscape water balance in the SWAT model. Unpublished Master's thesis, Cornell University, Ithaca, NY, USA.

White, K. L. and Chaubey, I. (2005). Sensitivity analysis, calibration, and validation for a multisite and multivariable SWATmodel. *Journal of the American Water Resources Association* **41**(5): pp. 1077–1089.

Wilby, R. L. and Christian W. D. (2007). Using SDSM Version 4.2. A decision support tool for the assessment of regional climate change impacts – User Manual.
URL: http://www.staff.lboro.ac.uk/~cocwd/SDSM/index.html [accessed 13 Feb 2011].

Williams, J. R. (1969). Flood routing with variable time or variable storage coefficients. *Transactions of the American Society of Agricultural Engineers* **12**(1): pp. 100–103.

Williams, J. R. (1995). Chapter 25. The EPIC model. In: Singh, V. P (ed.). Computer models of watershed hydrology. Highlands Ranch, CO, USA.

WMO. World Meteorological Organization (2009[6]). Guide to Hydrological Practices, Volume II: Management of Water Resources and Applications of Hydrological Practices. Geneva, Switzerland.

Wu, K. and Xu, J. (2005). Applicability of SWAT for three coastal watersheds in Louisiana. Watershed Management to Meet Water Quality Standards and Emerging TMDL (Total Maximum Daily Load), Proceedings of the Third Conference 5-9 March 2005. Atlanta, Georgia, USA.

WSSD (2002). Report of the World Summit on Sustainable Development. Johannesburg, South Africa, 26 August- 4 September 2002. New York City, NY, USA.

WWDSE, Water Works design and Supervision Enterprise (2007). Evaluation of Aynalem wellfield and selection of additional prospect for Mekelle town water supply. Addis Ababa, Ethiopia.

WWDSE, Water Works design and Supervision Enterprise (2008). Geomorphological report on Wolkaite irrigation study and design project. n.p.

Xu, C.-Y. (2000). Modeling the effect of climate change on water resources in central Sweden. *Water Resources Management* **14**(3): pp. 177–189.

Yazew, H. E. (2005). Development and Management of irrigated land in Tigray, Ethiopia. PhD thesis, Wageningen Universiteit and UNESCO-IHE Institute for Water Education, Delft, The Netherlands.

Yousuf, M.B. (2007). Numerical Groundwater Flow Modeling of the Dire Dawa Area. Master's thesis, Addis Ababa University, Ethiopia.

Zeleke, G. and Hurni, H. (2001). Implications of Land Use and Land Cover Dynamics for Mountain Resource Degradation in the Northwestern Ethiopian Highlands. *Mountain Research and Development* **21**: pp. 184–191.

Zeray, L., Roehrig, J. and Chekol, D. A. (2007). Climate Change Impact on Lake Ziway WatershedWater Availability, Ethiopia [FWU Water Resources Publications; 6]. Siegen, Germany.

Zhang, L., Dawes, W. R., Walker, G. R.(2001). Response of mean annual evapotranspiration to vegetation changes at catchment scale. *Water Resources Research* **37**(3): pp. 701–708.

Additional documents:

Canadian Institute for climate studies: HadCM3 A2 and B2 emission Scenario
http://www.cics.uvic.ca/scenarios/sdsm/select.cgi [accessed February 12, 2011].

Data access integration: CGCM3 A2 emission scenario
URL: http://loki.qc.ec.gc.ca/DAI/CGCM3_predictors-e.html [accessed March 5, 2013]

Ethiopia's Climate-Resilient Green Economy strategy (CRGE, 2011).

http://www.undp.org/content/dam/ethiopia/docs/Ethiopia%20CRGE.pdf

Laboratory Testing manual of Civil Engineering – Mekelle University (2000).(Adapted from American society of testing Material and the United Republic of Tanzania, Ministry of Work, 2000).

11 Appendices

11.1 Annex 1 - Weather Generator Statistic and Probability Value

The statistical data needed to generate representative daily climate data for the sub basins for SWAT model is using the weather generator (WGN file). When the user specifies that simulated weather will be used or when measured data is missing, climatic data will be generated. Following values were calculated for weather stations used in the research.

TMPMX (mon): Average or mean daily maximum air temperature for month (°C):

$$\bar{T}_{mx,mon} = \frac{\sum_{d=1}^{N} T_{mx,mon}}{N}$$

Where: T *maxmon* is the mean daily maximum temperature for the month (^{o}C)

PR_W(1,mon) : Probability of a wet day following a dry day in the month:

$$P(W|D) = \frac{days_{W/Di}}{days_{dry\ i}}$$

Where: *Pi(W/D)* is the probability of a wet day following a dry day in month *i*, *daysW/D,i* is the number of times a wet day followed a dry day in month *i* for the entire period of record,and *daysdry,i* is the number of dry days in month *i* during the entire period of record.

PR_W(2,mon) : Probability of a wet day following a wet day in the month:

$$P(W|W) = \frac{days_{W/Wi}}{days_{wet\ i}}$$

Where: *Pi(W/W)* is the probability of a wet day following a wet day in month *i*, *daysW/W,i i* is thenumber of times a wet day followed a wet day in month *i* for the entire period of record, and*dayswet,i* is the number of wet days in month *i* during the entire period of record.

TMPMN(mon): Average or mean daily minimum air temperature for month (°C):

$$\mu_{\mathrm{mn,mon}} = \frac{\sum_{\mathrm{d=1}}^{\mathrm{N}} \mathrm{T_{mn,mon}}}{\mathrm{N}}$$

Where $\mu_{mn,mon}$ is the mean daily minimum temperature for the month (°C), *Tmn,mon* is the dailyminimum temperature on record *d* in month *mon* (°C), and *N* is the total number of dailyminimum temperature records for month *mon*.

TMPSTDMX(mon): Standard deviation for daily maximum air temperature in month (ºC):

$$\sigma_{\mathrm{mx,mon}} = \sqrt{\frac{\sum_{\mathrm{d=1}}^{\mathrm{N}} \left(\mathrm{T_{mx,mon}} - \mu_{\mathrm{mx,mon}}\right)^2}{\mathrm{N}-1}}$$

Where: $\sigma_{mx,mon}$ is the standard deviation for daily maximum temperature in month *mon* (ºC),*Tmx,mon* is the daily maximum temperature on record *d* in month *mon* (°C), m*mxmon* is theaverage daily maximum temperature for the month (°C), and *N* is the total number of dailymaximum temperature records for month *mon*.

TMPSTDMN(mon): Standard deviation for daily minimum air temperature in month(°C):

$$\sigma_{\mathrm{mn,mon}} = \sqrt{\frac{\sum_{\mathrm{d=1}}^{\mathrm{N}} \left(\mathrm{T_{mn,mon}} - \mu_{\mathrm{mn,mon}}\right)^2}{\mathrm{N}-1}}$$

Where $\sigma_{mx,mon}$ is the standard deviation for daily minimum temperature in month *mon* (ºC),*Tmn,mon* is the daily minimum temperature on record *d* in month *mon* (°C), m*mnmon* is theaverage daily minimum temperature for the month (°C), and *N* is the total number of dailyminimum temperature records for month *mon*.

PCPMM(mon): Average or mean total monthly precipitation (mm H_2O):

$$\overline{\mathrm{R}}_{\mathrm{mon}} = \frac{\sum_{\mathrm{d=1}}^{\mathrm{N}} \mathrm{R_{day,mon}}}{\mathrm{Yrs}}$$

Where: $\bar{R}_{mon}$ is the mean monthly precipitation (mm H2O), *Rday,mon* is the daily precipiation forrecord *d* in month *mon* (mm H2O), *N* is the total number of records in month *mon* used tocalculate the average, and *yrs* is the number of years of daily precipitation records used incalculation.

PCPSTD(mon): Standard deviation for daily precipitation in month (mm H2O/day).Calculated based on following formula:

$$\sigma_{mon} = \sqrt{\frac{\sum_{d=1}^{N}\left(R_{mn,mon} - \bar{R}_{mon}\right)^2}{N-1}}$$

Where $\boldsymbol{\sigma_{mon}}$ is the standard deviation for daily precipitation in month *mon* (mm H_2O), *Rmon* is themean monthly precipitation (mm H_2O), *Rday,mon* is the daily precipiation for record *d* in month*mon* (mm H_2O), *N* is the total number of records in month *mon* used to calculate the average,and *yrs* is the number of years of daily precipitation records used in calculation.

PCPSKW(mon): Skew coefficient for daily precipitation in month:

$$g_{mon} = \frac{N.\sum_{d=1}^{N}\left(R_{day,,mon} - \bar{R}_{mon}\right)^3}{(N-1)(N-2)(N-3)}$$

Where g_{mon} is the skew coefficient for precipitation in the month, *N* is the total number of dailyprecipitation records for month *mon*, *Rday,mon* is the amount of precipitation for record *d* in month*mon* (mm H_2O), *Rmon* is the average precipitation for the month (mm H_2O), and *mon* is thestandard deviation for daily precipitation in month *mon* (mm H_2O). (Note: daily precipitationvalues of 0 mm are included in the skew coefficient calculation).

PR_W(1,mon) : Probability of a wet day following a dry day in the month:

$$P(W|D) = \frac{days_{W/Di}}{days_{dry\ i}}$$

Where *Pi(W/D)* is the probability of a wet day following a dry day in month *i*, *daysW/D,i* is the number of times a wet day followed a dry day in month *i* for the entire period of record,and *daysdry,i* is the number of dry days in month *i* during the entire period of record.

PR_W(2,mon) Probability of a wet day following a wet day in the month:

$$P(W|W) = \frac{days_{W/Wi}}{days_{wet\ i}}$$

Where *Pi(W/W)* is the probability of a wet day following a wet day in month *i*

PCPD(mon): Average number of days of precipitation in month.

$$\overline{\boldsymbol{d_{wet,i}}} = \frac{days_{wet,i}}{yrs}$$

Where $\overline{\boldsymbol{d_{wet,i}}}$, , is the average number of days of precipitation in month *i*, *dayswet,i* is the numberof wet days in month *i* during the entire period of record, and *yrs* is the number of years ofrecord.

RAINHHMX(mon): Maximum 0.5 hour rainfall in entire period of record for month.This value represents the most extreme 30-minute rainfall intensity recorded in the entire period of record.

SOLARAV(mon): Average daily solar radiation for month (MJ/m2/day).Calculated based on following formula:

$$\boldsymbol{\mu_{mon}} = \frac{\sum_{d=1}^{N} H_{days,mon}}{N}$$

Where $\mu_{\boldsymbol{mon}}$ is the mean daily solar radiation for the month (MJ/m2/day), *Hday,mon* is the totalsolar radiation reaching the earth's surface for day *d* in month *mon* (MJ/m2/day), and *N* is thetotal number of daily solar radiation records for month *mon*.

DEWPT(mon): Average daily dew point temperature in month (ºC):

$$\boldsymbol{\mu_{dew,mon}} = \frac{\sum_{\boldsymbol{d=1}}^{\boldsymbol{N}} \boldsymbol{T_{dew,mon}}}{\boldsymbol{N}}$$

Where $\mu_{\boldsymbol{dew,mon}}$ is the mean daily dew point temperature for the month (ºC), *Tdew,mon* is thedew point temperature for day *d* in month *mon* (ºC), and *N* is the total number of daily dew pointrecords for month *mon*.

WNDAV(mon): Average daily wind speed in month (m/s).Calculated based on following formula:

$$\boldsymbol{\mu_{wnd,mon}} = \frac{\sum_{\boldsymbol{d=1}}^{\boldsymbol{N}} \boldsymbol{\mu_{wnd,mon}}}{\boldsymbol{N}}$$

Where m*wndmon* is the mean daily wind speed for the month (m/s), m*wnd,mon* is the average windspeed for day *d* in month *mon* (m/s), and *N* is the total number of daily wind speed records formonth *mon*.

11.2 Annex2 - Monthly discharge data collected from different sources

STATION: Geba N r. Mekele, 121004 (H2)						BASIN: Tekeze		DRAINAGE AREA: 2440 Sq.Km.				
year	Jan	Feb	Mar	Apr	May	Jun	Jul	Aug	Sep	Oct	Nov	Dec
1967						4.50	182.35	254.17	23.24	6.80	4.65	2.43
1968	1.80	1.40	1.60	2.19	3.79	3.13	122.71	78.72	5.46	2.61	2.86	2.64
1969	4.91	5.87	4.95	4.85	23.76	1.15	120.74	78.71	2.67	0.66	0.27	0.32
1970	0.42	1.15	0.53	3.19	0.03	1.57	112.83	131.19	10.95	1.20	0.39	0.28
1971	0.23	0.09	1.39	0.91	4.99	2.53	40.36	63.20	2.60	0.02	0.47	0.29
1972	0.16	0.07	6.18	19.60	15.12	22.95	94.34	38.80	2.18	0.41	0.56	0.22
1973	0.09	0.04	0.03	3.09	2.11	0.07	107.37	230.65	19.08	4.80	2.10	0.75
1974	0.40	0.16	0.67	1.28	2.67	7.84	49.93	44.18	4.37	1.29	1.02	0.74
1975	0.80	0.69	4.76	5.10	0.34	7.20	72.19	171.76	48.79	5.22	3.10	2.65
1976	2.10	3.12	3.36	4.59	2.79	4.36	25.26	39.82	9.06	2.02	3.06	1.80
1977	1.29	0.89	7.95	0.34	4.82	4.15	97.92	111.78	5.57	8.10	3.47	2.76
1978												
1979									22.34	2.00	1.01	2.15
1980	1.15	4.29	5.04	5.60	2.21	9.72	315.57	286.69	5.67	1.54	0.57	0.67
1981	0.40	0.27	2.70	4.65	1.09	0.55	116.72	107.80	42.86	19.90	11.67	6.18
1982	4.93	3.59	17.75	6.06	7.44	4.32						
1991											0.43	0.61
1992	0.39	0.64	5.52	0.66	26.64	0.94	55.96	236.67	7.38	1.29		1.29
1993	0.85	6.50					154.74	104.60	22.96	6.38	0.50	0.36
1994	0.28	0.52	6.27	13.54			159.65	350.60		7.14	1.10	0.95
1995	0.41	1.22	16.88		15.10	0.99	64.48	132.91	16.24	1.19	0.97	0.88
1996	0.61	0.25	3.66	1.47	10.00	***170.00***	***535.50***	***1357.00***				36.51
1997										4.96	0.75	
1998			0.08	0.76	3.65	0.11	87.23	297.90				20.08
1999					0.75	5.48		219.34	49.30			2.76
2000	1.43	0.63	0.46	0.50	0.66	0.69	66.38	256.30	22.81			1.18
2001	0.58	0.43	1.68	0.66	0.57	1.85			33.82			6.10
2002							14.11	65.16	7.09	2.68		4.86
2003	1.31	1.78	0.77	1.64	0.45							
Mean	**1.17**	**1.60**	**4.39**	**4.03**	**6.14**	**12.10**	**123.64**	**211.73**	**17.35**	**4.01**	**2.05**	**3.98**
Max	**4.93**	**6.50**	**17.75**	**19.60**	**26.64**	**170.00**	**535.50**	**1357.00**	**49.30**	**19.90**	**11.67**	**36.51**
Min	**0.09**	**0.04**	**0.03**	**0.34**	**0.03**	**0.07**	**14.11**	**38.80**	**2.18**	**0.02**	**0.27**	**0.22**
STDEV	**1.36**	**1.93**	**4.90**	**4.79**	**7.74**	**36.53**	**114.79**	**272.71**	**15.20**	**4.50**	**2.67**	**7.88**
75%	**0.25**	**0.30**	**1.09**	**0.80**	**0.92**	**0.00**	**46.21**	**27.78**	**7.10**	**0.98**	**0.25**	**0.00**
85%	**0.00**	**0.00**	**0.00**	**0.00**	**0.00**	**0.00**	**4.67**	**0.00**	**1.60**	**0.00**	**0.00**	**0.00**

		Hunting Technical Service										
	*	Tekeze Master Plan Processed data										
	#	Hydrology Department Data										
	June	July	August									
1994			350.6	Suspect High Data								
1996	170	535.5	1357.0	Rating is not valid for high flows above stage 1.5 m								
	Q = 35.51(H +0.096) ^ 2.395											
		For high flows (H > 1.0 m), the exponent need to be reduced to about 1.7 which correpsond the channel control Manning derived exponent.										

11.3 Annex 3 - Soil and water assessment tool model output for different land use and climate scenarios in mm.

SURQ is for surface runoff in mm, LATQ is the lateral/interflow, and GW_Q is groundwater / base flow and WYLD is total water yield or stream flow.

Sub basin	Using 1972 Land cover Map				Using 2003 Land cover map			
	SURQ mm	GW_Q mm	LATQ mm	WYLD mm	SURQ mm	GW_Q mm	LATQ mm	WYLD mm
1	23.62	0.51	135.40	159.52	23.2	0.5	103.0	126.7
2	22.57	8.83	81.72	113.12	18.1	5.5	71.5	95.0
3	48.65	18.44	6.34	73.43	54.9	5.5	17.8	78.2
4	52.65	10.22	45.30	108.17	22.8	6.3	42.6	71.8
5	42.59	13.28	14.95	70.82	44.0	14.4	0.9	59.3
6	28.32	23.51	6.66	58.48	28.0	20.7	6.6	55.3
7	60.82	19.14	1.00	80.96	59.0	12.6	1.4	73.1
8	50.19	77.49	18.43	146.11	75.7	57.6	18.7	152.0
9	25.16	17.42	133.86	176.45	17.8	20.0	97.2	135.0
10	49.59	15.23	3.94	68.77	41.0	15.3	1.8	58.2
11	157.70	41.12	37.12	235.94	130.9	46.0	42.8	219.6
12	148.22	75.61	19.24	243.07	119.2	74.2	20.3	213.7
13	14.08	129.21	35.74	179.02	36.8	113.9	40.8	191.5
14	43.53	105.69	22.37	171.58	39.3	103.8	16.3	159.5
15	22.53	126.86	38.97	188.36	50.7	106.5	42.9	200.1
16	111.61	41.46	72.21	225.28	49.3	48.5	67.0	164.8
17	20.65	102.87	102.34	225.86	51.3	95.8	66.0	213.0
18	174.83	68.94	14.40	258.16	133.4	56.0	15.9	205.4
19	146.16	35.40	10.01	191.57	160.5	21.3	12.0	193.9
20	4.55	58.36	151.56	214.47	17.3	63.0	122.5	202.7
21	23.00	56.00	87.17	166.17	33.7	53.1	70.7	157.4
22	27.30	94.33	29.15	150.78	7.2	107.7	25.6	140.4
23	116.64	31.79	38.82	187.25	92.2	23.8	29.1	145.1
Average	**61.52**	**50.94**	**48.12**	**160.58**	**56.80**	**46.61**	**40.58**	**143.99**

Sub-basin	2030 H3A2a climate data				2030H3B2a climate data				2030CGCM3A2a climate data			
	SURQ mm	GWQ mm	LAT mm	WYLD mm	SURQ mm	GWQ mm	LAT mm	WYLD mm	SURQ mm	GWQ mm	LATQ m	WYLD mm
1	65.8	2.0	123.6	191.4	70.5	2.7	119.9	193.0	61.1	1.8	85.93	148.8
2	31.3	10.2	92.4	133.9	36.1	11.4	88.8	136.3	30.9	7.8	62.66	101.4
3	116.2	16.2	20.0	152.5	125.7	16.3	20.1	162.1	107.9	11.4	14.89	134.2
4	40.6	15.9	52.9	109.4	46.9	19.2	44.2	110.2	39.8	12.7	28.69	81.2
5	52.2	25.0	3.6	80.8	60.3	24.0	3.6	88.0	56.1	18.0	2.56	76.7
6	36.3	36.2	10.1	82.6	46.1	35.6	9.1	90.8	44.6	23.2	5.73	73.5
7	104.1	18.8	3.9	126.8	115.3	19.5	4.0	138.9	98.6	14.0	3.10	115.7
8	13.7	35.6	22.3	71.6	18.5	35.9	21.8	76.3	19.2	21.9	15.39	56.6
9	25.4	29.0	109.7	164.1	29.1	32.4	108.1	169.7	25.1	28.4	77.64	131.2
10	49.1	27.7	7.5	84.3	57.7	26.4	7.8	91.9	54.1	19.7	5.59	79.4
11	54.7	33.1	38.3	126.1	61.8	34.2	38.2	134.2	54.4	28.1	27.91	110.4
12	97.7	54.2	18.7	170.6	108.1	55.8	18.1	182.0	94.5	43.1	11.93	149.6
13	5.6	80.5	35.3	121.5	8.0	85.4	34.8	128.2	7.0	67.4	23.47	97.8
14	44.8	76.6	14.6	136.0	42.4	81.9	15.0	139.3	33.9	64.0	10.12	108.0
15	7.0	80.5	37.0	124.4	10.0	84.5	36.7	131.2	8.7	66.3	25.49	100.5
16	77.3	36.2	61.6	175.2	69.4	44.0	63.4	176.8	53.9	37.8	46.45	138.2
17	7.3	71.0	55.1	133.4	9.8	75.5	55.0	140.3	8.3	60.2	39.06	107.5
18	104.1	43.1	13.9	161.2	116.1	41.4	13.1	170.6	101.1	29.9	8.82	139.8
19	92.1	19.7	10.1	121.8	110.9	18.9	9.7	139.5	98.0	10.6	6.71	115.3
20	9.8	47.7	115.1	172.6	11.2	53.2	115.3	179.6	9.6	45.8	82.98	138.3
21	30.7	44.3	65.8	140.8	43.0	43.2	63.6	149.8	39.6	31.4	44.64	115.6
22	9.1	91.9	25.2	126.2	32.1	89.9	22.5	144.6	36.8	67.7	14.17	118.7
23	116.0	17.9	26.7	160.6	133.5	18.1	26.5	178.2	124.2	10.7	18.76	153.7
Average	**51.77**	**39.72**	**41.8**	**133.4**	**59.2**	**41.3**	**40.8**	**141.3**	**52.5**	**31.4**	**28.8**	**112.7**

11.4 Annex4 - Climate scenarios

The Special report for emission scenarios (SRES) team defined four narrative storylines that describing the relationships between the forces driving greenhouse gas and aerosol emissions and their evolution during the 21st century. They are labeled A1, A2, B1 and B2.

A1 storyline and scenario family describe a future world of very rapid economic growth, global population that peaks in mid-century and declines thereafter, and the rapid introduction of new and more efficient technologies. Major underlying themes are convergence among regions, capacity building and increased cultural and social interactions, with a substantial reduction in regional differences in per capita income. The A1 scenario family develops into three groups that describe alternative directions of technological change in the energy system.

A2 storyline and scenario family: regionalization, emphasis on human wealth regional, intensive (clash of civilizations) and describe a very heterogeneous world. The underlying theme is self-reliance and preservation of local identities. Fertility patterns across regions converge very slowly, which results in continuously increasing population. Economic development is primarily regionally oriented and per capita economic growth and technological changes are more fragmented and slower than in other storylines.

B1 storyline and scenario family: globalization, emphasis on sustainability and equity Globalized, extensive (sustainable development) and describe a convergent world with the same global population, that peaks in mid-century and declines thereafter, as in the A1 storyline, but with rapid change in economic structures toward a service and information economy, with reductions in material intensity and the introduction of clean and resource-efficient technologies. The emphasis is on global solutions to economic, social and environmental sustainability, including improved equity but without additional climate initiatives and slower than in other storylines

B2 storyline and scenario family: regionalization, emphasis on sustainability and equity Regional, extensive (mixed green bag). The B2 storyline and scenario family describes describe a world in which the emphasis is on local solutions to economic, social and environmental sustainability. It is a world with continuously increasing global population at a rate lower than A2, intermediate levels of economic development, and less rapid and more diverse technological change than in the B1 and A1 storylines. While the scenario is also oriented towards environmental protection and social equity, it focuses on local and regional levels.

Special submission report on Emission scenarios predictor variables downloaded and used in SDSM

No	Predictor variable	Predictor Description	No	Predictor variable	Predictor Description
1	mslpaf	Mean sea level pressure	14	P5zhaf	500hpa divergence
2	P_faf	Surface air flow strength	15	P8_faf	850 hpa* airflow strength
3	P_uaf	Surface zonal velocity	16	P8_uaf	850 hpa zonal velocity
4	P_vaf	Surface meridian velocity	17	P8_vaf	850 hpa meridian velocity
5	P_zaf	Surface vorticity	18	P8_zaf	850 hpa vorticity
6	P_thaf	Surface wind direction	19	P850af	850 hpa geospatial height
7	P_zhaf	Surface divergence	20	P8thaf	850 hpa wind direction
8	P5_faf	500 hpa* airflow strength	21	P8zhaf	850hpa divergence
9	P5_uaf	500 hpa zonal velocity	22	r500af	Relative humidity at 500 hpa
10	P5_vaf	500 hpa meridian velocity	23	r850af	Relative humidity at 500 hpa
11	P5_zaf	500 hpa vorticity	24	rhumaf	Near surface relative humidity
12	P500af	500 hpa geospatial height	25	shumaf	Surface specific humidity
13	P5thaf	500 hpa wind direction	26	tempaf	Mean temperature at 2 m

*hpa is a unit of pressure, 1 hpa=1 mbar=100 pa

11.5 Annex 5 - Soil analysis

Sample Hydrometric analysis is based on the procedure of the Geotechnical Laboratory Manual adapted ASTM (originally known as the American Society for Testing and Materials) AASHTO (American Association of State Highway and Transportation Officials) standard. The following are the tests modified for the geotechnical laboratory of Mekelle University:

1. Prepare the control jar by adding 125 ml of 4% sodium metaphosphate ($NaPO_3$) solution and sufficient distilled water to produce 1000 ml. (This solution can be made by mixing 40g of dry chemical with enough water to make 1000 ml). Put the hydrometer into the control cylinder and record zero and meniscus correction; then record the temperature by putting the thermometer in it.
2. Weigh out exactly 50g of soil passing the No. 200 sieve. Mix the soil with 125 ml of 4% sodium metaphosphate ($NaPO_3$) solution. Allow the soil mixture to stand about 12 hours.
3. At the end of the soaking period, transfer the mixture to a dispersion (or malt mixer) cup and add tap water until the cup is about two-thirds full. Mix for 1 minute. After mixing, carefully transfer all the contents of the dispersion cup to the sedimentation cylinder. Rinse any soil in the dispersion cup by using a plastic squeeze bottle or adding stabilized water and pour this into the sedimentation cylinder. Now add distilled water to fill the cylinder to the 1000 ml mark.
4. Cap the sedimentation cylinder with a No. 12 rubber stopper and carefully agitate for about 1 min. Agitation is defined as turning the cylinder upside down and back 60 turns for a period of 1 min. An upside down and back movement is 2 turns.
5. Put the sedimentation cylinder beside the control cylinder and start the stopwatch immediately. This is cumulative time t = 0. Insert the hydrometer into the sedimentation cylinder.
6. Take hydrometer readings at cumulative times t = 0.25 min., 0.5min., 1 min. and 2 min. Always read the upper level of meniscus. Remove and place the hydrometer in the control jar.

7. Continue taking hydrometer and temperature readings at approximate elapsed times of 8, 15, 30 and 60 min. and then 2, 4, 8, 24 and 48 hr. For each reading, insert the hydrometer into the sedimentation cylinder about 30 sec before reading is due. After the reading is taken, remove the hydrometer and put it back into the control cylinder.

Hydrometer Analysis (Texture)
(Sedimentation Method)

Volume of suspension cc
Specific gravity of soil
Specific gravity of water
unit wt of water g/cc

Sample 005

Sample No.	Time of Reading	Elapsed time t (min)	Actual Hydro-meter Reading	T (°C)	Compo site correc-tion	Corrected Hydro-meter reading	Effect. depth L (mm)	L/t	√(L/t)	K , from table	Parti cle Ø D(mm)	% fines
1.00	0.14	0										
2.00	0.14	2	1.03	23.0	0.0	1.02	9.70	4.85	2.20	0.01	0.03	72.95
3.00	0.14	4	1.02	23.0	0.0	1.02	10.35	2.59	1.61	0.01	0.02	64.99
4.00	0.14	6	1.02	23.0	0.0	1.02	11.00	1.83	1.35	0.01	0.02	57.02
5.00	0.14	8	1.02	23.0	0.0	1.02	11.30	1.41	1.19	0.01	0.02	53.84
6.00	0.15	10	1.02	23.0	0.0	1.02	11.50	1.15	1.07	0.01	0.01	50.65
7.00	0.15	20	1.02	23.0	0.0	1.01	12.10	0.61	0.78	0.01	0.01	44.28
8.00	0.16	30	1.02	23.0	0.0	1.01	12.30	0.41	0.64	0.01	0.01	41.10
9.00	0.18	60	1.01	23.0	0.0	1.01	12.60	0.21	0.46	0.01	0.01	37.91
10.00	0.22	120	1.01	23.0	0.0	1.01	13.05	0.11	0.33	0.01	0.00	33.13
11.00	0.31	240	1.01	24.0	0.0	1.01	13.40	0.06	0.24	0.01	0.00	28.99
12.00	0.47	480	1.01	24.0	0.0	1.01	13.70	0.03	0.17	0.01	0.00	25.80
13.00	0.14	1440	1.01	23.0	0.0	1.01	13.90	0.01	0.10	0.01	0.00	21.98

Particle size		% Clay	%	% out of 100
0.002	clay	25.09	25.1	25.1
0.002-0.05	Silt	72.95	47.9	47.9
0.05-0.075	Fine sand		27.1	27.1

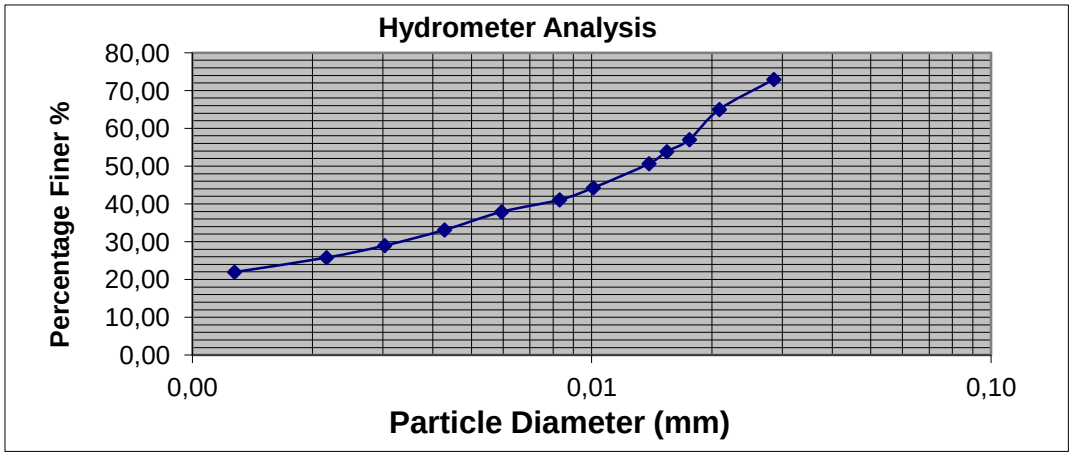

Sample wet sieve analysis

The calculation procedure is based on the Geotechnical laboratory manual prepared at MekelleUniversity Department of Civil Engineering. The test procedure for sieving is as follows:

1. Take a representative oven dried sample of soil that weighs about 500 g. (this is normally used for soil samples the greatest particle size of which is 4.75 mm)
2. If soil particles are lumped or conglomerated crush the lumped and not the particles using the pestle and mortar.
3. Determine the mass of sample accurately. Wt (g)
4. Prepare a stack of sieves. sieves having larger opening sizes (i.e lower numbers) are placed above the ones having smaller opening sizes (i.e higher numbers). The very last sieve is #200 and a pan is placed under it to collect the portion of soil passing #200 sieve. Here is a full set of sieves. (#s 4 and 200 should always be included)
5. Make sure sieves are clean, if many soil particles are stuck in the openings try to poke them out using brush.
6. Weigh all sieves and the pan separately. (Fill in column 3)
7. Pour the soil from step 3 into the stack of sieves from the top and place the cover, put the stack in the sieve shaker and fix the clamps, adjust the time on 10 to 15 minutes and get the shaker going.
8. Stop the sieve shaker and measure the mass of each sieve + retained soil. (fill in column 4)

9.

Sieve size (mm)	Weight of sieve	wt of sieve+ retained soil	Mass Retained (gm)	Percent retained (%)	Com.% retained	Percentage finer (%)
37.50	1705.96	1705.96	0.00	0.00	0.00	100.00
28.00	1727.22	1751.59	24.37	2.44	2.44	97.56
20.00	1617.33	1624.12	6.79	0.68	3.12	96.88
14.00	1356.9	1375.58	18.68	1.87	4.98	95.02
10.00	1324.81	1364.81	40.00	4.00	8.98	91.02
5.00	1372.25	1456.85	84.60	8.46	17.44	82.56
2.36	1245.13	1349.81	104.68	10.47	27.91	72.09
1.18	491.63	584.1	92.47	9.25	37.16	62.84
0.60	492.08	600.24	108.16	10.82	47.97	52.03
0.30	279.03	446.57	167.54	16.75	64.73	35.27
0.15	442.88	656.59	213.71	21.37	86.10	13.90
0.075	414.57	485.22	70.65	7.07	93.16	6.84
pan	314.57	377.34	62.77	6.28	99.44	0.56

SUL 026	%	from 500gram%Sand andAbove		
		%age distribution		
Gravel	17.4	0.0	Not include	
Sand	75.7	92.3		
Finner	6.3	7.7	Going to sedimentation analysis to separate clay and silt	
	82.0	100.0		

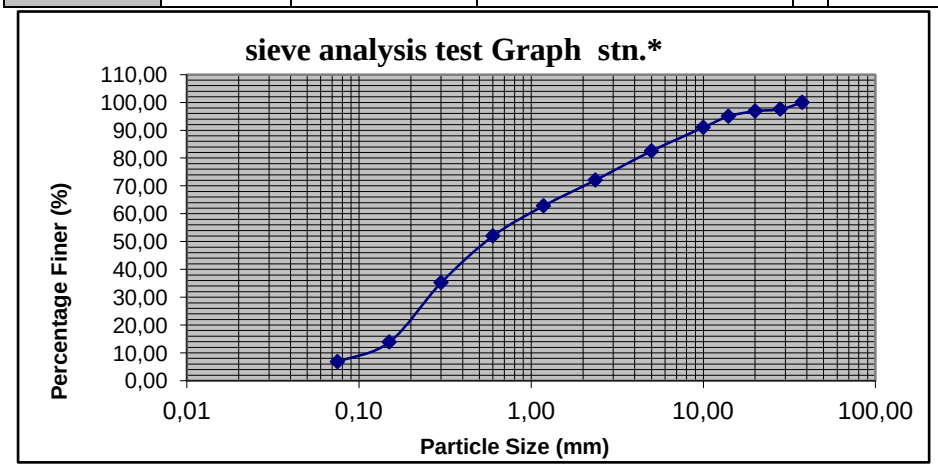

Sample soil textural analysis result using USDA soil classification triangle

Soil code	Elevation (m.a.s.l)	Percent Distribution			Soil Texture	Specific gravity
		Sand	Clay	Silt		
S001	3089	47.82	16.96	35.23	loam	2.69
S002	2833	16.72	15.42	67.86	silt loam	2.74
S010	2788	76.75	9.42	13.83	Sand Loam	2.60
S011	2353	66.65	13.83	19.52	Sandy Loam	2.71

S012	2390	19.38	35.95	44.67	Silt Clay Loam	2.66
S013	2507	98.62	0.63	0.74	Sand	2.66
S014	2318	99.73	0.09	0.18	Sand	2.63
S015	2354	88.90	5.88	5.22	Sand	2.71
S016	2369	68.16	16.00	15.84	Sand Loam	2.50
S017	2651	98.85	0.50	0.65	Sand	2.58
S018	2265	62.51	18.90	18.58	Sand Loam	2.45
S019	2291	32.44	47.98	19.58	Clay	2.43
S020	2343	97.94	0.85	1.21	Sand	2.63
S021	2339	68.92	8.00	23.08	Sand Loam	2.60
S022	2456	26.88	25.08	48.04	Loam	2.43
S023	2292	29.35	44.73	25.92	Clay	2.36
S024	2296	80.99	6.77	12.24	Loamy Sand	2.60
S027	2087	71.26	9.39	19.36	Sandy Loam	2.71
S028	2287	33.51	15.29	51.20	Silty Loam	2.74
S029	2462	48.70	13.21	38.09	Loam	2.60
S030	2080	19.33	44.09	36.59	Clay	2.71
S031	2006	95.43	2.62	1.94	Sand	2.58

Curriculum Vitae

The curriculum vitae is not available in the onlie version due to data privacy.

Erklärung

Hiermit bestätige ich, dass ich die vorliegende Arbeit selbstständig verfasst und keine Hilfsmittel außer den angegebenen verwendet habe. Die Stellen der Arbeit, die anderen Werken wörtlich oder inhaltlich entnommen sind, wurden durch Angabe der Quelle kenntlich gemacht.

Die Arbeit hat in gleicher oder ähnlicher Form noch keiner Prüfungsbehörde vorgelegen.

29. October 2013 _____

Abraha Adugna